General Disclaimer

One or more of the Following Statements may affect this Document

- This document has been reproduced from the best copy furnished by the organizational source. It is being released in the interest of making available as much information as possible.

- This document may contain data, which exceeds the sheet parameters. It was furnished in this condition by the organizational source and is the best copy available.

- This document may contain tone-on-tone or color graphs, charts and/or pictures, which have been reproduced in black and white.

- This document is paginated as submitted by the original source.

- Portions of this document are not fully legible due to the historical nature of some of the material. However, it is the best reproduction available from the original submission.

ERDA/NASA/3-20064/77/1
NASA CR-135230
DDA EDR 9068

STUDY AND PROGRAM PLAN
FOR
IMPROVED HEAVY DUTY GAS TURBINE ENGINE
CERAMIC COMPONENT DEVELOPMENT

(NASA-CR-135230) STUDY AND PROGRAM PLAN FOR IMPROVED HEAVY DUTY GAS TURBINE ENGINE CERAMIC COMPONENT DEVELOPMENT Final Report (Detroit Diesel Allison, Indianapolis, Ind.) 161 p HC A08/MF A01 CSCL 13F G3/85

N77-32033

Unclas 46224

H. E. Helms

DETROIT DIESEL ALLISON DIVISION OF GENERAL MOTORS
Indianapolis, Indiana 46206

May 1977

Prepared for the

NATIONAL AERONAUTICS AND SPACE ADMINISTRATION
Lewis Research Center
Cleveland, Ohio 44135

Contract NAS3-20064

As a Part of the

ENERGY RESEARCH AND DEVELOPMENT ADMINISTRATION
Division of Transportation Energy Conservation
Heat Engine Highway Vehicle Systems Program

1. Report No.	2. Government Accession No.	3. Recipient's Catalog No.
NASA CR-135230		

4. Title and Subtitle	5. Report Date
STUDY AND PROGRAM PLAN FOR IMPROVED HEAVY DUTY GAS TURBINE ENGINE CERAMIC COMPONENT DEVELOPMENT.	May 1977
	6. Performing Organization Code
7. Author(s)	8. Performing Organization Report No.
H. E. Helms	EDR 9068
	10. Work Unit No.
9. Performing Organization Name and Address	
Detroit Diesel, Division of General Motors Corporation Post Office Box 894 Indianapolis, Indiana 46206	11. Contract or Grant No. NAS 3-20064
	13. Type of Report and Period Covered
12. Sponsoring Agency Name and Address Energy Research and Development Administration Division of Transportation Energy Conservation Washington, D. C. 20545	Contractor Report
	14. Sponsoring Agency Code Report No.
	ERDA/NASA/3-20064/77/1

15. Supplementary Notes
Final Report. Prepared under Interagency Agreement EC-77-A-31-1011
Project Manager, W. Goette, Transportation Propulsion Division,
NASA Lewis Research Center, Cleveland, Ohio 44135

16. Abstract

A five-year program plan was generated from the study activities with the objectives of demonstrating a fuel economy of 213 mg/W·h (0.35 lb/hp-hr) brake specific fuel consumption by 1981 through use of ceramic materials, with conformance to current and projected Federal noise and emission standards, and to demonstrate a commercially viable engine.

Study results show that increased turbine inlet and regenerator inlet temperatures, through the use of ceramic materials, contribute the greatest amount to achieving fuel economy goals. Further, improved component efficiencies (for the compressor, gasifier turbine, power turbine, and regenerator disks show significant additional gains in fuel economy. Fuel saved in a 500,000-mile engine life, risk levels involved in development, and engine-related life cycle costs for fleets (100 units) of trucks and buses were used as criteria to select work goals for the planned program.

17. Key Words (Suggested by Author(s))	18. Distribution Statement
Heavy Duty Gas Turbine Engine Fuel Economy Component Efficiencies Life Cycle Costs Ceramic Components	Unclassified—Unlimited STAR Category 85 ERDA Category UC-96

19. Security Classif. (of this report)	20. Security Classif. (of this page)	21. No. of Pages	22. Price*
Unclassified	Unclassified	155	

* For sale by the National Technical Information Service, Springfield, Virginia 22151

FOREWORD

Work accomplished in this contracted effort was performed by a large team of experts at Detroit Diesel Allison Division of General Motors Corporation. Largest contributors to this work were:

Design Activities:	B. C. Hall, John Hayes, John Wertz, James Lunsford, David Decker
Regenerator Activities	Sam Thrasher, Michael Simetkosky Harris Gaston
Life Cycle Costs:	Carlton Curry
Performance Analysis:	James Wooten, Terry Knickerbocker
Materials:	Dr. Peter Heitman
Program Coordination and Reporting:	Roger Dycus, Dennis Schroff

The Carborundum Company contributors were Dr. John Coppola, Bill Long, Carl McMurtry and Dr. Ed Knight.

The Harrison Radiator Division of General Motors Corporation contributors were Paul Beatenbaugh, Vince Nicolia and Robert Hagen.

TABLE OF CONTENTS

TABLE OF CONTENTS (Cont)

LIST OF ILLUSTRATIONS

LIST OF TABLES

SUMMARY

A study was conducted to establish a viable program to improve the specific fuel consumption, by use of ceramic materials in the Detroit Diesel Allison Model 404 industrial gas turbine engine (herein called the base line engine). These ceramic materials permit increases in cycle operating temperatures and contribute to improved component efficiencies. The overall program objectives, using ceramic materials, were to accomplish the following goals:

- Improve the specific fuel consumption from 274 mg/W·h (0.45 lb/bhp-hr) to 213 mg/W·h (0.35 lb/bhp-hr) in a five-year program
- A commercially viable engine
- Conformance with current and projected noise and emission standards

The study conducted assessed (1) the improvements that can be made to the current engine by use of ceramic materials and component efficiency improvements, (2) truck and bus performance and life cycle costs from engine improvements, and (3) the risk or technical feasibility of engine improvements to achieve the fuel consumption goal in five years. The study established that the fuel consumption objective could be met by the use of ceramics in the regenerator disks and seals, turbine inlet vanes and stationary turbine tip shrouds, turbine inlet plenum, gasifier rotor blades, combustor, and exhaust diffusers along with component efficiency improvements in the compressor, turbines (gasifier and power), and regenerator disks. At a turbine inlet temperature of 1204°C (2200°F), the fuel consumption is within 2% of the goal, and at 1371°C (2500°F) the goal was exceeded.

At the 213 mg/W·h (0.35 lb/bhp-hr) sfc level, fuel savings achieved were 116,000 litres (30,600 gal) per truck or 100,000 litres (26,500 gal) per bus in a typical 805,000-kilometre (500,000-mile) engine life. In addition, it was shown that the engine-related life cycle costs of a typical highway truck or an intercity bus are improved by 5% to 15% (depending on the ceramic materials and fuel costs that are assumed). Noise and emission regulations can be met by the improved engines with minimal development.

The development risks associated with ceramic materials vary with the components—the regenerator being the lowest risk and the turbine rotor blade the highest risk in the time chosen for the program. Components selected for development are considered to be feasible for demonstration in the program planned.

An engine development plan was prepared, using the results of the study effort, which addressed the overall program objectives. The steps involved in the program are to increase the turbine inlet temperature successively from 1002°C (1835°F) (base line engine) to 1038°C (1900°F) to 1132°C (2070°F) to 1241°C (2265°F) with stepwise increases in the numbers of ceramic components, and to the aerodynamic component efficiencies. Ceramic regenerators are the first

components to be tested in the engine. Next, ceramic turbine inlet vanes and stationary rotor tip shrouds are introduced with a modest temperature increase. In the 1132°C (2070°F) engine, the ceramic turbine inlet plenum and gasifier rotor blades are introduced. Finally, in the 1241°C (2265°F) engine, a ceramic combustor, an exhaust diffuser, and power turbine nozzles are introduced along with improved aerodynamic components and the fuel consumption goal demonstrated.

In the development plan, ceramic components will be tested in considerable depth with rigs as well as engines to establish the feasibility of introducing ceramic components into production engines. Data achieved will be carefully and thoroughly integrated into a probabilistic design methodology procedure. The objective of this activity will be to establish design techniques which consistently predict ceramic material behavior. With the design method, proper material specifications, demonstrated inspection and quality control techniques, and significant rig and engine experience, the applicability of ceramic materials to a commercial engine can reasonably be expected to be established.

INTRODUCTION

This investigation is a part of an overall study of gas turbine engine fuel consumption improvements that is being managed by the Lewis Research Center of the National Aeronautics and Space Administration under sponsorship of the Energy Research and Development Administration. The study, reported herein under contract number NAS3-20064, involves the assessment of the potential for improving the Detroit Diesel Allison (DDA) Model 404 industrial gas turbine engine, herein called the base line engine, as applied to line haul trucks and highway buses through the use of ceramic components and aerodynamic efficiency improvements. The output of the study was used to generate a viable program plan for the development and implementation of the recommended modifications.

Detroit Diesel Allison has been active in developing an industrial gas turbine for more than twenty years. In this time, the all-metal gas turbine engine has progressed from an installed specific fuel consumption of approximately 426 mg/W·h (0.7 lb/bhp-hr) to 274 mg/W·h (0.45 lb/bhp-hr). Further, more than three million miles of truck, bus, and other vehicles usage have been compiled. Including development test stand running, more than 200,000 hours of engine operation have been completed. These engines are the Model 404, rated at 224 kW (300 hp), and the Model 505, rated at 291 kW (390 hp). A third engine, the Model 605, is planned for the same engine block and gearbox (95% commonality of parts); it is rated at 347 kW (465 hp).

The objective of this long-term development program has been to provide a new engine which can successfully compete in the heavy duty engine market place. Typical applications for this type engine are in highway heavy duty trucks, intercity buses (coaches), generator sets, boats, air compressors, and heavy duty equipment (loaders, scrapers, haulers, etc). To compete successfully in the market place, the engine must give fuel economy that is equal to or better than that of current heavy duty engines, must meet all government regulations on noise or emissions, must possess the durability and reliability characteristics equal to those of engines, and must not cost significantly more than the engines it is to replace. Most of these requirements have been met by the all-metal engine, and volume production is receiving serious consideration.

Advanced versions of development and production gas turbine engines receive continuous consideration, and ceramic engine components have been the subject of studies for many years. High risk has been assigned to ceramic gas turbine engine components, and only minimal funding has been affordable for this high technology area. With the recent emphasis, by government, on expediting the ceramic materials technology, a program to introduce ceramics in the base line engine was conceived and presented for government support. Benefits offered by ceramic materials are evident from their potentially high-strength, high-temperature characteristics. Higher turbine inlet temperature, higher regenerator operating temperature, and the potential for low cost are some of the benefits to be derived. Recent progress, evolving from government supported programs, has begun to indicate the potential of such ceramics as

silicon nitride, silicon carbide, and alumina-silicate materials. Other materials, such as sialons, lithium-alumina-silicate, and magnesium-alumina-silicate, are also candidate materials under development.

Specific problems arise in trying to incorporate ceramic components in any engine. The brittle nature of ceramics establishes a need for a new design methodology which recognizes the probabilistic nature of inherent flaws from fabrication. Design must provide attachments between ceramic and metal parts which properly distribute contact loads since, unlike metals, ceramic materials break rather than yield and redistribute local loads. Thermally induced stresses resulting from either transient or steady-state operating conditions must be accurately predicted over a complete operating cycle and geometry, or operation must be varied to accept the limitations of the ceramic materials. Inspection methods historically used for metals must be modified or new techniques must be developed to sort good fabricated parts from bad fabricated parts. New fabrication techniques must be forthcoming to produce consistently reliable, low-cost ceramic parts. Testing must be monitored closely to ascertain properly the environmental conditions which cause failures or produce chemical instability in ceramic parts. These and other problems must be solved to bring ceramic materials to a state of production readiness. In the program, each of these problems will be addressed in developing ceramic components for the engine.

Proper program planning and technical advances can be achieved only with a careful assessment of the current state of the art and by realistic projections of how improvements may be accomplished. A study to make assessments of potential improvements to the base line engine was established, and the results are reported herein. In the study, ceramic materials and the resulting improved component efficiencies were incorporated as candidate means of achieving the improved fuel economy objective of the program in the time frame specified (by the end of 1981).

A sequence of evaluation and study was established and a set of criteria was selected for choosing improvements for the base line engine. The study sequence selected was as follows.

- Assess sensitivities of engine parameters that might be changed. An increment of change in parameter yielding a 1% change in specific fuel consumption (sfc) was established.
- Select components for improvement from the sensitivity study based on ceramic materials capabilities and on feasible component efficiency or performance improvements. Technical specialists studied current and projected improvements and established goals.
- Calculate performance improvements of the engine and vehicles with the improved engines. Steps in improvement were selected to obtain maximum experience with current engine geometry and parts. This course was pursued to minimize program hardware costs and maximize the potential for early introduction of ceramic components in the production engine.

- Establish preliminary designs of engines for each increment of improvement.
- Evaluate costs for improvements to the base line engine (current all-metal engine). This included ceramic and metal engines produced at the rate of 6000 engines per month.
- Calculate life cycle costs to establish the customer benefits for having the improved engines at each step in development.
- Apply selection criteria for establishing work to be accomplished in the development program.
- Plan the program recognizing time, funding, and technical feasibility for accomplishment. Allow for iterations in work for ceramic components and for learning methods on design, fabrication, and test.
- Establish program schedule, manpower requirements, costs, and program management.

The engine cycle and program activity selection criteria were based on the following factors:

- Applicability to the base line engine
- Fuel savings accomplished
- Risk level for technical accomplishment
- Costs imposed on customers from engine-related life cycle cost studies (a typical line haul truck and a highway bus were used as base line vehicles.)

All components selected are applicable to either early or advanced versions of the base line engine. Each step recommended shows a fuel saving. The risk level was considered medium for all ceramic components except for the turbine rotor blade, which was assessed as high risk. The risk level for component efficiencies was considered medium. A recommendation for reconsideration of temperature goals is to be exercised in the program as progress is achieved.

The work accomplished under this contract consisted of a rigorous design study to establish a program plan for introducing ceramic materials into a current industrial gas turbine engine and to obtain improved fuel economy. The balance of this report describes the details of how this work was accomplished and of the results obtained.

Improved fuel economy is bound to have a significant impact on buses and trucks used on United States highways. The improved heavy duty gas turbine engine emissions and noise (relative to diesel engines) will meet all current and projected regulations. The hours of testing proposed will begin to establish a viable commercial application of improved components and ceramic components. Success with the ceramic materials applied to the components will establish an excellent technology base applicable to other highway passenger cars and vehicles.

BASE-LINE ENGINE

DESIGN DESCRIPTION

The Detroit Diesel Allison Model 404 and 505 industrial gas turbine engines, which are currently in the latter stages of development, are regenerative, free-turbine-type, heavy duty industrial engines. These engines are sized and configured for vehicular, marine and stationary applications. Their principal vehicular applications are in line haul (highway) trucks, highway buses, and transit coaches. The engine is also suited to off-highway applications, such as for track-laying vehicles, either industrial or military. Typical stationary applications include electric generator sets and air compressors. The multifuel capability of the engine is a particularly attractive feature for these applications. The two engine models, which have the same frame size and are basically identical with respect to mechanical design configuration, have different power ratings by virtue of differences in their compressor and turbine aerodynamic capacities. Approximately 90% of the parts are common between these two models.

For this investigation, the Model 404 engine will be used as the base-line engine because its 224 kW (300 hp) power rating makes it applicable to the line haul truck as well as the highway bus. The basic external arrangement of this engine is shown in Figure 1; its basic gas path is shown schematically in Figure 2. These illustrations show that the engine consists of a gasifier

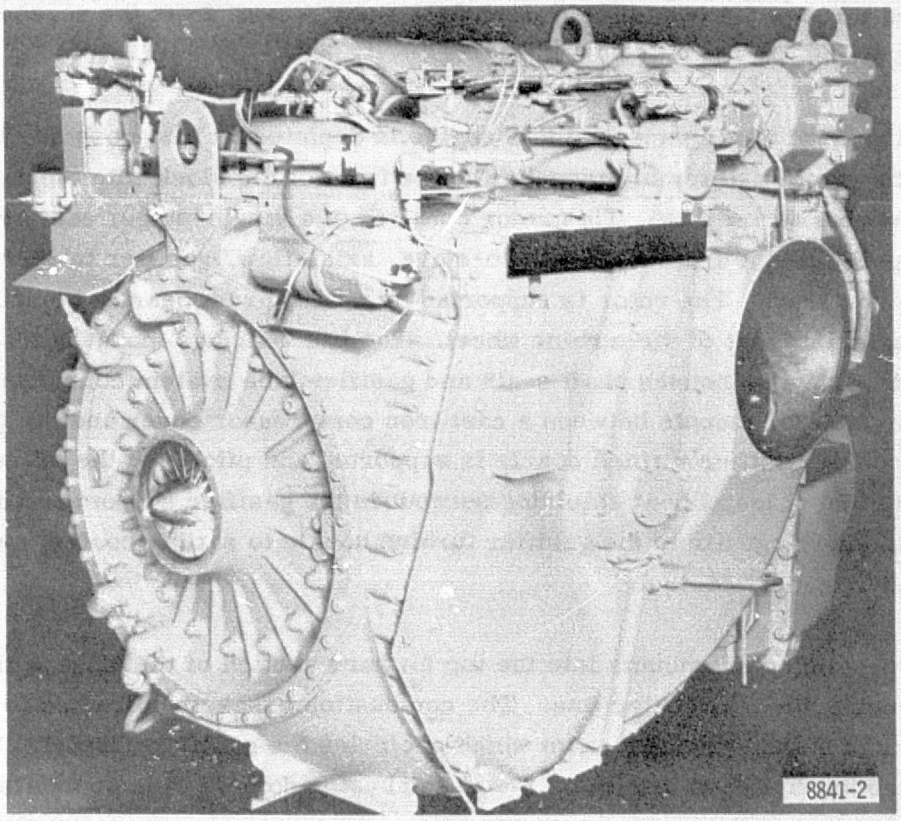

Figure 1. Base line engine.

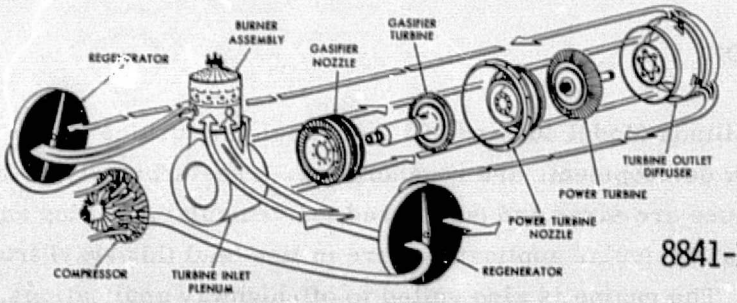

Figure 2. Engine airflow schematic.

assembly, a power turbine, a combustor, a regenerator system, a reduction and accessory drive gearbox, a power transfer system, and a fuel management system. The primary structural frame of the engine is a two-piece cast iron block. Air enters the single-stage, radial compressor from an inlet filter and silencer. The air discharging from the impeller flows through a vane-type diffuser and is then directed to the regenerator covers at the sides of the engine. The compressor discharge air then flows inward through the regenerator disks to the combustor. The gases from the combustor are directed to the gasifier turbine nozzle by the turbine inlet plenum. After the gas expands through the gasifier turbine, it flows through a transition to the power turbine. After expansion through the power turbine, the gases are directed outward through the two regenerator disks and then exit from the regenerator covers into the exhaust pipes.

The mechanical general arrangement of this engine is depicted by the cross section drawing of Figure 3. The gasifier assembly mounts into the front of the block with the axis of rotor rotation on the engine center line. This rotor consists of a single-stage, cast aluminum, compressor impeller at the front and a single-stage, axial-flow, gasifier turbine wheel attached to a common shaft. The rotor is supported by a ball thrust bearing behind the impeller and a roller bearing in front of the turbine wheel. The two bearings mount into a cast iron gasifier support which also houses shaft seals and gasifier lube system components. A vane-type compressor diffuser mounts between a cast iron compressor cover and the gasifier support. The air-cooled gasifier turbine nozzle is supported and piloted at the aft end of the gasifier support. Sheet metal heat shielding surrounds the gasifier support and also serves to duct compressor discharge air to the gasifier turbine nozzle to satisfy cooling requirements and shaft seal environment control.

A single-can-type combustor mounts into the top forward section of the block with its axis aligned on the engine vertical center line. The combustion gases are directed to the gasifier turbine by means of a sheet metal plenum which encircles the gasifier support. The single fuel nozzle and igniter are attached to a sheet metal combustor dome. This dome also supports

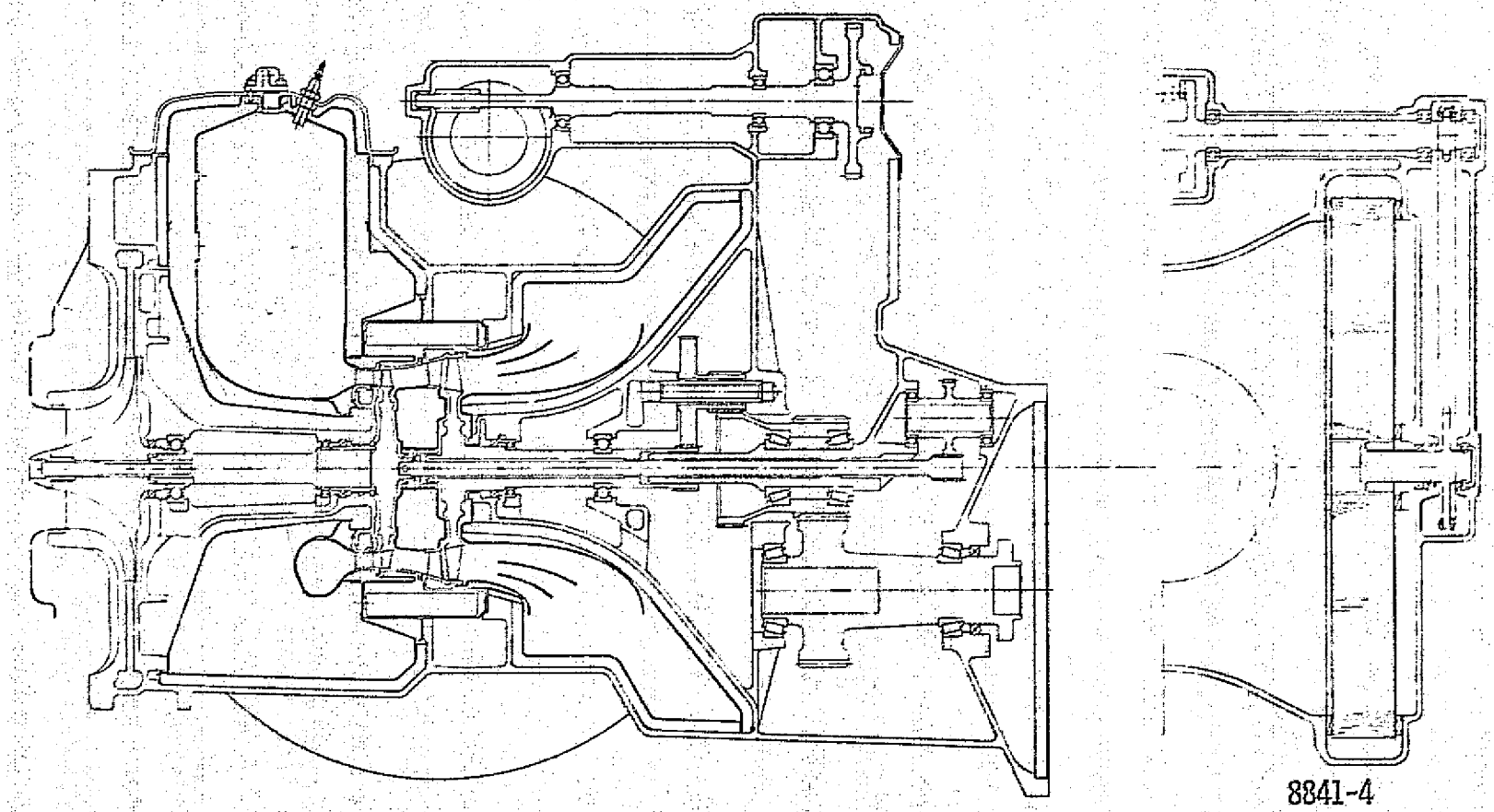

Figure 3. Engine general arrangement.

the combustor. Internal surfaces of the block, which would be exposed to hot gases and radiation from the combustor and turbine inlet plenum, are protected by insulation material and sheet metal liners.

The single-stage, axial-flow power turbine, which is aligned with and to the rear of the gasifier turbine, consists of a nozzle assembly supported from the block center bulkhead and a rotor supported on two bearings. These two bearings—a roller bearing immediately behind the turbine wheel and a ball thrust bearing at the aft end of the rotor shaft—are mounted in the forward case of the gearbox. A sheet metal exhaust diffuser encircles the power turbine rotor support structure.

The regenerator system consists of two metal matrix disks, disk seals, cast iron regenerator covers, and a disk drive system. A disk is mounted in each side of the block so that the axis of rotation is on the engine transverse horizontal center line. Each disk is supported and driven by a sprocket and shaft assembly which is supported from the regenerator covers. These sprockets are driven by roller chains which are, in turn, driven by sprockets connected by shafts to the regenerator drive gearbox at the top center of the engine. The regenerator drive gearbox mounts to and is driven from the front case of the main engine gearbox. The regenerator covers bolt to the block and direct the compressor discharge airflow from the block inward through the forward portion of the disks and direct the turbine exhaust gas outward through the rear portion of the disks to the exhaust pipes.

The main engine gearbox contains the reduction gearing between the power turbine rotor and the engine output shaft and gearing for accessory drives. The engine lube pump and related components are assembled in this gearbox. The engine accessories and the regenerator drive system are driven by the gasifier rotor. Other accessories as required for different applications can be mounted to the gearbox driven by the power turbine. Also, a simple gear substitution within the gearbox provides a change in output speed and/or a reversal in rotation as desired for a particular application. A shaft which attaches to the rear of the gasifier rotor and extends through the power turbine rotor into the gearbox provides the drive from the gasifier rotor. This shaft is interconnected by suitable gearing to an oil-cooled, oil-pressure-modulated, multiple-plate clutch which, in turn, is geared to the power turbine rotor. This system constitutes the mechanical portion of the power transfer system. When the clutch is fully locked up, the engine operates as a single-shaft engine.

The principal components of the fuel management system are an electronic control, a relay box, an electric fuel metering valve, an electric clutch servovalve, a throttle sensor, a compressor inlet temperature sensor, and thermocouples and speed pickups. This system provides for automatic sequencing of engine starting functions, automatic scheduling of fuel flow and turbine inlet temperature, automatic programming of power transfer clutch engagement, road speed governor function, and automatic shutdown protection against abnormal conditions during starting and operation. The system is designed to operate on either 12- or 24-volt d-c power.

The engine was sized and configured to meet the performance characteristics, reliability, endurance life, life-cycle cost, maintainability, emissions and competitive production cost requirements of the intended applications.

The engine was designed to have a time between overhaul (TBO) of 7500 hr in the highway truck application, with the majority of the parts having a minimum life of 15,000 hours. Design criteria with respect to wear rates, oxidation rates, and allowable stress levels were established to be consistent with these goals. A detail description of the components used in the base line engine is contained in the appendix.

PERFORMANCE AND OPERATION

The industrial gas turbine performance objective is to provide general-purpose engines, competitive in fuel economy with other commercially available power sources in the same horsepower range, meeting current and projected noise and emission standards. The power rating of the base line engine at 224 kW (300 hp) (at SAE standard day conditions) was selected on the basis of a variety of applications including trucks, buses, off-highway vehicles, boats, air compressors, and generator sets. In many of these applications, the duty cycle is such that most of the fuel is consumed at engine throttle settings above 50% power. For this reason, an additional requirement is to maintain the sfc vs hp curve as flat as possible between 50% and 100% power and, with the sfc at 50% power, no more than 8% above that at 100% power.

The sfc requirements were established to be competitive on an installed basis with diesel engines used in the same applications. This ruled out nonregenerative cycles. In addition, part-load temperature control must be used to flatten the sfc curve. The wide range of loads to be driven also favored the two-shaft approach to match a variety of output rpm and torque combinations. The simplest configuration meeting these requirements is the low-pressure-ratio centrifugal compressor driven by a single-stage gasifier turbine combined with a single-stage power turbine. Because of the engine size limitations for truck and bus applications, the regenerator offered better performance and lower material cost than the recuperator. Table I shows the base line engine cycle parameters at 100% power. This engine has a design point sfc of 274 mg/W·h (0.45 lb/hp-hr).

The control of turbine temperature is by means of power transfer which consists of a slipping clutch in which one set of plates is geared to the gasifier shaft and the other to the power turbine shaft, as shown in Figure 4. Thermocouples at the gasifier turbine inlet sense the temperature to be controlled by a closed-loop system which drives a servovalve modulating the pressure applied to the plates of the slipping clutch. In the normal range of operation, the relative speeds are such that increasing clutch pressure extracts power from the gasifier shaft, raising the turbine inlet temperature to the desired level. This power, minus slip losses, is transferred to the output shaft. Turbine inlet temperature is maintained constant as power is reduced until the regenerator temperature limit of 774°C (1425°F) is reached. As power is reduced

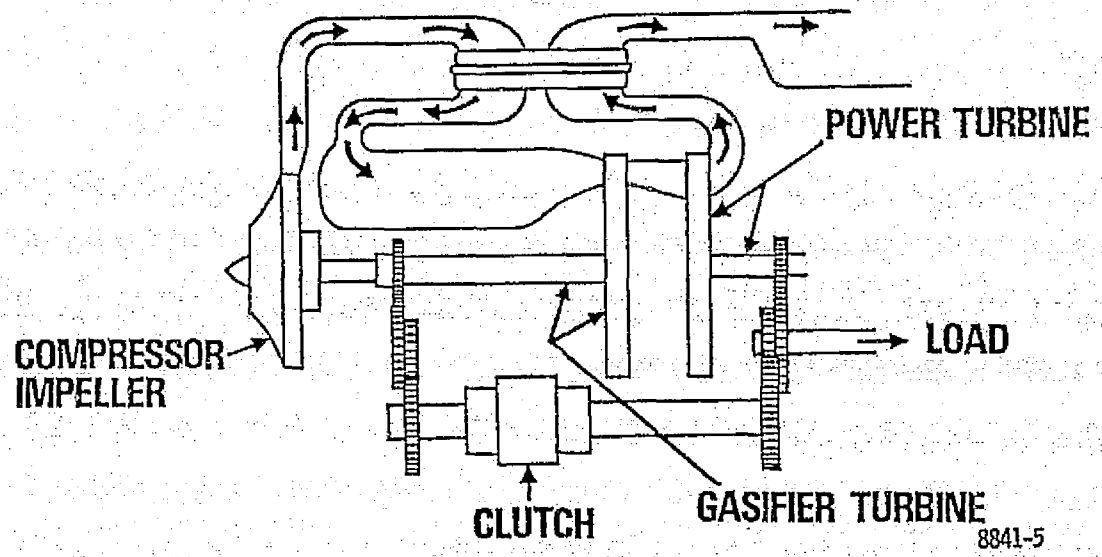

Figure 4. Power transfer.

TABLE I. BASE-LINE ENGINE MAXIMUM POWER CYCLE PARAMETERS

Turbine inlet temperature	°C (°F)	1002 (1835)
Compressor pressure ratio		4.00
Compressor airflow	kg/s (lb/sec)	1.56 (3.45)
Compressor efficiency	%	82.4
Gasifier turbine efficiency	%	87.0
Power turbine efficiency	%	89.7
Burner efficiency*	%	97.6
Regenerator effectiveness	%	88.9
Regenerator leakage	%	4.92
Regenerator inlet temperature	°C (°F)	692 (1278)
Turbine rotor cooling	%	1.71
Block and turbine shroud cooling	%	3.56
Gasifier nozzle vane cooling	%	1.00
Overboard leakage	%	1.21
Total pressure loss**	%	11.8
Mechanical loss	W (hp)	17.9 (24.0)
Shaft power	W (hp)	224 (300)
Specific fuel consumption	mg/W·h (lb/hp-hr)	274 (0.45)

*Includes cycle heat loss
**Includes inlet and exhaust loss

further, the regenerator temperature is maintained at the maximum limit until the gasifier reaches idle speed (53%), at which time the clutch is completely disengaged. The clutch is also locked up to provide engine braking for downhill operation and for power turbine overspeed protection. For generator sets, the clutch is disengaged for starting, then locked up at rated speed for accurate governing. This method of temperature control also has several advantages as a result of the closed-loop system. First, accessory loads applied to the gasifier do not affect turbine temperature, thus minimizing changes in output power and engine life. Second, trimming or selection of components on the production line is not required to maintain the desired temperature. Third, fouling or deterioration of engine components in service has a minimum effect on power and engine life.

Most of the proposed vehicle applications are in a weight class where vehicle acceleration is slow and where an engine idle-to-maximum acceleration time up to 4 seconds is acceptable. This acceleration can be achieved by disengaging the power transfer clutch and raising turbine temperature about 93°C (200°F), still under closed loop control. Because of the large heat capacity of the regenerator system, fuel flow is shut off completely for a deceleration with the throttle at idle. This fuel step, however, lowers turbine temperature by only 371°C (700°F), so the hot section temperature transients tend to be less severe than in most gas turbines although they are very frequent.

Performance development has been continuous, and improvements have been demonstrated by engine test stand calibrations of instrumented engines. The instrumentation was designed to permit the analysis of component performance for verification of test rig results on the separate components. The base line engine demonstrated performance is shown in Figure 5. Component development is continuing, and improvements will continue to be introduced in logical steps as the engine matures. These changes will be in addition to those which result from the higher temperature capabilities of ceramics and will be pursued in parallel with the ceramics program.

Field experience with base line engines has shown considerable scatter in fuel economy data when the vehicles are used by customer personnel in regular service, a result which is also evident for diesel-powered vehicles. If such variables as road speed, vehicle configuration, weight, tires, accessory loads, wind velocity, and ambient temperature are recorded, however, good correlation between measured and predicted fuel economy can be obtained. Controlled tests as well as routine operation are important parts of the field test program to permit the evaluation of fuel economy as well as reliability and durability. The responses of the engine and vehicle are another important aspect of field testing which has become an integral part of control system development. In general, the transients experienced during rapid changes from engine braking to maximum power are more severe in the vehicles than during dynamometer testing and are used to evaluate surge margin.

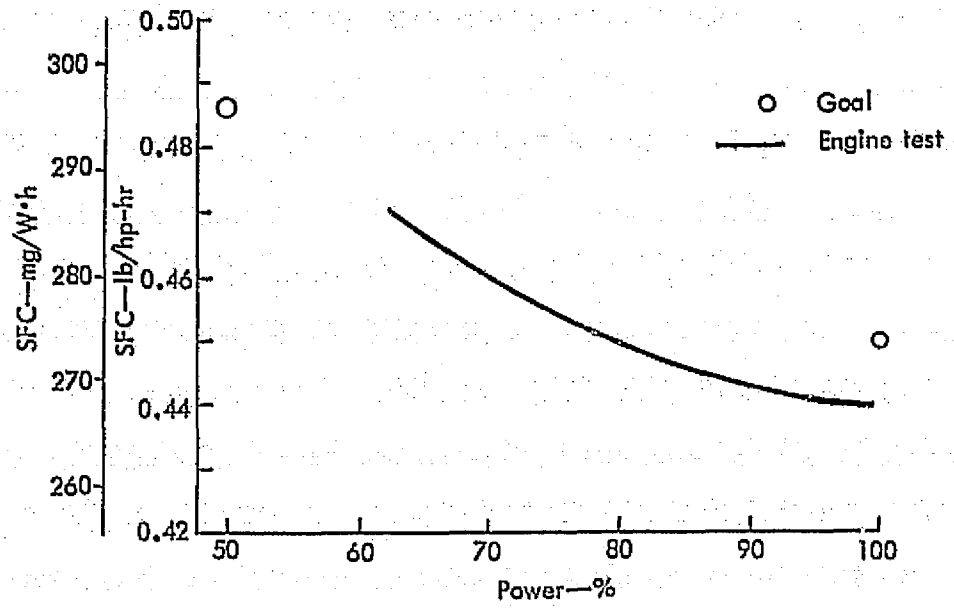

Figure 5. Base line engine performance

VEHICULAR APPLICATIONS

Two different vehicular applications were used in the study program for fuel economy and life cycle cost estimates: a highway tractor-trailer truck with a gross vehicle weight of 31,700 kg (70,000 lb), herein called a line haul truck, and a highway bus with a gross vehicle weight of 16,300 kg (36,000 lb). These vehicles are similar to those powered by base line engines during DDA's field test program. In addition, they are similar to production vehicles powered by diesel engines of the same power rating as the base line gas turbine. Listed in Table II are the pertinent vehicle characteristics for both application, frontal area, tire size, axle ratio, and type of transmission, that will be used in the study. Figure 6 shows the road load power requirements for both vehicles under level-road, steady-speed operating conditions. Shown also are the accessory load and drive line loss increments. The accessory loads are higher for the bus because of the heavy air conditioning and electrical system loads. Similarly, the bus data show higher drive line losses, primarily because a nine-speed manual transmission was selected for the truck as opposed to a four-speed automatic for the bus. The automatic is less efficient, primarily because of the oil pump and oil cooler losses. The automatic transmission was selected for the bus because it is becoming the standard configuration in the bus industry. The use of the nine-speed manual transmission in the truck data is typical of the heavy truck industry although nine forward speeds are not required with a free-turbine engine because of its inherent torque characteristics.

The scheduled maintenance during this period is summarized in Table III. These data are for a "mature" engine from which all of the early production and engineering deficiencies have been worked out. These data will be used in the life cycle cost analysis section of the study program.

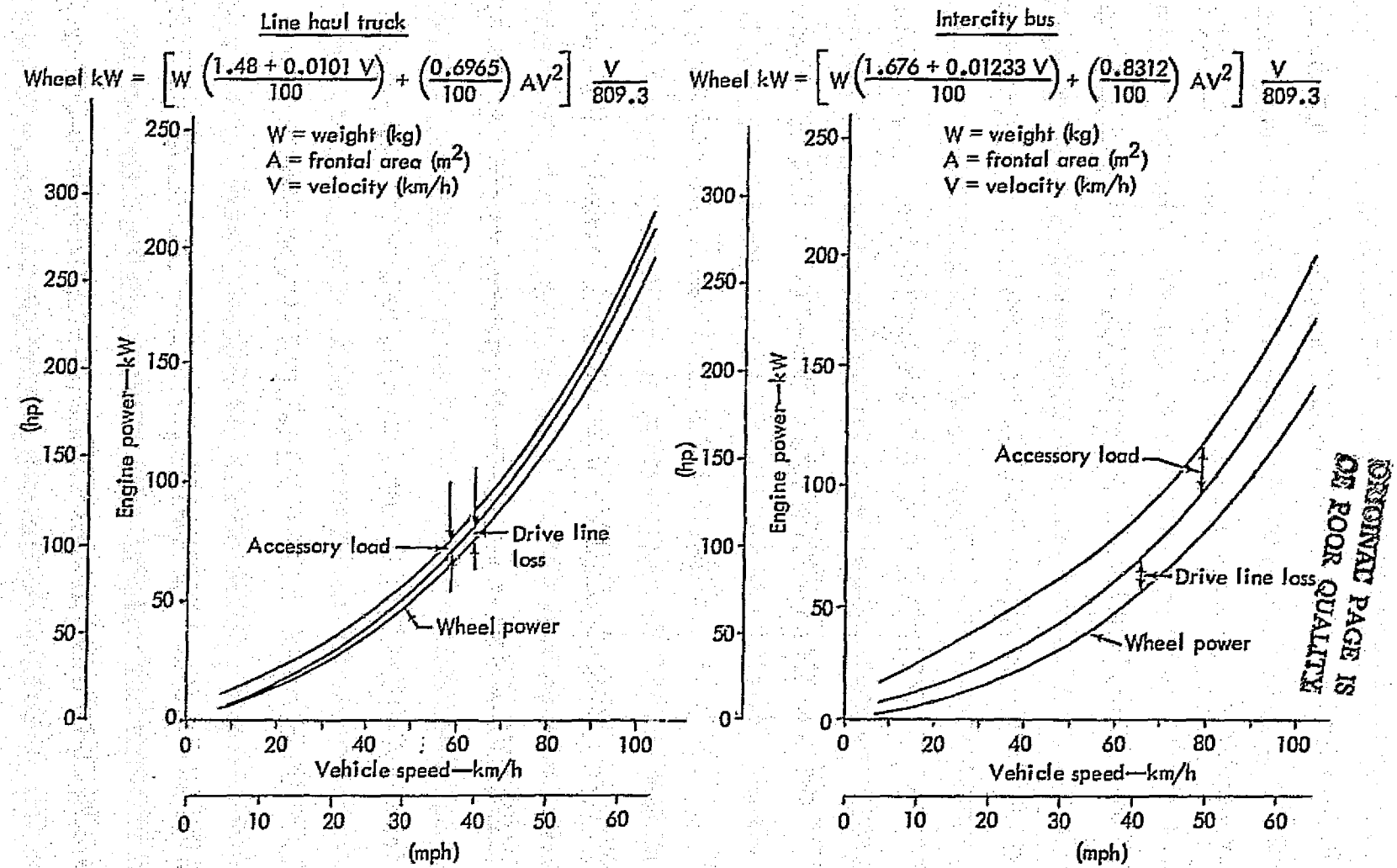

Figure 6. Road load power requirements.

TABLE II. VEHICLE CHARACTERISTICS

	Line haul truck	Intercity bus
Gross vehicle weight, kg (lb)	31,700 (70,000)	16,300 (36,000)
Frontal area, m^2 (ft^2)	9.48 (102)	6.9 (74)
Tire revolutions per kilometre (mile)	298 (480) (10 × 22 tires)	309 (497) (12.5 × 22.5 tires)
Axle ratio	4.886	4.330
Transmission	Fuller TR9509A (9-speed manual)	Allison HT 740 CT (4-speed automatic)

TABLE III. SCHEDULED MAINTENANCE, BASE-LINE ENGINE

Thousand kilometres (Thousand miles)	145 (90)	217 (135)	290 (180)	434 (270)	579 (360)	652 (405)	724 (450)	869 (540)
Change igniter	X		X	X	X		X	X
Clean air cleaner		X		X		X		X
Change oil		X		X		X		X
Change hot seal				X				X
Change fuel nozzle				X				X
Overhaul								X
Change turbine gas path components								
Regenerator components								
Other items as required								

METHOD OF ANALYSIS AND RESULTS

A study was conducted to identify means of achieving significant reduction in fuel consumption of the base line gas turbine engine. It was also of interest in this study to retain or improve the marketability of the engine for application in highway trucks and buses. Therefore, engine changes to achieve reduced fuel consumption cannot significantly increase engine purchase cost and vehicle operating cost or reduce engine reliability. The engine modifications must, in addition, provide environmentally acceptable emissions and noise characteristics.

BASE LINE PERFORMANCE SENSITIVITY

In the analysis, a performance sensitivity study of all the engine performance parameters affecting the base line engine was conducted. Input data for this program were determined from instrumented engine and component rig performance measurements along with some theoretical data. These parameters, their base line values, and their sensitivities, as determined by using a cycle matching computer program, are presented in Table IV. The parametric sensitivities shown represent the required change in the parameter basic value which is required to produce a 1% change in engine specific fuel consumption (sfc). The changes required in the component efficiencies for the compressor, combustor, gasifier turbine, power turbine, and regenerator are large compared with the potential technology improvements which can be expected in these components within the next few years. Therefore, the total engine improvement available from technology gain on these components must be only in the order of a few percent in engine sfc.

A similar review of the individual parametric pressure losses, leakages and cooling flows, power losses, and heat losses produces the same conclusion—i.e., no substantial gain is available from any single element.

The sensitivity to engine pressure ratio change shown indicates that a significant reduction in engine pressure ratio is required to produce a 1% benefit in engine sfc. The beneficial effect of reduced pressure ratio results from the sensitivity of engine sfc to regenerator leakage which is strongly pressure ratio dependent.

It is well known that gas turbine engines have shown significant reductions in sfc as engine cycle temperature is increased. The base line engine parametric sensitivity for temperature change is 12°C (22°F). In metal engines, air cooling of metal structures is necessarily required to achieve higher cycle temperatures. Engine performance penalties associated with this cooling utilization rapidly diminish the real fuel economy gains achievable with increasing engine temperature. However, with the view that ceramic materials can be evolved and applied structurally in engine components at temperatures up to approximately 1371°C (2500°F), then engine temperature change represents a truly significant potential for improvement in engine sfc.

TABLE IV. BASE-LINE ENGINE PERFORMANCE PARAMETERS AND SENSITIVITIES

Turbine inlet temperature = 1002°C (1835°F)

Specific fuel consumption (sfc) = 274 mg/W·h (0.45 lb/bhp-hr)

Parameter		Parameter value	Parameter sensitivity*
Component efficiencies, %			
Compressor		82.4	+0.66
Combustor		99.9	+1.00
Gasifier turbine		87.0	+0.92
Power turbine		89.7	+1.32
Regenerator effectiveness		89.8	+0.92
Pressure losses ($\Delta P/P$), %			
Inlet	1.50		
Regenerator air side	0.18		
Combustor and turbine inlet plenum	2.20		
Interturbine duct	0.69		
Turbine diffuser	2.75		
Regenerator gas side	3.06		
Exhaust	1.18		
		11.56	-0.80
Leakage and cooling flow**, %			
Turbine piston ring leakage	0.17		
Turbine rotor cooling	1.54		
		1.71	-0.62
Overboard leakage (splitlines and main bearing seals)		1.21	-0.74
Regenerator leakages, 5.12%			
Rim and crossarm cold seal and disk carryover		1.48	-0.70
Crossarm hot seal		1.96	-0.60
Rim hot seal		1.48	-1.47
Air side bypass		0.20	-1.66
Inner muff cooling		1.78	-1.66
Black and outer muff cooling		1.78	-1.66
Gasifier turbine nozzle cooling		1.00	-1.66
Power losses, kW (hp)			
Gasifier driven accessories (fuel pump, oil pump, regenerators)		6.71 (9.0)	-2.5 (-3.3)
Power turbine driven accessories		(0.0)	
Gearbox windage and friction		9.03 (12.11)	-2.3 (-3.0)
Gasifier main bearings		1.28 (1.72)	-2.5 (-3.3)
Power turbine main bearings		0.89 (1.19)	-2.3 (-3.0)
		17.91 (24.02)	
Heat losses, kW (Btu/min)			
Into lubrication system		5.25 (300)	-7.12 (-405)
External		10.54 (600)	-7.12 (-405)
Engine pressure ratio		4.0	-0.34
Engine cycle temperature, °C (°F)			
Turbine (rotor) inlet		1002 (1835)	12 (22)

* Sensitivities shown are the change in the parameter value to produce a 1.0% reduction in engine bsfc.

** Values are percent of supply point airflow

This study was conducted based on the extensive use of ceramic components in areas where cooled metal components would otherwise be required. It is acknowledged that the ceramics technology necessary to satisfy all of the engine requirements for all of the components studied is not available today. However, it is felt that the identification of the benefits of ceramics in specific applications can focus the rapidly evolving ceramics developments and technology to provide for availability within a few years.

IMPROVED ENGINE STUDY

A series of engines of increasing cycle temperature levels were conceived for this study. For these engines, the base line engine was used as a starting point; however, the number of ceramic components and component design improvements increased as the engine cycle temperature was increased. Specific engine temperature levels were selected which corresponded with the necessary replacement of the metal components because of life limiting thermal conditions. The first metal component that becomes life limited and must be replaced by a ceramic part is the gasifier nozzle and tip shroud. Without air cooling, it was shown to be life limited at the 954°C (1750°F) turbine inlet temperature level of an earlier version of the base line engine. All other metal components have acceptable lives up to 1038°C (1900°F) turbine inlet temperature. Above 1038°C (1900°F), ceramic blades must be used in the gasifier rotor.

The turbine inlet plenum and combustor walls are cooled by regenerated air. Figure 7 shows the effect of the engine rating temperature (at turbine inlet) on the regenerated air temperature for the design point (maximum power) and the maximum off-design operating conditions. This curve shows that above 1038°C (1900°F), the metal turbine inlet plenum becomes life limited and must be replaced by a ceramic part. Above 1200°C (2200°F), the combustor becomes limited and must be replaced by a ceramic part. These limiting points are shown as temperature ranges in Figure 7 because it is impossible to predict the hot spot temperature and its effect on a given component. Figure 8 shows the effect of engine rating temperature on power turbine inlet temperature and the associated life limiting points for the power turbine nozzle and rotor. A change to ceramic nozzles must be made above 1171°C (2140°F). The single-stage power turbine rotor is life limited at the same time and must be replaced by a two-stage design (metal rotors) operating at a lower speed to reduce the stress level. Above 1296°C (2365°F), ceramic blades must be used in the power turbine rotors.

Figure 9 shows the effect of engine rating temperature on turbine exhaust temperature along with the exhaust diffuser limiting temperature which occurs above 1135°C (2075°F). At this rating temperature, however, an improved metal part (better material) will suffice since the maximum off-design exhaust temperature of 982°C (1800°F) will be encountered for only a small percentage of the operating cycle. However, as the rating temperature is increased, the percentage of operating time spent at the 982°C (1800°F) turbine exhaust temperature condition will increase, thus requiring a change to a ceramic part.

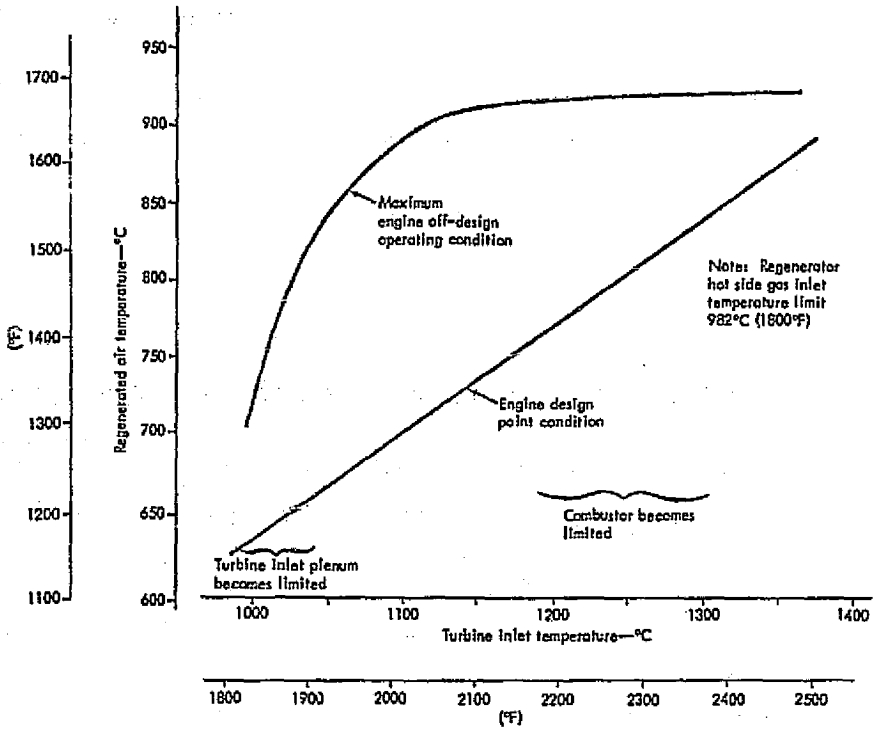

Figure 7. Effect of rating temperature on regenerated air temperature.

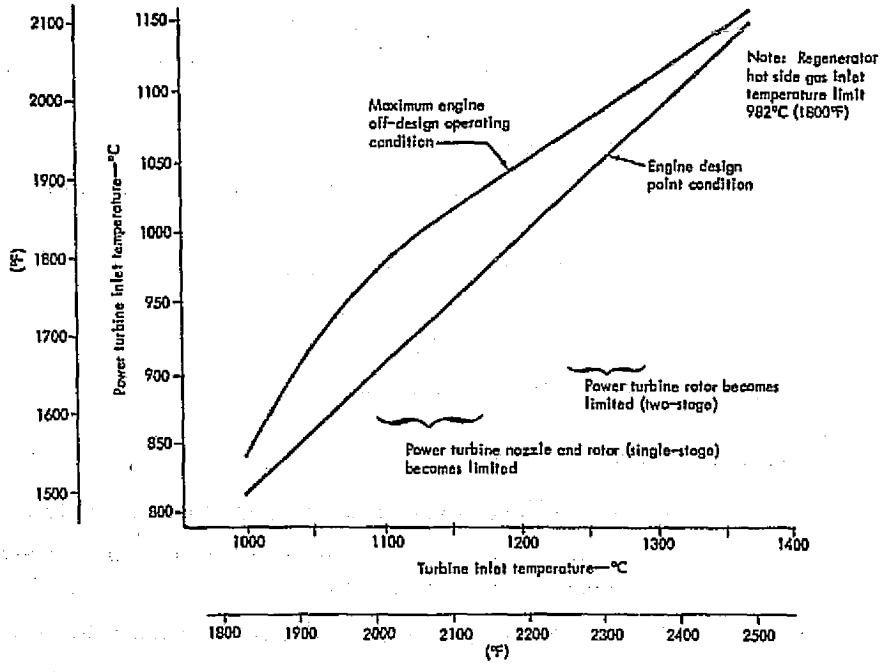

Figure 8. Effect of rating temperature on power turbine inlet temperature.

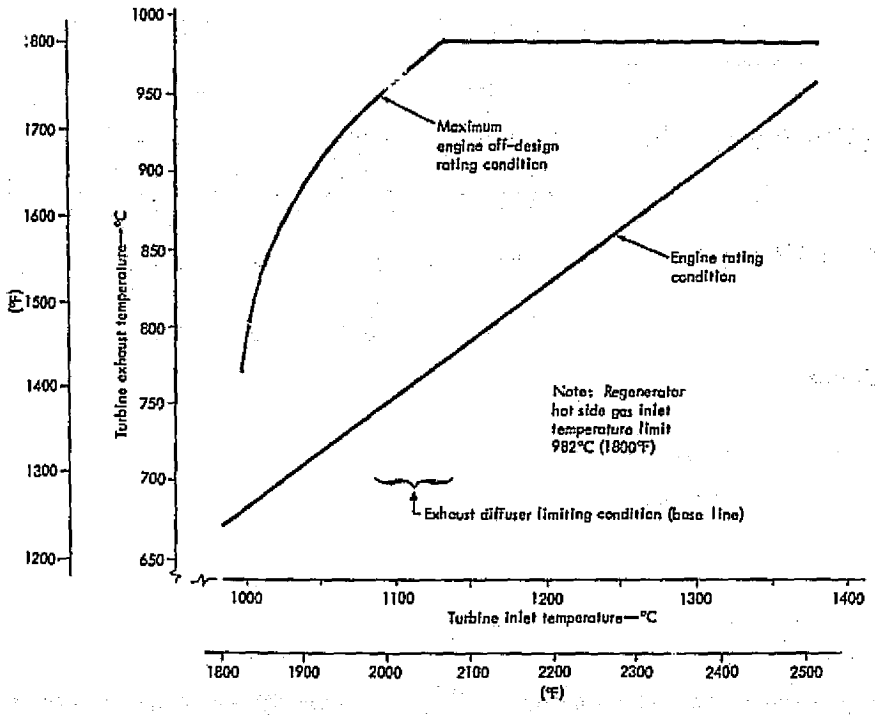

Figure 9. Effect of rating temperature on turbine exhaust temperature.

To flatten the part-load sfc curve, part-load temperature control is used in the base line engine which causes the regenerator hot side gas inlet temperature (turbine exhaust temperature) to increase as engine power is reduced. When the regenerator system temperature limit (704°C (1425°F) on the base line engine metal system) is reached, the engine control system starts reducing turbine inlet temperature to control the regenerator hot side temperature as power is further reduced. As the engine rating temperature is increased, the 704°C (1425°F) regenerator temperature limit will be encountered at ever increasing power levels. This raises the part-load low power sfc. Ceramic regenerator disks and seals will allow operation at higher part-load temperatures and are therefore included as an integral part of this analysis.

From the above knowledge of the life limiting temperatures of the various components, five engines were selected for the analysis. The cycle temperatures and ceramic component content of these study engines are presented in Table V with the base line engine included for reference. In addition, component aerodynamic improvements are incorporated in the compressor, gasifier and power turbines, and regenerator system for the 1204°C (2200°F) and 1371°C (2500°F) engine configurations as noted in Table V. The 1002°C (1835°F) study engine is identical with the base line engine except for the addition of ceramic regenerator disks and seals. Engine performance configurations were defined in which engine flows and losses were

TABLE V. CERAMIC COMPONENT CONTENT OF STUDY ENGINES

Engine Cycle Temperature °C (°F)	Base line 1002 (1835)	Study Engines 1002 (1835)	1038 (1900)	1132 (2070)	1204 (2200)	1371 (2500)
Regenerator Disk and Seals	M	C	C	C	C*	C*
Gasifier Nozzle and Tip Shroud	M	M	C	C	C*	C*
Plenum	M	M	M	C	C	C
Gasifier Rotor Blades	M	M	M	C	C*	C*
Single Stage Power Turbine	M	M	M	M		
Two Stage Power Turbine Nozzles					C*	C*
Two Stage Power Turbine Blades					M*	C*
Exhaust Diffuser	M	M	M	I	C	C
Combustor	M	M	M	M	M	C

M - metal component
I - improved metal component
C - ceramic component
* - aerodynamic improvements.

adjusted in concert with the temperature increases and component improvements to keep engine power constant at 224 kW (300 hp). These configurations were evolved in an iterative manner to facilitate the propor assignment of efficiencies and losses (flow, pressure, heat, and mechanical) as functions of the differing cycle conditions and mass flows. The effects of flow size on component efficiency were included. The final study engine performance definitions along with component characteristic maps were used to define engine off-design performance characteristics and maps. These engine performance maps were then used with the truck and coach vehicle characteristics and two typical vehicle routes to define vehicle road load fuel consumption characteristics and average route fuel consumption.

A mechanical configuration concept general arrangement layout was generated for each of the study performance configurations to provide a definition of the ceramic components and attendent engine changes. Volume production costs were obtained for all of the ceramic and metal parts unique to each of the engines.

Projection of engine reliability for the study engines proved to be impossible with any useful level of confidence. Therefore, the engines were assumed to have equal reliability independent of ceramic content or temperature level.

The engine cost, reliability assumption, and average vehicle mission fuel consumption data were utilized in a life cycle cost analysis performed for fleet operation of linehaul hi[illegible] trucks and highway buses.

Noise and exhaust emission evaluations of the study engine configurations were also performed.

Engine Performance

The performance configurations for the analysis study engines were evolved in an iterative manner to facilitate the proper assignment of efficiencies, flows, and losses as functions of differing engine cycle conditions and mass flows.

Since the line haul trucks and highway buses used in the analysis are both speed and weight limited, they are, therefore, maximum power limited for best fuel economy. It is then necessary to reduce engine airflow when increasing turbine inlet temperature in order to maintain a constant maximum rated power. Reducing the flow results in decreased compressor and turbine efficiencies, for a given technology level, as shown in Figure 10, because of running clearance and other aerodynamic effects. The two lines shown represent the current component technology and the advanced technology expected to be available within the time frame of this program. The airflow reduction also has a negative effect on regenerator system and overboard leakages since they tend to be constant actual mass flows at a given cycle pressure. Therefore, these leakages, expressed as a percentage of the cycle flow, will increase. Technology advances in the area of regenerator leakage are expected to be available within the time frame of this program and were included in the performance analysis.

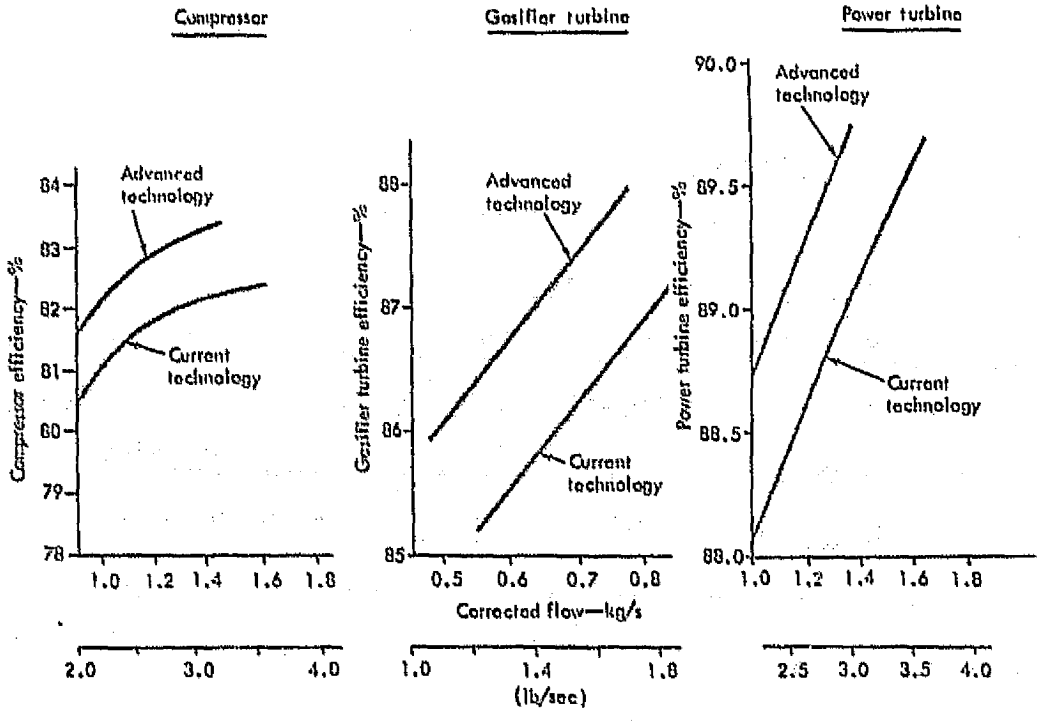

Figure 10. Effect of size on component efficiency.

A significant improvement in regenerator effectiveness will result from the airflow reduction, as shown in Figure 11. This improvement is a result of the increase in the heat transfer coefficient in passages. Lines are shown for the base line metal regenerators, the 0.008-mm (0.003 in.) thin-wall alumina silicate ceramic regenerators and an advanced technology ceramic regenerator. This curve also shows the significant benefits of using ceramic regenerators, derived primarily from the lower conduction losses with ceramic materials.

Another benefit of reducing the airflow is a reduction in cycle pressure losses for a given physical size engine (ducting, regenerator, etc). Some of this benefit will be lost, however, as gas temperatures increase. These effects are included in the performance analysis.

Table VI shows the cycle parameters at the maximum power rating [224 kW (300 hp)] of the base line and study engines determined at 29 °C (85 °F) and 152 m (500 ft) ambient conditions. Also shown is the maximum part load regenerator hot side temperature. The compressor, gasifier turbine, and power turbine performance characteristics for the 1038 °C (1900 °F) engine are the same as for the base line engine. The component characteristics for the thin-wall alumina silicate ceramic regenerator were also used in this engine. The base line compressor, gasifier turbine, and power turbine characteristics were flow scaled for size effects for the 1132 °C (2070 °F) engine. The thin-wall alumina silicate ceramic regenerator characteristics were adjusted for airflow effects.

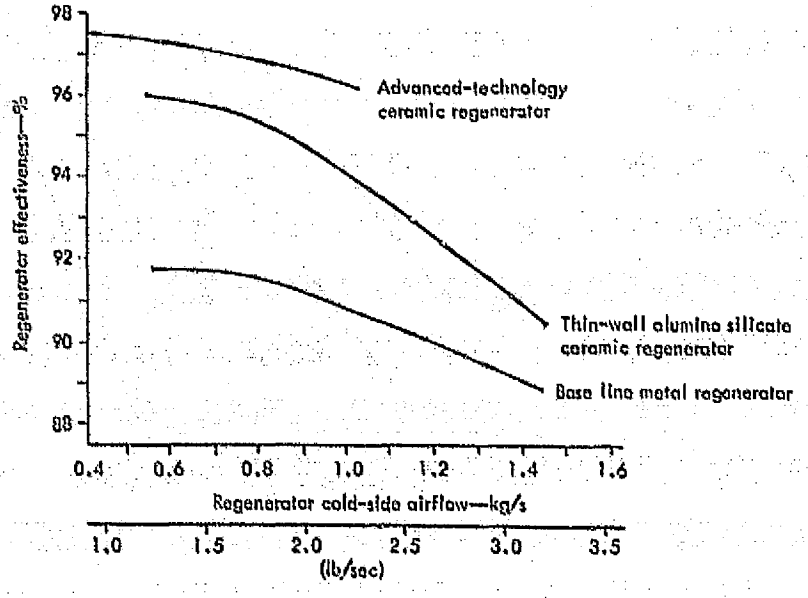

Figure 11. Effect of airflow on regenerator effectiveness.

TABLE VI. CYCLE PARAMETERS AT MAXIMUM POWER - STUDY ENGINES

Turbine Inlet Temperature	°C	(°F)	1032 (1235)*	1092 (1885)****	1038 (1900)	1132 (2070)	1204 (2200)***	1371 (2500)***
Max Power Regenerator Temp	°C	(°F)	632 (1278)	695 (1283)	722 (1331)	792 (1458)	839 (1543)	953 (1755)
Max Part Load Regenerator Temp	°C	(°F)	774 (1425)	856 (1591)	883 (1648)	979 (1795)	982 (1850)	982 (1800)
Compressor Pressure Ratio			4.09	4.09	4.09	4.09	4.09	4.09
Compressor Airflow	kg/s	(lb/sec)	1.56 (3.45)	1.56 (3.45)	1.56 (3.45)	1.38 (2.95)	1.15 (2.54)	0.962 (2.12)
Compressor Efficiency		%	82.4	82.4	82.4	82.2	82.0	82.2
Gasifier Turbine Efficiency		%	87.0	87.0	87.0	86.4	87.1	85.6
Power Turbine Efficiency		%	89.7	89.7	89.7	89.0	89.2	88.2
Burner Efficiency		%	97.6	97.6	97.6	97.6	97.8	97.8
Regenerator Effectiveness		%	88.9	90.5	90.6	93.3	96.2	97.0
Regenerator Leakage		%	4.92	4.92	4.92	5.75	5.25	6.29
Turbine Cooling (Wheels & Seals)		%	1.71	1.71	1.83	2.63	3.04	3.69
Stator & Turbine Shroud Cooling		%	3.56	3.56	3.56	3.56	3.56	3.56
Gasifier Vane Cooling		%	1.69	1.69	0.0	0.0	0.0	0.0
Overboard Leakage		%	1.21	1.21	1.21	1.42	1.29	1.54
Total Pressure Loss**		%	11.8	12.0	13.0	12.5	10.3	9.5
Mechanical Losses	W	(hp)	17.9 (24.0)	17.9 (24.0)	17.9 (24.0)	17.9 (24.0)	15.9 (21.4)	15.9 (21.4)
Shaft Power	W	(hp)	224 (300)	224 (300)	224 (300)	224 (300)	224 (300)	224 (300)
Specific Fuel Consumption	mg/W-h	(lb/hr-hr)	274 (0.45)	274 (0.45)	252 (0.425)	245 (0.404)	217 (0.357)	203 (0.344)
SFC Improvement Over Base Line		%		0	5.5	10.2	20.7	23.5

* Base-Line Engine
** Includes Inlet and Exit Loss
*** Technology Advancement
**** Ceramic Regenerators

For the 1204°C (2200°F) and 1371°C (2500°F) engines, the base line compressor performance characteristics were scaled to the advanced technology levels shown in Figure 10. A new, advanced-technology, single-stage gasifier turbine and a two-stage power turbine are introduced and scaled for flow size effects. Other technology advancements in these engines include:

- Reduced heat rejection (shown as burner efficiency)
- Reduced overboard leakage
- Reduced mechanical losses
- Increased regenerator effectiveness (per Figure 11) through increased frontal area, improved flow distribution, or advanced technology in matrix design

Maximum-power specific fuel consumption is shown in Figure 12 for the base line and the five study engines. The discontinuity in the sfc curve shown in Figure 12 between the 1132°C (2070°F) and the 1204°C (2200°F) engines is the result of the incorporation of advanced-technology components. Of the 11.6% sfc improvement between the two engines, 3.9 percentage points are attributable to the 72°C (130°F) increase in cycle temperature and the other 7.7 percentage points to the advanced-technology components. Figure 12 also shows a diminishing improvement in sfc as temperature is increased from 1204°C (2200°F) to 1371°C (2500°F). As noted in Table VI, the 1204°C (2200°F) engine shows a 20.7% sfc improvement over the base line engine while the 1371°C (2500°F) engine has an improvement of 23.5%.

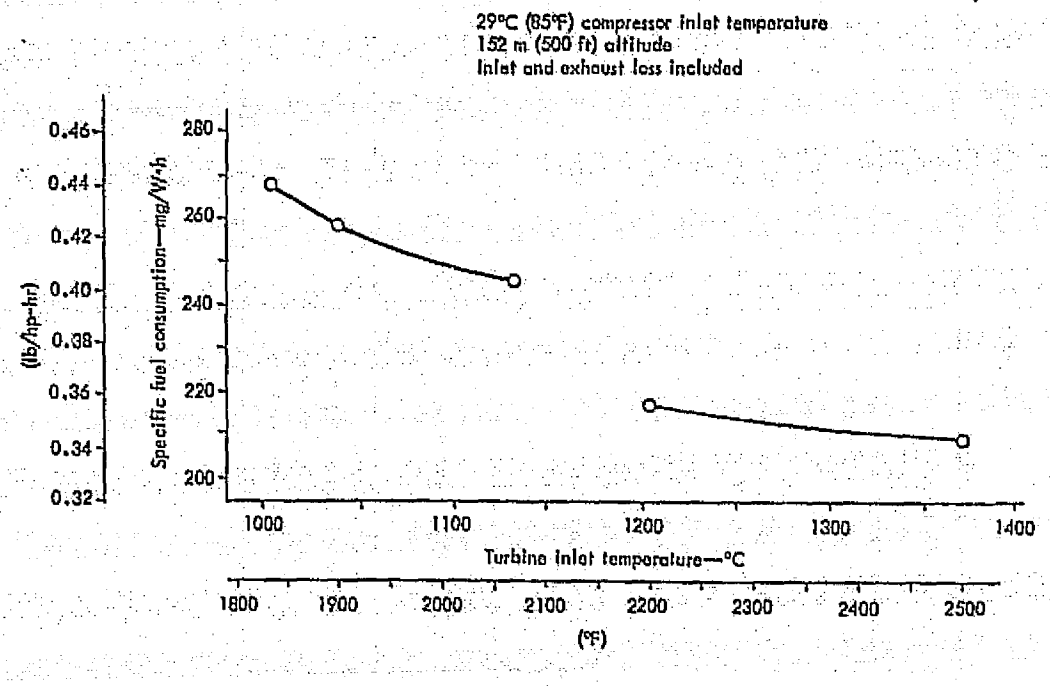

Figure 12. Max power sfc vs turbine inlet temperature.

The base line engine performance sensitivities indicated that the specific fuel consumption is improved as cycle pressure ratio is reduced. However, this trend is reversed at higher cycle temperatures, as shown in Figure 13, which is a plot of sfc versus pressure ratio for the 1371 °C (2500 °F) engine. For this engine, the optimum pressure ratio is 4.7. The benefit is small, however—less than a 1% improvement.

The part-power sfc of the engines is shown in Figure 14. The part-power sfc improvement of the 1002 °C (1835 °F) study engine (base line engine with ceramic regenerators) is caused by the increased hot-side temperature limit of the ceramic regenerator 982 °C (1800 °F) versus 774 °C (1425 °F) for the base line metal regenerator . Part-power sfc improvements similar to the maximum power improvements are sustained for the 1038, 1132, and 1204 °C (1900, 2070, and 2200 °F) engines. The part-power performance of the 1371 °C (2500 °F) engine approaches the 1204 °C (2200 °F) performance levels at approximately 50% power because of the reduction of turbine inlet temperature required to maintain the 982 °C (1800 °F) temperature limit at the regenerator hot-side inlet.

Full engine performance maps showing fuel flow over the full power range at various output shaft speeds for the base line and study engines are shown in Appendix B, as are performance maps for the advanced-technology gasifier and power turbine used in this analysis. A station-by-station tabulation of the cycle parameters at 100% and 50% power and idle for the base line and study engines is also given in the appendix.

In summary, significant sfc improvements (20% or better) over the full usable engine power range are possible by increases in turbine inlet temperature, through the use of ceramic components, and by improved efficiencies through the use of advanced technology components.

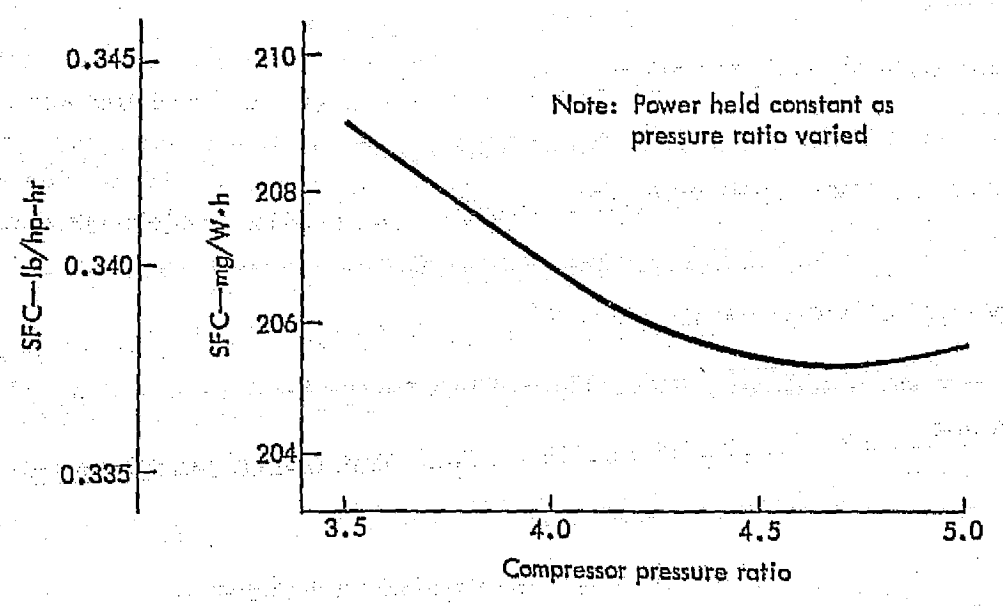

Figure 13. Effect of compressor pressure ratio on sfc—1371°C (2500°F) engine.

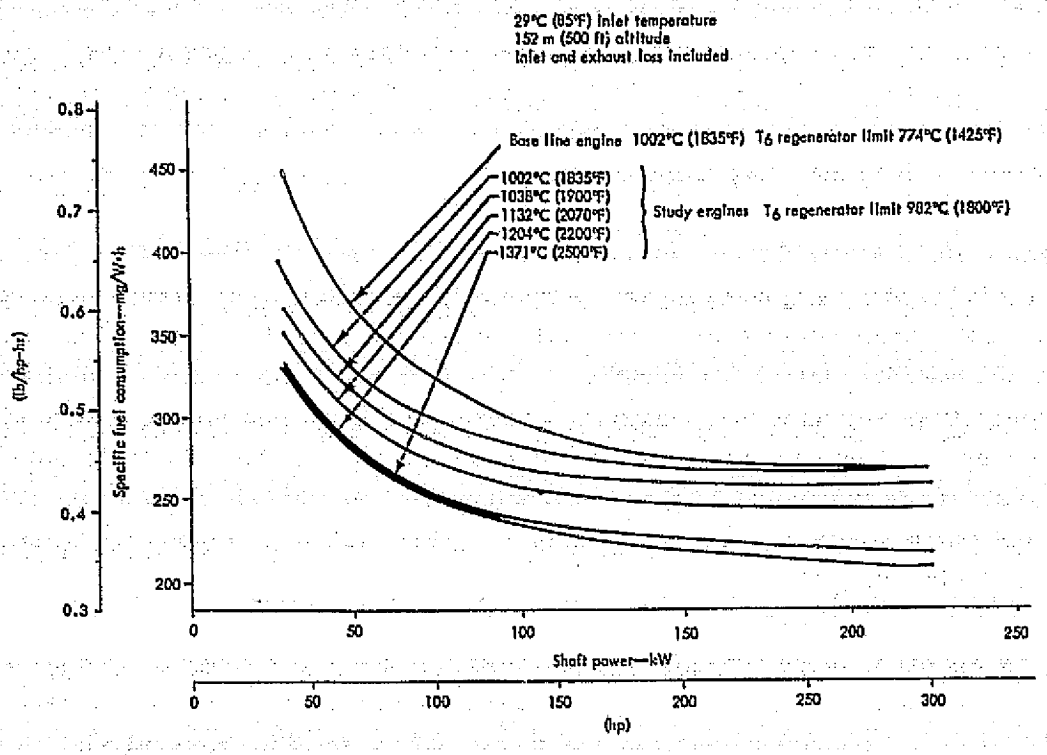

Figure 14. SFC vs power.

However, only three additional percentage points of sfc improvement are achieved by increasing the temperature from 1204°C (2200°F) to 1371°C (2500°F), and this improvement is not sustained at part power because of the 982°C (1800°F) regenerator temperature limit.

Vehicle Simulation

Vehicle fuel consumption was determined for the line haul truck and intercity bus, using the base line and study engine performance estimates. The vehicle characteristics and road load power requirements are discussed in the "Base Line Engine" section of this report (ref Table II and Figure 6). A vehicle/route simulation computer program was used to predict vehicle performance. Input to the program includes vehicle characteristics (vehicle aerodynamics, engine, transmission, and driveline) and the route profile versus time (starts/stops, speed limits, and grades). Two routes were selected:

- Chicago to Boston (Interstates 80 and 90)—1626.2 km (1010.5 miles) rolling terrain, eight starts/stops.
- Los Angeles to Salt Lake City (1962 Trailways Bus Route)—1176 km (731 miles) mountainous terrain, 89 starts/stops.

A maximum speed limit of 96 km/h (60 mph) was imposed on each route.

Tables VII and VIII show tabulated percent time at engine speed and net torque for each vehicle and route. These distributions reflect the differing power demands and operating requirements of the vehicles.

Average predicted fuel consumption is shown in Table IX and is plotted against turbine inlet temperature in Figure 15. As expected, these data show a significant improvement in vehicle fuel economy as the cycle temperature and the aerodynamic component technology level is increased.

The effect of axle ratio was investigated (Table X), using the 1371°C (2500°F) study engine for both the truck and bus vehicles. The effects were found to be negligible with the base line ratios selected being optimum.

Curves showing the level road fuel consumption against vehicle speed along with the average fuel consumption and route speed are shown in Appendix B for both vehicles and routes for using the base line and the five study engines.

Figure 16 shows the total fuel savings, compared with the base line engine, for both vehicles for the average route based on an 805 000-km (500,000-mile) engine life.

Gas turbine engines are sensitive to ambient inlet conditions, and the data presented herein are for 29°C (85°F) and 152-m (500 ft) altitude (SAE rating conditions). The following data are shown to illustrate this sensitivity to inlet conditions and to quantify the realistic improvement the turbine offers relative to data shown in this study. These data at 16°C (60°F), sea level inlet conditions were not used to impact recommendations or conclusions from the study program. Figure 17 shows that lower temperatures produce lower specific fuel consumption values. Altitude has little effect on sfc. The increase in sfc below 4°C (40°F) is caused by the reduction in turbine inlet temperature needed to avoid compressor surge. The average ambient temperature in the United States is 13°C (56°F) (Ref 1). At this condition, sfc is reduced approximately 5% from the SAE rating conditions.

Vehicle performance for the base line and study engine configurations calculated at 16°C (60°F), sea level, ambient conditions is presented in Table XI and Figure 18 for comparison with the 29°C (85°F), 152-m (500-ft) inlet condition. Table XII shows a percentage improvement for the line haul truck and intercity bus installations.

Study Engine Configuration

General arrangement layout drawings were made to identify the ceramic components and additional engine changes (not requiring ceramic components) associated with each of the analysis study engines [1038°C (1900°F), 1132°C (2070°F), 1204°C (2200°F), 1371°C (2500°F) cycle temperatures]. The unique parts for each of these engines were defined in sufficient detail to evaluate

TABLE VII. PERCENT TIME AT ENGINE SPEED AND TORQUE—LINE HAUL TRUCK

ENGINE SPEED (RPM)	600	800	1000	1200	1400	1600	1800	2000	2200	2400	2600	2800
ENGINE TORQUE N-m (lb ft)	LOS ANGELES TO SALT LAKE CITY											
1356 (1000)												
1085 (800)			0.06	0.02	0.02	0.02	0.02	0.02	1.89	0.09		
813 (600)									6.84	18.08	27.52	8.64	2.14
542 (400)									0.02	0.34	8.52		0.50
271 (200)									0.03	3.79	7.50	0.05	0.47
0		0.14	0.04	0.06	0.04	0.05	0.04	0.02	0.07	2.31	4.82	0.43	0.38
-271 (-200)								0.04	0.08	0.32	2.02	0.28	0.24
-542 (-400)								<0.01	0.38	0.79	0.65	0.17	0.03
	CHICAGO TO BOSTON											
1356 (1000)												
1085 (800)			<0.01		<0.01				3.53	0.29			
813 (600)									0.33	15.79	44.76	1.76	0.64
542 (400)										0.89	21.61		
271 (200)										0.59	5.14		
0		0.02	0.01	0.01	0.01	0.01	0.01	0.01	0.08	0.13	2.44	0.02	
-271 (-200)								<0.01	0.01	0.01	0.71		
-542 (-400)									0.10	0.11	0.98		

TABLE VIII. PERCENT TIME AT ENGINE SPEED AND TORQUE—INTERCITY BUS

ENGINE SPEED (RPM)	600	800	1000	1200	1400	1600	1800	2000	2200	2400	2600	2800
ENGINE TORQUE N-m (lb ft)	LOS ANGELES TO SALT LAKE CITY											
1356 (1000)		0.01	0.02	<0.01								
1085 (800)	<0.01	0.23	0.05	0.08	0.09	0.32	0.33	<0.01				
813 (600)						0.18	2.86	11.78	14.68	6.58	3.17	0.10
542 (400)					0.21	0.33	0.40	0.42	23.86	0.49	2.55	2.06
271 (200)	0.01		0.03	0.06	0.26	2.90	0.64	2.06	9.38		1.40	
0	0.68	0.57	0.48	0.19	0.50	1.12	0.30	0.48	3.36	0.20	0.71	0.07
- 271 (-200)							0.26	0.14	1.31	0.48	0.16	<0.01
-542 (-400)							0.58	0.31	0.49	<0.01	0.06	<0.01
	CHICAGO TO BOSTON											
1356 (1000)		<0.01	<0.01									
1085 (800)		0.02		<0.01	<0.01	0.02	0.77					
813 (600)							0.38	5.91	26.51	1.15	0.95	0.05
542 (400)								1.58	52.93		0.02	0.19
271 (200)						0.03	0.03	0.56	6.35			
0	0.09	0.14	0.15	0.07	0.06	0.04	0.01	<0.01	1.94			
-271 (-200)												
-542 (-400)							0.03	0.02				

TABLE IX. VEHICLE FUEL CONSUMPTION

Vehicle and Engine	Fuel Consumption—km/ℓ (mpg)			
	Los Angeles to Salt Lake City	Chicago to Boston	Average Route	Average Improvement
Line Haul Truck—4.886 Axle Ratio				
Base Line 1002°C (1835°F) Engine	1.47 (3.45)	1.64 (3.85)	1.55 (3.65)	---
Base Line Engine With Ceramic Regenerators	1.53 (3.60)	1.68 (3.95)	1.57 (3.69)	1.1%
1038°C (1900°F) Engine	1.59 (3.75)	1.74 (4.10)	1.67 (3.94)	7.9%
1132°C (2070°F) Engine	1.68 (3.95)	1.83 (4.30)	1.76 (4.15)	13.7%
1204°C (2200°F) Engine	1.91 (4.50)	2.06 (4.85)	2.00 (4.70)	28.8%
1371°C (2500°F) Engine	1.98 (4.65)	2.12 (5.00)	2.05 (4.82)	32.0%
Intercity Bus—4.330 Axle Ratio				
Base Line 1002°C (1835°F) Engine	1.64 (3.85)	1.76 (4.15)	1.70 (4.01)	---
Base Line Engine With Ceramic Regenerators	1.70 (4.00)	1.78 (4.20)	1.75 (4.12)	2.7%
1038°C (1900°F) Engine	1.78 (4.20)	1.87 (4.40)	1.82 (4.28)	6.7%
1132°C (2070°F) Engine	1.85 (4.35)	1.95 (4.60)	1.91 (4.49)	12.0%
1204°C (2200°F) Engine	2.12 (5.00)	2.19 (5.15)	2.16 (5.09)	26.9%
1371°C (2500°F) Engine	2.17 (5.10)	2.23 (5.25)	2.20 (5.17)	28.9%

NOTE: SAE STD Day Engine Performance

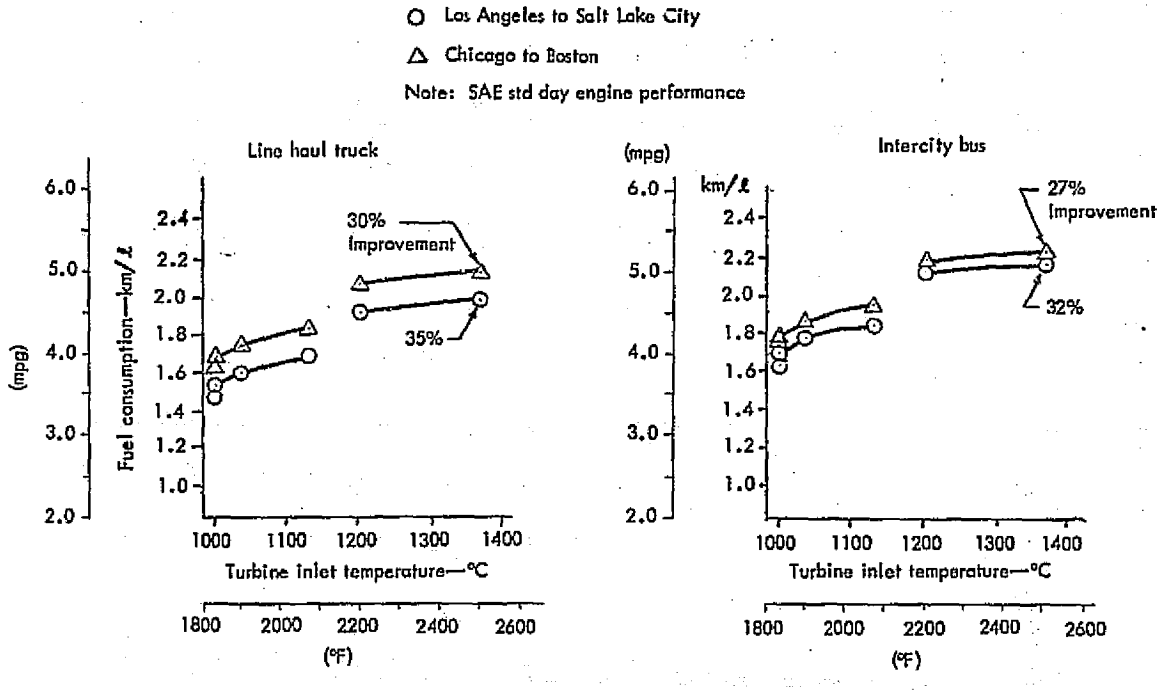

Figure 15. Improvement in fuel economy with increasing temperature.

TABLE X. EFFECT OF AXLE RATIO ON FUEL CONSUMPTION
[1371 °C (2500°F) Study Engine]

Vehicle	Axle Ratio	Ratio %Δ	Los Angeles to Salt Lake City		Chicago to Boston	
			Average Speed km/h (mph)	Fuel Consumption km/ℓ (mpg)	Average Speed km/h (mph)	Fuel Consumption km/ℓ (mpg)
Line Haul Truck	4.625	-5.3	74 (46)	1.95 (4.59)	93 (53)	2.10 (4.94)
	*4.886	0.0	74 (46)	1.98 (4.65)	93 (58)	2.12 (5.00)
	5.290	+8.3	74 (46)	1.95 (4.60)	93 (58)	2.11 (4.97)
	5.570	+14.0	74 (46)	1.93 (4.54)	93 (58)	2.09 (4.91)
Intercity Bus	4.110	-5.1	80 (50)	2.13 (5.02)	95 (59)	2.23 (5.24)
	*4.330	0.0	80 (50)	2.17 (5.10)	95 (59)	2.23 (5.25)
	4.625	+6.8	80 (50)	2.15 (5.06)	95 (59)	2.23 (5.25)
	4.880	+12.7	80 (50)	2.15 (5.05)	95 (59)	2.22 (5.23)

*This Axle Ratio Was Used As A Base Line.

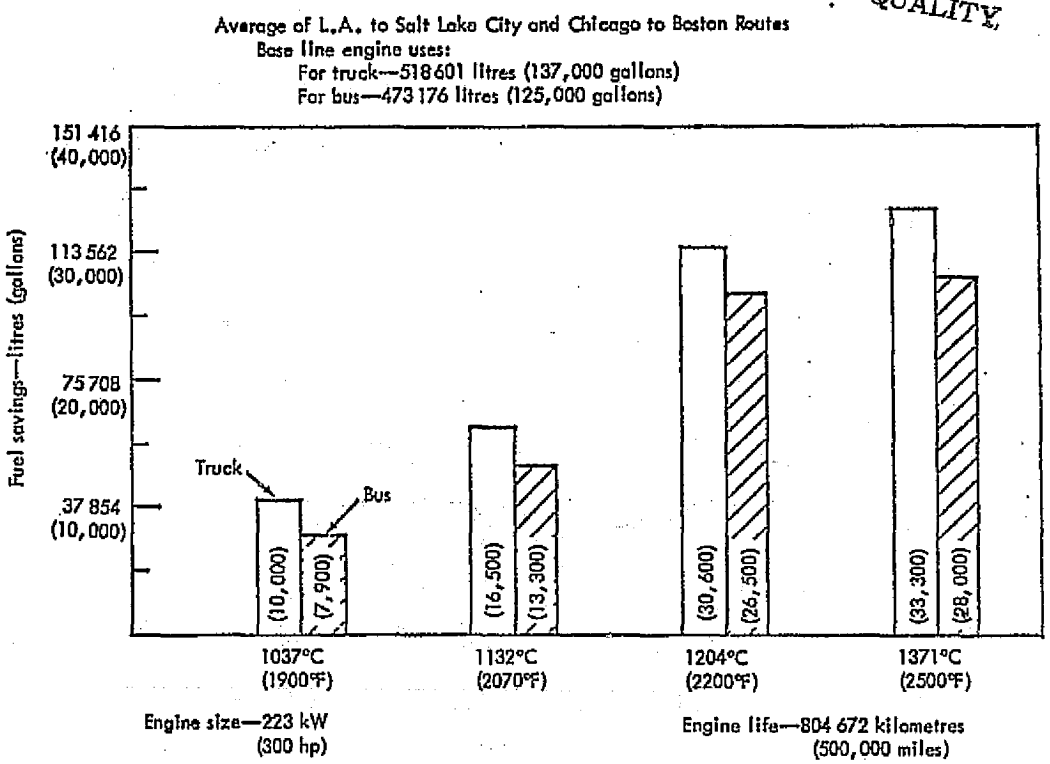

Figure 16. Fuel savings of study engines.

TABLE XI. VEHICLE FUEL CONSUMPTION AT 16°C (60°F) AMBIENT

Vehicle and Engine	FUEL CONSUMPTION—km/ℓ (mpg)		
	Los Angeles to Salt Lake City	Chicago to Boston	Composite
Line Haul Truck			
Base Line 1002°C (1835°F) Engine	1.61 (3.78)	1.69 (3.97)	1.65 (3.89)
Base Line Engine & Ceramic Regenerators	1.63 (3.84)	1.74 (4.09)	1.69 (3.98)
1038°C (1900°F) Engine	1.71 (4.02)	1.80 (4.23)	1.76 (4.14)
1132°C (2070°F) Engine	1.82 (4.28)	1.89 (4.45)	1.86 (4.38)
1204°C (2200°F) Engine	1.99 (4.67)	2.13 (5.01)	2.07 (4.86)
1371°C (2500°F) Engine	2.03 (4.77)	2.16 (5.08)	2.10 (4.95)
Intercity Bus			
Base Line 1002°C (1835°F) Engine	1.69 (3.98)	1.81 (4.26)	1.76 (4.14)
Base Line Engine & Ceramic Regenerators	1.77 (4.17)	1.86 (4.37)	1.82 (4.28)
1038°C (1900°F) Engine	1.83 (4.30)	1.92 (4.52)	1.88 (4.42)
1132°C (2070°F) Engine	1.90 (4.48)	2.02 (4.75)	1.97 (4.63)
1204°C (2200°F) Engine	2.18 (5.13)	2.24 (5.28)	2.22 (5.22)
1371°C (2500°F) Engine	2.19 (5.16)	2.27 (5.33)	2.24 (5.26)

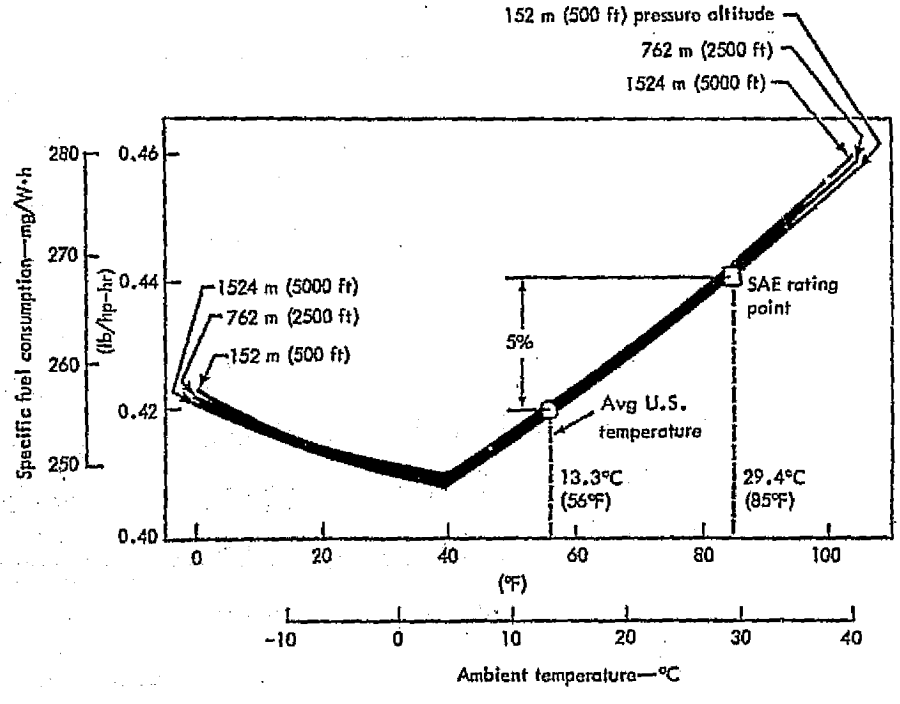

Figure 17. Effects of ambient conditions on base line engine sfc.

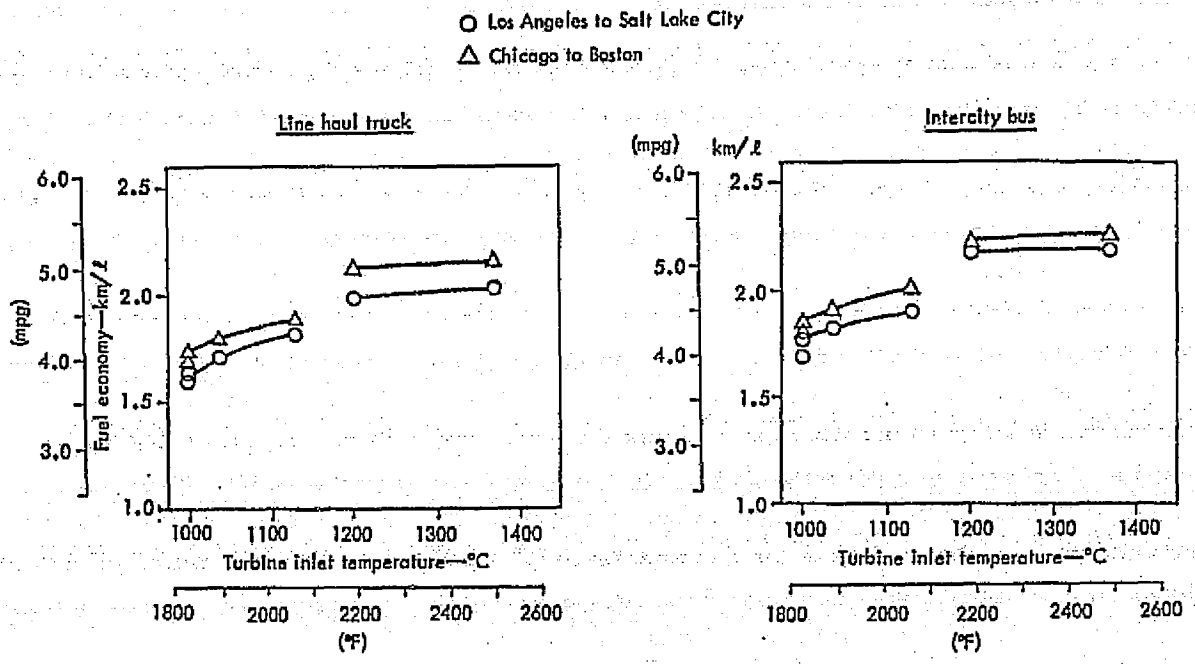

Figure 18. Improvement in fuel economy with temperature at 16°C (60°F) ambient.

TABLE XII. AMBIENT EFFECT ON VEHICLE FUEL CONSUMPTION
[SAE to 16°C (60°F) ambient inlet comparison]
Composite Route Simulation

Engine	% Improvement	
	Truck	Bus
Base Line 1002°C (1835°F) Engine	6.4%	3.5%
Base Line Engine With Ceramic Regenerators	7.6%	4.0%
1038°C (1900°F) Engine	5.4%	3.3%
1132°C (2070°F) Engine	5.7%	3.1%
1204°C (2200°F) Engine	3.5%	2.8%
1371°C (2500°F) Engine	2.4%	1.8%

probable volume cost and development effects. Parts lists were then prepared to identify the specific changes which each engine would require from the base line engine. Additional descriptions of the engines, components, and parts are given in the "Program Plan" and "Technical Approach" sections.

1038°C (1900°F) Engine Configuration

The general arrangement layout and part numbers for the turbine for the 1038°C (1900°F) engine are shown in Figure 19. The concept adopted for the gasifier turbine nozzle uses individual ceramic vanes (-1) with integral end platforms which form the flow path inner and outer walls. The individual vanes are located between a continuous ceramic ring (-3) on the inner diameter and the continuous ceramic tip shroud ring (-2) on the outer diameter. The approach attempts to diminish the individual ceramic part size, complexity, and thermally introduced stress. This assembly of vanes and rings is centered from a tang/slot pattern which centers the tip shroud indirectly from the engine block. Each of the individual vanes is keyed at the leading edge of the inner and outer platforms to an embossed sheet metal plate which provides the proper circumferential spacing to the vanes and reacts the vane tangential aerodynamic loads. The vane axial aerodynamic and pressure loads are reacted from the vanes to the ceramic inner and outer continuous rings. The rings contact a continuous surface on metal parts (-13 and -5) to accommodate both the load reaction and and sealing. The metal part (-13) which effects this axial location function at the vane outer platform can be shimmed (-15) to ensure that the proper vane inner and outer platform axial relationship is maintained.

The gasifier turbine tip shroud (-2) defined in Figure 19 is a complete ring of relatively simple section shape. It incorporates slots to engage on the centering tangs of the supporting metal parts (-13) and a low density ceramic on the bore to provide an abradable material for rubbing the gasifier turbine rotor blades.

This engine incorporates ceramic thin wall regenerator disks and utilizes an engine block in which the cross-arm members are flat rather than contoured as is required to accommodate the thermally induced deflection of the metal regenerator.

1132°C (2070°F) Engine Configuration

The burner and turbine general arrangement for the 1132°C (2070°F) engine is presented in Figure 20. This engine incorporates the same ceramic gasifier turbine nozzle and tip shroud concept described previously but also has a ceramic turbine inlet plenum and ceramic gasifier turbine rotor blades. The ceramic plenum is configured in three parts (-16, -17, -18) to facilitate withdrawal of a part or patterns from casting or molding tooling and also to diminish the part-induced thermal stresses. The three parts consist of a forward element (-17), a rear element (-18), and the center hub (-16). The parting surfaces between these elements are defined as simple planes to facilitate finishing to a flat condition. The contact loads induced between the plenum elements by the engine combustor pressure drop are supplemented by sheet metal details which clamp the elements together. The plenum is loaded into contact with the gasifier nozzle outer platform by a metallic wave spring (-22) provided at the plenum hub. A ceramic seal ring (-23) at the plenum outlet diameter prevents bypass leakage of regenerated air past the combustor. A similar sealing function is provided at the hub by metal details (-27, -26). The

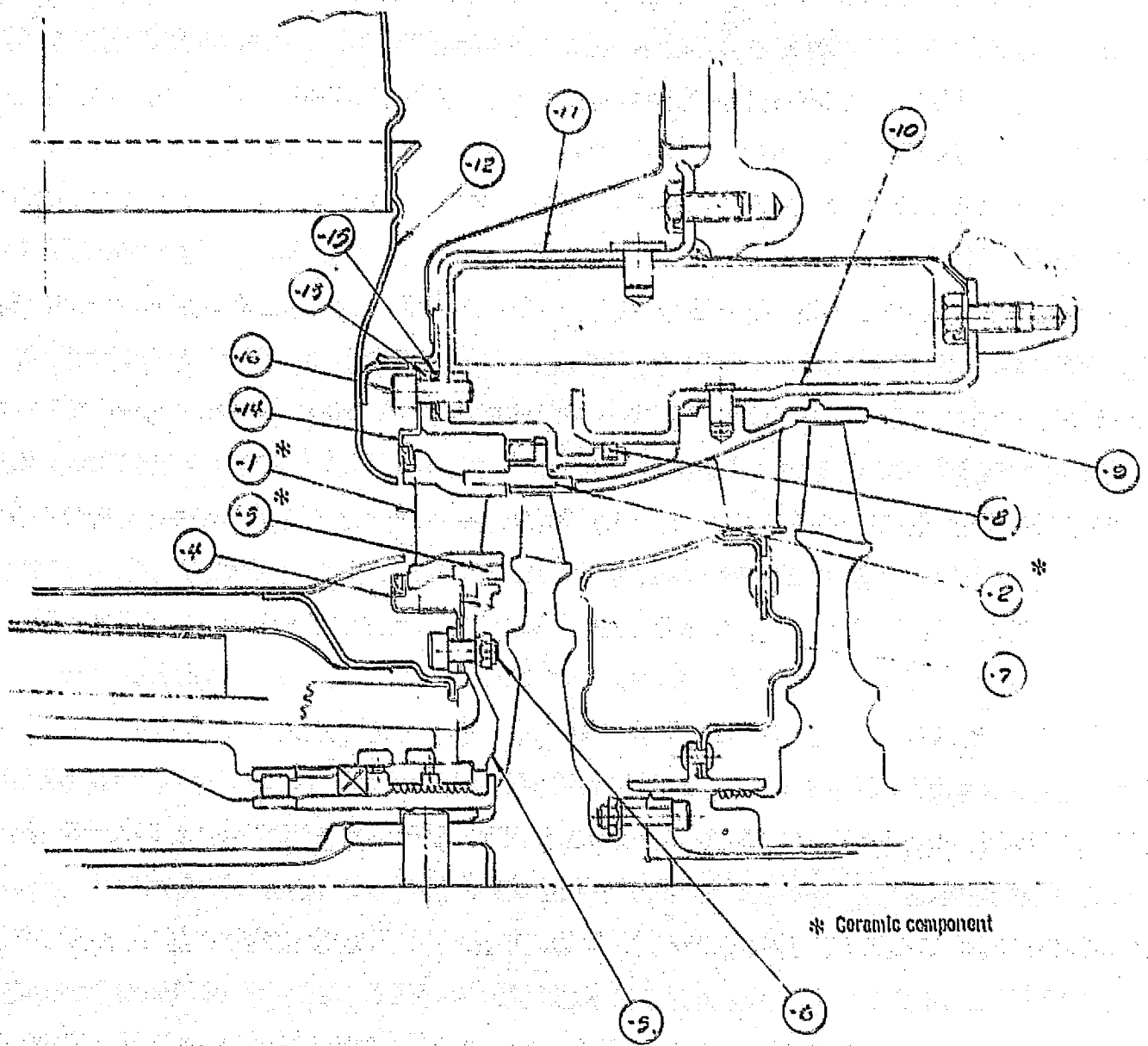

Figure 19. Turbine general arrangement for 1038°C (1900°F) study engine.

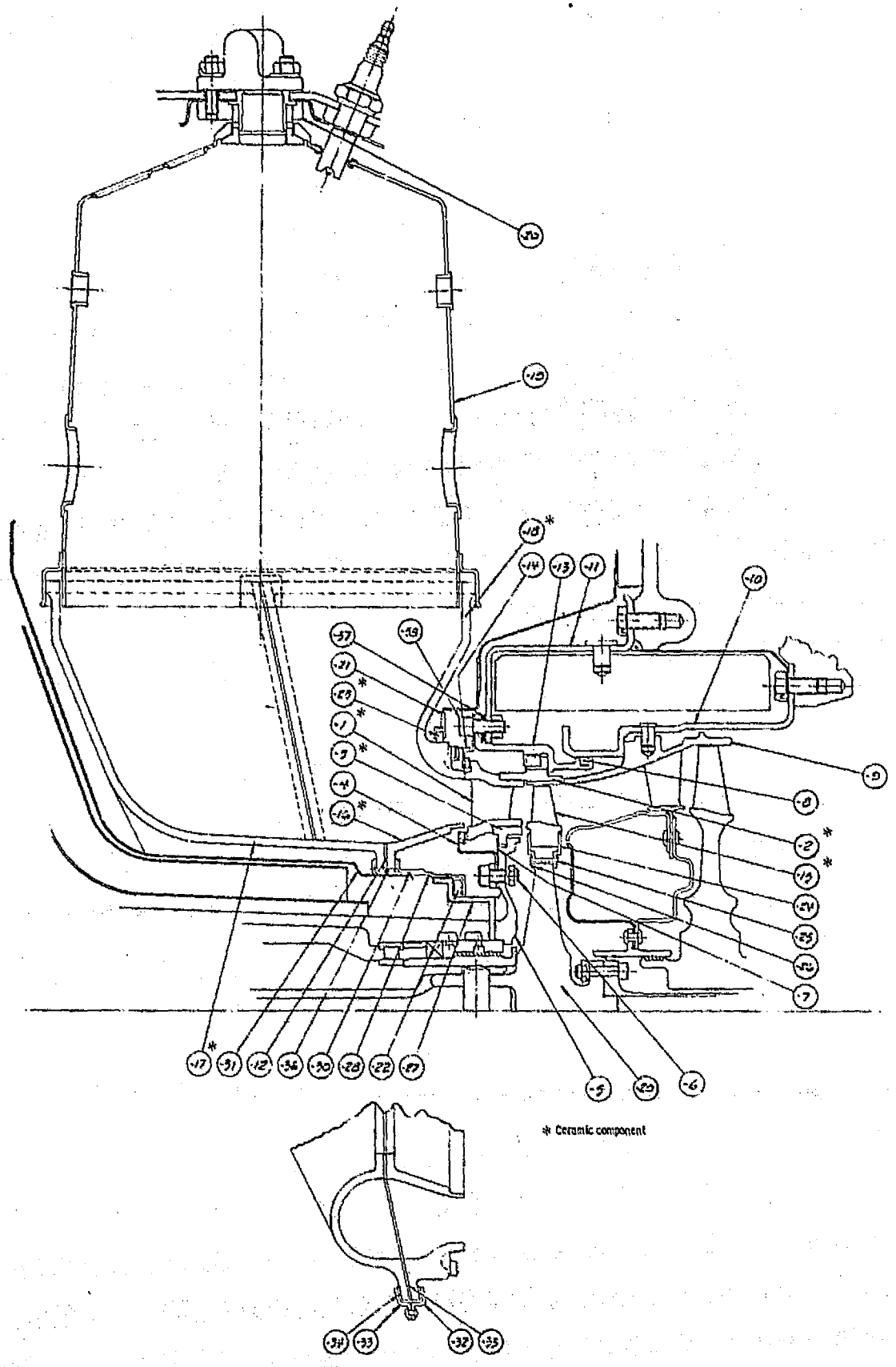

Figure 20. Combustor and turbine general arrangement for 1132°C (2070°F) study engine.

ceramic turbine blade (-15) uses a relatively conventional platform and stalk configuration with a single lug dovetail. The stalk and dovetail are aligned with the airfoil to minimize induced bending from centrifugal effects. The turbine blades are retained axially in the wheel by segmented ring elements at both the forward (-26) and rear (-24) wheel faces. These elements are retained to the wheel by a coned pilot surface and by rivets (-25). The segmented ring elements also seal the cavities between blades to prevent flow leakage under the blade platforms.

Several turbine section metal parts are reconfigured to facilitate location or sealing of the ceramic components.

The combustor liner mounting at the fuel nozzle is modified to provide flexibility which permits the combustion liner to engage the plenum without significant loads from misalignment.

The combustor outlet gas conditions for this engine exceed the engine thermocouple capability; therefore, the engine control logic is modified to schedule fuel flow using temperatures sensed at the regenerated exit (combustor inlet) and turbine outlet stations.

The engine includes the aforementioned ceramic thin-wall regenerator disks with associated seals and block contour changes.

1204°C (2200°F) Engine Configuration

The burner and turbine general arrangement for the 1204°C (2200°F) engine is shown in Figure 21. This engine incorporates a new turbine flow path of reduced diameter to reflect the engine mass flow reduction to maintain power output constant. In addition, the power turbine is changed to a two-stage configuration to increase efficiency and reduce the blade stress levels by operation at reduced power turbine rotor speed. The two-stage power turbine also eliminates the inter-turbine duct and the associated pressure loss. A metal prechamber combustor is shown as a part of this engine configuration. Efficiency increases are also specified for the compressor and gasifier turbines.

The general configuration and construction of the ceramic gasifier turbine nozzle, gasifier turbine tip shroud, turbine inlet plenum, and gasifier turbine rotor blades are the same as those in the 1204°C (2070°F) engine previously discussed.

This engine incorporates ceramic nozzles in both power turbine stages. Individual vanes (-63, -64 and -60, -61) with integral hub and tip platforms are used in these stages in a manner similar to the gasifier vanes. The vane hub platforms engage an annular channel in a continuous ceramic ring (-38 and -48) which forms the inner band and effects the stator-to-rotor seal. The inner ring incorporates a low-density coating on the inner diameter to reduce abrasion on the rotor seal knives. Six of the vanes (-64 and -61) in each of the stages incorporate a

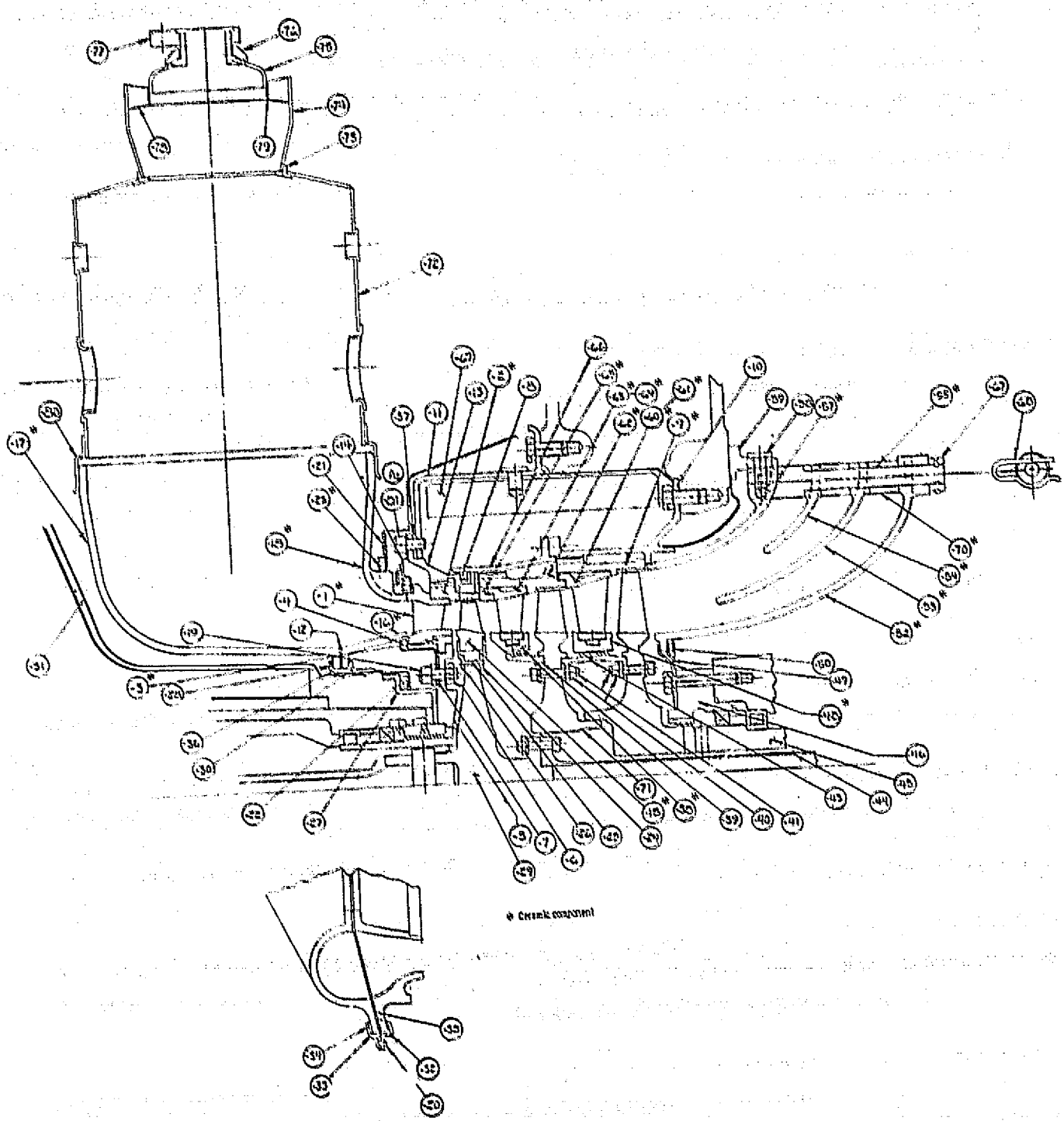

Figure 21. Combustor and turbine general arrangement for 1204°C (2200°F) study engine.

cylindrical projection at the hub end which engages a hole in the inner ring to provide a ring antirotation feature. The axial fit of the vane hub platforms into the inner ring annular channel controls the twist displacement of the vanes about their axis. The vane tip platforms are trapped at assembly between continuous ceramic rings (-65 and -62, -62 and -9).

A tang on each of the vane outer platforms engages slots in the outer continuous rings to provide circumferential spacing and react the vane row aerodynamic torque. The radial dimensional fit of the vanes, outer rings, and inner rings controls the vane radial position and the relative axial position of the inner ring to the outer rings. Circumferentially continuous surfaces are provided on the outer rings to react the vane aerodynamic axial loads and to provide seal lands to prevent vane bypass leakage. The outer rings are centered through a key/slot pattern to metal members which are supported from the engine block bulkhead.

Stationary shroud rings are provided over the power turbine rotors as an integral part of the power turbine vane outer rings.

The ceramic turbine exhaust diffuser consists of contoured inner wall (-52), outer wall (-57) and two splitters (-53 and -54) which are all surfaces of revolution except for their mounting features. The splitters and inner wall are all located radially from the outer wall by six sets of rods and spacers (-55, -70, -67, -68). The six ceramic rods (-55) engage axial holes in the outer wall (-57) to provide a slip fit for assembly. The inner wall (-52) is retained axially and oriented circumferentially by sheet metal details (-49 and -50) at its forward flange. The diffuser outer wall is located both radially and axially from a set of radial pins (-58) through a flange (-59) mounted on the engine block.

Thin-wall ceramic regenerator disks are used with this engine with increased effectiveness because of improved matrix geometry and/or increased frontal area with improved flow distribution. Reduced leakage is also assumed.

The control changes identified for the 1132°C (2070°F) engine are also used with this engine. Improved insulation is required to protect the engine block against the higher cavity temperatures, and the block cross-arm construction is modified to isolate the cross-arm thermal growth from constraint by the block.

1371°C (2500°F) Engine Configuration

The general arrangement for the turbine and combustor sections of the 1371°C (2500°F) engine is presented in Figure 22. This engine incorporates the same flow path as the 1204°C (2200°F) engine, and the configuration and construction of the gasifier turbine nozzle, gasifier tip shroud, plenum, gasifier turbine rotor, power turbine nozzles and tip shrouds, and turbine exhaust diffuser are also similar. The 1371°C (2500°F) engine, in addition, incorporates ceramic power turbine rotor blades and a ceramic combustor.

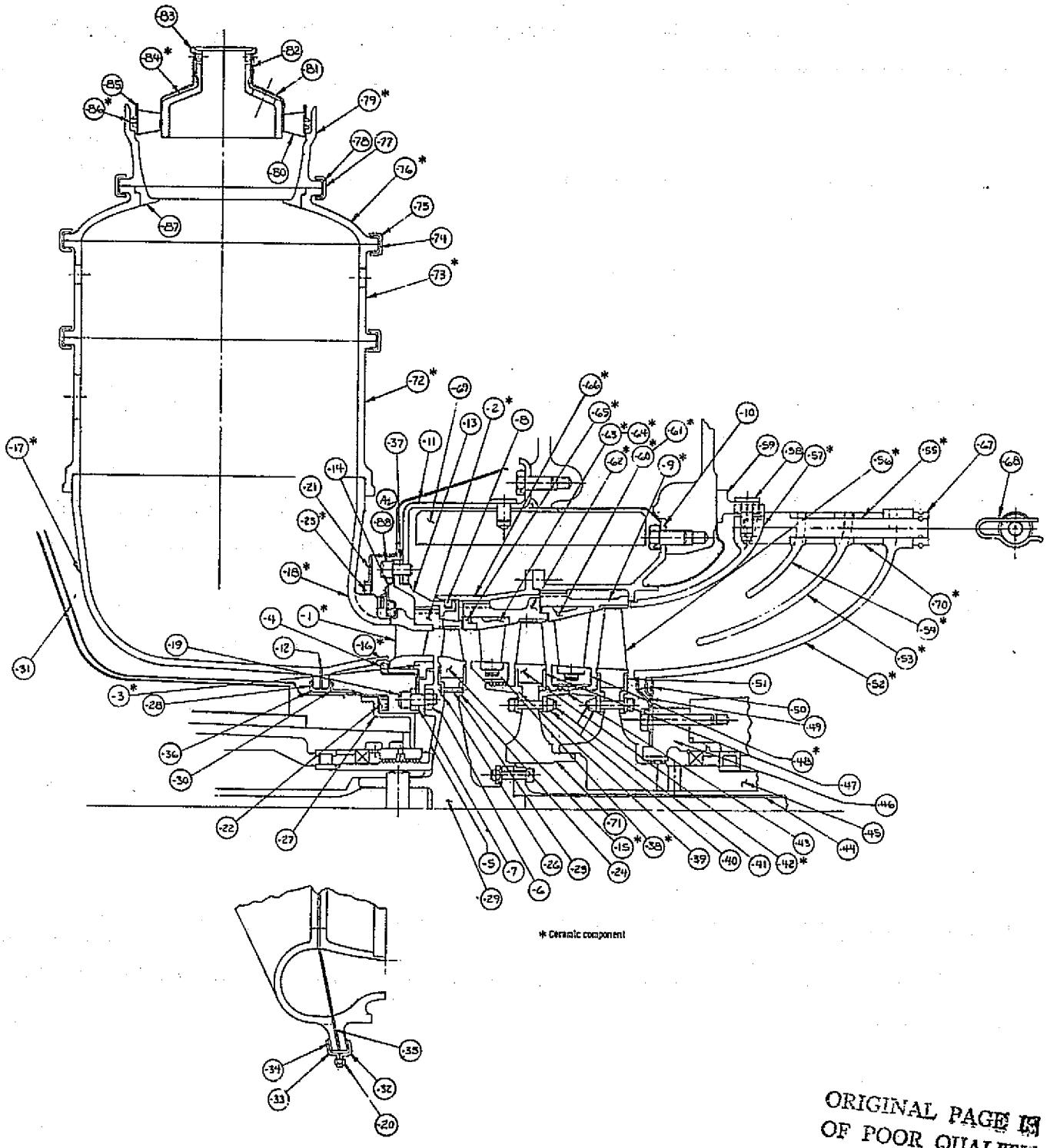

Figure 22. Combustor and turbine general arrangement for 1371°C (2500°F) study engine.

The ceramic blades (-42 and -56) in both of the power turbine stages provide an integral platform at the airfoil hub, a stalk transition section, and a single lug dovetail. The blade dovetails are aligned with the airfoil to minimize bending stresses induced by centrifugal loading. The blades are retained axially in the turbine wheels by flanged cover plates and seal plates (-39, -47, -43 and -51) which are piloted to the turbine wheels and retained by the power turbine rotor assembly bolts (-40 and -41).

The ceramic combustor comprises a series of cylindrical shells (-72, -73, -76, -79) to restrict the axial temperature difference occurring in any one part. A separate ceramic ring (-87) is incorporated at the exit of the prechamber section where high local heat transfer can occur. (Thermal isolation of the combustor dilution holes may similarly be required.) The combustor cylindrical sections are joined using sheet metal bands (-75, -77) which impose a slight clamping effect in addition to the small compressive load which exists because of the operating combustor drop. The prechamber dome (-84) is also a ceramic cylindrical section which is located by a sheet metal sheel (-82) that supports the metal swirl vane assembly (-80, -81, -82, -83, -85). The swirl vane assembly is sealed at the prechamber outer wall (-79), using a ceramic seal ring (-86). The combustor is located by engagement with the turbine inlet plenum and the prechamber swirl assembly. The prechamber swirl assembly clamps to the combustor cover in conjunction with the fuel nozzle assembly.

The improved compressor, gasifier turbine, and regenerator characteristics are retained from the 1204°C (2200°F) engine, as is the control logic.

Noise

Exterior sound level tests were performed in 1971 and 1976 to compare diesel and gas turbine-powered intercity buses. The tests were conducted in accordance with the SAE J 366 procedure for acceleration and deceleration operating modes below 57 km/h (35 mph). The specified test site layout is shown in Figure 23. The test results are presented in Table XIII as "A" scale weighted sound pressure levels. The turbine-powered bus in both acceleration test series has produced sound levels diminished by at least 5 dB from those of the diesel. The deceleration test series results have been about equivalent for the turbine and diesel. The turbine-powered bus currently satisfies the 80-dBA limits proposed for 1978 by the California Standards and proposed for 1980 by the Federal Standards. The diesel-powered bus value of 85.3 exceeds the current California Standard of 83 dBA.

The base line engine has three sources of noise: compressor inlet, exhaust, and the gear case. The use of inlet air cleaners greatly attenuates noise originating from the compressor. The remaining engine noise is believed to be primarily exhaust related. Exhaust noise is the product of three components: combustion noise, turbine noise, and jet or pipe flow noise. Turbine noise occurs at the rotor blade passage frequency which (for the base line engine) is well above the audible range. Jet or pipe flow noise will decrease because the engine exhaust velocity will decrease from 66.1 m/s (217 ft/sec) to 32.3 m/s (106 ft/sec) for the 1371°C (2500°F) engine.

Note: Test layout for heavy trucks and buses per SAE J366

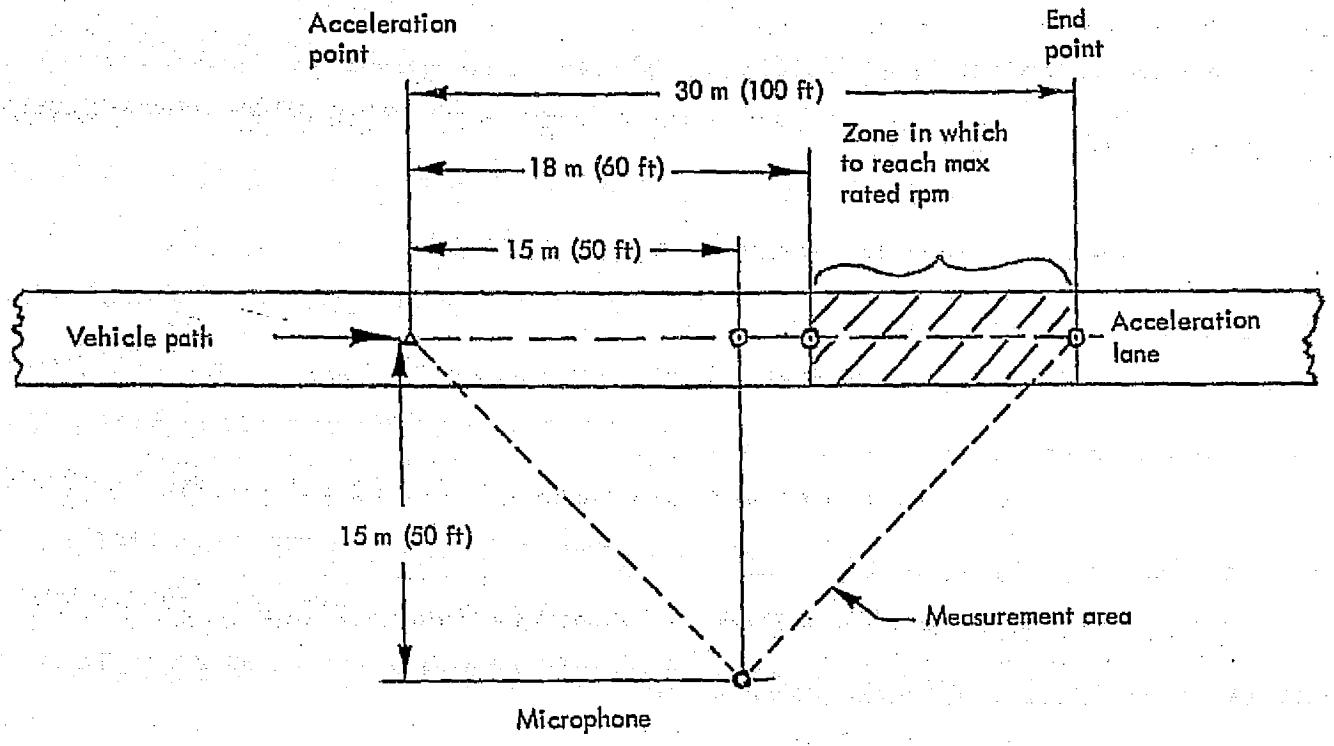

Figure 23. Exterior sound level test site layout.

TABLE XIII. EXTERNAL NOISE COMPARISON, DIESEL- AND TURBINE-POWERED BUS

	1971 Tests		1976 Tests	
Engine	Diesel 8V-71	Turbine 404-1	Diesel 8V-71	Turbine 404-3
Coach Model	Challenger MC-7	Challenger MC-7	Challenger MC-7	Turboliner MC-7
Transmission	Allison HT 740	Allison HT 740 CT	Spicer 4 Spd	Allison HT 740 CT
Average Sound Pressure Levels - db "A" Scale Weighted				
SAE J366 Operation				
Acceleration				
Left Side	84	79	85.3	76.5
Right Side	80	77.5	82.5	76.9
Deceleration				
Left Side	76	75	78.8	76.1
Right Side	76	75	76.8	77.4

Combustion noise will also decrease as the turbine inlet temperature is increased. This is based on the use of three combustion noise prediction models, the results of which are shown in Figure 24. These data are based on a 954°C (1750°F) turbine inlet temperature because the engines used in the intercity bus sound level tests were earlier versions of the base line engine and were rated at that temperature. Except for the turbomachinery flow size and cooling, these earlier engines are nearly identical with the current base line engine. A reduction in combustion noise of 4 to 9 dB is predicted (depending on which model is used) for the 1371°C (2500°F) engine. This projection is consistent with DDA experience where engine cycle developments leading to reduced fuel consumption have also reduced engine exhaust noise. The predicted reduction is shown as an incremental reduction in sound power level. Because the combustion noise spectra have been shown to be essentially constant (refer to NASA TM X71627), the reduction in combustion sound power will translate directly to a reduction on the "A" weighted scale. Vehicle noise, however, will probably show a lesser reduction because other vehicle noise sources will provide a noise floor which will mask the full effect of lower engine exhaust noise.

Three combustion noise prediction models were used in this study. The methods recommended by the NASA Aircraft Noise Prediction Program (ANOPP) and proposed by the SAE A21 Committee for Aircraft Noise are identical in form except for the inclusion of a turbine attenuation term in the A21 method, which accounts for the lower noise predicted by the A21 method as compared with the ANOPP method. The third prediction model was developed for the FAA

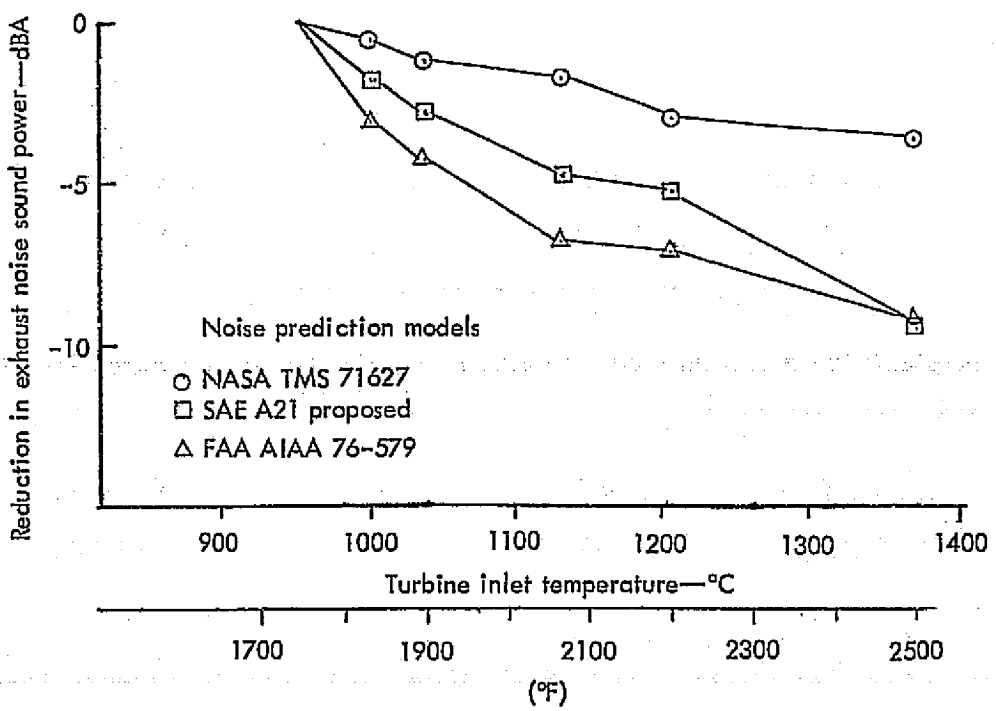

Figure 24. Effect of increasing cycle temperature on exhaust noise.

under contract DOT-FA75-WA-3663. This model attempts to describe the combustion noise generation process in a more theoretical and rigorous way than the ANOP or A21 methods. Attenuation through the regenerator is not included in any of the models used. However, this attenuation should be constant at all cycle temperatures because the regenerator represents a constant insertion loss.

Emission Analysis of Study Engines

An analysis was performed to predict the emission characteristics of the study engines. The program goals require maintenance of emission levels within known and projected legal requirements. The existing standard most applicable to the gas turbine would be the Heavy Duty Engine/Vehicle emission control requirement for diesel on-highway vehicles. For 1977, these standards are as follows:

1977	Constituent, mg/W·h (g/hp-h)			
Standard	HC	CO	NO_x	HC + NO_x
Federal	---	54 (40)	---	21.4 (16.0)
California	1.3 (1.0)	33 (25)	10 (7.5)	6.7 (5.0) (Optional)

At a public hearing on October 5, 1976, the California Air Resources Board passed the following standards for heavy-duty diesel engines used in highway vehicles:

Model Year				
Effective	HC*	CO	NO_x	HC + NO_x
1979	2.0 (1.5)	33 (25)	10 (7.5)	6.7 (5.0) (Optional)
1980	1.3 (1.0)	33 (25)	---	8.0 (6.0)
1983	0.7 (0.5)	33 (25)	---	6.0 (4.5)

*Measured with flame ionization analyzer.

New Federal standards for heavy duty diesel engines are also being considered for 1978. The proposed new rules set emission levels as follows:

HC	CO	HC + NO_x
2.0 (1.5)	33 (25.0)	13.4 (10.0)

Projected standards are very difficult to predict and are sometimes postponed because of other considerations, such as new instrumentation base lines, cost, and fuel economy trade-offs. For this reason, it is advisable to concentrate our attention to the 1980 California emissions levels when estimating the point in time when combustor development may be required. It is also recognized that the 1983 California standards will require additional combustor development.

Gaseous pollutant emissions were predicted for the advanced models of the diffusion flame combustor. The emissions were predicted as a function of combustor geometry and inlet conditions by means of a "characteristics time model" developed at Purdue University under the direction of Professor A. M. Mellor. The substance of this emission prediction model is described in a paper presented to the Sixteenth Symposium (International) on Combustion held at MIT, Cambridge, Massachusetts in August, 1976 and published by the Combustion Institute, Pittsburgh, Pa. The title of the paper is Characteristic Times for Combustion and Pollutant Formation in Spray Combustion by Tuttle, Colket, Bilger, and Mellor.

Emissions predictions were made for the four study engine cycles at the combustion inlet conditions of each power level of the 13-mode Federal Heavy Duty Diesel Cycle. This represents 100%, 75%, 50%, 25%, and 2% power points at both intermediate and maximum engine output speeds plus three (3) idle conditions for each engine cycle. The weighted composite results, in units of milligrams per watt hour (grams per brake horsepower hour) are listed in the following tabulation:

	Base Line	Study Engines			
	Engine	1038°C	1132°C	1204°C	1371°C
Constituent	Actual Data	(1900°F)	(2070°F)	(2200°F)	(2500°F)
HC*	0.19 (0.14)	0.4 (0.3)	0.3 (0.2)	0.4 (0.3)	0.3 (0.2)
NO_x	5.36 (4.00)	5.2 (3.9)	7.1 (5.3)	5.4 (4.0)	8.0 (6.0)
HC + NO_x	5.55 (4.14)	5.6 (4.2)	7.4 (5.5)	5.8 (4.3)	8.3 (6.2)
CO	1.57 (1.17)	2.3 (1.7)	1.6 (1.2)	2.3 (1.7)	1.3 (1.0)

*HC values are estimated from previous DDA experience with HC/CO ratios and the predicted CO value. The base line data represent actual measurements.

The results show that gaseous emissions for the four engine configurations remain very near or below the tentative 1980 standard. The amount by which the HC + NO_x emissions are predicted to exceed the projected standard for the 1371°C (2500°F) cycle engine is so small that only minor modifications will be required to be made to the combustor in order to meet the legal requirements. To meet the 1983 standard, additional development will be required.

The pollutant of most concern is NO_x which is predicted to increase about 53% in progressing from the 1038°C (1900°F) cycle to the 1371°C (2500°F) cycle. This increase is largely because of the higher combustor inlet air temperatures and the associated higher flame temperatures. A discontinuity in the predicted emissions trends occurs between the 1132°C (2070°F) and the 1204°C (2200°F) engines because of a combustor size adjustment which would occur at this phase if the engine output horsepower were held constant. The prechamber combustor will have very little effect on the emissions because it will be of the diffusion flame variety. The emissions were predicted and are compared above for a constant 224 kW (300 hp) engine. All emissions except NO_x should be reduced as the cycle temperatures increase. HC, CO, and smoke all would benefit (be reduced) from these more favorable combustion environments.

Engine Cost

Detail part definitions were generated for all of the ceramic and metal parts which are unique to the turbines and combustors of the analysis study engines. This was done only in sufficient detail to facilitate the generation of part pricing data. The definitions include basic part size, shape and features, critical dimensions and tolerances, special surface finish requirements, and materials (where possible) and are shown on the engine general arrangement layout drawings (Figures 19, 20, 21, and 22).

Part production volumes equivalent to 6000 engines per month were assumed for the part pricing activities. The 6000 per month engine production rate is consistent with the engine "maturity" level used in the life-cycle-cost analyses.

Volume production costs were provided for all of the unique metal parts by the Detroit Diesel Allison Production Manufacturing Department. The basis for this pricing was the same as that for the base line engine volume production part manufacturing costs.

The volume production prices for all of the ceramic component details were generated by the Research and Development Division, Carborundum Company, Niagara Falls, New York.

Volume pricing data for the regenerator system disks and seals were provided by Harrison Radiator Division of General Motors, who supplied the equivalent data for the base line engine regenerator parts.

Pricing increases in the block insulation were assumed as a percent of base line block insulation prices for the 1204°C (2200°F) and 1371°C (2500°F) engines. Anticipated changes to the basic engine block are not, however, expected to increase engine production cost.

The engine electronic control assembly has adequate sensor and amplifier quantities and microprocessor capacity for application to the advanced engines to operate at turbine inlet conditions up to 1371°C (2500°F). Thermocouple locations will be changed as the local environments in the engines exceed thermocouple durability temperature limits, and control logic will be changed to reflect the revised sensor locations. However, engine control system costs will not change significantly as a result of these sensor location and control logic modifications.

A summary of the 6000 engines per month volume production parts costs is presented for each of the significant component changes and for each of the analysis study engines in Table XIV.

TABLE XIV. COMPONENT COST DATA FOR STUDY ENGINES

(6000/month engine production volume)

Percent Of Base Line Engine Parts Cost	Component Replacement (and Associated Parts)	Parts cost increase as a percentage of base-line engine cost*			
		1038°C Engine (1900°F)	1132°C Engine (2070°F)	1204°C Engine (2200°F)	1371°C Engine (2500°F)
14.2	Ceramic Regen Disk and Seals	3.6	3.6	3.6	3.6
5.0	Ceramic Gasifier Nozzle and Tip Seal	-0.8	-1.1	-1.1	-1.1
1.5	Ceramic Gasifier Rotor Blades		1.5	1.2	1.2
1.3	Ceramic Turbine Inlet Plenum		2.9	2.9	2.9
2.3	Ceramic Power Turbine Nozzles (2 Stage)			5.4	5.4
2.3	Metal Power Turbine Rotor (2 Stage)				
	Ceramic Power Turbine Blades (2 Stage)				4.7
0.9	Turbine Exhaust Diffuser			7.9	7.9
1.5	Metal Pre-Chamber Combustor			0.7	
	Ceramic Pre-Chamber Combustor				2.9
100	Total Engine	2.2	7.2	22.8	27.5

*$\frac{\text{(Replacement Component Cost) - (Base Line Part Cost)}}{\text{(Base Line Engine Parts Total Cost)}} \times 100\%$

The summary shows an increasing total engine parts cost with increasing engine cycle tempera level and with increasing ceramic component content. The ceramic components are in general more expensive than their base line engine metallic counterparts. However, metal components with operating capability at the study engine temperature levels would similarly be more expensive than the base line components and would result in additional associated performance deterioration. The one exception is the gasifier turbine nozzle, wherein the base line metallic counterpart price reflects a complex air-cooled assembly. In this case, the ceramic component replacement assembly provides a cost reduction.

The ceramic components which are dependent on ceramic casting practices show relative cost increases of substantial magnitude compared with the counterpart metallic components:

Component		Relative Cost Increase
Turbine Inlet Plenum (2.9/1.3) × 100%	=	220%
Turbine Exhaust Diffuser (7.9/0.8) × 100%	=	990%
Combustor (2.9/1.5 + 7) × 100%	=	130%

Of the 22.8% engine parts cost increase of the 1204°C (2200°F) engine over the base line engine, 5.2% is attributable to the incorporation of the two-stage improved power turbine and the pre-chamber combustor:

Component	Increase (%)
Two-Stage Metal Power Turbine Nozzle	2.3
Two-Stage Metal Power Turbine Rotors	2.2
Metal Pre-chamber Combustor	0.7
	5.2%

This assumes that an additional metal power turbine nozzle would have about the same cost as the base line part.

The engine assembly and test costs are assumed to be the same as those of the base line engine. In addition, it is assumed the engine selling price will reflect the same percentage markup over cost as the base line engine.

Life Cycle Cost Analysis

Life cycle costs for the base line and study engines were evaluated. The ceramic engine parts were recognized for each engine. Relative values for fuel, maintenance material and labor, and engine acquisition costs were calculated and used in a computer model. This model is the result of work done since 1968 and represents a "state-of-the-art" analysis tool. The modular capacity of the model was exercised to fit an assumed maintenance concept.

A line haul truck profile was used to develop a maintenance and operating scenario for the various engines. This scenario is shown in Table XV with respect to basic data input. These values were selected to apply an 805 000-kilometre (500,000-mile) average for each truck. The labor rates used do reflect the labor costs common to larger line haul truck operations. Typical maintenance allocations by percent for each level of maintenance are shown in Figure 25. These allocations are further modified, using the scheduled maintenance concept as defined in the base line engine description (ref Table III). The percent allocations were held constant for each of the study engines.

The life cycle cost analysis results for the line haul truck are presented in Figures 26 through 29. All values in the comparison tables are shown as a percent of the base line engine operating at 1002°C (1835°F). Examination of the sensitivity data indicates that the cost has a break point between 1132°C (2070°F) and 1204°C (2200°F). This substantial improvement reflects not only a more efficient cycle but also technology improvements in the form of higher efficiency components. Comparison curves are shown which indicate the effect of omitting the technology improvements and relying only on the basic cycle improvement.

TABLE XV. LINE HAUL TRUCK LIFE CYCLE COST ANALYSIS INPUT DATA

Program Assumptions	
• Fleet Size	100 Tractors
• Utilization	14 500 km (9,000 Miles) Per Month For Each Tractor
• Average Speed	72 Kilometres Per Hour (45 MPH)
• Maintenance Levels	Garage: In-Frame; Out-Of-Frame Rebuild: Major Repair; Overhaul
• Engine Turn-Around	Maximum Of One Month At All Levels
• Labor Rate	$17.00 Per Man-Hour At All Levels
• Program Time	60 Months
• Fleet Age	Uniformly Distributed Over 805 000 km (500,000 Mile) Age Profile)

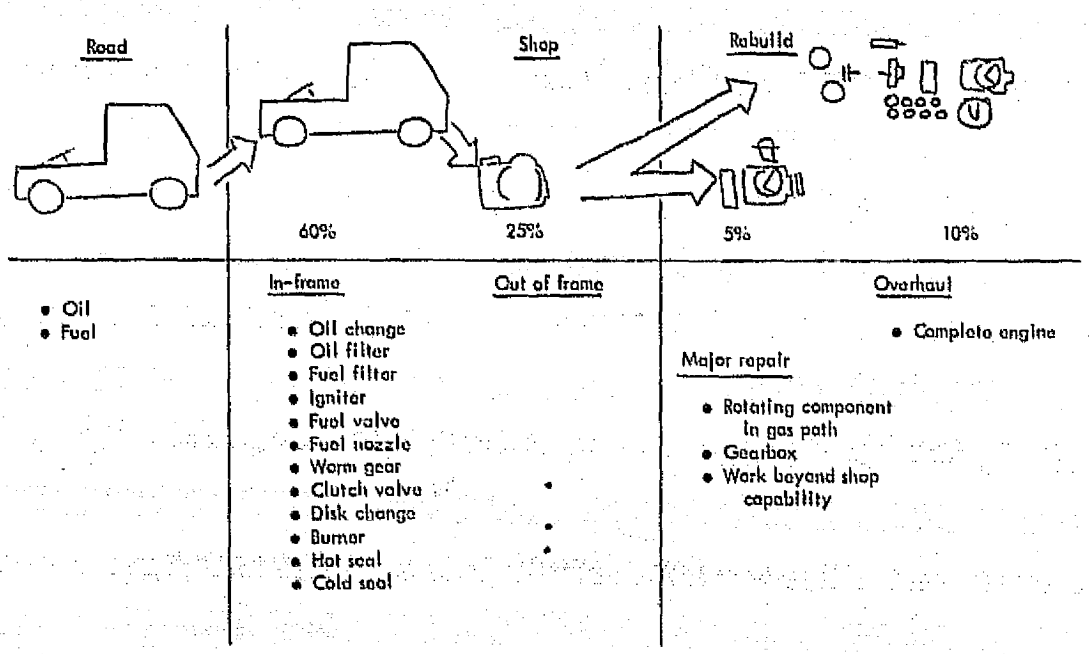

Figure 25. Typical line haul truck maintenance allocations.

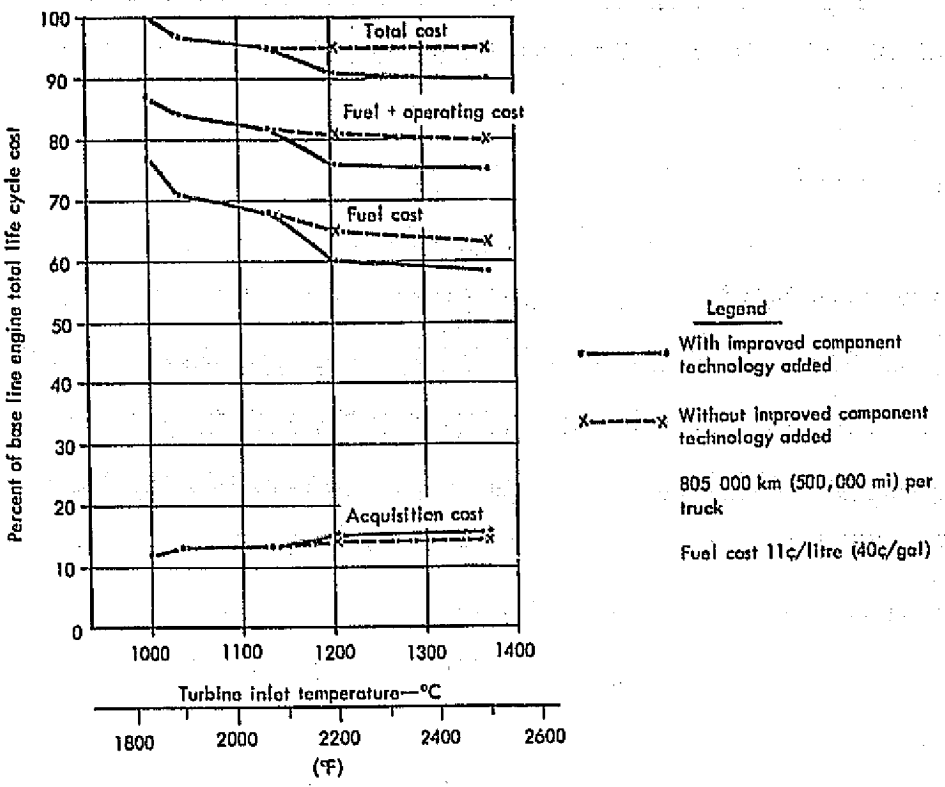

Figure 26. Effect of cycle temperature on line haul truck.

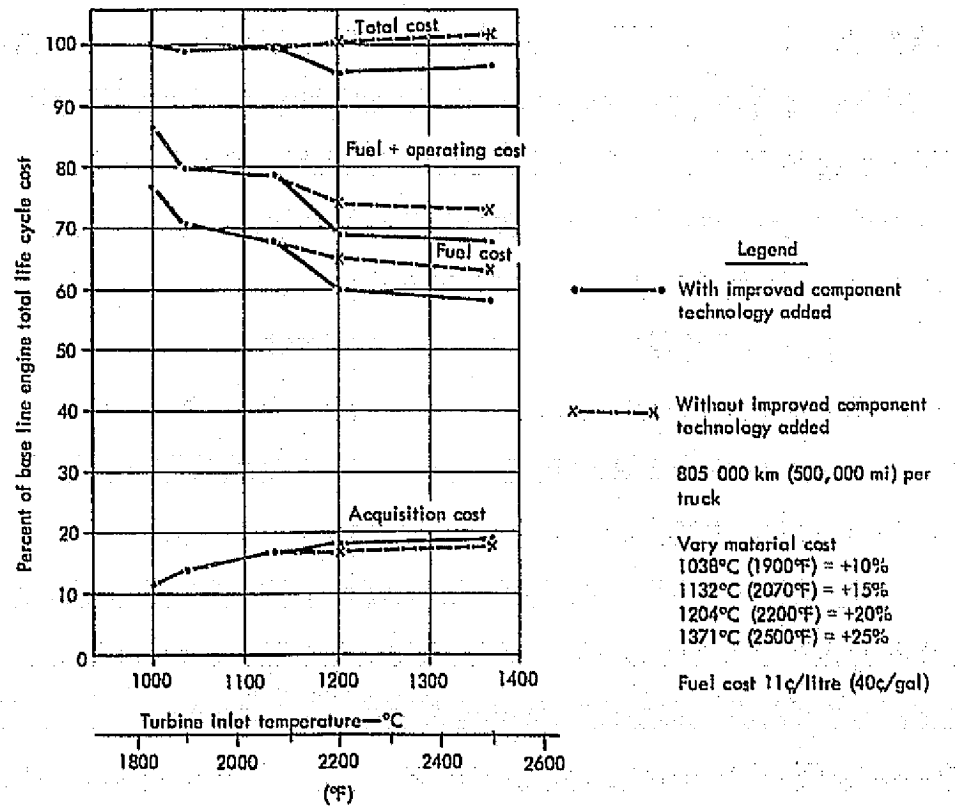

Figure 27. Line haul truck cycle cost adjusted for increased ceramic material cost.

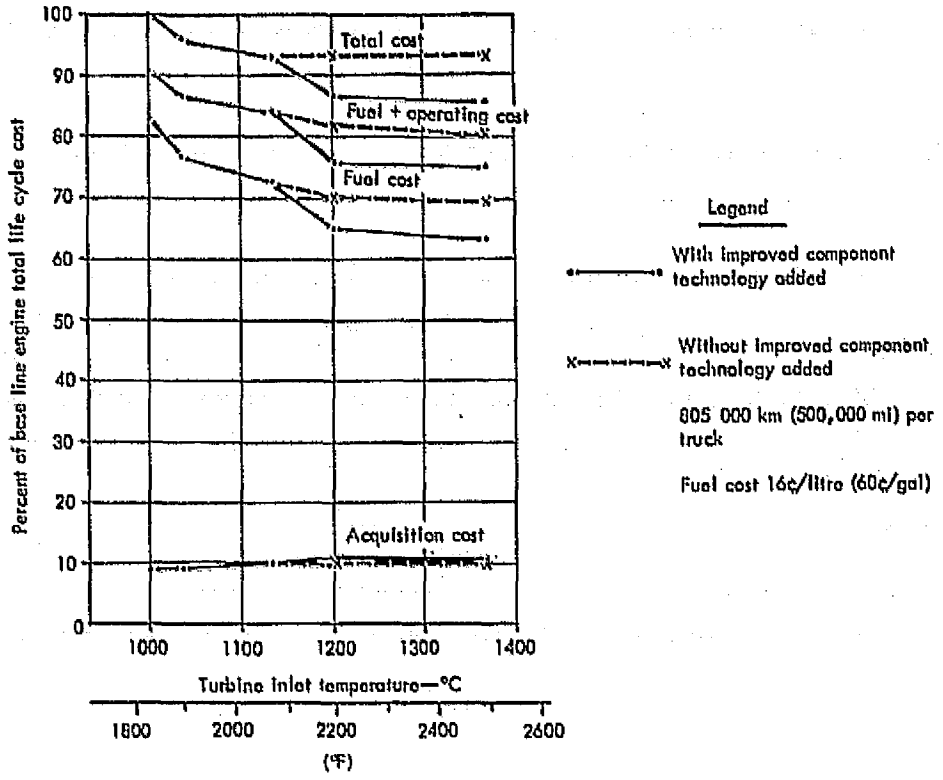

Figure 28. Line haul life cycle cost adjusted for increased fuel price.

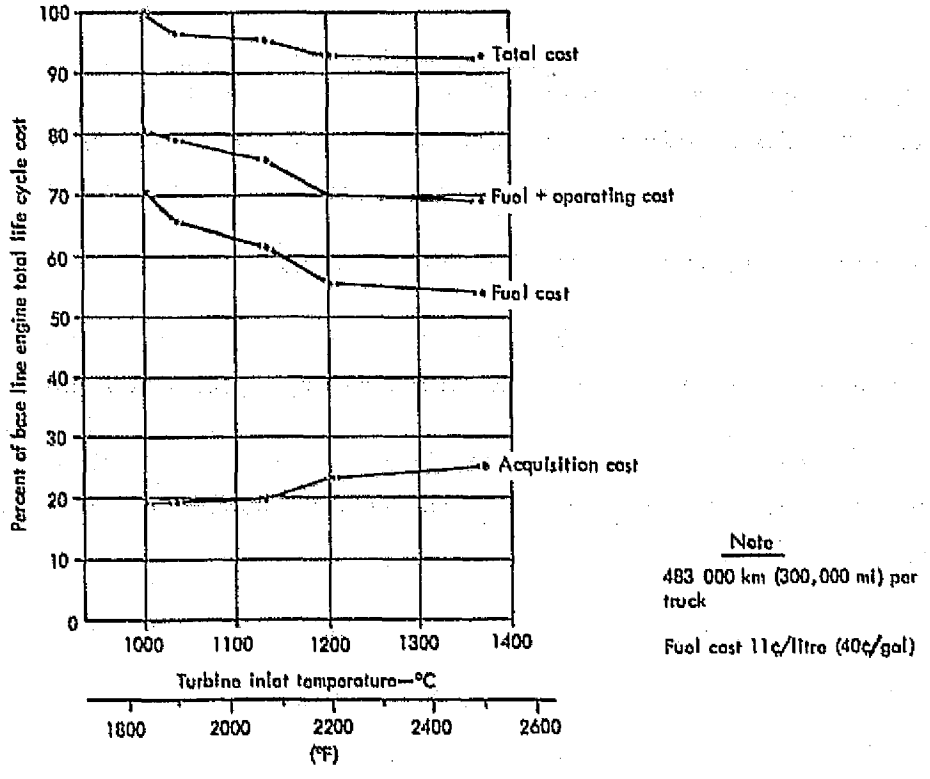

Figure 29. Line haul truck life cycle cost adjusted for reduced length of ownership.

The basic effect of the increased cycle temperature is shown both with and without recognition of the component technology improvement in Figure 26. This curve indicates that there is no benefit in increasing temperature beyond 1132°C (2070°F) unless improved efficiency components are introduced. Further, only a minor drop in life cycle costs is shown for the 1371°C (2500°F) engine compared to the 1204°C (2200°F) engine even with improved components.

Recognizing that the confidence for ceramic material prices decreases as more ceramic material is introduced, the sensitivity for an assumed increase in the cost of the ceramic materials with temperature is shown in Figure 27. The material content was varied in 5% steps for each engine after the 1038°C (1900°F) configuration. There was an initial material adjustment of 10% for the 1038°C (1900°F) engine. With this assumption, the 1204°C (2200°F) engine shows the lowest life cycle cost.

Fuel may be the principal cost driver. In the previous calculations, a cost of 11 cents per litre (40 cents per gallon) for fuel was used. Figure 28 shows the impact of fuel at 16 cents per litre (60 cents per gallon). The percentage contribution of the higher-cost fuel represents a substantial increase to the cost of operation. Even with the higher fuel cost, the 1371°C (2500°F) engine life cycle costs are only slightly better than the 1204°C (2200°F) engine.

The previous data were aimed at an average distance of 805 000 km (500,000 miles) per tractor. Since some users are concerned about cost to first overhaul, a 483 000 km (300,000 mile) per tractor data set was calculated. These data are depicted in Figure 29, which shows a relatively small change in life cycle cost, with the 1204°C (2200°F) engine as the optimum.

It appears that the 1038°C (1900°F) and 1204°C (2200°F) engine configurations show the most benefit in cost saving. The 1132°C (2070°F) version is marginally better than the 1038°C (1900°F) version. When one considers the relative risk of operating the engine at higher temperatures, it would seem that a question could be raised concerning overall engine reliability. However, a basic premise of this study was that the associated metal parts complementing the ceramic engines would maintain a constant premature removal rate.

An intercity bus application generally follows the cost trends of the truck. The bus life cycle cost is somewhat more labor intensive because of installation constraints. However, there were no other significant trend changes over a line haul truck. Specific values of fuel and the labor-material mix will change. A summary of the operational values is listed in Table XVI. However, Figures 30, 31, and 32 indicate curve shapes very similar to those of the truck, even with these changes introduced.

TABLE XVI. INTERCITY BUS LIFE CYCLE COST ANALYSIS INPUT DATA

Program Assumptions	
● Fleet Size	100 Bus Fleet
● Utilization	26 500 km (16,500 miles) Per Month For Each Bus
● Average Speed	72 Kilometers Per Hour (45 MPH)
● Maintenance Levels	Garage In-Frame Out-Of-Frame Rebuild Major Repair Overhaul
● Engine Turn-Around	Maximum Of One Month At All Levels
● Labor Rate	$17.00 Per Man-Hour At All Levels
● Program Time	60 Months
● Fleet Age	Uniformly Distributed Over 805 000 km (500,000 Mile) Age Profile

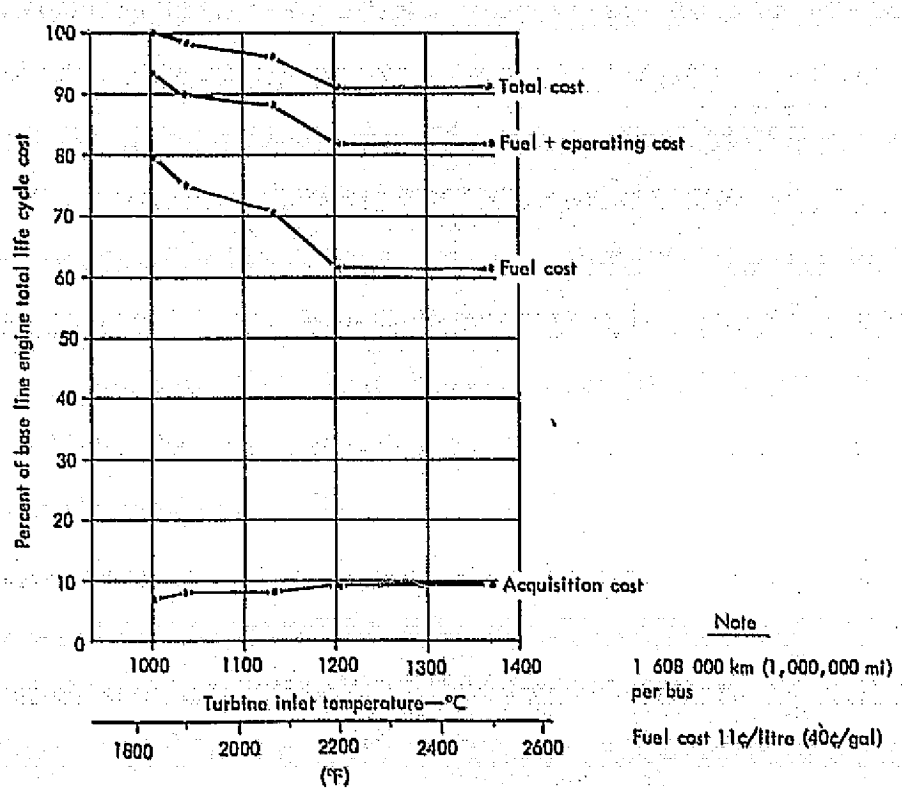

Figure 30. Effect of cycle temperature on intercity bus life cycle cost.

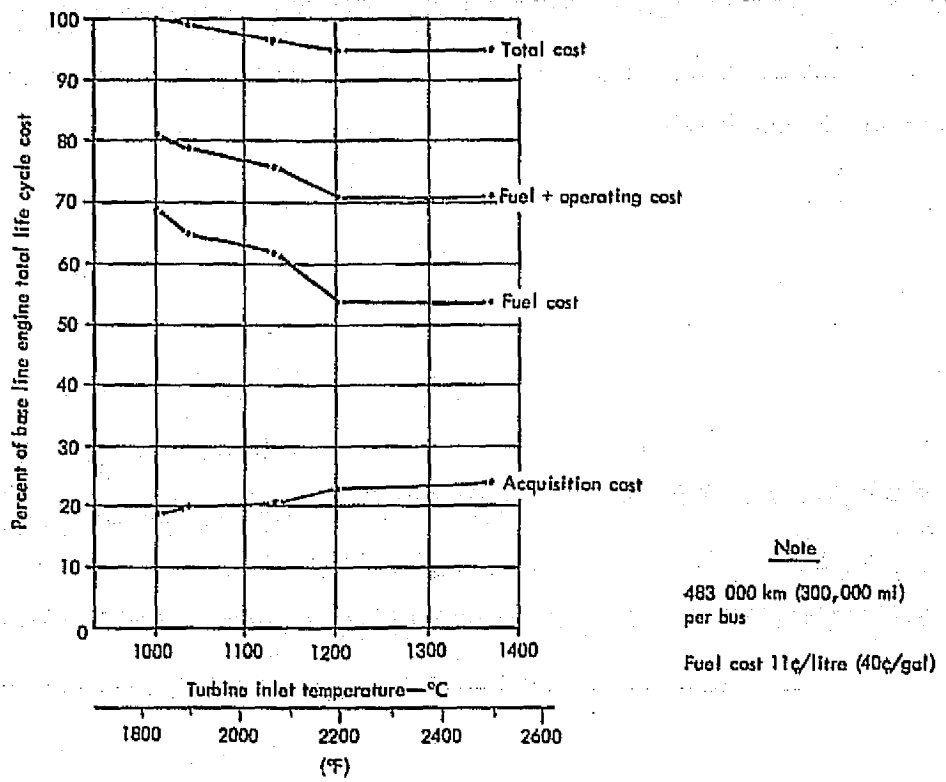

Figure 31. Intercity bus life cycle cost adjusted for reduced period of ownership.

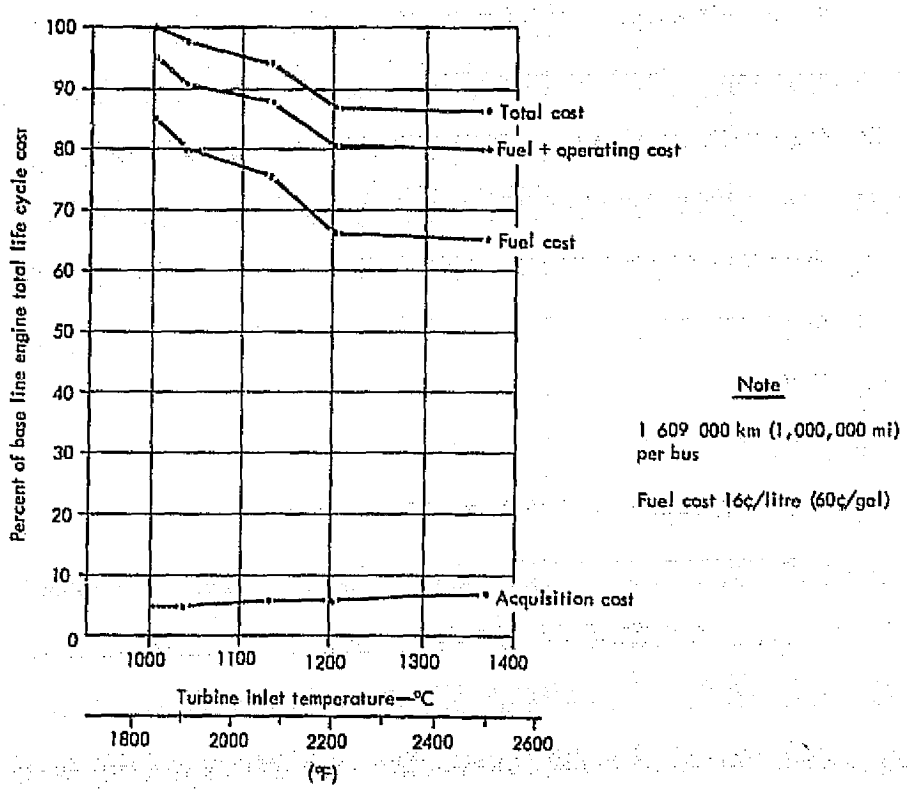

Figure 32. Intercity bus life cycle cost adjusted for increased fuel cost.

The principal reason for more labor being required in the operation of the bus is that less maintenance can be done "in-frame." Current bus designs do not allow regenerator disks and seals to be changed in-frame in the manner that a "cab-over" semi-tractor truck will allow. Therefore, the garage level labor content increases in the operating cost category over a truck application. Fortunately, the relative total percentage does not vary a great deal, thereby preserving the general curve shapes common to the line haul truck.

In summary, the view from a life cycle cost standpoint seems to center on three recommendations:

1. The 1038°C (1900°F) level of ceramic content should be pursued.
2. The 1204°C (2200°F) level of ceramic content and technology appears very attractive from a cost/benefit weighting.
3. The 1371°C (2500°F) level should be deemphasized pending more "building block" technology work. The potential fuel savings are desirable, but today's understanding of the other engine items which must also be low cost adds a degree of risk. This risk does not appear to be substantially offset by life cycle cost savings.

Life cycle cost analyses were prepared for the line haul truck and intercity bus applications using sea level, 15.6°C (60°F) vehicle simulation data and a 16 cents per litre (60 cents per gallon) fuel cost (projected 1980 cost). These data are compared with the previous results (SAE standard day) for the truck and the bus in Figures 33 and 34, respectively. A significant reduction in life cycle cost is shown for sea level, 15.6°C (60°F) day operation, with the base line engine showing the greatest improvement.

Marketability

The market concept for the range of ceramic engines was based on an extension of the all-metal base line engine. It was considered that the metal engine would be offered at a competitive price to a comparably rated power diesel when installation considerations were included. Also, benefits toward meeting environmental constraints were not credited to the turbine, nor were they assessed against the diesel installation. One could have some concern that the higher temperature ceramic engines might move outside the competitive price range. Therefore, the importance of the operating and support costs to offset the investment cost becomes very significant. One could conclude from this preliminary study that the 1204°C (2200°F) engine would represent the upper limit that would probably fit a competitive market. The 1371°C (2500°F) engine will need more development to provide further reductions in life cycle costs in order to be accepted.

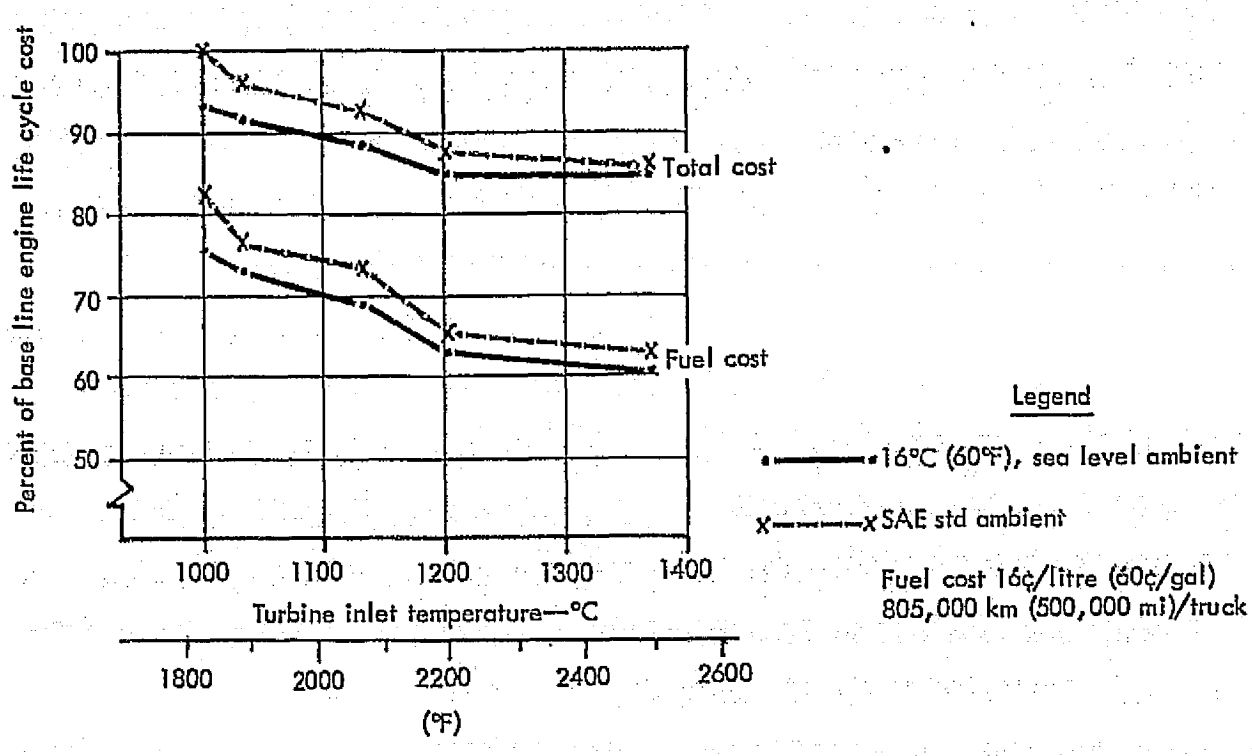

Figure 33. Line haul truck life cycle cost—effect of ambient conditions.

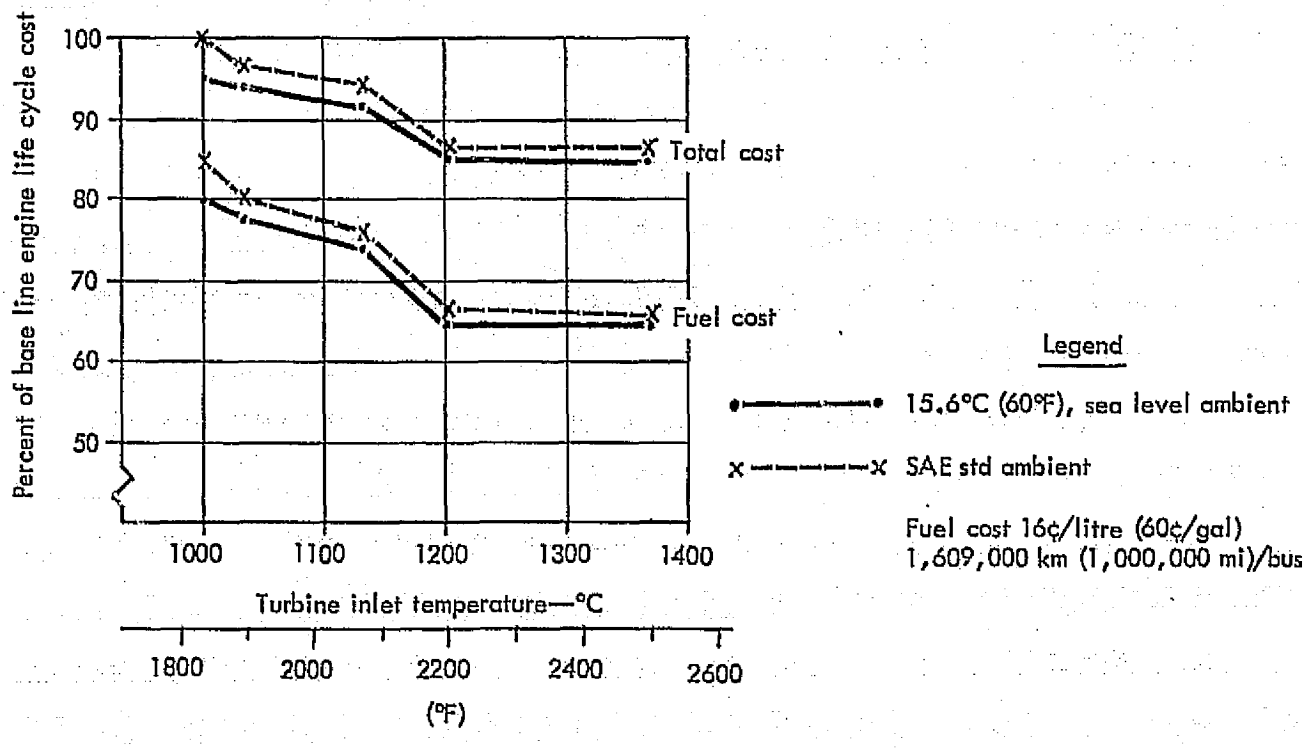

Figure 34. Intercity bus life cycle cost—effect of ambient conditions.

STUDY CONCLUSIONS AND RECOMMENDATIONS

The purpose of the foregoing study was to use selection criteria on performance [213 mg/W·hr (0.35 lb/hp-hr) sfc], durability (qualify ceramic parts for use in a base line gas turbine program), and cost (competitive for truck and bus applications) and establish a program plan for an improved engine which could be demonstrated by the end of 1981. Based on the study results discussed, the following conclusions were drawn:

1. Ceramic components can be introduced into the current base line engine and a 213-mg/W·hr (0.35 lb/hp-hr) sfc can be demonstrated by 1981. The risk of successful completion of this work is considered high because of the high technology involved in applying ceramic components to gas turbine engines.
2. Ceramic components (which permit increased turbine and regenerator inlet temperatures) as well as improved component efficiencies are required to meet the performance objective by 1981.
3. Ceramic materials require substantial characterization and development activity to achieve the durability required to qualify ceramic components for introduction in a production engine.
4. Program planning should emphasize the early durability evaluation of ceramic regenerators and early development testing of ceramic vanes, blades, and tip shrouds.
5. Approximately a 1204°C (2200°F) turbine inlet temperature is the near-term limit of temperature capability for ceramic materials and for achieving the 213-mg/W·h (0.35 lb/hp-hr) sfc goal. At this turbine inlet temperature, fuel savings are approximately 29% for a line haul truck and 27% for a highway bus.
6. Life cycle costs show fuel cost to be extremely important to overall cost and that improved sfc will become overriding in importance as fuel costs increase. (It appears that fuel will cost much more than 60 cents per gallon by 1981). This fact should lend increasing importance to the fuel conservation aspects of future powerplants.
7. The cost of ownership of line haul trucks and highway buses is reduced by 9% by achieving the 1204°C (2200°F) operational capability. Only a 1% additional reduction is realized by achieving 1371°C (2500°F) (based on current knowledge of ceramics). The increased risk with minimum assessed payoff does not justify a program plan which goes much above the 1204°C (2200°F) level.
8. Integral ceramic turbine blade and wheel rotor assemblies require more than five years to develop to a stage of readiness for initial production engines. This technology should result from a program funded separately from the one planned herein.
9. Noise and emission standards through 1980 regulations can be met by 1204°C (2200°F) engines. Work on combustors should be performed in the planned program to meet proposed emission standards for 1983 and beyond.

PROGRAM PLAN

PROGRAM OBJECTIVES

Two primary objectives were selected for the planned program:

1. Incorporate ceramic components into the base line engine to demonstrate the applicability of current ceramic materials technology by the end of 1981.
2. Demonstrate improved fuel consumption from the benefits derived by having improved ceramic and aerodynamic components. The fuel consumption improvement desired is to change from a 274-mg/W·h (0.45 lb/hp-hr) to a 213-mg/W·h (0.35 lb/hp-hr) sfc by the end of 1981.

The program also has two secondary objectives:

1. Meet current and projected federal noise and emission regulations.
2. Demonstrate commercial capability for the improved engines.

These objectives were established with NASA/ERDA at the inception of the program and were used as criteria in the study conducted. The scope of the schedule, technical accomplishment, and endurance testing was defined by these objectives, the feasibility fo meeting the objectives was assessed in the study program.

RISK FACTORS

The program plan which follows recognizes the relatively "high risk" of incorporating ceramic components in a gas turbine, and the plan is intended to permit iterations on materials and geometry of ceramic components.

The risk factor for incorporating ceramic components varies with each component. Risk levels were assigned as follows (lowest risk factor is lowest number, highest risk is highest number):

1. Regenerator
2. Combustor
3. Stationary Turbine Tip Shrouds
4. Turbine Nozzle Guide Vanes
5. Turbine Inlet Plenum
6. Turbine Exhaust Diffuser
7. Turbine Rotor Blades—Metal Wheel
8. Turbine Rotor Blades and Wheel

These risk factors recognize the current state of the art demonstrated in the various industry programs to incorporate ceramic materials in gas turbine engines. A second ranking of ceramic components was made to illustrate the performance benefits possible in the program. The following list shows the relative performance payoff; the lowest numbers indicate the highest payoffs, and the highest numbers the lowest performance gains.

1a. Regenerators
1b. Turbine Nozzle Guide Vanes
1c. Turbine Rotor Blades
2. Stationary Turbine Tip Shrouds
3. Turbine Inlet Plenum
4. Combustor
5. Turbine Exhaust Diffuser

Two items are noteworthy in comparing these two lists of components. First, ceramic turbine rotor blades and wheels were not considered to be feasible in the time frame of the objectives and were dropped from the second listing. This combined blade and wheel ceramic technology component development should be pursued in a separate program of longer duration. Second, three components are ranked in the highest performance payoff category (regenerators, vanes, and blades). This equal ranking reflects the importance of each component in achieving the increased turbine inlet temperatures required for obtaining the 213-mg/W·h (0.35 lb/hp-hr) sfc objective. The regenerators and vanes give immediate benefits at the 1038°C (1900°F) level, and their development should be given emphasis. The ceramic rotor blades (or optional air-cooled blades) are required at the 1132°C (2070°F) and 1241°C (2265°F) turbine inlet temperatures and should also receive early program emphasis because their learning curve for application will be the steepest of all components shown.

Two benefits of ceramic components are derived in gas turbine performance: higher cycle temperature and improved component efficiencies. Significant concentration on both of these in the development program is required to achieve the performance objective established. The following plan is presented as a suggestion of an approach toward achieving the potential benefits offered by ceramic materials.

PROGRAM PLAN SUMMARY

The incorporation of ceramic components and component efficiency improvements leading to the demonstration of the 213-mg/W·h (0.35 lb/hp-hr) specific fuel consumption goal will be achieved stepwise through successive increases in turbine inlet temperature. A detailed description of the program plan including demonstrator engine performance, configuration, and testing is given in the remainder of this section.

Demonstration Engine Performance and Configuration

The engine configurations and cycle temperatures which are necessary to satisfy the development and demonstration activities outlined for the program are very nearly identical with those conceived for the study program. Only three significant differences exist:

- The study engine configured for 1204°C (2200°F) will be designed to operate at 1241°C (2265°F) to achieve the 213-mg/W·h (0.35 lb/hp-hr) specific fuel consumption objective. The component performance required to meet this objective is discussed later in this section.
- The 1241°C (2265°F) demonstration engine will use the ceramic pre-chamber combustor that was configured for the 1371°C (2500°F) study engine to obtain acceptable life.
- The flow capacities of the turbines and compressor will be coordinated with the base line program to exploit the availability of components to the fullest extent and minimize program costs. The horsepower of the engines will not remain constant. Table XVII presents the various stages of engine performance demonstrated from the base line as temperature is increased to the 1241°C (2265°F) turbine inlet temperature engine.

The part-load fuel consumption of the 1002°C (1835°F) demonstrator engine (base line engine with ceramic regenerators) will not be as good as was predicted in the study program because the regenerator inlet temperature will be limited to 774°C (1425°F) by seal wearface material temperature limits. At full power, the trade-off in increased ceramic regenerator pressure drop offsets its increased effectiveness, resulting in slightly lower power—218 kW (293 hp)—at the same specific fuel consumption of 274 mg/W·h (0.45 lb/hp-hr).

In the 1038°C (1900°F) demonstrator engine, the use of the ceramic regenerator is continued, and the gasifier turbine nozzle vane assembly and rotor tip shroud are replaced with ceramic components. This will permit the rotor inlet temperature to be raised to 1038°C (1900°F), thereby increasing the power to 231 kW (310 hp) and lowering the sfc to 262 mg/W·h (0.43 lb/hp-hr). These power and sfc improvements carry through the entire power range and will be demonstrated on the test stand and in a vehicle.

The next step in the program is to replace the gasifier turbine inlet plenum and the gasifier turbine rotor blades with ceramic parts. The turbine inlet temperature can then be raised to 1132°C (2070°F), and the engine power and sfc are raised to 261 kW (350 hp) and 243 mg/W·h (0.40 lb/hp-hr), respectively. These increases carry through the full power range. Demonstrations will be made on the test stand and in the vehicle.

TABLE XVII. PERFORMANCE DEMONSTRATION ENGINES

[29°C (85°F), 152 m (500 ft) altitude]

			Ref Base Line				
Engine Performance							
Turbine Inlet Temperature	°C	(°F)	1002 (1835)	1002 (1835)	1038 (1900)	1132 (2070)	1241 (2265)
Max Part Load Regenerator Temperature	°C	(°F)	774 (1425)	774 (1425)	899 (1650)	979 (1795)	982 (1800)
Design Capability Of Regenerator	°C	(°F)	774 (1425)	774 (1425)	982 (1800)	982 (1800)	982 (1800)
Compressor Airflow	kg/s	(lb/sec)	1.56 (3.45)	1.56 (3.45)	1.56 (3.45)	1.56 (3.45)	1.37 (3.03)
Shaft Power	kW	(hp)	224 (300)	218 (293)	231 (310)	261 (350)	287 (385)
Specific Fuel Consumption	mg/W•h	(lb/hp-hr)	274 (0.45)	274 (0.45)	262 (0.43)	243 (0.40)	213 (0.35)
Test Stand Demonstration			Yes		Yes	Yes	Yes
Vehicle Demonstration					Yes	Yes	Yes
Introduction of Ceramic Components							
Regenerator Disk And Seal			M	C	C	C	C
Gasifier Nozzle Assembly			M	M	C	C	C
Gasifier Tip Shroud			M	M	C	C	C
Plenum			M	M	M	C	C
Gasifier Rotor Blades			M	M	M	C	C
Two Stage Power Turbine Nozzle			*	*	*	*	C
Two Stage Power Turbine Rotor Blades			*	*	*	*	M
Exhaust Diffuser			M	M	M	M	C
Combustor			M	M	M	M	C

M - Metal
C - Ceramic
* - Single Stage Metal

The next step in the demonstration program is to redesign the entire hot section gas path to make use of advanced component technology to raise the level of performance of each part. With reference to the all-metal base line engine, the compressor efficiency is raised 1.0% from 82.4% to 83.4% and the corrected flow capacity is reduced from 1.66 kg/s (3.65 lb/sec) to 1.45 kg/s (3.20 lb/sec) at a constant 4.0 pressure ratio. The gasifier turbine is redesigned for a 1.0% efficiency improvement from 87.0% to 88.0%, and the corrected flow capacity decreases from 0.835 kg/s (1.84 lb/sec) to 0.745 kg/s (1.73 lb/sec) to match the reduced flow capacity of the compressor. The power turbine is redesigned from one to two stages with ceramic nozzle vane assemblies. The efficiency of the power turbine is unchanged from that of the single-stage base line engine at 89.7%. As in the gasifier turbine, the power turbine corrected flow capacity is reduced, from 1.62 kg/s (3.58 lb/sec) to 1.38 kg/s (3.04 lb/sec), for proper matching with the gasifier section. Regenerator effectiveness increases 6.1% from 88.9% to 95.0%. Regenerator leakage and pressure drop increase by 0.4% (4.9% to 5.3%) and 0.6% (3.2% to 3.8%), respectively; however, regenerator leakage flow is reduced from 0.075 kg/s (0.165 lb/sec) to 0.069 kg/s (0.152 lb/sec), and total cycle pressure loss is reduced by 1.1% from 11.9% to 10.8% as the result of the reduced cycle mass flow. The details of how these component improvements are to be accomplished are discussed in the Technical Approach section. Ceramics are used in the combustor and power turbine exhaust diffuser. These changes allow the gasifier rotor inlet temperature to be raised to 1241°C (2265°F) to attain the sfc goal of 213 mg/W·h (0.35 lb/hp-hr).

The compressor sets the engine flow capacity size, and the resultant power level is 287 kW (385 hp). If the compressor were to be resized smaller to maintain 224 kW (300 hp), the gasifier shaft rotational speed would have to be increased and a complete redesign of the high-speed shafting and gearing would be necessary. This would result in additional expense, effort, and time.

Engine Development Plan

The initial activity scheduled in the engine development program is the evaluation of the durability and chemical stability of ce. ic regenerator disks in an existing engine with a 774°C (1425°F) regenerator temperature limit.

The next activity is the rig evaluation of rim-driven ceramic regenerator disks, individual ceramic gasifier nozzle vanes, and an individual ceramic gasifier tip shroud and the incorporation of these parts into two base line engines for test demonstration at 1038°C (1900°F) turbine inlet temperature with a 774°C (1425°F) regenerator temperature limit. These first two 1038°C (1900°F) engines are designated as Design I. A regenerator system development program for the advancement of regenerator performance and mechanical technology in the areas of ceramic matrix geometry, seals, and drive system is begun and is continued throughout the program.

The initial experience gained from these activities is applied to design fabrication, component test, and engine test (two engines) of improved ceramic regenerator disks and associated parts, integrated ceramic gasifier vanes and nozzle assembly, and integrated ceramic tip shroud. The designation of these two engines is Design II. These turbine parts are also tested to the 1038°C (1900°F) turbine inlet temperature condition. The regenerator temperature limit is increased to 982°C (1800°F); however, the engine is capable of producing a regenerator inlet temperature of only 899°C (1650°F) as indicated in the study program earlier in this report.

An activity for design studies, fabrication of test specimens, and bench testing of the ceramic gasifier blade to metal turbine wheel attachment configuration is also begun near the start of the program.

A further increase in engine turbine inlet temperature to 1132°C (2070°F) is scheduled as the next activity for improvement of the engine. This temperature increase is supported by design, fabrication, component test, and engine test of an improved ceramic regenerator system and gasifier nozzle assembly and tip shroud with the incorporation of ceramic gasifier turbine rotor blades and a ceramic turbine inlet plenum. The engine electronic control system is also modified for this engine to accommodate engine control logic that is compatible with temperature sensors located in the lower temperature regions at turbine outlet conditions and combustor inlet conditions.

Component improvement programs for several of the engine aerodynamic components are conducted concurrently with the testing. This testing involves the compressor, regenerator, gasifier turbine, and power turbine and is directed toward providing the specific performance characteristics required for the 1241°C (2265°F) engine configuration, 213 mg/W·h (0.35 lb/hp-hr) sfc, which is the next program step. Turbine exhaust diffuser aerodynamic development is also conducted to ensure compatibility with the power turbine and to provide an improved flow distribution to the regenerator system.

The engine configured for development and demonstration of the 1241°C (2265°F) turbine inlet temperature level incorporates the improved aerodynamic components and the ceramic components improved from those previously engine tested and the addition of ceramic power turbine nozzles, a ceramic combustor, and a ceramic exhaust diffuser.

An overview of this program as has been outlined is presented in Figure 35.

A detailed description of the test plan follows.

Rig Testing

The testing program formulated was conceived to address specific requirements applicable to the content of ceramic materials in the engine. These specific requirements vary from component to component. For example, ceramic regenerators and their testing represent a relatively

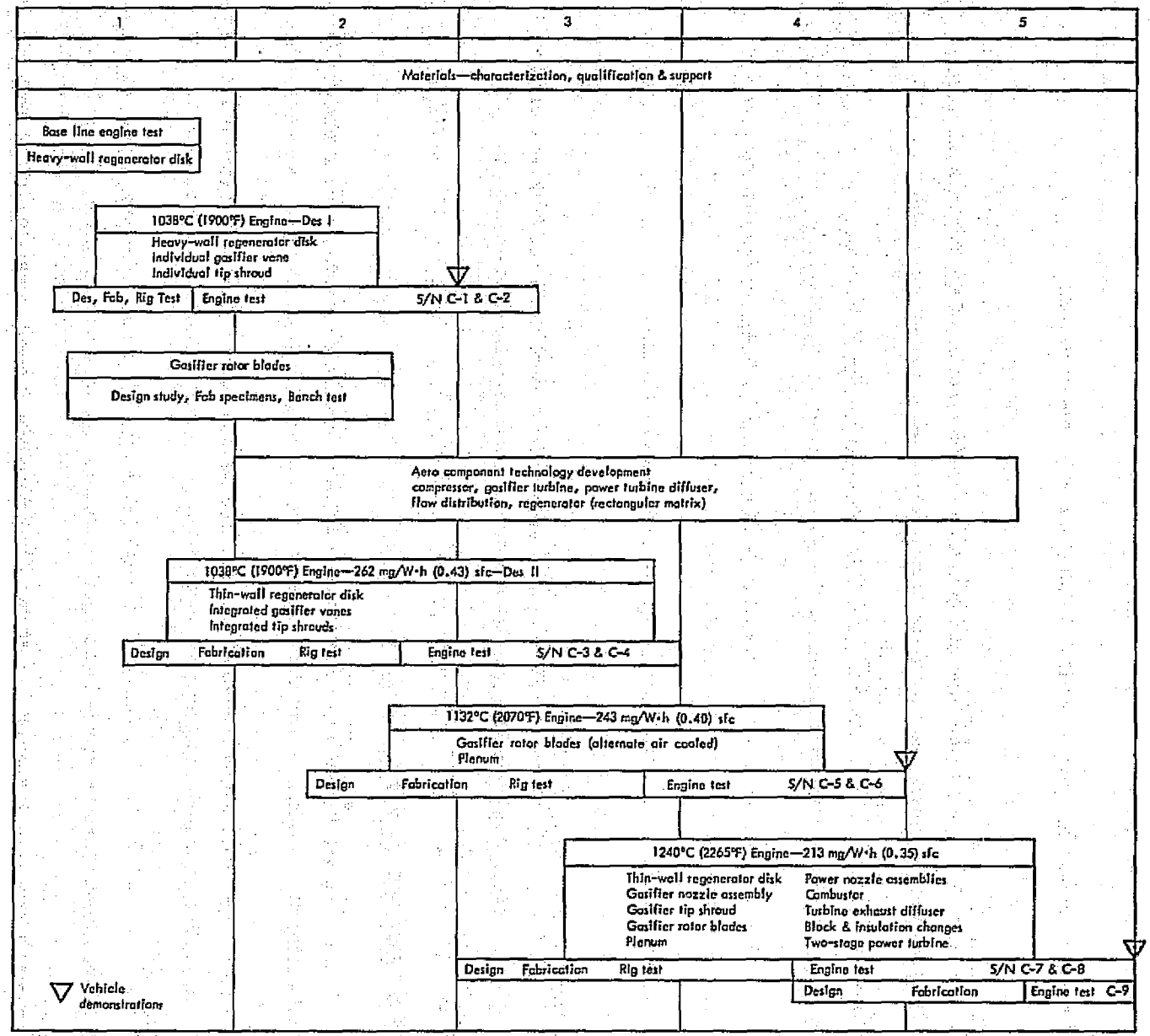

Figure 35. Heavy duty gas turbine engine program schedule.

straightforward step as opposed to ceramic turbine rotor blades. This suggests that a reasonably firm test plan for regenerator evaluations can be formulated, whereas the test plan for rotor blades (because of the higher learning curve) will be more subject to change with program activities. Stationary ceramic components represent a development risk between regenerator disks and rotor blades, and testing will be conducted on a demand basis.

Iterations from one step to the next design step were of prime consideration in establishing the plans for the rigs and engine. Because of the unknown performance of the ceramic designs to be evaluated, the test plans shown (while used to establish program costs and manpower) will be subject to adjustment and may vary significantly with program execution.

In formulating the rig and engine test plans, the rig programs were established to be relatively short tests, cyclic in nature, with a level of instrumentation that should help identify problems to be encountered or performance characteristics as required. It was found that engine testing could be accomplished for approximately the same cost (or less) as rig tests in many cases. Engine testing is preferred to rig testing because of the realistic environment in the engine and the inability of rigs to exactly reproduce the engine environment.

The rig testing and engine testing candidate plans are discussed in the following paragraphs. The target numbers of hours, numbers of components, numbers of tests, or numbers of rig builds are given depending on which of these factors is most significant from a technical accomplishment consideration. Table XVIII is a summary of the rig test plan.

Regenerator Rig Testing

The regenerator rig will be used to evaluate the various regenerator system configurations developed during the program. The drive system for the regenerator plus system performance (disks and seals) are evaluated under actual steady-state engine conditions over the speed range Drive torque, disk effectiveness, pressure drop, and seal leakage data are obtained during rig testing. In year 3, a high-temperature rig will be used to evaluate ceramic regenerator hardware at temperatures to 982°C (1800°F).

During the first year, two regenerator rig test programs are planned. The first is designed to evaluate hub-driven ceramic disk and seal hardware and provide feedback for the design activity. The second test program is intended to evaluate the first rim-driven ceramic disk hardware which was designed early in the year. These two test programs will accumulate testing which will provide drive system functional checkout and torque data and disk effectiveness and pressure drop and seal leakage data. Limited durability data will be also obtained.

TABLE XVIII. CANDIDATE TESTS—BENCH AND RIG PROGRAM

Year	1	2	3	4	5
Rig Test Programs					
Burner and Cascade Rig	430 hr	445 hr	560 hr	790 hr	420 hr
Cold Flow Rig	6	6 Gasifier Nozzles	6 Gasifier Nozzles	6 Gasifier Nozzles 12 Power Turbine Nozzles	6 Gasifier Nozzles 12 Power Turbine Nozzles
Regenerator Internal Leakage Rig	14 Disks	10 Disks	10 Disks	8 Disks	8 Disks
Regenerator Seal Leaf Leakage Rig	12 Seals	12 Seals	12 Seals	12 Seals	12 Seals
Regenerator Rig—High Temperature	192 hr	224 hr	224 hr	324 hr	284 hr
Vibration Rig	Nozzle & Shroud	Nozzle, Plenum, & Blades	Nozzle, Plenums, & Blades	Nozzles, Plenum, Blades, & Exhaust Diffuser	Nozzles, Plenums, & Exhaust Diffuser
Spin Pit	No	34 Tests	34 Tests	34 Tests	4 Tests
Compressor Rig Tests	No	6 Builds	3 Builds	3 Builds	---
Turbine Rig Tests	No	4 Builds	2 Builds	2 Builds	---

During years 2 through 5, regenerator hot rig testing of each regenerator system configuration will be conducted. Starting with year 3, testing will be at a maximum temperature of 1800°F. Two supporting ambient temperature rigs are provided to help develop regenerator system components. A disk internal leakage rig will be used to measure the leakage through the walls of the matrix that occurs as the result of fabrication defects or material porosity. A seal leaf leakage rig will be used to measure seal leaf leakage over the engine pressure (speed) range. These ambient temperature rigs will be used to evaluate a majority of the disks and seals to be tested in the regenerator hot rig. These data will provide feedback to the next stage of design activity.

Cold Flow Rig Testing

The cold flow rig will be used to evaluate the various gasifier and power turbine nozzle configurations developed during the program. Information to be obtained will consist of nozzle flow capacities, data for prediction of engine operating characteristics, and functional checks on ceramic components under aerodynamic loading. The cold flow rig will be capable of simulating engine pressure and flow conditions over the speed range with ambient temperature air.

During each of the first three years, six gasifier nozzle assemblies will be tested. The first-year configuration will feature individual vanes in a metal ring; the following years will feature ceramic assemblies with integral shrouds. The fourth- and fifth-year configurations will consist of ceramic gasifier and two-stage power turbine nozzle assemblies with integral shrouds. Each year, 18 tests of the gasifier and two-stage power turbine nozzles will be conducted.

Burner and Cascade Rig Testing

The burner and cascade rig will be used to evaluate the various turbine nozzle and shroud assemblies, metal and ceramic combustor, plus metal and ceramic plenums developed during the program. The burner and cascade rig provides testing of components with aerodynamic loading plus thermal effects that simulate actual engine conditions. In the fourth year, a high-temperature burner and cascade rig will be used to evaluate ceramic components at temperatures up to 1241°C (2265°F).

Various combustor configurations plus turbine nozzle and shroud assemblies will be tested during all five years. For the first year and part of the second year, combustor testing will be concentrated on metal configurations; the remaining combustor tests will be with ceramic components. During the second year, ceramic plenum work will begin and will continue through the fifth year. During all five years, burner rig work in support of engine testing will be conducted as required. The following is a summary of the work planned for the burner and cascade rig:

Year	Component tested
1	Metal combustor and engine support Separate ceramic gasifier tip shroud Individual ceramic gasifier nozzle vanes
2	Metal combustor (ceramic simulator) and engine support Gasifier nozzle & shroud assembly Ceramic plenum
3	Introduce high temperature burner rig Metal combustor (ceramic simulator) and engine support Gasifier nozzle & shroud assembly Ceramic plenum
4	Metal combustor and engine support Ceramic combustor Ceramic plenum Gasifier nozzle & shroud assembly Power turbine nozzle & shroud assembly
5	Metal combustor and engine support Ceramic combustor Ceramic plenum Gasifier nozzles shroud assembly Power turbine nozzle & shroud assembly

Vibration Testing

Vibration bench testing consists of two parts: (1) shaker table frequency surveys for all of the various stationary ceramic parts and (2) more extensive testing of turbine blades. For each turbine blade design, a frequency survey of 10 separate blades is run from 0 to 30,000 Hz to locate resonances. Mode shapes are mechanically measured on two blades, the stress distribution in the blade is measured on one blade, fatigue strength is determined for five blades, and the damping characteristics are defined for 1 blade (19 total blade tests per design). Excitation of the blade is provided by an acoustic siren. The following is the breakdown for vibration testing:

Year 1	
One gasifier nozzle with individual ceramic vanes	shaker table
One separate gasifier nozzle shroud	
Year 2	
One integrated gasifier shroud and nozzle	shaker table
One metal inlet plenum	
One gasifier blade design (2 materials)	38 blade tests
Year 3	
One gasifier nozzle and shroud	shaker table
Two ceramic inlet plenums	
One new gasifier blade design (2 materials)	38 blade tests
Year 4	
One new gasifier nozzle and shroud	shaker table
Two power turbine nozzles	
One new plenum	
One ceramic exhaust diffuser	
One new gasifier blade design (2 materials)	38 blade tests
One power turbine design (2 stages)	38 blade tests
Year 5	
One new gasifier nozzle design	shaker table
Two new power turbine nozzles	
Two new plenums	
One exhaust diffuser	

Spin Pit Testing

The spin pit will be used to evaluate the various ceramic gasifier blade configurations developed during the program. Spin pit testing provides centrifugal loading of the blade and blade to wheel attachment at ambient temperatures.

Spin pit testing will begin in the second year with testing of the gasifier blades. Thirty-four tests are planned to evaluate the blades and blade attachment. The third and fourth years will also include 34 tests each year. The 34 tests are described as follows:

- Spin two blades to overspeed failure - 10 tests
  (two ceramic materials × 5 tests)
- 110% proof spin tests on blades - 12 tests
  (two materials × 6 engine tests)
- 110% proof spin tests on rotor assemblies - 6 tests
  (two materials × 3 rotor assemblies)
- Cyclic spin tests 10% to 110% - 500 cycles - 6 tests
  (two materials × 3 tests)

Spin pit testing in the fifth year will consist of 110% proof spin tests of four rotor assemblies.

Compressor Rig Testing

Compressor rig testing will be accomplished to achieve an increase in efficiency while decreasing compressor airflow from 1.56 kg/s (3.45 lb/sec) to 1.37 kg/s (3.03 lb/sec). Corrected flows (NASA std) drop from 1.66 kg/s (3.65 lb/sec) to 1.45 kg/s (3.20 lb/sec). In the initial year of the program, design analysis and correlation of existing data will lead to new design parameters to be evaluated in subsequent years. In year two, six compressor rig builds are identified, and in each build more than one design variation will be evaluated (such as rematching, alternate diffuser passages and variations in instrumentation readings, yaw probe surveys of temperature, pressure and angle). All tests will be heavily instrumented to provide maximum diagnostic data on which to base further development.

Additional compressor builds are shown in each of the two subsequent years to achieve refinements and improvements to compressor efficiency. This type compressor program is necessary to achieve the technology improvement being sought.

Turbine Rig Testing

Turbine rig testing is required to achieve two program objectives:

- Incorporate ceramic components in the turbine
- Incorporate improved turbine efficiency while preserving the basic engine configuration

The incorporation of ceramic turbine vanes and blades will require new aerodynamic configurations of these airfoils. The current air cooled metal vane is not near to optimum for minimum thermal and mechanical stresses in ceramic vanes and must be replaced with a new row of airfoils. Similarly, ceramic blades will require a new configuration in the rotor because of aerodynamic, vibration, and structural considerations. A turbine rig program is mandatory to achieve these changes. Simultaneously, an opportunity to achieve improved aerodynamic

performance is presented and will be utilized to achieve the projected fuel savings in the program objective. This turbine rig program will be the evaluation phase of performance parameters achieved with the new configurations required to place ceramic components in both the gasifier and power turbines.

The power turbine in the current engine is structurally inadequate above the 1132°C (2070°F) temperature level and must be replaced with a new two-stage power turbine to run the 1241°C (2265°F) turbine inlet temperature conditions. This requires evaluations in the turbine rig program to consolidate and improve performance in hand and achieve improved performance necessary for the program objective.

The turbine rig test program is designed to evaluate new airfoils required including ceramic optimized geometries. Specific tests planned are

- Nozzle Vane Aspect Ratio Evaluation
- Rotor Blade Aspect Ratio and Tip Clearance Tests
- Trailing Edge Thickness Effects (blade and vane)
- Airfoil Surface Roughness Effects (blade and vane)
- Gasifier and Power Turbine Performance Analysis Tests

In addition to the new turbine airfoils and flowpath walls, the turbine exhaust diffuser will be new and must be evaluated. A rig program to achieve optimum power turbine performance (considering regenerator blockage) by proper exhaust diffuser geometry design will be conducted. This program will also provide as uniform a flow into the regenerator as possible to maximize regenerator effectiveness.

Builds on the turbine test rigs will be initiated in the second year of the program addressing the 1132°C (2070°F) engine and continue through the fourth year of the program when the 1241°C (2265°F) turbine geometry will be completed.

Engine Testing

Three types of engine testing are planned in this program to accomplish the following:

- Evaluate ceramic component capabilities in special, accelerated tests
- Evaluate engine performance (specific fuel consumption, emissions, horsepower, component efficiencies, etc)
- Evaluate durability of ceramic materials and other engine components operating with typical duty cycles encountered in buses and trucks. This endurance will be accumulated at advancing turbine inlet temperatures [1033°C (1900°F) to 1241°C (2265°F)].

Figure 36 is a summary of the engines planned in the program and target endurance hours used for planning purposes. In recognition of the fact that high-risk programs require adjustments to planning as progress shows either greater or less success than planned, adjustments to the proposed hours will be made as technical accomplishment, timing, and funds will permit. An objective of this program is to qualify ceramic components for introduction in a production engine program. The endurance hours shown will provide the opportunity to address this objective.

Figure 36 indicates that advancing turbine inlet temperature progresses from the current engine, 1002°C (1835°F), to the program target engine of 213 mg/W·h (0.35 sfc) over the five-year period in definite steps. Each step is designed to provide increasing technology for a succeeding step in temperature and performance. This evaluation of technology should promote both early acceptance of ceramic components and an advanced temperature capability applicable to highway gas turbine engines.

Work Breakdown Structure

The recommended work breakdown structure (WBS) for the proposed five-year plan is shown in Table XIX. This WBS is the result of many iterations to provide a manageable and concise way of tracking the technical progress and financial expenditures by work packages.

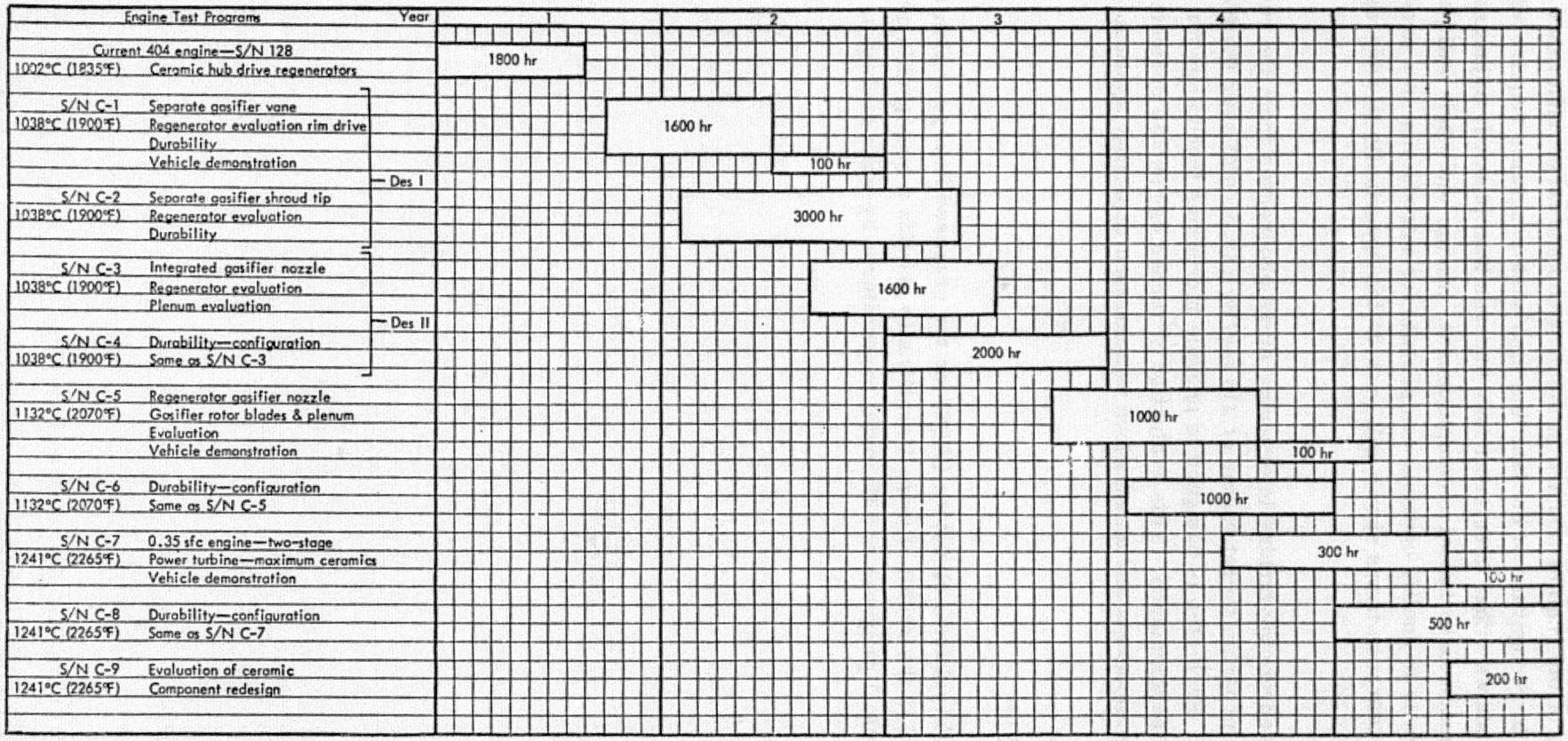

Figure 36. Candidate hours—engine test program.

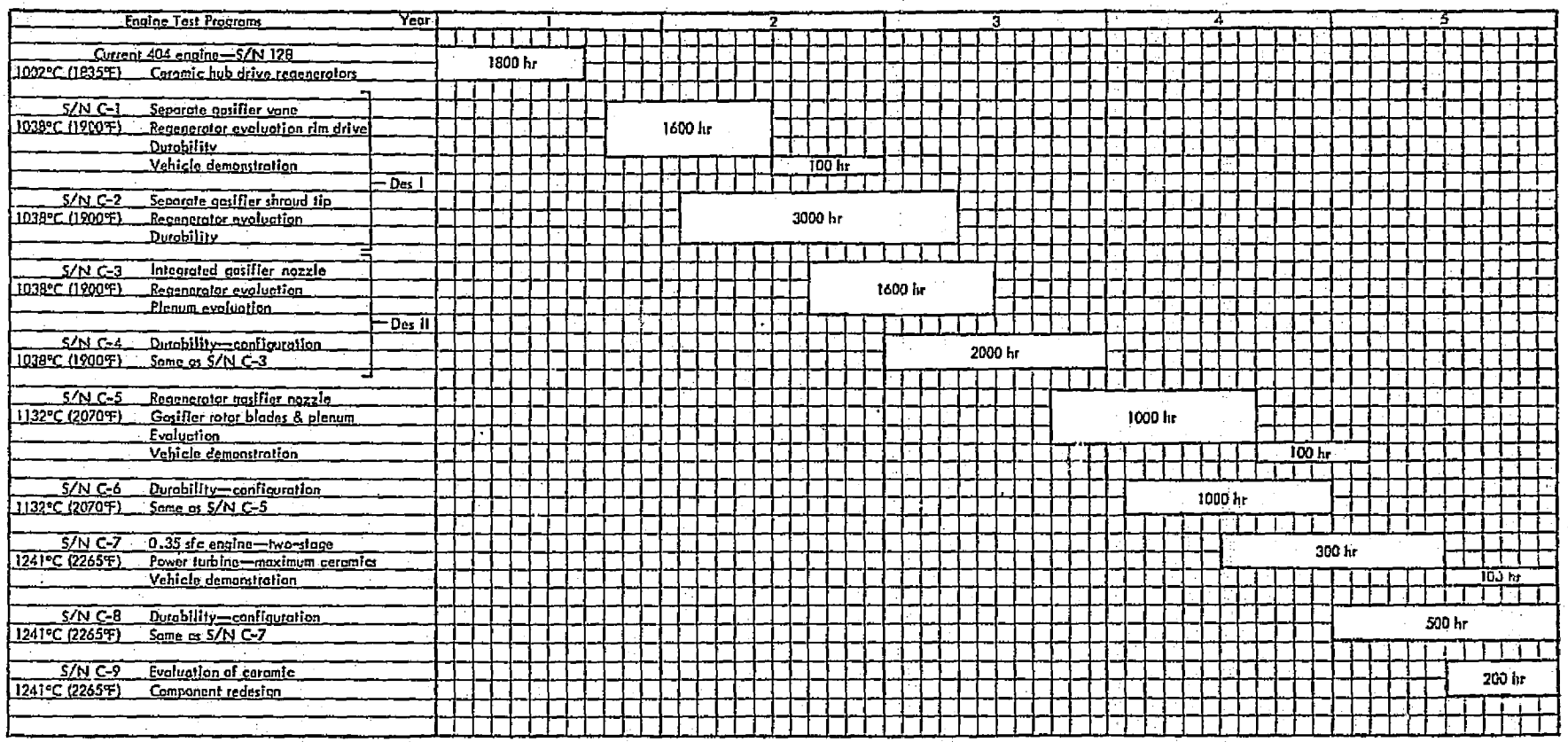

Figure 36. Candidate hours—engine test program.

TABLE XIX. WORK BREAKDOWN STRUCTURE

1.0 Engines
- 1.1 Design
  - 1.1.1 Design Engine Modifications
  - 1.1.2 Design Two-Stage Metal Power Turbine
  - 1.1.3 Performance Analysis
  - 1.1.4 Support for Design, Fabrication, and Test
  - 1.1.5 Engine Controls
  - 1.1.6 Compressor
- 1.2 Procurement and Fabrication
  - 1.2.1 Engine Hardware (nonceramic)
  - 1.2.2 Assembly Tools
  - 1.2.3 Test Equipment—Instrumentation, etc
- 1.3 Bench and Rig Tests
  - 1.3.1 Controls Bench Test
  - 1.3.2 Two-Stage Metal Power Turbine Vibration Test
  - 1.3.3 Compressor Vibration Test
- 1.4 Engine Assembly and Test
  - 1.4.1 Hub Drive Regenerator Test Engine
  - 1.4.2 1038°C (1900°F) Basic Engine—Design I
    - 1.4.2.1 Engine S/N C-1
    - 1.4.2.2 Engine S/N C-2
  - 1.4.3 1038°C (1900°F) Basic Engine—Design II
    - 1.4.3.1 Engine S/N C-3
    - 1.4.3.2 Engine S/N C-4
  - 1.4.4 1132°F (2070°F) Improved Engine
    - 1.4.4.1 Engine S/N C-5
    - 1.4.4.2 Engine S/N C-6
  - 1.4.5 1240°C (2265°F) Improved Engine
    - 1.4.5.1 Engine S/N C-7
    - 1.4.5.2 Engine S/N C-8
    - 1.4.5.3 Engine S/N C-9
- 1.5 Vehicle Test
  - 1.5.1 Engine S/N C-1
  - 1.5.2 Engine S/N C-5
  - 1.5.3 Engine S/N C-7

2.0 Ceramic Materials Development
- 2.1 Materials Characterization
- 2.2 Component Materials Qualification
- 2.3 Support for Design, Fabrication, and Test

3.0 Ceramic Regenerator
- 3.1 Design and Development
- 3.2 Procurement and Fabrication
- 3.3 Rig Test
  - 3.3.1 Regenerator Hot Performance Rig
  - 3.3.2 Seal Leaf Leakage Rig
  - 3.3.3 Disk Internal Leakage Rig
  - 3.3.4 Regenerator System Bench Tests

4.0 Ceramic Combustor and Turbine Components
- 4.1 Design
  - 4.1.1 Gasifier Turbine Nozzle and Shroud
  - 4.1.2 Gasifier Turbine Blade
  - 4.1.3 Turbine Inlet Plenum
  - 4.1.4 Power Turbine Nozzle
  - 4.1.5 Combustor
  - 4.1.6 Turbine Exhaust Diffuser
- 4.2 Procurement and Fabrication
  - 4.2.1 Gasifier Turbine Nozzle and Shroud
  - 4.2.2 Gasifier Turbine Blade
  - 4.2.3 Turbine Inlet Plenum
  - 4.2.4 Power Turbine Nozzle
  - 4.2.5 Combustor
  - 4.2.6 Turbine Exhaust Diffuser
- 4.3 Bench and Rig Tests
  - 4.3.1 Gasifier Turbine Nozzle and Shroud
    - 4.3.1.1 Burner Rig Test
    - 4.3.1.2 Vibration Test
    - 4.3.1.3 Cold Flow Test
  - 4.3.2 Gasifier Turbine Blade
    - 4.3.2.1 Interface Material
    - 4.3.2.2 Burner Rig Test
    - 4.3.2.3 Vibration Test
    - 4.3.2.4 Spin Test
  - 4.3.3 Turbine Inlet Plenum
    - 4.3.3.1 Burner Rig Test
    - 4.3.3.2 Vibration Test
  - 4.3.4 Power Turbine Nozzle
    - 4.3.4.1 Burner Rig Test
    - 4.3.4.2 Vibration Test
    - 4.3.4.3 Cold Flow Test
  - 4.3.5 Combustor
    - 4.3.5.1 Burner Rig Test
    - 4.3.5.2 Vibration Test
  - 4.3.6 Turbine Exhaust Diffuser
    - 4.3.6.1 Burner Rig Test
    - 4.3.6.2 Vibration Test

5.0 Component Aerodynamic Research
- 5.1 Test Equipment Design
  - 5.1.1 Compressor
  - 5.1.2 Turbines
  - 5.1.3 Turbine Exhaust Diffuser
  - 5.1.4 Regenerator Flow Distribution
- 5.2 Rig and Test Equipment Hardware
  - 5.2.1 Compressor
  - 5.2.2 Turbines
  - 5.2.3 Turbine Exhaust Diffuser
  - 5.2.4 Regenerator Flow Distribution
- 5.3 Testing and Data Reduction
  - 5.3.1 Compressors
  - 5.3.2 Turbines
  - 5.3.3 Turbine Exhaust Diffuser
  - 5.3.4 Regenerator Flow Distribution

6.0 Program Management
- 6.1 Program Management
- 6.2 Reporting Requirements

TECHNICAL APPROACH

This section is a description of the technical approach toward implementing the engine development plan. The ceramic component design and the design approach are discussed for each ceramic part, as are the metal component modifications. The aerodynamic component development details for the compressor, turbines, and exhaust diffuser and the regenerator flow distribution are also discussed. Finally, the details of the material aspects of ceramic component design including the materials development program are presented.

CERAMIC COMPONENTS

Regenerator System

Although the regenerator system of the base line engine represents a highly developed aerodynamic/thermodynamic component, substantial improvements in engine performance can be projected with continued development effort. The base line sensitivities presented in Table IV indicate that engine performance improvements can result from increased regenerator operating temperature capability, increased effectiveness, reduced leakage, and reduced pressure loss. These improvements must also have inherently acceptable reliability/durability characteristics. In addition, the regenerator disk mount and drive systems must be designed and developed to accommodate significantly higher temperatures.

Disks and Seals

The five-year plan includes the development of a rim-driven ceramic regenerator system with a performance level matched with the 1241 °C (2265 °F) engine components to produce 213 mg/W·h (0.35 lb/hp-hr) sfc. At least two disk matrix geometries and two ceramic materials will be evaluated.

The first year is devoted to demonstrating the feasibility of an alumina silicate (AS) regenerator featuring rim drive and hub support. The rim drive ring gear will be elastomer mounted. Performance will be compromised because of disk and seal size limitations dictated by the engine block casting.

The hot seals to be used in the initial test activities will utilize a nickel oxide crossarm wear face and a graphite rim wear face. The maximum temperature capability of the regenerator system will be limited to 774 °C (1425 °F) by graphite oxidation.

The design emphasis late in the first and early in the second year will be on an improved-performance regenerator system plus improvements in the rim drive-hub mount system as indicated by previous testing. New technology will be incorporated into the seals, disk, and drive system. The performance improvements are planned to result from development of the thin-

wall AS material disk or a new rectangular matrix disk plus seal design improvements. The maximum temperature capability of the seal design will be 982°C (1800°F), which is adequate for operation of the 1241°C (2265°F) engine. Testing during the second year will evaluate the first year hardware.

The design emphasis late in the second and early in the third year will be on performance and on achieving the 982°C (1800°F) maximum seal temperature capability. Performance improvements will be explored with a new ceramic disk rectangular matrix geometry and or flow area changes. A new ceramic disk material will also be evaluated. Any rim drive system modifications indicated by previous testing will be incorporated.

Testing during the third year will evaluate the second year hardware.

Design activities late in the third year will provide a second round of performance improvement work. Two ceramic materials and matrix geometries will be evaluated along with seal and drive system improvements indicated by third year rig testing. The 982°C (1800°F) maximum temperature capability will be maintained in the seal design.

The design emphasis during the fourth year will be on defining the best performance configuration with the best durability life at 982°C (1800°F) maximum temperature. Testing of the third year hardware will be used to define the best ceramic disk material and matrix geometry. Seal and drive system improvements indicated by previous testing will be incorporated.

During the fifth year, fabrication and test evaluation of the fourth year design hardware will be accomplished, ending with an engine demonstration of 213 mg/W·h (0.35 lb/hp-hr) sfc at 1241°C (2265°F) turbine inlet temperature with a 982°C (1800°F) regenerator inlet temperature limit.

Disk Drive and Mounting

The dominant tasks involved in the design and development of a rim drive system for a ceramic regenerator disk are defined in terms of essentially two features, each of which is directly related to the disk rim gear: first, the gear-to-disk attachment, and second, the support system for the gear and disk assembly. The balance of the rim drive system, in contrast, is within the scope of experience in the base line engine development program, which includes a rim drive system for hub-mounted metal disks. (In another variation of the metal disk/hub drive regenerator system used in the base line engine, testing of hub-driven ceramic disks will be conducted.)

The difficulty of satisfactorily attaching a peripheral gear to a ceramic disk is well known and arises primarily from two inherent characteristics of ceramic: its very low thermal coefficient of expansion and its lack of ductility. (These characteristics, in fact, must be thoroughly addressed when ceramic parts are mounted in any metal engine parts subjected to elevated temperatures.)

Design of a gear and disk assembly in which a 360-degree band of elastomer is used as the attachment medium was begun. Elastomer appears promising as a short-term solution to the attachment problem, but the capability of any elastomer to adequately retain its properties over extended periods of engine operation at the significantly higher disk temperatures that will result from the scheduled increases in turbine temperature is unknown. Early in the program, heat transfer, stress, and deflection analyses of the elastomer-bonded gear and disk assembly will be made to ensure the optimization of the initial design. Other attachment concepts will be studied and analyzed as their merits may warrant; then at least one alternate will be selected for test evaluation.

The selection of the best method of supporting the gear and disk assembly, at the hub or rim, requires a careful trade-off study of several design considerations. A hub mount is attractive because of its greater simplicity and resultant lower cost, but it imposes greater loads upon the disk matrix, which transmits both the pinion-to-gear separating load and the weight of the gear and disk to the hub spindle. Therefore, a rigorous stress analysis of the disk matrix, particularly in the hub area, is essential for determining the disk's tolerance for these loads. In a rim mount system, the hub is essentially unloaded and the disk rim is not subjected to the pinion-to-gear separating load as in the case of a hub mount, except to the extent that the gear is distorted out of round by the pinion and/or the rim support rollers. In either support system, the disk matrix is also subjected to stresses arising from thermal gradients and face seal friction. A rim support system requires more bearings (a pair for each rim roller), although they are far more accessible for oil or grease lubrication than one in the hub, where a spherical carbon bearing is a leading candidate.

The drive system will be affected by the scheduled increases in engine operation temperature in at least two areas: first, by the rise in the disk rim temperature, which is particularly significant in the case of an elastomer gear attachment; and second, by the greater thermal transients in the engine block and regenerator, insofar as they affect the center-to-center distance between the drive pinion and gear. Although the pinion and gear mesh will be relatively insensitive to the variations in tooth engagement that result from the thermal gradients, sufficient clearance must be provided to avoid interference at any time.

Design studies of the hub and rim support systems were started, but the hub support was selected as the best starting point for regenerator evaluation testing because of its much greater adaptability to the existing engine housing castings and also because of experience with hub-mounted disks. As a result, testing will begin earlier, and at less expense, than would be possible with a rim support system. Meanwhile, analytical work will proceed on both systems; if the results indicate that a rim support system should be developed in addition to, or in lieu of, the hub support system, then appropriate action will be taken. It is recognized, of course, that the pertinent analyses may indicate that the two systems are equally feasible, in which case the ultimate choice would be made on the basis of evaluation of test results (with emphasis on durability) and/or cost comparisons.

Four basic rim drive configurations will be designed and analyzed, with fabrication and systematic test evaluation following as necessary. (These are designated as Designs "A," "B," "C," and "D.") These four designs represent the drive combinations that are possible with two disk support designs (hub or rim) and two gear-to-disk attachment designs (elastomer or an alternate design yet to be selected). Other design variations in the drive system are certain to be introduced and/or some of these four eliminated as rig and engine test evaluation proceeds, but these four are the major ones that will receive attention at the onset of the program.

Design "A" - elastomer attachment/hub support - has been selected as the initial candidate for fabrication and test evaluation in the regenerator rig and an engine. Design "B" - elastomer attachment/rim support - will also be released for both rig and engine test evaluation, although the scope of that testing will be contingent upon the results of Design "A" testing. For example, if the durability of the Design "A" drive system hub features are sufficiently promising (even though design modifications may be necessary), testing of Design "B" may be limited to the rig, or postponed. In any event, Design "C" will be released shortly after Design "B" to assure the timely availability of an alternate gear-to-disk attachment that avoids the use of elastomer. It will be adapted to either or both the hub and rim support systems (resulting in Design "C" or Design "D," respectively), depending upon their development status.

Ceramic Gasifier Nozzle and Tip Shroud

Improvements in engine specific fuel consumption require significant increases in turbine inlet temperature. Substantial oxidation and sulfidation improvements for small metal gasifier nozzle vanes with elevated turbine inlet temperature cannot be achieved with currently known alloy and coating combinations unless elaborate cooling schemes are employed. Sensitivity studies indicate that a 1% increase in gasifier nozzle cooling air decreases engine sfc by 0.6%.

Introduction of a gasifier ceramic vane will eliminate the need for cooling the gasifier nozzle at current turbine inlet temperature levels and also will permit escalating the turbine inlet temperature levels as required in the program. The ceramic gasifier nozzle scheme is discussed in this report (see Figure 19). At present, it is anticipated that this design scheme can be used as the turbine inlet temperature is escalated. Some revision will be required to accommodate flow path changes and possible material changes; however, the basic design scheme offers sufficient flexibility to allow the design modifications for increased temperature to be based on design test experience.

The introduction of a ceramic gasifier tip shroud is based primarily on the need to achieve improved gasifier rotor clearance. Ceramic materials offer the advantage of having a low coefficient of thermal expansion which consequently permits closer control of the rotor tip clearance. Therefore, a ceramic rotor tip shroud combined with an abradable coating permits major improvements in the control of rotor tip clearance over the current metal design. In

addition, increases in turbine inlet temperature will also require either improved materials and coatings for oxidation resistance or additional cooling air to maintain metal temperature near current levels. Use of a ceramic tip shroud will allow the scheduled increases in turbine inlet temperature without increases in shroud cooling air. The combination of improved rotor tip clearance and the ability of a ceramic shroud to function without increases in cooling air will effect improvements in engine sfc. The design scheme selected for the ceramic gasifier turbine tip shroud is shown in Figure 19 and discussed in the study section of this report. The basic design selected can be used as the turbine inlet temperatures is increased. However, as was the case for the ceramic gasifier nozzle, modification will be required to accommodate change in flow path size.

The turbine general arrangement for the 1132°C (2070°F) engine is shown in Figure 20; that of the 1241°C (2265°F) engine is presented in Figure 21. Examination of these arrangements shows that the gasifier nozzle and shroud concepts are similar to the design presented in Figure 19; the differences are related entirely to the flow path changes. The construction details of the ceramic nozzle and tip shroud are described in the 1038°C (1900°F) study engine description earlier in this report.

To gain experience with ceramic turbine parts, the first two 1038°C (1900°F) development engines, designated Design I engines, will use modified versions of the ceramic nozzle and tip shroud described earlier. The first engine will be built and tested with a ceramic tip shroud and a base line metal nozzle assembly. The second engine will be built and tested with ceramic vanes installed in place of half of the metal vanes and a metal tip shroud. These designs are designated as individual ceramic tip shroud and individual ceramic vanes as opposed to the integrated ceramic tip shroud and vane assemblies used in the third and fourth 1038°C (1900°F) engines, which are designated Design II engines.

Ceramic Gasifier Turbine Rotor Assembly

The primary benefit associated with the incorporation of ceramics in the gasifier turbine rotor assembly is to permit increased engine cycle temperature levels without the associated severe penalties for rotor blade cooling using engine cycle air. Aerodynamic blade shape penalties are also incurred when air cooling is applied to turbines in the small flow size of the base line engine. At temperatures above 1038°C (1900°F), the gasifier turbine metal blade life is reduced rapidly, and beginning with the 1132°C (2070°F) engine, the blading temperature capability must be significantly upgraded. A new configuration will be designed which would have potential for development for the 1241°C (2265°F) application. Gasifier blade and disk temperature capability is significantly upgraded through the use of ceramic blades.

A composite construction utilizing ceramic blades in a metal wheel was selected for this effort. A unitized ceramic rotor was considered to be beyond the scope of near-term ceramic capabilities at the rotational technology level of the engine. The rotor assembly is shown in

Figure 37, and a preliminary sketch of the blade geometry is shown in Figure 38. The ceramic turbine blade shown incorporates a relatively conventional platform and stalk configuration with a single lug dovetail. The stalk and dovetail are aligned with the airfoil to minimize bending induced by centrifugal effects. The turbine blades are retained axially in the wheel by segmented ring elements at both the forward and rear wheel faces. These elements are retained to the wheel by a coned pilot surface and by rivets. The segmented ring elements also seal the cavities between blades to prevent leakage of turbine working gas around the blade row.

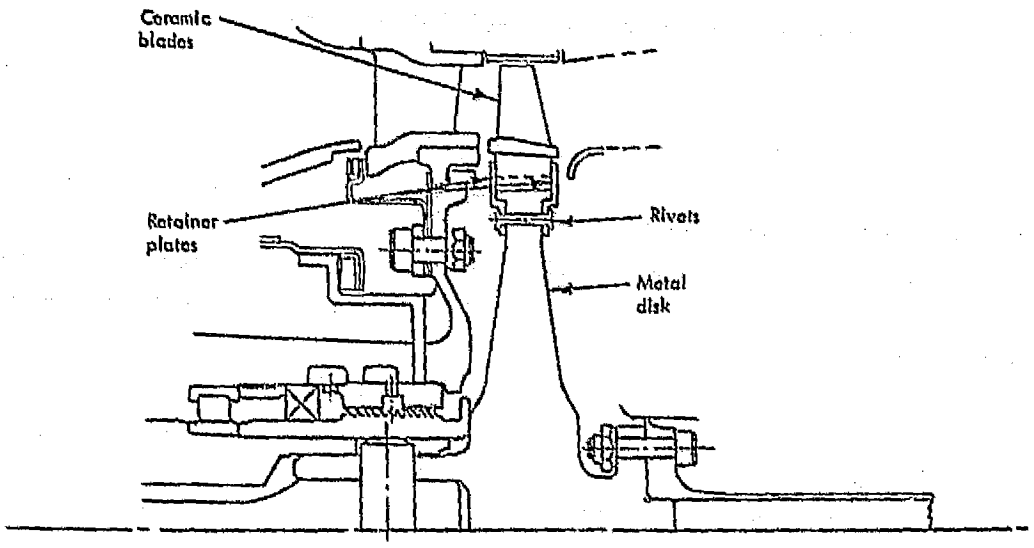

Figure 37. Gasifier turbine configuration for 1132°C (2070°F).

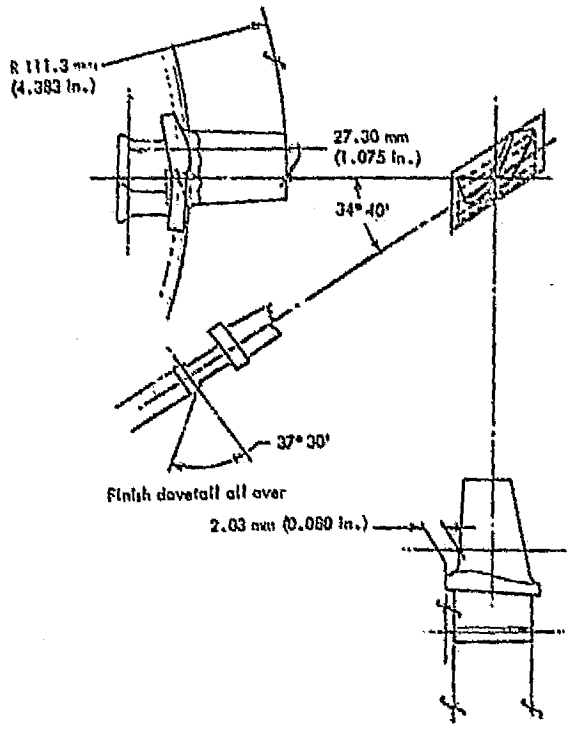

Figure 38. Ceramic gasifier turbine blade.

The selected geometry for the blade can be provided from any of the currently available high-strength silicon carbide or silicon nitride materials. Further, any of the currently used processes, such as molding, slip casting, and "iso-pressing," can be used to form the green body. Dimensional tolerance capabilities of many processes are not established, but the design can be machined as required including machining all over to meet required tolerances in development stages.

The gasifier rotor design provides a disk geometry with inherent advantages for improved cyclic life. Disk outermost continuous fibers are not exposed to the gas path, and thermal protection is provided by the blades and blade retainer plates. This will significantly reduce radial temperature gradients and resulting stress levels during transient conditions. However, careful attention must be given the blade attachment dovetail design to provide adequate cyclic life in this area.

Blade, attachment, and disk will be designed with the same criterion used for the base line metal rotor (15,000 hours useful life and with adequate cyclic life—assuming 7500 start-stop cycles and 37,500 run-brake-run cycles). This can be accomplished with currently available design methodologies. A well developed computer program is available which can optimize the dovetail shape while recognizing a wide range of material characteristics, stress limits, dimensional limitations, and low cycle fatigue limits. Other tools including two-dimensional and three-dimensional heat conduction and stress analyses will be used. However, design criteria are dependent upon adequate statistical materials property data for both metals and ceramics. Active pursuit of the candidate ceramic materials characterization program is imperative if success is to be achieved in the blade and attachment design.

Revisions in gasifier turbine airfoil shape and flow path radii will be required between the 1132°C (2070°F) and 1241°C (2265°F) engine designs to obtain desired performance levels. However, the same blade attachment concept will be used in both engines, and the experience gained in the 1132°C (2070°F) engine program will be directly applicable to the 1241°C (2265°F) design.

To partially offset increased gas temperature effects on turbine disk temperature gradients and resulting thermal stress levels, disk cooling airflow rates are increased for both rotors as follows:

	1002°C (1835°F) Base line engine	1132°C (2070°F) Engine	1241°C (2265°F) Engine
Gasifier Disk Front Face	0.53%	0.75%	0.89%
Gasifier Disk Rear Face	0.55%	0.50%	0.63%

These increased flow rates are included in the engine performance analyses.

Ceramic Power Turbine Nozzle and Tip Shroud

The increasing temperature levels in the program necessitate a change to a ceramic material in the power turbine nozzle assembly as the metal long-term oxidation limits are exceeded as established in the study section of this report. This change is required in the 1241°C (2265°F) engine in order to meet the 15,000-hour life objective. A major redesign activity is scheduled to achieve a configuration that is compatible with the life requirements and avoids the performance penalty associated with the use of cooling air.

The design will feature a two-stage power turbine with ceramic nozzles in both stages. The two-stage design is required to improve the power turbine efficiency, which is discussed subsequently. The maximum local (hot spot) gas temperatures at the first- and second-stage nozzles will be 1171°C (2140°F), and 1082°C (1980°F), respectively, at design point conditions. These temperatures will increase approximately 55°C (100°F) at off-design operating conditions.

The design will also feature ceramic power turbine rotor tip shrouds in the two-stage power turbine design. The ceramic tip shrouds allow improvement in rotor tip clearance and also eliminate the need for cooling a metal shroud. Both of these advantages translate into improved engine sfc.

The scheme for the ceramic power turbine nozzle design is shown in Figure 21. The construction details are described under the 1204°C (2200°F) study engine description earlier in this report. This arrangement must satisfy the 15,000-hour life criteria and the aerodynamic and vibratory constraints needed for a production engine.

Ceramic Turbine Inlet Plenum

The metal temperatures achieved in the base line engine turbine inlet plenum have essentially reached the temperature capability for uncooled metals. The incorporation of surface boundary cooling in the plenum could extend its operating gas temperature capability to some intermediate level. This cooling would not represent an engine performance penalty if regenerated air were used. However, at the engine cycle temperatures of interest in this program, regenerated air is inadequate for cooling of the plenum. To avoid the engine performance penalty associated with the use of compressor discharge air for cooling, a ceramic turbine inlet plenum will be used.

Figure 7 illustrates the gas temperature characteristics and indicates the metal plenum limits. A change to a ceramic plenum appears to be necessary at the 1038°C (1900°F) engine rating temperature to meet the 15,000-hour life objectives because the plenum inner surface "sees" engine rating temperature levels and the outer surface "sees" regenerated air temperatures. However, the ceramic plenum will not be introduced until the 1132°C (2070°F) engine because

of the risk associated with introducing a complex ceramic part early in the demonstration program. In addition, the life of the metal plenum should be adequate for the demonstration and scheduled durability of the 1038°C (1900°F) engine.

The construction of a ceramic plenum has been conceived as shown in Figure 20. The ceramic plenum is configured in three parts to facilitate withdrawal of the part or patterns from casting or molding tooling and also to diminish the part-induced thermal stresses. The construction details are described under the 1132°C (2070°F) study engine description earlier in this report. Initially, a metal combustor will be piloted on the OD of the plenum entrance, but in the final 1241°C (2265°F) engine, a ceramic combustor will engage the plenum opening. The unsupported combustor shell will impose a slight compressive load on the plenum inlet flange.

Life of the ceramic plenum will be a function of the ceramic material oxidation/deterioration characteristics and ceramic material fracture characteristics resulting from the surface temperature distributions and mechanical stresses, neither of which can be adequately predicted at this stage. During the program, this information will be developed along with the tools to make a life assessment.

Ceramic Combustor

The base line engine uses regenerated air (combustor inlet) to provide cooling to the combustor dome and walls by transpiration, using Lamilloy® * material.

As the engine rating temperature is increased in the program, the temperature of the cooling air available for transpiration cooling of the combustor walls becomes a critical factor. Figure 7 depicts this temperature characteristic and the associated values as limited by the metal temperature of the combustor walls. It is apparent that a change to a ceramic material is required at the 1241°C (2265°F) engine rating temperature.

In addition, a continuous burning combustor is currently in development for the base line engine, which employs a pre-chamber to sustain combustion at very low fuel flows. This combustor will diminish only slightly the engine dynamic braking capacity but will significantly reduce the thermal shock effects on the turbine and regenerator systems which resulted from the combustor relights. The low emission capability is also significantly improved with the pre-chamber configuration. Therefore, the pre-chamber combustor configuration is introduced during the program.

The technology for a ceramic combustor is not as well established, and this phase of the combustor development program will be more extensive. The ceramic combustor will be designed following accepted guidelines for the aerodynamic design of combustors. Thus, such concerns as reaction rate and heat release rate will determine the basic combustor size. Exhaust

*Lamilloy is a registered trademark of the General Motors Corporation.

temperature pattern and requirements and emission requirements will govern the appropriate flow splits and pressure drop. In addition, the problems peculiar to the design of a ceramic combustor require substantial input in such areas as heat transfer and stress. Various regions of the ceramic liner will be modeled in order to determine transient temperature response. Particular attention will be paid to the areas between holes in the combustor and to areas of ceramic and metal interfaces. A finite element model, along with the heat transfer results, will be used in order to predict the local stress distributions in the liner walls. Naturally, as changes in the design are made during development of the ceramic combustor, the results of these analyses must be reviewed. The design of the ceramic combustor must therefore be an iterative loop.

The initial combustor for the 1241°C (2265°F) cycle will consist of a metallic structure made to the shapes and dimensions planned for the desired ceramic version. A ceramic combustor is not easily patched and reworked, as is a metal combustor, so the simulated combustor will eliminate some of the difficulty in the transition from a metal (Lamilloy) combustor to a ceramic combustor. This will permit elimination of any aspects in the design of the combustor which are incompatible with a ceramic design while reworking of the combustor is still relatively easy.

When an acceptable design has been established with a Lamilloy combustor, a ceramic combustor will be fabricated. This ceramic combustor will be rig tested and modified as necessary to establish a design sufficient for engine layout and design. While engine design is under way, combustor rig development will continue. This nine-month period will permit the necessary "fine tuning" of the ceramic design to prepare it to run in the engine. Continued iterations of these practices will be utilized throughout the continued engine development and test program.

A preliminary design of a ceramic combustor has been conceived as shown in Figure 22. The construction of this combustor is described in the 1371°C (2500°F) study engine configuration section of this report. It is anticipated that the pre-chamber combustor technology will be available for incorporation in the 1241°C (2265°F) engine.

The principal difference between the metal and ceramic combustors will be in durability. The life of the ceramic version will be dependent on surface temperature distribution (thermal gradients) and the ceramic material strength characteristics. At this time, there is insufficient information to make a life prediction, but the information and the necessary analytical tools will be developed during the program.

Ceramic Exhaust Diffuser

The increasing temperature levels in the program necessitate a change to a ceramic material in the turbine exhaust diffuser as the metal long-term oxidation limits are exceeded. Figure 9 shows the gas temperature characteristics and indicates the point at which the metal exhaust diffuser is limited. A change to a ceramic material is required in the 1241°C (2265°F) engine in order to meet the 15,000-hour life objective. It is important to note that the average temperature level of the exhaust diffuser at the engine rating condition is not limiting. The actual limitation arises at the off-design operating conditions when the radial temperature profile is superimposed on higher average temperature levels. In this situation, the splitters are particularly vulnerable to local hot spots.

A design scheme for a ceramic exhaust diffuser has been conceived as shown in Figure 21. The construction details are described under the 1204°C (2200°F) study engine description earlier in this report. The walls are simple, annular shapes and are attached to the engine structure through keying arrangements to accommodate differential thermal growth. Splitters are incorporated, as in the metal design, to improve the aerodynamic stability of the diffusing passage. The splitters are also mounted through a slot and post arrangement to accommodate thermal growth.

Relatively high costs associated with the cast ceramic diffuser members indicate that a composite construction using metal inner and outer walls and ceramic splitter elements would be more cost effective. Gas temperatures are diminished along the walls by temperature profile effects whereas the splitters are exposed to the local gas temperature hot spot. This approach will be evaluated during the detail part design phase.

The size and shape of the exhaust diffuser flow passage will be designed to obtain optimum loss characteristics, and, consequently, a negligible performance change is anticipated. The life of the ceramic exhaust diffuser will principally be a function of the surface temperature and strength distribution of the ceramic material which cannot be adequately predicted at this stage. Information developed in the materials characterization effort and the use of elemental models will be combined to make a life assessment as the program progresses.

OTHER ENGINE MODIFICATIONS

Engine Controls

The controls mechanization for the engines will be similar to that currently applied in the base line engine. However, control modifications of two types are proposed for application to the elevated-temperature engines.

The initial modifications would alter only the control settings and dynamics. These changes along with improvements in sensor capability will accommodate the needs for the 1038°C (1900°F) and 1132°C (2070°F) engines.

The control logic and parameters for the 1241°C (2265°F) engine will be significantly different from those of the previous configuration because the high cycle temperatures will make direct sensing and closed-loop control of turbine inlet temperature impractical. Instead, the fuel limiting will most probably be open-loop, based on the utilization of burner inlet temperature along with other engine parameters. The power transfer control may continue to be closed-loop, most probably based on controlling the regenerator inlet (power turbine exit) gas temperature. Also, at this time, the basic electronic control mechanization would be of the microprocessor rather than the analog discrete component type.

Gasifier Turbine Rotor for 1038°C (1900°F) Engine

The base line gasifier rotor will be used without change for the 1038°C (1900°F) engine. Gasifier blade inlet temperature is increased from 1002°C (1835°F) to 1038°C (1900°F). A preliminary review of turbine blade life potential indicates that the gasifier blade stress rupture life would no longer meet the design criterion of 15,000 hours on a mission basis but would have approximately a 4500-hour life, which is considered adequate for the ceramic gasifier nozzle and tip shroud development program.

Cyclic life of the turbine disks will be adversely affected by increased gas temperatures. However, the disks are considered satisfactory for the desired program with minor revisions in cooling flow rates as follows:

	1002°C (1835°F) Base line engine	1038°C (1900°F) Engine
Gasifier Disk Front Face	0.53%	0.64%
Gasifier Disk Rear Face	0.55%	0.55%

(% is percent of compressor mass flow)

The increased flow rates are modest and are included in the performance analyses.

Power Turbine Nozzle for 1038°C (1900°F) and 1132°C (2070°F) Engines

Substantial oxidation and sulfidation improvements will be required for the current power turbine nozzle as the rated turbine inlet temperature is elevated to achieve the specific fuel consumption objectives. Some improvement can be achieved in long-term oxidation and sulfidation resistance by upgrading the power turbine alloy and combining it with a protective coating. The engine configuration rated at 1038°C (1900°F) will have gas conditions that

produce power turbine nozzle metal temperature levels approaching 935°C (1715°F). The existing Hastelloy S alloy and design configuration is satisfactory for use with this engine. The next step in turbine inlet temperature is to a level of 1132°C (2070°F), and metal temperature estimates for the power turbine nozzle approach 1021°C (1870°F). This temperature level will not permit engine testing using the existing Hastelloy S hardware. However, engine operation at this temperature can be achieved by converting to an improved material, such as Mar-M509 alloy, with a corrosion-resistant coating. In addition to the improved material and coating, long-term life (15,000 hr) might require air cooling of the airfoils since the metal temperature predicted is approximately 39°C (70°F) higher than the current temperature level accepted for long life.

Power Turbine Rotor for 1038°C (1900°F) and 1132°C (2070°F) Engines

In the base line engine, the power turbine inlet design point gas temperature is 814°C (1498°F), which increases to 845°C (1554°F) and 938°C (1720°F) in the 1038°C (1900°F) and 1132°C (2070°F) engines, respectively. A preliminary review of power turbine blade stress rupture life potential indicates that life is more than adequate for the 1038°C (1900°F) engine and would have approximately a 7000-hr life in the 1132°C (2070°F) engine application. This is just under half the engine design goal of 15,000 hr but is considered adequate for the development program involving ceramic components in other locations in the engine. Therefore, the base line power turbine rotor will be used without modification in the 1038°C (1900°F) and 1132°C (2070°F) engines.

Cyclic life of the power turbine disk will be adversely affected by increased gas temperatures. However, the disk is considered satisfactory for the desired program with minor revisions in cooling flow rates as follows:

	1002°C (1835°F) Base line engine	1038°C (1900°F) Engine	1132°C (2070°F) Engine
Power Disk Front Face	0.23%	0.40%	0.50%
Power Disk Rear Face	0.15%	0.22%	0.33%

(% is percent of compressor mass flow)

The increased flow rates are modest and are included in the performance analyses.

Two-Stage Power Turbine Rotor

At a gasifier turbine inlet temperature of 1241°C (2265°F), the power turbine design point rotor inlet temperature will be 1040°C (1905°F). A significant change to the power turbine is required because the base line power blade stress-rupture life drops to a very low level at this temperature. To accommodate required blade metal temperatures, a two-stage power turbine

operating at reduced speed (and stress levels) will provide desired performance and required life without the use of ceramic blading. The power turbine rotor general arrangement for the 1241°C (2265°F) engine is shown in Figure 39.

The power turbine rotor assembly utilizes two integral disk and blade cast wheels which are cantilever mounted on a steel shaft. The second-stage disk is inertia welded to the shaft as in the base line power rotor. The first-stage wheel is centered by a hub pilot to the second-stage wheel and retained by multiple bolts to a continuous seal drum which is, in turn, bolted to the second-stage wheel. A continuous interstage seal ring is also secured to the first-stage power turbine wheel front face using the wheel mounting bolts. This construction was selected because of its simplicity and does not alter the currently developed quill shaft and gasifier turbine wheel attachment or the power rotor shaft and bearing arrangement. Tentative materials selected for power rotor components include Waspaloy for the two seal rings and Mar-M246 with a corrosion-resistant coating for the two wheels.

Power turbine rotor design criteria require a 15,000-hr useful life and adequate cyclic life including 7500 start-stop cycles and 37,500 run-brake-run cycles. Designing for minimum production part cost (with such features as blade passage pullability) is emphasized. Other criteria involving blade vibration characteristics will be the same as observed in the base line engine design.

Rotor disk face cooling flow rates have been tentatively selected for use with these parts and are included in the performance analyses.

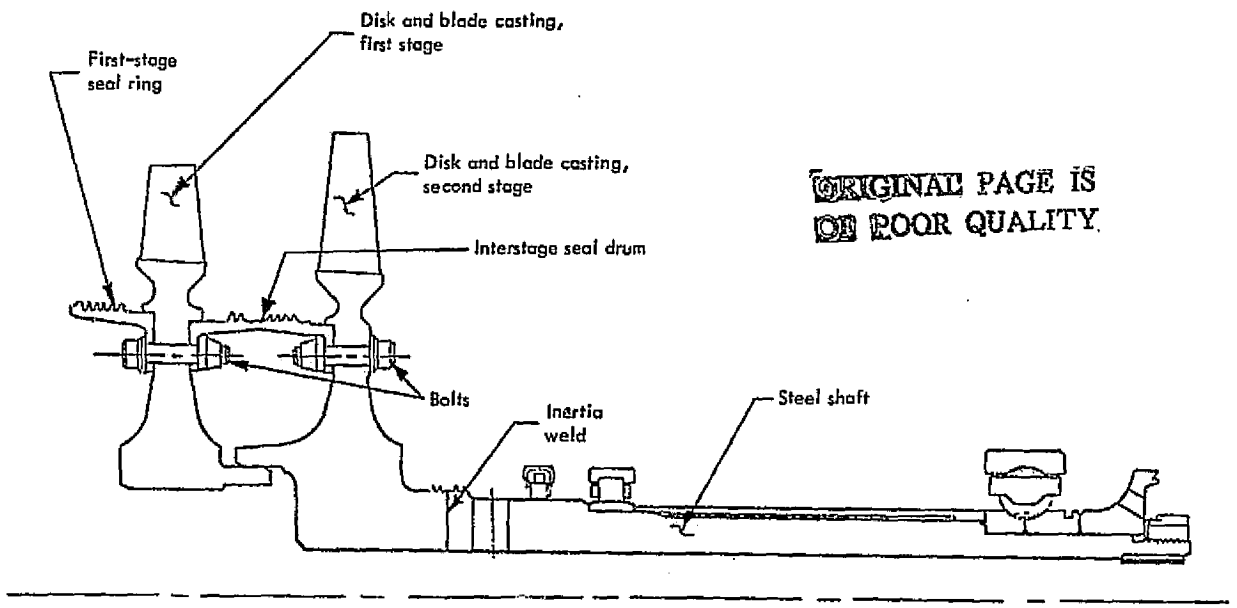

Figure 39. Advanced engine two stage power turbine rotor.

Combustor for 1038°C (1900°F) and 1132°C (2070°F) Engines

An analysis of combustor wall temperatures for a Lamilloy combustor has shown that existing technology is sufficient to permit the design and development of metallic combustors suitable for use in the 1038°C (1900°F) and 1132°C (2070°F) engines. Because of the higher cycle temperatures in the 1132°C (2070°F) engine, the Lamilloy for the combustor in that engine will have to be made from a higher grade of stainless steel material, such as Haynes 188 or perhaps the new Incoloy alloy MA 956. The design and development of the combustors for the 1038°C (1900°F) and 1132°C (2070°F) engines will draw heavily on experience as well as existing technology, and these phases in the combustor development program will follow conventional design procedures.

Engine Insulation

Changes to the engine block insulation will be required to maintain the engine block metal temperatures at acceptable levels and to limit the engine heat rejection as engine cycle temperatures increase. The existing engine block and bearing support housings are protected by insulating blankets and/or sheet metal liners. However, the regenerated air temperature which is exposed to the large combustor and forward block cavity is increased during the course of the program from approximately 704°C (1300°F) in the base line engine to 943°C (1730°F) in the 1241°C (2265°F) engine. (These values are associated with the part-power operation of the engine.) The block rear cavity, which contains the turbine exhaust gas, must accommodate a similar increase from 774°C (1425°F) to 983°C (1800°F).

Engine Block

The engine block crossarm in the base line engine is exposed without insulation for a very limited surface area to the gas temperatures which prevail in the block forward and rear cavities—704°C (1300°F) and 774°C (1425°F), respectively—at the engine power transfer operating condition. A cored passage within the crossarm is provided to accommodate cooling air, which is supplied from the compressor discharge location, to diminish the block crossarm temperature.

At the elevated gas conditions which will exist in the 1241°C (2265°F) engine—943°C (1730°F) in the forward cavity and 982°C (1800°F) in the rear cavity—a separate facing member is expected to be required to isolate the block casting from direct contact with these gas conditions. This member must, in addition, be free to grow relative to the block to avoid severe induced thermal stresses and distortions.

The engine block and regenerator cover crossarm lands are flat in this engine rather than contoured since the ceramic regenerator disks do not exhibit the thermal expansion associated with metal regenerator disks.

It is also anticipated that the engine block will require modification to accommodate a larger regenerator disk drive gear. Several factors are interacting to indicate this:

- If improved disk matrix technology is not achieved, a greater disk effective flow area will be required
- Regenerator seal face widths may need to increase to satisfy durability and leakage goals
- The current skewing of passages in current ceramic disks leaves approximately 7.6 mm (0.30 in.) of disk rim ineffective.
- If elastomer is retained for the gear-to-disk connection system, a substantial radial width may be required for thermal isolation of the elastomer.

The initial program activities will permit an evaluation of these problems.

The block may also require a change to accommodate relocation of the rim drive system in conjunction with the cavity increase.

AERODYNAMIC COMPONENT DEVELOPMENT

The analysis program results indicated that a significant contribution in accomplishing the 213 mg/W•h (0.35 lb/hp-hr) objective of the 1241°C (2265°F) engine would come from near-term component performance improvements, even though the contribution from any one component is small. Also, this engine will necessarily feature a flow path reduced in size from that of the current base line engine. As the flow path size becomes smaller, the scaling factors influencing compressor and turbine performance become more significant and must be given proper consideration if the desired component efficiencies desired are to be achieved. The factors influencing component performance can best be evaluated by rig testing. Consequently, the rig testing will include the compressor, gasifier turbine, power turbine, turbine exhaust diffuser, and the effect of the exhaust diffuser on regenerator flow distribution and effectiveness. The programs scheduled for each of these components are described in more detail in the following paragraphs.

Compressor

Performance objectives for the 1241°C (2265°F) engine require improvements in component efficiency as well as an increase in turbine inlet temperature. Usable compressor efficiency, for instance, must be raised a full percentage point above that of the base line compressor. This increase in efficiency must be obtained in conjunction with a corrected flow decrease from 1.65 kg/s (3.65 lb/sec) to 1.45 kg/s (3.2 lb/sec). A compressor redesign is required to accomplish these objectives.

The compressor design effort encompasses a three-month period. This design period includes not only aerodynamic design but also stress analysis, dynamic analysis, and mechanical design. Fabrication of component rig test pieces including instrumentation will be completed in six

months. Eight more months will be devoted to testing and analysis to develop the compressor to its full potential. A total of six compressor builds are planned. These tests will include a new-design base line test, rematch as necessary, alternate diffusers, rotor exit yaw probe surveys of temperature pressure and angle, and, possibly, a rotor-only test. All tests will be heavily instrumented to provide maximum diagnostic data on which to base further development.

Continual compressor rig support at a reduced level is provided during the 1241°C (2265°F) engine demonstration activity.

Gasifier Turbine

The gasifier turbine development effort is directed toward evaluating size effects for the reduced flow path. Initially, aerodynamic analyses will be performed to establish a preliminary flow path for the 1241°C (2265°F) engine. A gasifier turbine rig will be designed and fabricated to permit early testing of the preliminary flow path components. The activities are scheduled to begin during the second year of the program and will allow the test results to be introduced into the initial design of the engine.

Items to be tested are (1) rotor blade aspect ratio and tip clearance effects, (2) nozzle vane aspect ratio, (3) rotor blade and nozzle vane trailing edge thickness effects, (4) rotor blade and nozzle vane airfoil surface roughness effects, and (5) performance testing of the 1241°C (2265°F) engine hardware. These test areas are outlined as follows:

Rotor Blade Aspect Ratio Test and Rotor Clearance Test

The objective of this test is to evaluate the cost versus performance trade-off associated with reducing the blading aspect ratio (reduced number of blade, constant solidity) for the smaller size. Three aspect ratios would be tested on the new, reduced-size turbine rig to complete the size effect versus aspect ratio trade-off study. In addition, the rotors would be tested with at least two different clearances. These data would then be used to perform trade-off studies and to provide the insight needed for possible turbine improvements.

Nozzle Vane Aspect Ratio

The objective of this test is to evaluate the effect of nozzle vane aspect ratio (vary number of nozzle vanes while maintaining constant solidity) on turbine performance. Two different aspect ratios will be tested in the small engine size. The data from this program would be used for correlation with the base line size hardware. These data will provide the information needed to perform trade-offs between endwall losses and Reynold number (size) effects on performance.

Trailing Edge Thickness Effect (Rotor Blade and Nozzle Vane)

The objective of this test is to assess the effect of increased airfoil trailing edge thickness on aerodynamic performance. Currently, the effect of blade trailing edge thickness on performance is being investigated in the base line hardware program under other funding. This effort will be extended to include the 1241°C (2265°F) engine size hardware for blade as well as vane airfoils. The blade and vane will be tested separately and together. The information gained would provide the data needed to determine the aerodynamic design of ceramic blade and vane trailing edge radii for engine hardware.

Rotor Blade and Nozzle Vane Surface Roughness

The objective of this effort is to evaluate the effect of airfoil surface roughness on aerodynamic performance and to provide the basis to correlate a boundary layer loss model with surface roughness. In the test program, the hardware from the programs described would be used, and the effect on turbine performance would be evaluated for at least two different surface finishes. The data from these two tests would give size effect and surface roughness effect turbine performance data that could be applied to the engine.

1241°C (2265°F) Engine Gasifier Turbine Test

The testing as outlined for evaluating the size effects on turbine performance will be integrated into the engine design. This hardware will be tested in a rig to assess the aerodynamic performance. The data obtained will provide the basis for correlating the aerodynamic design tools with the performance obtained. This test will also influence the aerodynamic design for the engine redesign, scheduled in the fourth year of the program.

Power Turbine

The 1241°C (2265°F) engine incorporates a two-stage power turbine. Aside from including the additional stage, the power turbine design will be smaller in size that that of the base line engine. The objective of this program is to provide aerodynamic data for the power turbine design that can be used to verify the design before committing it to the actual engine configuration. The effort would tie in the testing of the base line size single-stage power turbine design with the aerodynamic considerations for the two-stage 1241°C (2265°F) engine power turbine design.

Rig testing will include the evaluation of two-stage turbine aerodynamic base line performance, rotor blade tip clearance, and airfoil resets. The initial two-stage turbine base line testing will be completed before the engine design and will ensure that the aerodynamic techniques used have been correlated with test results. The program also provides for rig testing of airfoil resets prior to committing them to the final two-stage power turbine design. In addition to the

basic aerodynamic data obtained, the data can be correlated with the single-stage test data to identify at what point it is most advantageous aerodynamically to change from a single-stage to a two-stage power turbine.

Exhaust Diffuser

The power turbine exhaust diffuser performance is dependent on the inlet gas conditions exiting the power turbine and is also dependent on the downstream blockage effects from the regenerator system. The program is consequently broken down into two distinct areas of investigation: (1) exhaust diffuser performance without downstream influence to achieve optimum power turbine performance and (2) exhaust diffuser performance to achieve optimum power turbine performance with the influence of the regenerator cover blockage. These programs are discussed here. A supplemental program to evaluate exhaust diffuser influence on regenerator disk effectiveness is discussed under the next subheading.

The turbine exhaust diffuser must provide not only efficient pressure recovery but also proper hot gas distribution to the regenerator matrix. The objective of this program is to design and develop the turbine exhaust diffuser for the 1241°C (2265°F) engine. Initially, an exhaust diffuser will be designed and fabricated for the two-stage power turbine. This diffuser will be base line rig tested, and five iterations are expected to be made before the final exhaust diffuser configuration is determined. The configurations will be tested, using the two-stage power turbine rig to more nearly simulate engine operating conditions. The combined effects of power turbine Mach number, swirl angle, and tip leakage will be evaluated because these combined effects influence the exhaust diffuser static pressure recovery. Following data analysis, a final design will be fabricated and tested with the redesigned (reset airfoils) two-stage power turbine. The data obtained from this program will provide the necessary input for the design of the turbine exhaust diffuser.

The next test is to define the downstream influence of the regenerator cover on the turbine exhaust diffuser and power turbine system performance. Further, the program will be used to optimize the turbine exhaust diffuser and regenerator cover configurations that provide the best power turbine aerodynamic performance. This effort will complement the previously described exhaust diffuser work. Initially, a rig test will be conducted, using a two-stage power turbine, an exhaust diffuser, and a regenerator cover to determine the effects of the cover blockage. These data will be used to assess the cover influence on the flow redistribution in the exhaust diffuser and on the exhaust diffuser pressure recovery. Two subsequent modifications to the exhaust diffuser geometry will be tested with the reset two-stage power turbine to assess the final exhaust diffuser design.

Regenerator Flow Distribution

The regenerator effectiveness is influenced by the flow distribution into the heat transfer matrix from the turbine exhaust diffuser. Modifications in flow distribution to the regenerator matrix for improved regenerator effectiveness can influence the performance levels of the exhaust diffuser and power turbine. The objective of this program is to determine the regenerator performance with the two-stage power turbine and exhaust diffuser configuration and to determine if improvements in regenerator effectiveness can be achieved without compromising the established turbine diffuser/power turbine system performance.

The program effort will be closely related to the exhaust diffuser program. Initially, circumferential and radial pressure and temperature measurements will be made to map the regenerator disk core energy distribution. These data will be combined with known cold-side flow distributions to determine overall regenerator effectiveness. Minor modifications to the flow distribution will be made to optimize regenerator effectiveness without compromising the established diffuser/power turbine system performance.

DESIGN WITH CERAMIC MATERIALS

The inherent characteristics and properties of ceramic materials differ sufficiently from metallic structural material properties to require special attention at all phases of the design effort. In some cases specifically different practices are necessary.

The need for change in design practice is not a new phenomenon to gas turbine engine experience. Materials use has continually progressed to lower ductility levels through the incorporation of higher-strength steel alloys, superalloys, and high-strength titanium. The necessary changes in design methodology have addressed refined criteria definitions, improved fatigue characterization through finite element modeling and combined loading conditions, use of fracture mechanics technology, and application of probability/reliability practices. The advent of ceramic materials, therefore, represents a logical extension of these changes in the design disciplines.

The detailed structural analysis techniques employed for final design evaluation are based on the finite element method. Finite element computer programs using plate, ring, and cube elements for efficiently and accurately analyzing gas turbine components are available. The ability to adjust the finite element size from the small elements needed in areas of high stress concentration to large elements in lower stress areas results in a considerable reduction in analytical effort without a sacrifice of accuracy. Automated model generation and output plotting features are used extensively to facilitate rapid evaluation of candidate designs. These basic element types are employed for modeling engine components, depending on their geometric characteristics. Many of the critical components can be accurately analyzed, using the two-dimensional plate or ring elements; however, the three-dimensional cube element is required for complete general modeling of geometric shapes and loading conditions.

The established metallic materials quality control practices and their relatively large critical flow size at low stress levels usually permit design optimization activities to concentrate on the reduction of part-peak stresses. However, the greater flow sensitivity of ceramic materials and their generally greater strength variability requires that design activities for ceramic parts must consider flaws of significant size even in low-stress areas of the parts. Therefore, design failure probability evaluations of ceramic parts must address the stress distribution of the entire part. Comparative designs can most easily be assessed by comparison of a failure probability value on risk of rupture index associated with the entire part. Design procedures will be evaluated to provide a direct coupling of the existing finite element model stress output with the ceramic material volume/stress/probability and surface area/stress/probability characteristics to provide the desired risk of rupture distribution and part index.

A design procedure for general application to all of the ceramic components in the program is available. The plan begins with the identification of appropriate background data and progresses through the preliminary design, detail design, and fabrication/test phases. A continual information exchange is maintained with the materials test program and nondestructive inspection (NDI) program. Iterative design loops are used to provide direct feedback of test data and results to the analytic activities and thereby provide for revision of geometric configurations.

The parametric studies conducted as a preliminary design activity are used to establish the sensitivity of component dimensions, material properties, environmental factors, and part functional requirements on part stress, life, or cost objectives. Thus, the critical parameters or parametric combinations can be identified and component preliminary design activities can be rapidly converged to optimization. If revised engine or component operating limits are implied, their sensitivity can also be evaluated.

Component design criteria, critical analysis conditions, material selections, and a geometric configuration are all defined from the preliminary design activities to initiate the detail design effort. Materials test and NDI programs are also defined to ensure that proper emphasis is placed on the identified critical parameters.

A component heat transfer analysis, using finite element modeling techniques, starts the detail design analytic activities. The output from this model is then incorporated in similar finite element models for determination of stress and deflection, critical flaw size/location, and permissible initial flaw size. The necessary materials properties for these analyses are continually updated from the materials test program. Also, component data obtained from rig and engine tests can be fed back through these analytic models for correlation of the analytic techniques. This feedback provides improved analytic predictive capability for evaluation of subsequent geometric configurations and environmental conditions. The flaw size/location information generated can be used for revision of the NDI program.

In the component fabrication and test phase of the plan, the ceramic specimens and components are initially subjected to materials and NDI testing for verification of desired properties, characteristics, and quality. However, the initial rig or engine test for some components may be performed with a metal part fabricated to simulate the characteristics of the ceramic component. This practice will permit the evaluation of selected critical environmental situations without major risk to either the simulated ceramic component or other rig or engine parts. Proof tests will be defined to simulate the part limiting operational conditions, and parts will be proof tested for quality segregation prior to functional rig or engine testing.

Evaluation of Regenerator Disk and Seal Materials

The regenerator design plan requires that materials development work be conducted to assist in component development and evaluation of a rim drive ceramic regenerator disk and seal system. This support will address the needs in the following areas:

- Experimental test and evaluation
- Materials and processing - engineering design
- Component fabrication - shop/inspection
- Failure analysis

A detailed description of the five-year program plan is given in the following paragraphs.

- First year—The current ceramic disk hot seal (nickel oxide/calcium fluoride (NiO/CaF_2) hot crossarm, graphite rim wear face) is temperature limited in the rim area to approximately 774°C (1425°F) by graphite oxidation.

  During the first part of this period various mixtures of plasma-sprayed NiO/CaF_2 coatings will be lab evaluated on the friction and wear test rigs to determine their suitability as a high- and low-temperature (to replace graphite) seal wear face material. Rig testing of the various mixtures will be evaluated against the alumina silicate (AS) 152-mm (6 in.) regenerator disk triangular matrix. The materials having the best coefficient of friction at various temperatures and good wear properties will be implemented into the design of full-scale hardware. Thermal stability tests will be conducted on "selected" coating/wear face materials over various substrates in the evaluation of a coating-to-substrate compatibility. The details for the test parameters, specimen configuration, and test rig descriptions for the aforementioned tests are presented following the program plan review.

- Second year—The materials and design emphasis in the second year will be on an improved-performance regenerator system. The maximum capability of the seal design will be 982°C (1800°F). In addition, improved performance resulting from the development of the thin-wall AS ceramic disk is planned. The thin-wall AS disk matrix will be friction and wear tested and evaluated against the "current selected" seal-wear face material. Evaluation of

- Third year—The seal-wear face materials evaluation and design emphasis during this period will be on obtaining improved performance and obtaining a maximum seal capability of 982°C (1800°F).

  Performance improvement plans are to evaluate and incorporate (1) a new ceramic material (probably magnesia alumina silicate—MAS) in addition to the AS disk, (2) a rectangular matrix geometry, and (3) flow area changes. Sufficient lab testing of materials, disk, and seal systems will be conducted to assist the design and implementation of full-scale hardware.

- Fourth year—This period of work effort calls for defining the seal material and disk configuration that will give the best performance and durability at 982°C (1800°F). Materials Engineering support will continue to address the needs of the program plan.

- Fifth year—Assistance in the fabrication, inspection, and test evaluation of the fourth year design hardware will be accomplished, resulting in an engine demonstration of 213 mg/W·h (0.35 lb/hp-hr) sfc at 1241°C (2265°F) turbine inlet temperature and regenerator inlet temperature of 982°C (1800°F).

Initial Friction and Wear Test

All initial friction and wear testing during the scope of this evaluation will be conducted on seal-wear face materials over a temperature range of 204°C to 982°C (400°F-1800°F) at sliding velocities of 6.4 and 32 m/min (21 and 105 ft/min) with normal forces of 69 kPa (10 psi). In addition, long-range wear rates for each candidate coating during the first year will be established at temperatures of 316°C and 774°C (600°F and 1425°F) at 32 m/min (105 ft/min) sliding velocity and 69 kPa (10 psi) load. Pending design requirements, wear rates at temperatures up to 982°C (1800°F) will also be conducted on selected wear face materials.

Thermal Distortion and Warpage Test

Thermal distortion and warpage tests of various coating systems will be conducted in duplicates in the evaluation of a coating-to-substrate compatibility at preselected test temperatures. The material systems will be subjected to a maximum of six heating and cooling cycles over a temperature range of 21°C to a maximum of 982°C to 21°C (70°F to 1800°F to 70°F) for the measurement of possible deflection at various test temperatures. After each cycle, total warpage of the coating-to-substrate system is measured and then retested up to six cycles or whenever stability occurs.

Materials Selection—Turbine Flow Path Parts

In selecting candidate ceramic materials for application in the turbine flow path, four criteria must be met: (1) mechanical, physical and chemical properties must be compatible with component design requirements, (2) materials must be definable to allow processing parameters

to be frozen during component development, (3) material must be fabricable into complex shapes with a minimum of diamond grinding, and (4) a competent manufacturing source must be available. Using these criteria, tentative materials selections have been made for use in the 1038°C (1900°F) and 1132°C (2070°F) engine phases. These selections are shown in Table XX, along with probable green body fabrication techniques. Also included are some of the emerging materials which will be factored into the program as they mature.

TABLE XX. CANDIDATE CERAMIC MATERIALS TURBINE FLOW PATH

Component	Material	Fabrication Technique
Vane Assemblies	RB SiC	Transfer Molding
	RB Si_3N_4	Injection Molding
Turbine Tip Shroud	RB SiC	Compression Molding
	MAS	Isostatic Pressing
Blades	Sintered - SiC	Transfer Molding
Plenum	RB SiC	Slip Casting
	Impregnated SiC	Slip Casting
Emerging Materials	CNTD SiC	Gas Phase Deposition
	Sintered Si_3N_4	Molded, isostatic, etc.
	SiC/C composites	Molded, isostatic, etc.

Materials Testing and Evaluation Program

A complete characterization of the mechanical, physical, and chemical properties of candidate ceramic materials is an absolute requirement for the effective support of the component development tasks. Such a program consists basically of five subtasks:

- Generation of material properties including thermal expansion, thermal conductivity, specific heat, elastic modulus, Poisson's ratio, and strength required to employ a linear elastic probabilistic approach to structural design
- Generation of time-dependent properties including thermal fatigue, creep, and crack propagation characteristics with emphasis on the probabilistic nature of these properties
- Evaluation of environmental effects including oxidation, hot corrosion, and erosion which could cause property degradation of candidate materials during long-term use
- Development of the relationship between material structure and mechanical properties with special emphasis on establishing the size, type, and distribution of strength-limiting defects
- Development of high-resolution inspection technique to detect critical size defects in candidate ceramic materials

A program of this scope should be applied only to mature materials whose processing is sufficiently well established to justify freezing all process parameters for the duration of a component development phase. Newly emerging materials, however, will be continually monitored in a timely fashion and factored into the program as appropriate.

During the first year, data will be generated in four materials—RB SiC, RB Si_3N_4, MAS, and sintered SiC—to a temperature of 1149°C (2100°F) and in sufficient depth to support the design effort for a functional vane/shroud assembly for the 1038°C (1900°F) engine and the initial blade studies. Characterization to 1371°C (2500°F) will be completed for all four materials during the second year. In addition, a subtask to develop new nondestructive evaluation (NDE) techniques will be started during the second year. During the third year, two more mature materials will be completely characterized for application in the 1241°C (2265°F) engine. Also, the NDE will continue. In the fourth year, a final mature material will be evaluated for use in the final iteration of the 1241°C (2265°F) engine. The NDE development program should be completed. Finally, in the fifth year, selected materials will be examined at temperatures to 1538°C (2800°F) in an effort to assess the feasibility of raising turbine inlet temperature to 1371°C (2500°F).

The following are detailed descriptions of the testing procedures to be applied. A summary of the NDE development program is also given.

Thermal Properties

Thermal conductivity, thermal expansion, and heat capacity will be measured from room temperature to the expected flow path hot spot temperature.

Specific heat will be determined, using a Bunsen ice calorimeter in which heat given up by the specimen melts ice which is in equilibrium with outgassed distilled water in the closed calorimeter well. Mercury enters the system from an external weight accounting source to make up the change in volume. The weight of the mercury making up the volume change is directly proportional to specimen enthalpy or heat liberated by the specimen when cooling from an elevated temperature to the ice point. The values of the changes in enthalpy and temperature can then be used in calculating the specific heat.

Thermal conductivity will be determined from thermal diffusivity measurements, using the flash laser technique. In this technique a thin, disk-shaped specimen is positioned in the isothermal zone of a furnace and the front face is heated by a short-duration laser pulse. As the heat pulse travels through the specimen, the back face temperature rise is recorded as a function of time. This temperature-time history is directly related to thermal diffusivity. Thermal conductivity can then be calculated from the values of thermal diffusivity, specific heat, and density.

Thermal expansion studies will be performed, using a direct-view dilatometer. The expansion and contraction of the test specimen are measured directly by tracking, during heating and cooling, the relative displacement of fiducial marks on tantalum end caps located at both ends of the specimen. To calculate expansion, the total expansion of end caps and specimen is calculated, after which the end cap expansion, obtained by previous dilatometer measurements, is subtracted from the total expansion.

Elastic Properties

Longitudinal and shear moduli and Polisson's ratio will be measured over the range of room temperature to the expected flow path hot spot temperature. Elastic properties will be measured by a thin-wire untrasonic pulse-echo technique. In this measurement technique, the test sample is attached by a long, thin wire to a modulus transducer that is capable of generating and detecting longitudinal and torsional waves. The sample is suspended in a furnace and excited by the transducer. The extensional and torsional wave velocities are measured independently, and the respective moduli are computed. Poisson's ratio is then calculated by elastic theory.

Material Strength

Strength and Surface Finish

The primary objective of this subtask is to establish the relationship between strength and surface finish for each ceramic material to establish the finish requirements for machined surfaces, particularly for blade attachment areas. In addition, an in-house ceramic machining capability is desirable for expediting the rework and alteration of components where necessary.

Preliminary grinding and cutting parameters for all candidate ceramic materials will be established from (1) available literature and (2) contacts with appropriate equipment and materials vendors. Initial studies will include fabrication of round rods and rectangular beams of each material, using a range of grinding parameters. Subsequently, the surfaces of each rod or beam will be characterized to establish surface finish and extent of damage. Specimens will then be tested to failure and subjected to fracture surface analysis. The results of these tests and analyses in conjunction with surface finish measurements will be used to arrive at grinding procedures for each of the candidate ceramic materials.

Material Defect Strength Distributions

In order to specify the probability of failure of a component subject to a given stress state or equivalently establish the maximum design stress at a specified level of reliability, a knowledge of the material defect strength distribution per unit volume is required. Such information, of course, is derived from experimentally measured fracture probability data. The usual approach has been to empirically correlate measured data, generated on a simple test configuration, with

a selected distribution function (e.g., the Weibull[2] power function), and then extrapolate to large complex geometries and low stress levels to obtain component failure probabilities. Such practices have seldom met with success. This should not be altogether unexpected because, aside from the difficulties associated with extrapolation to stress levels well below the range of measured values, defect populations in ceramics are quite often found to be multimodal[3] and, clearly, a single distribution function, such as that proposed by Weibull, cannot effectively describe the statistics of fracture under these circumstances.

Fortunately, work is now appearing in the literature[3,4] which suggests that the required defect strength distributions can, in fact, be obtained directly from measured fracture probability data and a knowledge of the location of the fracture controlling flaws without resorting to assumptions about the nature of the distribution function. Note that even with the validation of such techniques, extrapolation to stress levels below the range of measured data (i.e., low failure probabilities) is still prohibited because such extrapolations can yield unconservative estimates of component failure probabilities. This aspect can be minimized only by obtaining fracture probability data on specimens of relatively large volume or by testing a large number of specimens. The former approach is adopted in the following program.

To establish the required defect strength distributions (and, simultaneously, the applicability of the Weibull power function), a program is planned to (1) measure fracture probability data for a wide range of specimen sizes and (2) establish fracture origins for each specimen, where possible, through SEM fractographic analysis. These data will be analyzed in light of the aforementioned statistical techniques to arrive at valid defect strength distributions for each material given serious consideration in the component development efforts. In all, four specimen geometry-loading arrangements will be used: three- and four-point loading of rectangular beams, uniaxial tensile testing of cylindrical rods, and burst testing of rectangular cross section rings. Fifty specimens of each arrangement will be tested to ensure a statistically significant sample size. These four arrangements should cover a sufficiently wide stress range to be appropriate for most of the components under consideration in this program.

During the first year, the initial four candidate materials will be evaluated in four-point bending at room temperature and at two elevated temperatures. Test temperatures will be determined individually for each material from expected component operating temperatures in the 1038°C (900°F) engine. Testing of the remaining geometries will be completed in the second year.

Note that where strength is changing rapidly with temperature, sufficient additional testing to "fill" in the curve will take place. In this case, however, sampling size will be kept to a level (15-20) sufficient to determine mean strength values only.

Prior to testing, all specimens will be rigorously inspected. All specimens will be radiographed, examined with dye penetrant techniques, and scrutinized under a low-power light microscope. In addition, density and surface finish will be measured. Selected surfaces will also be examined in the scanning electron microscope.

Where possible, all testing will be instrumented with transducers so that acoustic emission signatures can be recorded. This information is not only useful in establishing material failure mechanisms but also important in accessing damage to components during proof testing.

Effect of Environmental Exposure on Material Strength

Bend specimens of each of the candidate materials will be exposed to an oxidizing environment for extended periods of time at two different temperature levels. The temperature levels for each material will be selected on the basis of preliminary oxidation measurements derived from (1) differential thermal analysis and (2) component operating temperatures. After exposure, bars will be tested to failure. Subsequently SEM techniques will be used to evaluate surface oxide character and fracture surface topography so that strength degradation, if any, can be related to critical microstructural features. Such information, in the case of degraded materials, is expected to lead to rational alterations in chemistry and/or structure so as to obviate the observed strength reductions.

Lot-to-Lot Material Strength Variability

Because the chemical properties of brittle materials are expected to have a general sensitivity to slight variations in raw materials and processing procedures, the lot-to-lot variability will be assessed for all materials for which design data are to be generated. This will be accomplished by fabricating separately and independently at least three lots of bend bars for each material of interest. Each lot will contain at least 50 specimens to ensure a statistically significant sampling size. Testing at room temperature will minimize the cost. All specimens will be fractographically analyzed to establish relationships between fracture stress and the size and nature of the defects causing failure. These data will be analyzed, along with the data developed initially in the subtask, using the appropriate statistical techniques.

Stress Intensity Factor/Crack Velocity

All candidate materials will be experimentally examined to assess whether a slow crack growth mechanism is the dominant time-dependent failure mechanism. The stress intensity factor can then be calculated.

Creep Rupture

The creep rupture properties of candidate materials will be measured. A direct tension test will be used to generate the required data. The use of such a testing procedure is required by the fact that valid creep data can be generated only when a statically determinate stress distribution is developed within the test specimen. For this reason, other samples and less expensive tests (e.g., bend testing) are not applicable.

Thermal Fatigue

The thermal fatigue behavior of candidate airfoil materials will be established in an operational fluidized bed test. In this test, a wedge-shaped specimen is cycled between fluidized beds maintained at different temperatures. Transient thermal stresses which simulate those found in airfoils are thus generated within the specimen.

A three-dimensional finite element transient thermal stress code is used to relate the stress state developed in the test specimen to the difference in bed temperatures. Thus, by selecting the proper bed temperatures as determined by thermal stress code, any desired transient can develop in the test specimen.

Microstructure and Fracture Topography

The microstructure of all candidate materials will be documented by both optical EMS and SEM micrography. Fracture surfaces of all test specimens will be examined and characterized in the scanning electron microscope. Such microstructural analysis will be used to establish both a structure/property relationship for the candidate material and a base line for hardware failure analysis.

Evaluation of Abradable Tip Seal Materials

A viable abradable seal material must not only demonstrate acceptable abradability, it must also possess sufficient resistance to hot gas and particulate erosion, thermal shock, and oxidation. Because these requirements oppose each other, trade-offs must be made so that an acceptable balance of properties is achieved. This task is designed to supply the data required to make the necessary trade-offs.

Oxidation and Corrosion

Viable ceramic turbine materials must possess long-term resistance to highly oxidizing environments which contain alkali metal and sulfur bearing compounds. Work by Ervin[5] has shown that the oxidation of silicon carbide in the presence of alkali metal glasses (e.g., $Na_2O \cdot 4SiO_2$) can be accelerated as much as a hundredfold.

Work in this laboratory, using a standard crucible test as developed for superalloys, has shown that silicon carbide can be strongly attacked by molten salts containing Na_2SO_4. More recently, Tressler et al.[6] have shown similar results for commercial grades of reaction-sintered and hot-pressed silicon nitride and silicon carbide, with the carbide suffering catastrophic attack. In-house work at DDA, on the other hand, has shown that preoxidized hot-pressed and chrome oxide-bonded as well as hot-pressed silicon nitride with large amounts of MgO are unaffected by molten $NaSO_4$-NaCl salts. Further, thermogravimetric study, using various SO_2/SO_3 ratios

in a nitrogen/oxygen mixture, has shown that after a short period of time the oxidation kinetics for hot-pressed silicon carbide over the temperature range of 982-1371°C (1800-2500°F) were equivalent to those in pure oxygen. This suggests that for this material, at least, high-sulfur fuel will have little effect on component performance.

Clearly, the effect of sulfur and alkali metals in the oxidation characteristics of turbine ceramics is poorly understood. Available information suggests that serious degradation of some materials could occur in the presence of these elements. Thus, a program to evaluate the effect of these elements on long-term oxidation is in order.

The task planned for this program will include two phases. In the first phase, a preliminary thermogravimetric study of all materials will be conducted to establish the sensitivity oxidation rates to various levels of sulfur and alkali metal compounds. The second phase will follow up with burner rig testing of suspect materials under conditions which will closely simulate the environment to be encountered by actual components.

Quality Assurance of Ceramic Components

Because ceramic materials are highly probabilistic in nature, design stresses are very sensitive to allowable risk and degree of material variability. An extensive quality assurance program is therefore essential to the successful utilization of ceramic materials in gas turbine engines. Such a program has two primary objectives:

- Reduction of property variability
- Early rejection of defective components

These objectives will be accomplished by implementation of a highly detailed nondestructive and destructive evaluation program.

Nondestructive Evaluation Program

The nondestructive phase of the quality assurance will be applied in four distinct stages as shown in Figure 40.

- Raw Material and Process Control—The fabrication of ceramic components must be closely controlled so that repeatable properties, insofar as possible, can be consistently obtained. Factors requiring control include: chemistry, particle size, shape and distribution, binder chemistry and content, open body processing parameters, and sintering time, temperature, pressure, and atmosphere. The primary burden for this task lies with the ceramic producer. All manufacturers selected to fabricate components will be required to maintain complete traceability records for all hardware and test specimens produced. This will allow the complete and detailed processing history, starting with the raw materials characteristics for specific individual components, to be examined as required.

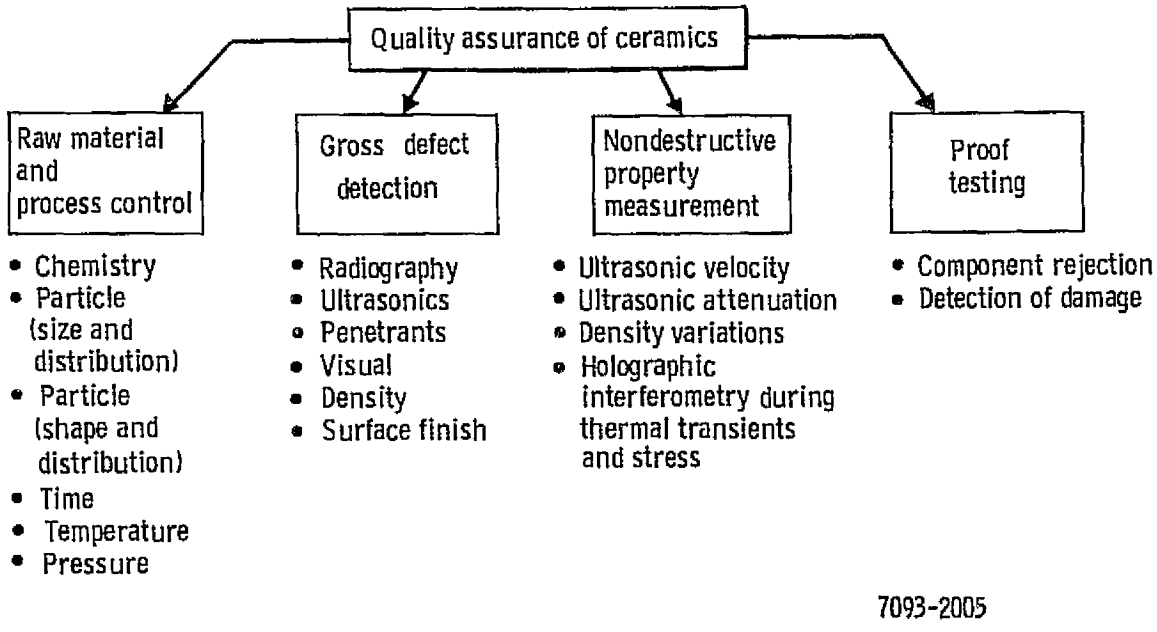

Figure 40. Major categories of quality assurance of ceramics.

- Gross Defect Detection—Normal nondestructive techniques will be used to find gross cracks, voids, and inclusions. The techniques to be used are very well known and will require little adaption for use with ceramic materials. However, the resolution limits of these techniques are well above the critical flaw size (10-100 μ) for ceramic materials. Thus, additional inspection techniques with increased resolution are required. Such techniques, including ultrahigh frequency ultrasonics, will be developed under a separate task and factored into the program as success dictates.
- Nondestructive Property Measurement—To assess variations of chemistry, density, and, in some cases, microstructure, property measurement techniques will be used. These techniques including ultrasonic velocity, ultrasonic attenuation, and density variation are widely known and have been successfully applied to ceramic systems in the past with good results. An additional technique potentially germane to ceramic material is being proposed: holographic interferometry during thermal as well as stress transients. This technique will be evaluated under a separate task and factored into the program as success dictates.
- Proof Testing—Because of the insufficient resolution of currently available defect detection techniques and the formidable difficulties in predicting component strength at realistic reliability levels by extrapolation of measured fracture probability data, proof testing is required to establish maximum defect sizes and thus an upper limit to component failure probability. To this end, all components will be proof tested prior to rig and/or engine testing. Tests designed to apply realistic loadings under simulated turbine environmental conditions will be used where possible. For example, in the case of inlet guide vanes and blades, a pressurized hot gas cascade facility will be used to induce thermal stresses to levels in excess of those expected to result from the most severe engine transients.

In addition, blades, because of the requirement of high-load-carrying capability, will be subjected to centrifugal and vibrational loading in specially designed spin and vibration tests. Further, all ring structures including turbine tip shrouds will be proofed with an internal pressurization test, using a rubber membrane and hydraulic fluid. Acoustic emission techniques will be used where possible to assess damage during proofing by comparing acoustic signatures with those measured during the laboratory mechanical property investigations.

Destructive Evaluation

Bend strengths of components will be evaluated from specimens either processed simultaneously with or cut directly from actual hardware.

Sampling size will be sufficient (30-50 specimens) to develop statistically significant data. In addition, selected components will be tested to failure during proofing. Fracture surfaces of all specimens and components will be examined to establish, where possible, the types and sizes of defects causing failure. The microstructures of all hardware will be examined in detail, using available EMS, SEM, and EMP techniques. The sum total of the information generated will be compared with that developed from laboratory test materials from which design data were obtained in an effort to assess expected component reliability and performance. In addition, this information is crucial to the successful evaluation of the results of component rig and engine testing.

Failure Analysis of Ceramic Materials

Material failure analysis is a requisite part of any program promoting the use of a "new" class of materials. It is especially meaningful with brittle materials because of the statistical nature of expected failures. Analysis of hardware failures allows the separation of poor design from material insufficiencies, defects, or improper fabrication procedures and suggests the appropriate corrective measures. Analysis of laboratory test specimens yields information on the detailed mechanisms which control the response of a given material. Such information gives insight into ways in which processing, chemistry, and microstructure can be altered to yield enhanced properties. Furthermore, this information feeds back into the hardware failure analysis and provides the base line.

Fractographic analysis is one of the most powerful tools for the failure analysis of an engine or rig component. A careful study of the minute features of the topography of a fracture, by scanning electron microscopy or by fracture replicas viewed on an electron microscope, provides a wealth of information concerning the failure mode. A handbook of fractographs for metallic materials has been published to aid in the identification of failure modes using transmission electron microscopy replication techniques. Fatigue, stress-corrosion, etc, are characterized by electron fractographs and the techniques used to produce them. There is no

comparable fractography handbook for ceramic materials. Furthermore, there is virtually no information relating failure mechanisms, particularly under conditions of high-temperature creep and fatigue, to microstructural features for the materials considered in this process.

During the screening and design data testing portion of the program, typical specimen fractures—produced in the ceramic materials by thermal shock, thermal fatigue, flexure, tensile, and creep-rupture loadings—will be documented by optical, scanning electron microscopy and transmission electron microscopy (replica) techniques. The handbook of standard fractographs, thus compiled will be used in failure analyses of rig and engine-run ceramic components.

The failure analyses of specimens as well as components will also include optical and electron microscopy studies of the microstructure, crack propagation, and arrest behavior in ceramic materials. As an example, an attempt will be made to determine how the critical flaw size of a ceramic body is related to its microstructural features, particularly the type, size, and distribution of phases and pores as well as grain sizes. If pores are larger than the average grain size, the critical flaw size will be related to pore diameter. On the other hand, if pore size is small with respect to grain size, the critical flaw size will be the grain diameter. The size of surface flaws introduced by machining is also related to microstructure. Because grain boundaries may be effective crack stoppers, the depth of penetration of such flaws is limited to about one grain diameter. The precise flaw depth is, of course, dependent not only on grain size but also on the severity of the machining operations. Surface finish would be expected to be more important in high-density than in low-density materials.

CONCLUSIONS

This document reports the results of a study program to establish how ceramic materials can be introduced into the Allison Model 404 industrial gas turbine engine. The following were the objectives for the study program engine development:

- Obtain improved fuel economy [Goal: 213 mg/W·h (0.35 lb/hp-hr) sfc at 100% power] by 1981 through the use of ceramic materials and improved component efficiencies.
- Meet current and projected federal emission and noise regulations.
- Commercial application capability in highway buses and trucks.

The study program was to produce a program plan to meet these objectives, recognizing the technical feasibility for meeting goals, costs for program plan, usage and cost of engines by truck or bus customers, and maximum applicability of advanced components to the current all-metal engines (which are planned for early production).

The following conclusions were established from the results of this study program.

1. The 213-mg/W·h (0.35 lb/hp-hr) sfc objective can be achieved by the end of calendar year 1981 with an engine operating at 1241°C (2265°F) turbine inlet temperature. This engine will incorporate ceramic components as follows:

   - Regenerator disks
   - Combustor
   - Turbine inlet plenum
   - Gasifier turbine inlet vanes
   - Gasifier turbine rotor blades
   - Gasifier turbine stationary tip shrouds
   - Power turbine inlet vanes
   - Turbine exhaust diffuser

   In addition to ceramic components, improved efficiency for the compressor, gasifier turbine, power turbine, and ceramic regenerator will be incorporated. A new, two-stage, metal power turbine is required for the 1241°C (2265°F) operating temperature. More than 90% commonality of parts with the current all-metal engine will be maintained.

2. Logical steps in turbine inlet temperature are from 1002°C (1835°F) to 1038°C (1900°F) to 1132°C (2070°F) to 1241°C (2265°F). These steps allow a sequential introduction of ceramic components to promote early qualification of ceramic components for further development and field evaluations preparatory to production.

The order of state of development of ceramic components is as follows:

- Ceramic regenerator disks—highest state of development
- Ceramic turbine gasifier inlet vanes
- Ceramic turbine stationary tip shrouds
- Ceramic combustor
- Ceramic turbine inlet plenum
- Ceramic exhaust diffusers
- Ceramic turbine rotor blade—least development, highest risk

3. Current and projected federal noise and emission standard can be met by all improved engines. Combustor development will be required to maintain a 25% production margin for NO_x.

4. A five-year program will achieve the target fuel economy with some ceramic components qualified for development leading to commercial engine production.

5. A major emphasis on ceramic material characterization, design methodology, nondestructive inspection, and techniques for rig and engine testing with ceramic components is required to meet program objectives.

6. Increasing the turbine inlet temperature to 1371°C (2500°F) does not appear to be technically feasible in a five-year time frame. Further, the best analysis with current technology does not show a payoff in engine-related life cycle costs for buses or trucks. This conclusion should be reevaluated in the third and fourth years of the program.

BASE LINE REGENERATOR SYSTEM

The base line engine regenerator system consists of two sets of hardware, one on each side of the engine. Figure 41 shows one set of regenerator hardware, which consists of an inboard seal, a stainless steel disk, an outboard seal, and two rub blocks. The disk is driven at the hub (see Figure 42) by a chain drive system with a viscous damper to damp frictionally induced vibrations in the system. The disk is a copper-brazed assembly, made from 0.05-mm (0.002 inch) thick stainless steel corrugated into a triangular shape and spirally wound on a sleeve. The seals have two sealing faces. One is a wear face (graphite on all surfaces except the hot seal crossarm (which is Met-Net) which contacts the rotating regenerator disk; the other face has a leaf structure which seals against the cast iron engine block surfaces. Two rub blocks, located on the outboard side of the disk with the outboard seal, are provided to maintain the disk in a position parallel to the engine block sealing surfaces.

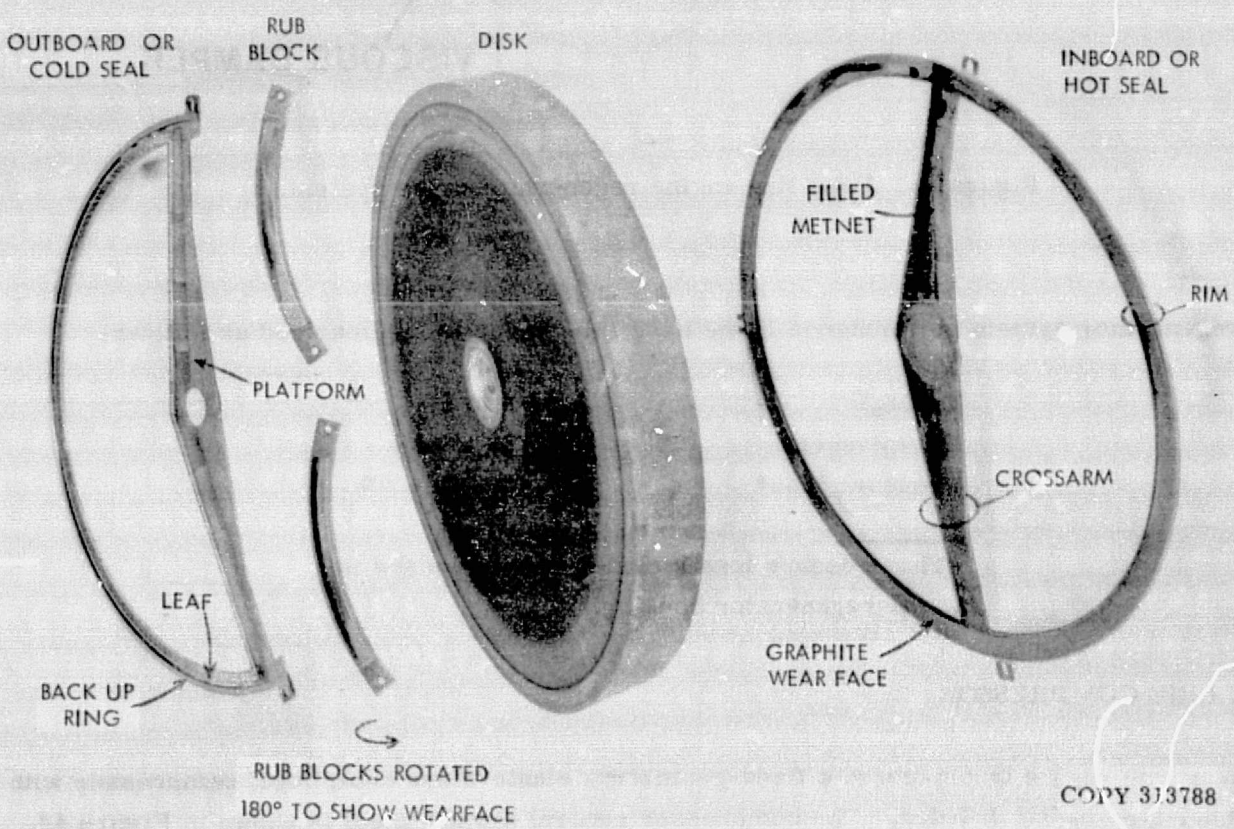

Figure 41. Base line metal regenerator disks and seals.

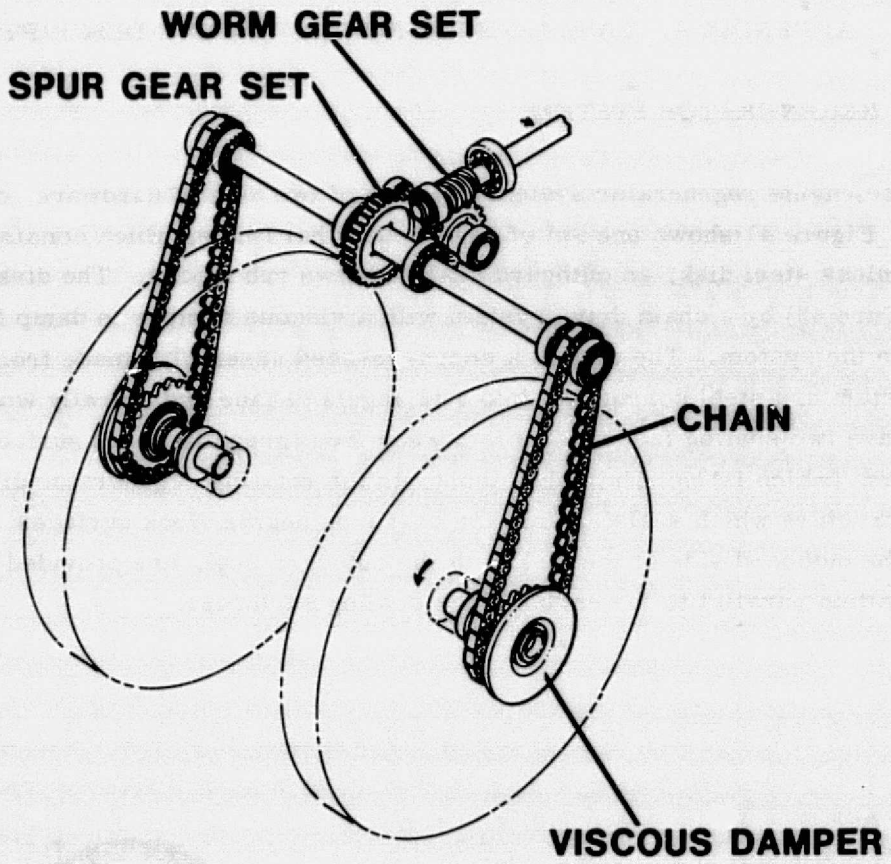

Figure 42. Base line engine regenerator drive system.

The regenerator system performance in the base line engine is summarized as follows:

Leakage	4 to 5%
Effectiveness	86 to 89%
Pressure loss*	3.3 to 4.0%

*The pressure loss includes ducting losses in the regenerator housing.

BASE LINE COMPRESSOR

The base line engine incorporated a fixed-geometry, single-stage centrifugal compressor with a channel-type radial diffuser. The compressor general arrangement is shown in Figure 43.

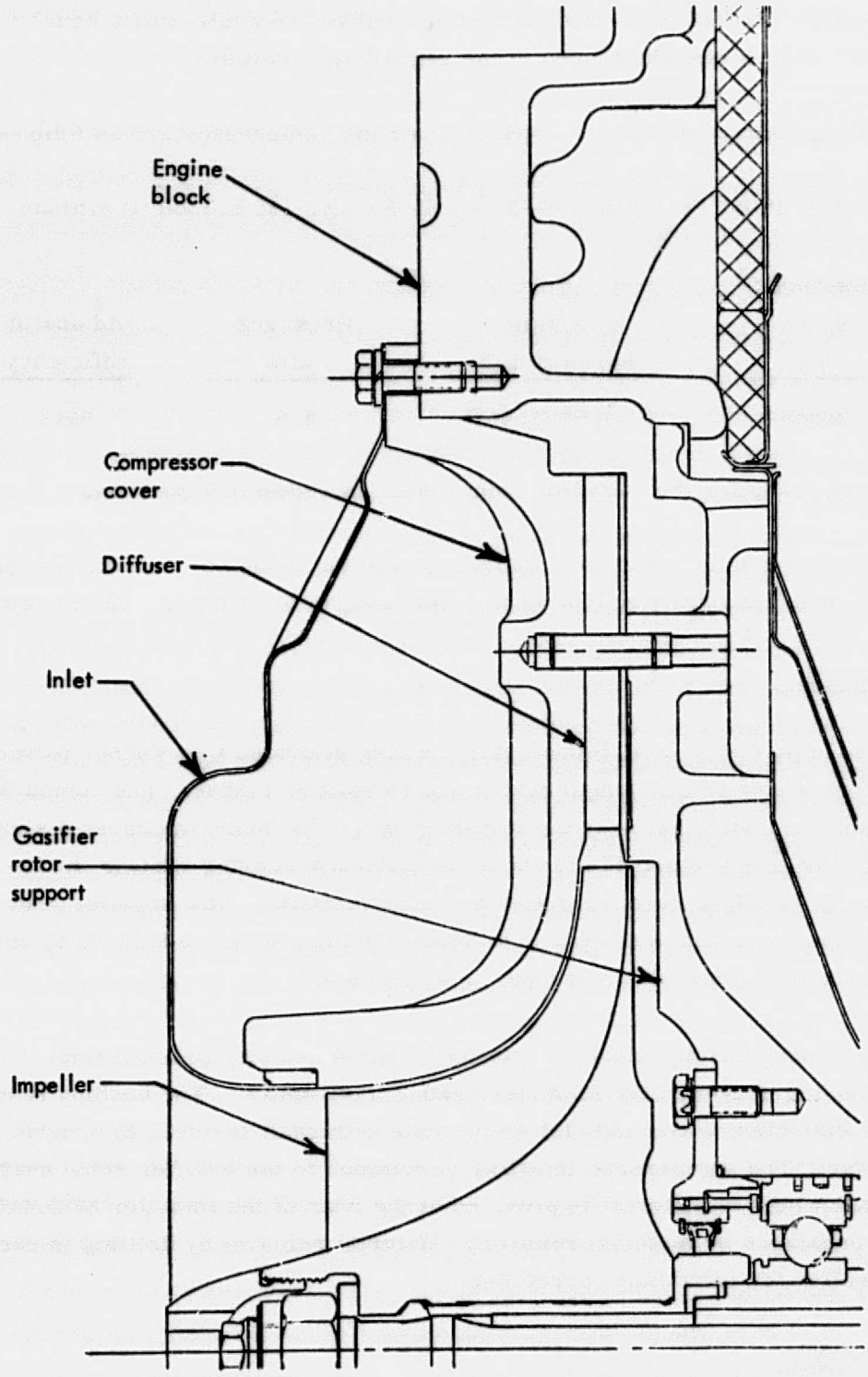

Figure 43. Base line compressor general arrangement.

The air is discharged from a diffuser into an irregularly shaped cavity in the engine block. This cavity contains a baffle at the top and bottom to effect an approximate equal division of the air to both sides of the block which open to the regenerator system.

The specific rating point performance objectives for the compressor are as follows:

Design Point Performance—29°C (85°F) day, 152 m (500 ft) altitude

Rotational Speed rpm	Airflow kg/s (lb/sec)	Pressure Ratio	Adiabatic Efficiency
36905	1.56 (3.45)	4.0	82.4

A full performance map for the base line compressor is shown in Figure 44.

The mechanical life objectives for the compressor are the same as those for the engine—i.e., two overhaul periods consisting of 7500 engine operating hours each (15,000 hr total).

Compressor Impeller

The compressor impeller is an aluminum alloy casting produced by a rubber pattern process. The impeller consists of 15 full-length blades and 15 splitter blades. The contours of the full and splitter blades are identical near the impeller exit. The blade thickness distribution in the inducer area was selected to provide for both adequate draft during casting and for sufficient stiffness to satisfy the blade resonant frequency requirements. The impeller blades have substantial backsweep at the impeller exit. The blade bending, which is induced by the backsweep, is reduced by providing high thickness taper in the blades.

A steel bushing is permanently installed into the impeller bore by press fitting. The bushing incorporates two interference pilot diameters and a drive spline. The bushing rear flange contains a pilot diameter, face, and slot which mate with shaft features to provide for impeller location and drive. The compressor impeller is retained to the gasifier rotor shaft with a single central tie bolt. A ring of material is provided at the rear of the impeller backplate to permit correction for unbalance by material removal. Material removal by drilling is permitted at the front of the impeller for unbalance correction.

Compressor Diffuser

The compressor diffuser is of the radial channel type and contains 24 passages with parallel front and rear surfaces. The front diffuser passage surface is provided by the diffuser rear plate. The additional passage geometry is provided by 24 equally spaced diffuser vanes.

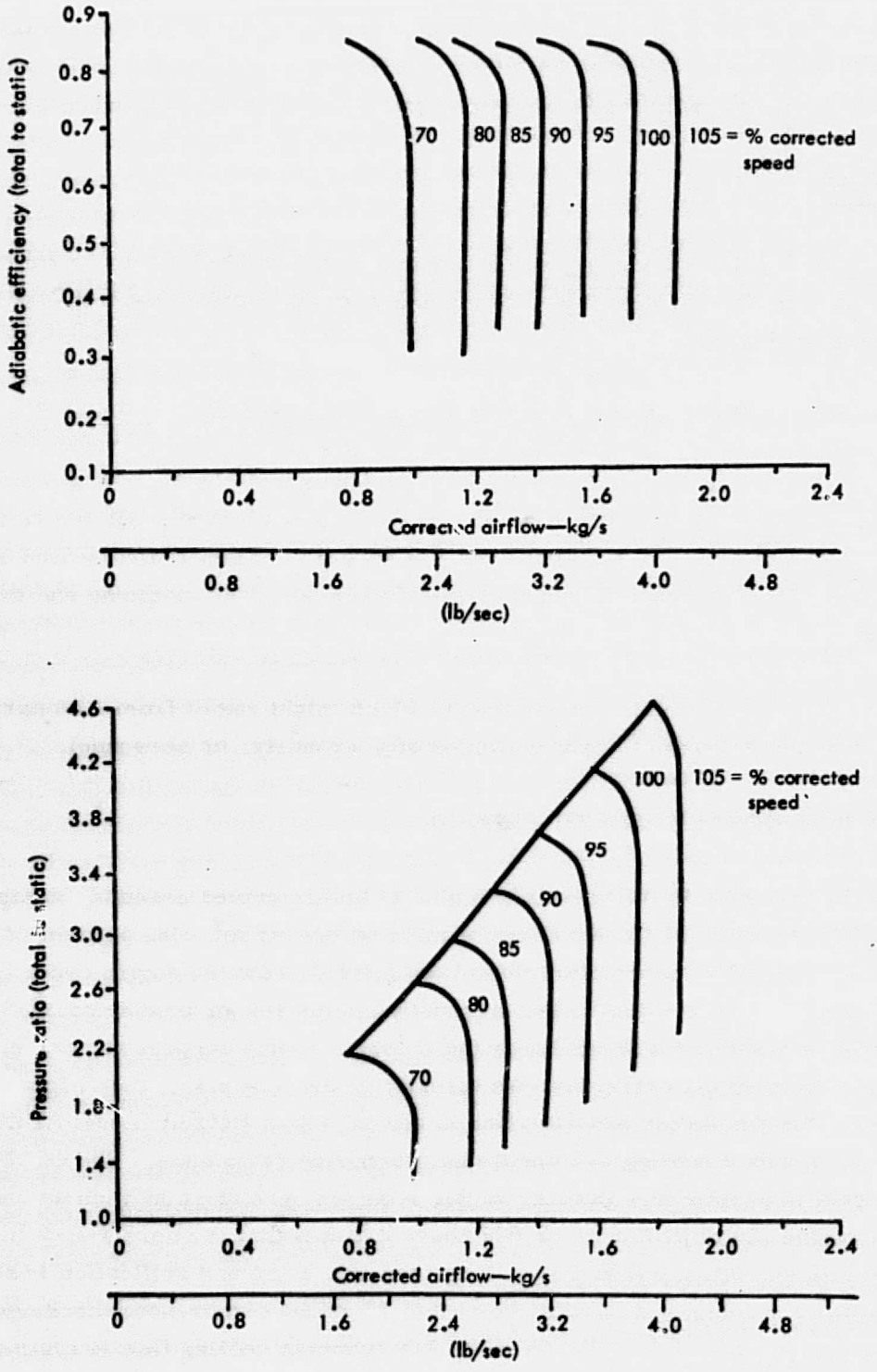

Figure 44. Base line compressor performance.

The diffuser is clamped between the gasifier bearing support and the compressor cover with 22 bolts which pass through holes in 22 of the diffuser vanes. A pin is pressed into each of the remaining two diffuser vanes, engaging both the compressor cover and the gasifier bearing support to provide accurate radial and circumferential location of the support to the cover.

Compressor Cover

The compressor cover is a sand casting which contains radial stiffening ribs on its front face. The cover bore and rear face are machined to a contour which matches the impeller blade tips at engine operating conditions.

The compressor cover also serves as the forward pressure diaphragm at the front of the engine to react the pressure loads associated with the compressor discharge pressure conditions. The gasifier rotor thrust bearing reaction, gasifier turbine nozzle loads, and gasifier bearing support pressure loads are additionally reacted into the engine block through the compressor cover-to-block outer splitline. The gasifier bearing support is aligned and located axially with respect to the engine block through the support-to-diffuser-to-cover clamping and the cover-to-block splitline.

The compressor cover must contain any fragments which might result from a compressor impeller failure to prevent damage to adjacent equipment, property, or personnel.

BASE LINE GASIFIER NOZZLE AND TIP SHROUD

The gasifier nozzle assembly in the base line engine is an air-cooled assembly designed to provide the desired life objective of 15,000 hours of mission operation. One percent of the compressor airflow is required to accomplish this at the 1002°C (1835°F) engine cycle temperature of the base line engine. The gasifier nozzle assembly comprises an annular nozzle casting with air-cooled airfoils, a gasifier tip shroud over the rotor, a nozzle support structure, and sealing features to prevent nozzle cooling air loss directly to the flow path. (See Figure 45.) The nozzle is cast from Martin Metals 509 alloy and is coated with a Detroit Diesel Allison-developed corrosion-resistant coating to improve hot corrosion resistance. The combustor outlet temperature profile results in a gasifier nozzle inlet temperature condition as shown in Figure 46. The engine life objective of 15,000 hours dictates that the nozzle peak metal temperature must not exceed 982°C (1800°F) for long term oxidation and sulfidation resistance. The gasifier nozzle heat transfer analysis shows that 1% of the compressor discharge flow will provide adequate cooling for the airfoils when the impingement cooling flow is distributed, as shown in Figure 47. Cooling air enters the vane impingement tubes at the hub and is distributed so that 0.6% of compressor discharge flow is distributed uniformly from the hub to the tip at the leading edge. This air then splits equally and flows between the tube and the suction and pressure sides of the airfoil. An additional 0.2% of cooling air is required at both the vane mid-channel suction side and the mid-channel trailing edge to provide proper cooling. The cooling

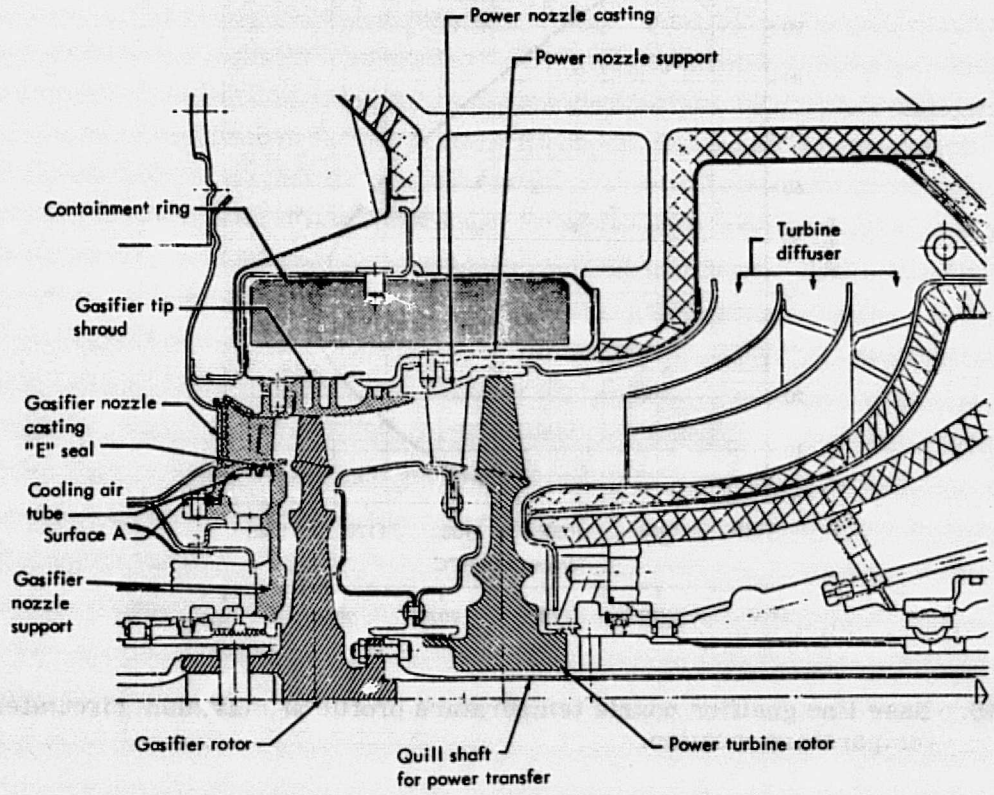

Figure 45. Base line engine turbine schematic.

air from the tube leading edge, suction side, and trailing edge exits from the airfoil through a vertical slot in the vane pressure surface near the trailing edge. In addition to the cooling air vane, a boundary of cooling air, 1.76% of compressor flow, is supplied along the gas path surfaces of the inner and outer bands.

Attention was given to the selection of the number of gasifier nozzle vanes to ensure that the gasifier blade vibratory modes did not intersect vane passage frequencies in the high-speed operating range. The gasifier blades are clear of the vane passage frequencies (20th engine order) in the operating range except for the fundamental mode interference just above idle rotor speed. The design maintained the axial vane trailing-edge-to-rotor-blade spacing in accordance with earlier development engine blade vibration experience.

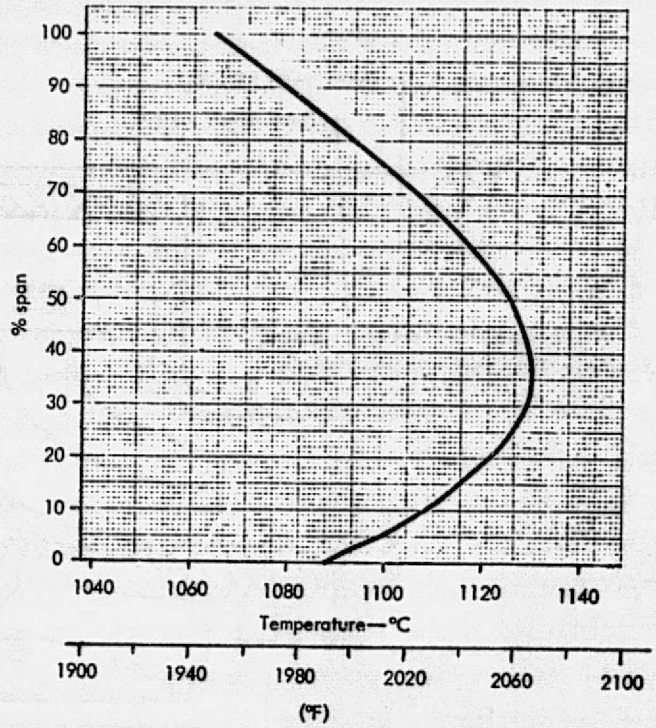

Figure 46. Base line gasifier nozzle temperature profile at maximum circumferential temperature location.

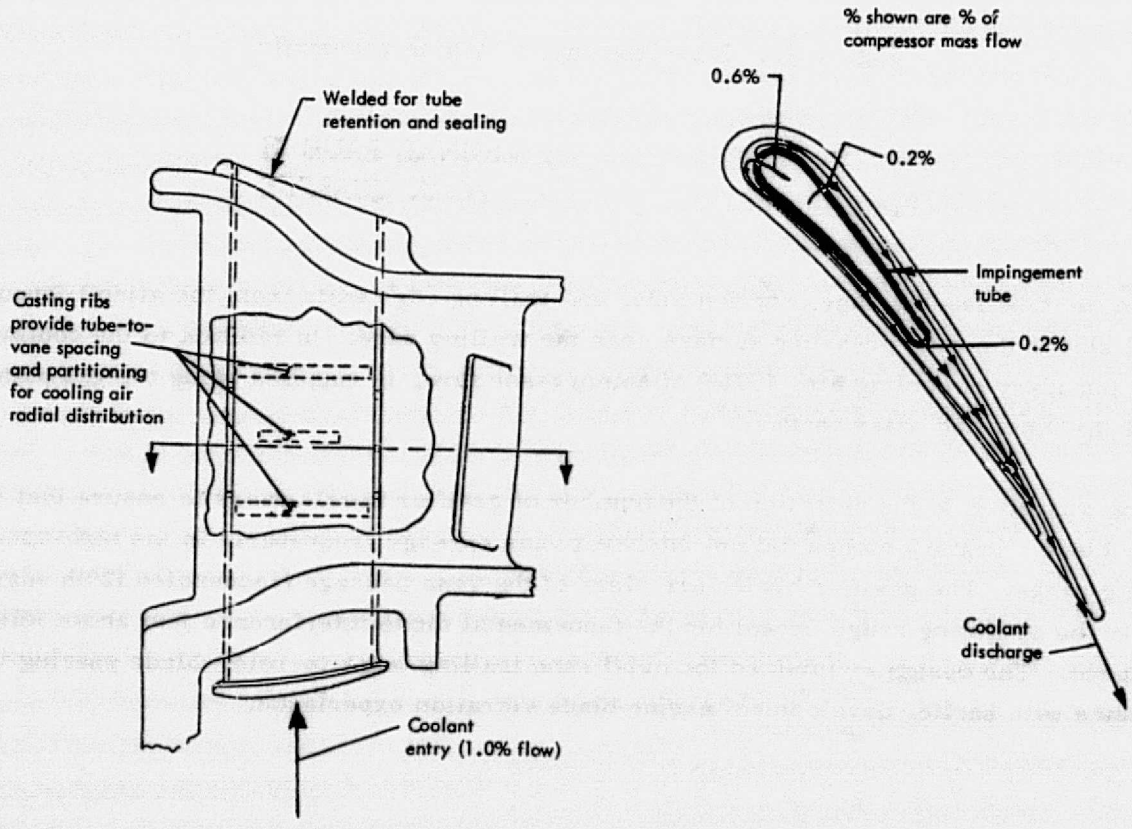

Figure 47. Base line gasifier vane cooling system.

The gasifier nozzle casting provides the support for the gasifier stationary rotor shroud. The shroud performs the following functions: (1) provides the gasifier rotor tip gas boundary and serves to control rotor tip clearance, (2) provides the support for the gasifier piston ring, (3) provides the primary restrictor to control the outer nozzle band cooling airflow, and (4) forms the outer flow path wall between the gasifier and power turbines. The shroud is attached to the rear of the gasifier nozzle outer band by five radially oriented headed pins which serve both as cross-key centering features and as axial retaining features. The headed pins are retained by weldment to the shroud. The shroud is cast in NX 188 material and is cooled to 704°C (1300°F) by three ribs that are exposed to a flow of cooling air. A sheet metal cover is provided at the periphery of the shroud to induce the flow of cooling air around and through the labyrinth formed by the shroud circumferential ribs and the staggered rib slots. This cooling air is then introduced into the flow path as outer nozzle band cooling air.

The gasifier nozzle loads induced by the shroud and the aerodynamic gas loading on the vanes are reacted by the gasifier nozzle support which is a structural member that is cast in Inco 718 material.

Sealing of the support and nozzle at the rear requires a compliant member to accommodate differential axial thermal growth. The compliance was achieved by using an "E" seal design fabricated from Inco 718 material.

Sealing is also required between the turbine inlet plenum and the nozzle support casting. This seal is achieved by engaging an extension of the plenum to the gasifier nozzle support when the engine is assembled.

The considerations outlined in materials selection, aerodynamics, air cooling, and mechanical design contribute to a gasifier nozzle and shroud assembly that is intended to provide 15,000 hours of useful life when used in the engine at a rated turbine rotor inlet temperature of 1002°C (1835°F).

BASE LINE GASIFIER TURBINE ROTOR

The base line engine features high-technology turbine design considering the long-life objectives of the engine. Turbine operating conditions are severe for a long-life engine and require air cooling of the gasifier nozzle and careful attention to blade reaction levels and taper ratios to achieve design life goals in the blading. Rotors are designed with useful life goals of two 7500-hour overhaul periods or 15,000 hours at mission operating conditions. The approach to the design of the turbines involved an iterative loop approach. This process began with the engine cycle definition and terminated with completion of the detail drawings. Between these two end points, appropriate technologies were selected for aerodynamics, cooling, vibration criteria, structural criteria, materials, combustor pattern, manufacturing methods, and quality. The resulting turbine general arrangement and secondary flow system are shown in Figure 48.

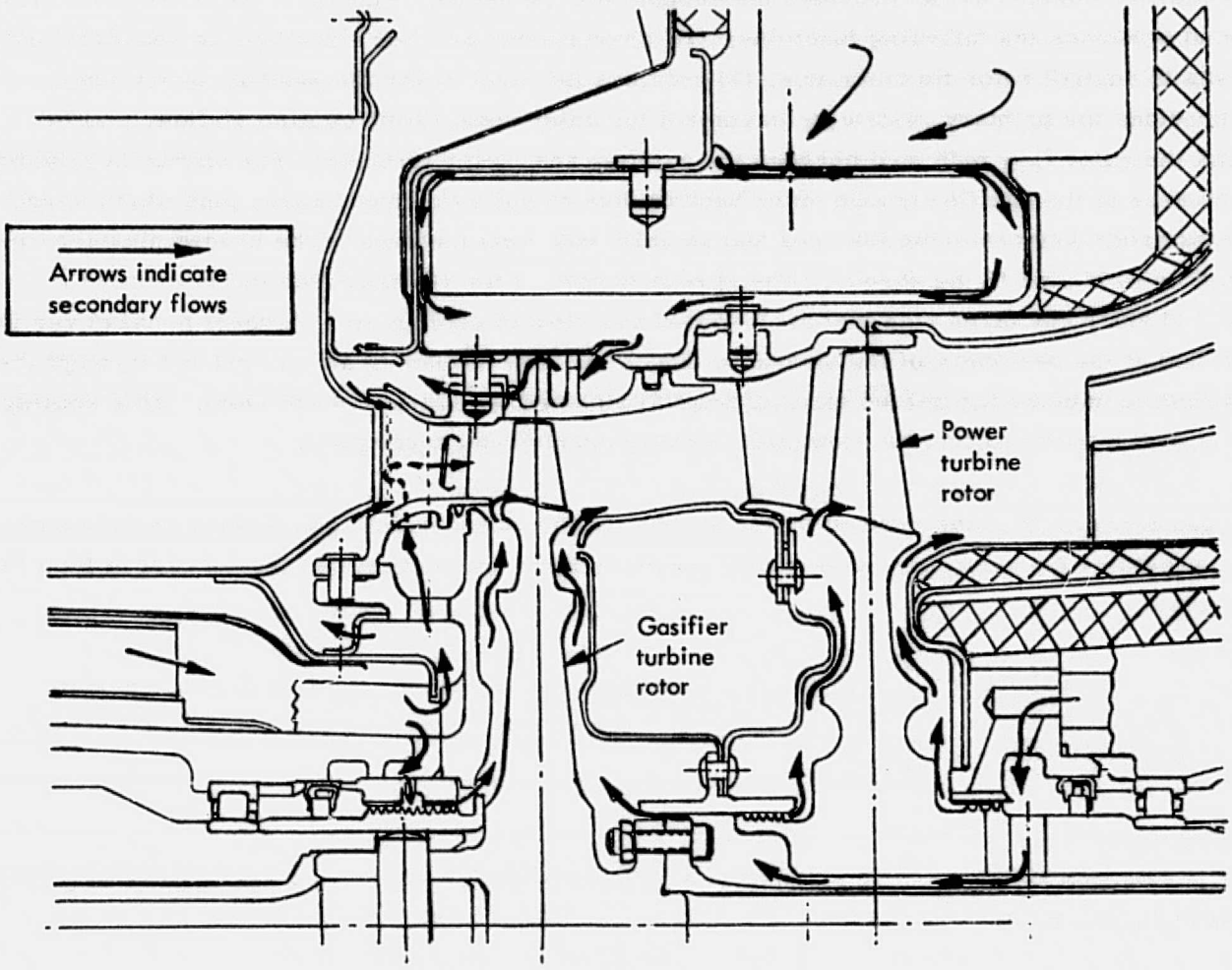

Figure 48. Base line engine turbine cooling system.

The gasifier turbine rotor comprises integral disk and blades which, by impulse and reaction, extract power from the main gas stream to drive the compressor, regenerator, and certain accessories and provide a portion of the engine power output. The rotor is of cast Mar-M246 material and the airfoils are coated with a DDA-developed coating for oxidation resistance. The gasifier rotor has 56 blades. It is secured to the shaft by a tie bolt which mates with the turbine wheel forward stub shaft and is retained by a transverse pin. The gasifier rotor shaft pilots on the outer diameter of the wheel forward stub shaft and extensions of the bolt retaining pin engagement slots in the shaft to provide the torsional connection between wheel and shaft. The energy absorbed by the gasifier rotor is transmitted to the compressor through the gasifier shaft and to the engine output during power transfer through the quill shaft. The quill shaft pilots on the rear of the gasifier disk and is retained by six bolts and nuts.

Turbine performance objectives were selected to match a performance cycle producing 224 shaft kW (300 hp) and 274 mg/W·h (0.45 lb/hp-hr) sfc. The turbine design point performance conditions are listed in Table XXI. The full turbine performance map is shown in Figure 49. The approach to aerodynamic design considered the application of several technological advances to improve performance or maintain performance in the configuration. The following are some of the more significant considerations:

- Vane endwall contouring was used in the gasifier turbine to reduce secondary flows and their attendant losses in the vane row.
- Controlled vortex velocity diagrams, which handle the continuity, momentum, and energy equations in a radial equilibrium flow solution, were used.
- Flow path radii and blades solidity were selected to minimize inertia of the gasifier rotor.

TABLE XXI. BASE LINE GASIFIER TURBINE DESIGN POINT CONDITIONS

Parameter	Value
Blade Inlet Total Temperature	1002°C (1835°F)
Vane Inlet Total Pressure	382.7 kN/m^2 abs (55.51 psia)
Blade Inlet Gas Flow	1.461 kg/s (3.221 lb/sec)
Blade Inlet Corrected Gas Flow	0.8328 kg/s (1.836 lb/sec)
Blade Inlet Fuel/Air Ratio	0.0115
Rotational Speed	36,905 rpm
Corrected Rotational Speed	17,770 rpm
Direction of Rotation as Viewed from the Rear of the Turbine	Counterclockwise
Power	309 kW (415 hp)
Work	212 kJ/kg (91.1 Btu/lb)
Corrected Work	49.1 kJ/kg (21.1 Btu/lb)
Expansion Ratio	2.065 (total-total)
Efficiency Goal	87.0 (total-total)

Vehicle mission simulation analyses were conducted to establish the sensitivity of turbine blade stress rupture life and turbine wheel cyclic life to the various vehicle operating modes and their distribution. These studies indicated that if a 2400-hr life can be provided in the gasifier turbine blade at the engine power rating condition, the blade will have a 15,000-hr life capability at the normal mission condition distribution. The 15,000-hr mission life objective is equivalent to 1 200 000 km (750,000 miles) (two overhaul periods). This study also indicated that the turbine wheels will be exposed to a large number of major thermal cycles during this 15,000-hour mission life.

Turbine disk cyclic life design criteria were defined by the two cycles as described below. The wheels must be capable of withstanding 7500 cycle A and 37,500 cycle B alterations without failure.

Design point parameters

Temperature = 1002°C (1835°F)
Expansion Ratio = 2.06 (total-to-total)
Efficiency = 87% (total-to-total)
Speed = 36,905 rpm (= 100% $N/\sqrt{\theta}$)

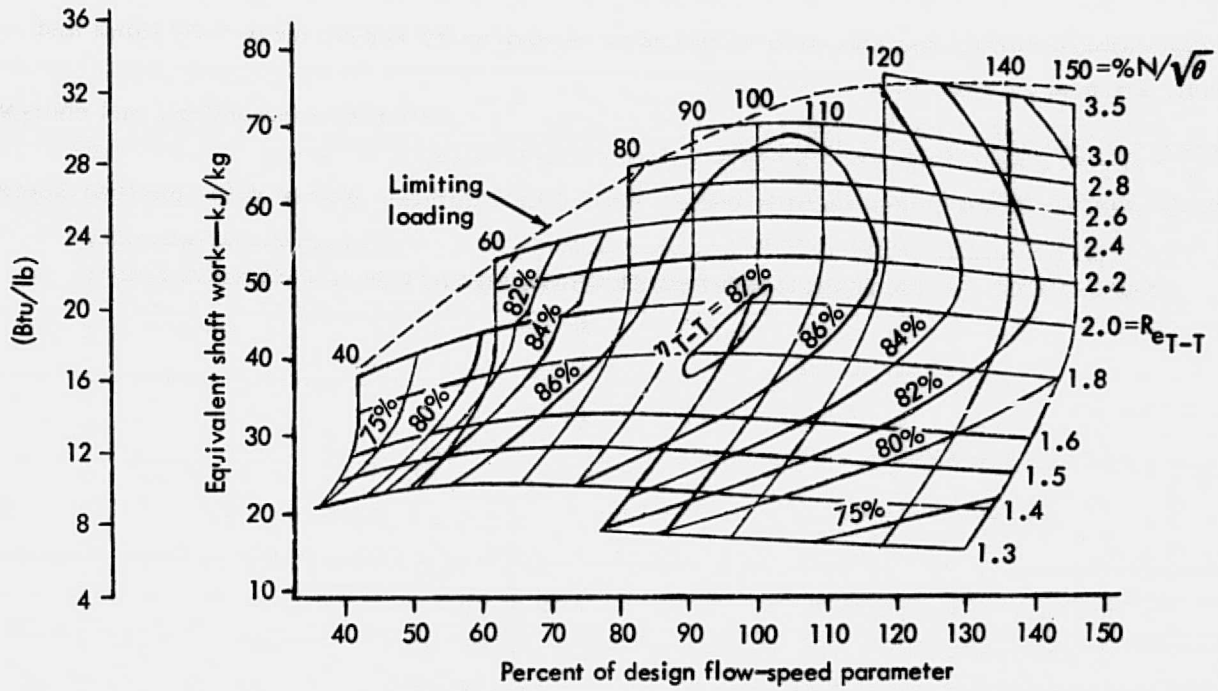

Figure 49. Base line gasifier turbine performance map.

Cycle A

A. Rapid acceleration from cold start to design point
B. Stabilize metal temperatures at design point
C. Dynamic braking from design point
D. Shutdown from dynamic braking

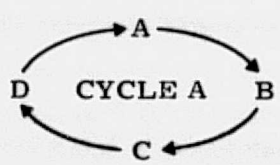

7500 Cycles

Cycle B

A. Dynamic braking from design point
B. Dynamic braking to design point

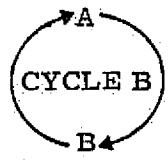

37,500 Cycles

In addition to blade stress-rupture life, disk cyclic life, and gasifier nozzle cooling requirements, a number of specific mechanical parametric limits were defined to ensure that the mechanical design objectives would be achieved in accord with the aerodynamic design of the turbine. The constraints addressed the following problems:

- Rotor degree of reaction and blade area distribution must satisfy blade life objectives
- Blade trailing edge radius must equal or exceed 0.254 mm (0.010 in) to ensure adequate cast part quality level
- Blade thickness distribution near the trailing edge at the base must taper radially to minimize fatigue concentration factor.
- Blade frequency must avoid coincidence with vane numbers within the engine operating speed range to avoid blade fatigue excitation.
- Axial spacing between vane trailing edge and blade leading edge must be equal to or greater than 10 mm (0.40 in.) in gasifier turbines and 6.3 mm (0.250 in.) in power turbines to diminish blade excitation.
- Turbine blade geometry must provide that the passage between adjacent blades can be extracted along a straight line without rotation to facilitate high-volume/low-cost foundry practice.
- Gasifier turbine nozzle vane shape must permit the incorporation of an untwisted impingement cooling tube within the vane.

The blade design for the gasifier turbine was completed and all aerodynamic and mechanical considerations were satisfied. Designing blades for pullability required the development of a new methodology.

"Pullability" refers to blade geometry which allows the passage shape between blades to be extracted on a straight line without rotation to facilitate high-volume/low-cost foundry practice.

The engine provides dynamic braking for vehicle operation. In the dynamic braking mode, the engine is motored up to 85% rated gasifier rotor speed in a fire-out condition. This operation quickly cools turbine rotor blading and disk rim, reversing normal disk temperature gradients.

Because of the criticality of accurate determination of disk and blade metal temperature, a two-dimensional finite element model was developed for heat conduction analysis. Heat transfer analysis methods were correlated with data obtained from a previous model gasifier wheel during engine test. Finite element two-dimensional model analysis methods were used to establish stress distributions in the turbine disks. Temperature and stress distributions were established for the following conditions:

- Fire-up from stabilized ambient conditions
- Stabilized conditions at design point
- Prolonged dynamic braking from design point

Based on computer stress comparisons with available low cycle fatigue data available for Mar-M246 material, the turbine disk designs have a satisfactory steady-state and cyclic life.

BASE LINE POWER TURBINE NOZZLE

The hot gases from the gasifier rotor are directed to the power turbine nozzle through an interstage duct. This duct is a diffusing passage whose inner wall is formed by the gasifier shroud. The inner duct material is Hastelloy X and has an estimated metal temperature 704°C (1300°F). The power turbine nozzle assembly arrangement is shown in Figure 50.

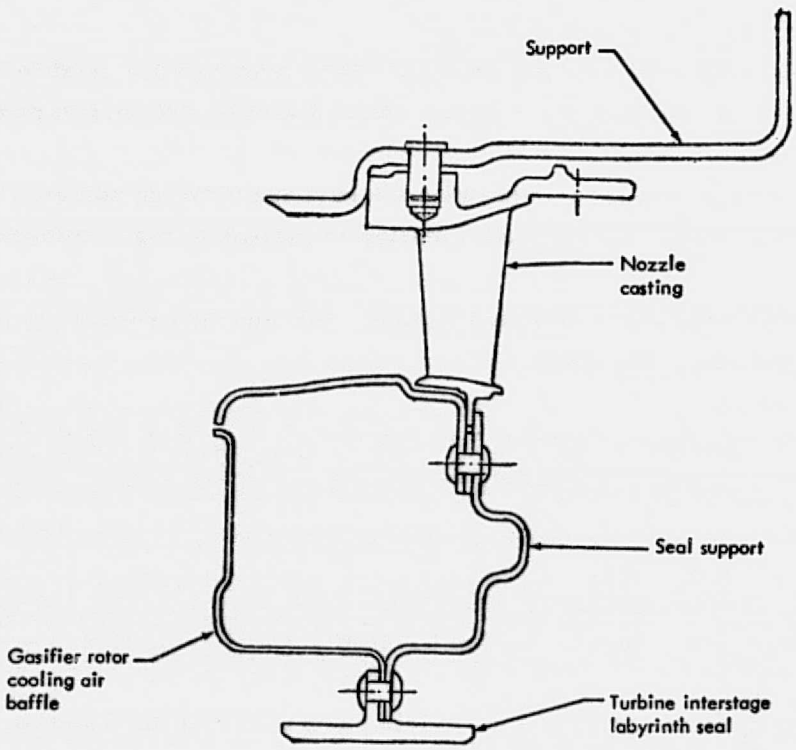

Figure 50. Base line power turbine nozzle assembly.

The power turbine nozzle is an investment casting in Hastelloy S alloy. The nozzle is supported at the outer band by five radially oriented headed pins that are, in turn, welded to an AISI-410 sheet metal support. The pins serve as a cross-key centering feature which permits the nozzle casting to grow thermally independent of the support. The number of headed pins and airfoils were selected jointly to permit slotting the nozzle inner band to effect a reduction of thermal stress level in the airfoils. The nozzle support is piloted and attached to the engine block and provides the piston ring seal bore feature. The nozzle inner band is flanged on the inside diameter and is slotted radially at five locations to provide a cross-key centering feature. The male portion of the key feature is provided by five tangs that project from a sheet metal ring that is positioned axially to the nozzle flange by the duct inner wall and by the interstage labyrinth seal supporting sheet metal. These sheet metal members are clamped together around the nozzle flange by ten rivets. The static member of the turbine labyrinth seal and the gasifier turbine rotor rear cooling air baffle are piloted to the supporting sheet metal and retained by six rivets. This design retains the radial centering feature required by the labyrinth seal and inner duct wall but permits the nozzle casting to grow thermally without induced thermal stress from the supported members.

The nozzle casting contains 40 airfoils cast integrally with the inner and outer bands. The Hastelloy S alloy selected for the casting does not require a coating when used in an engine with a rated gasifier turbine rotor inlet temperature of 1002°C (1835°F). The power turbine nozzle maximum metal temperature of 902°C (1655°F) occurs at the 35% span and is assumed to equal the stage gas temperature because air cooling is not employed. This temperature level (below the 954°C (1750°F) limit for Hastelloy S material) satisfies the 15,000-hour long-term oxidation and sulfidation requirement.

The power turbine rotor tip shroud is provided by a rearward extension of the nozzle outer band. The shroud incorporates a circumferential rib to provide increased stiffness to maintain the roundness of the power turbine blade track.

The materials selection, aerodynamic design, and mechanical design provide a power turbine nozzle assembly intended to provide 15,000 hours of life in the base line engine.

BASE LINE POWER TURBINE ROTOR

The power turbine rotor (Figure 51) comprises an integral disk and blades which, by impulse and reaction, extract power from the main gas stream to provide desired engine power output. In the base line engine, the power rotor is of cast Mar-M246 material and the airfoils are coated with a Detroit Diesel Allison-developed coating for oxidation resistance. The power rotor has 48 blades. The disk is inertia-welded directly to a steel shaft which supports the disk mass and transmits torque to the reduction gear system and power output shaft. The disk also provides the rotating labyrinth seal members for the front and rear disk cooling airflows. The cooling airflows metered by these labyrinth seals are approximately 0.14% at the front and 0.10% at the rear. The intent of these metered flows is to provide a supply of air that will prevent hot flow path gases from entering the disk cavity.

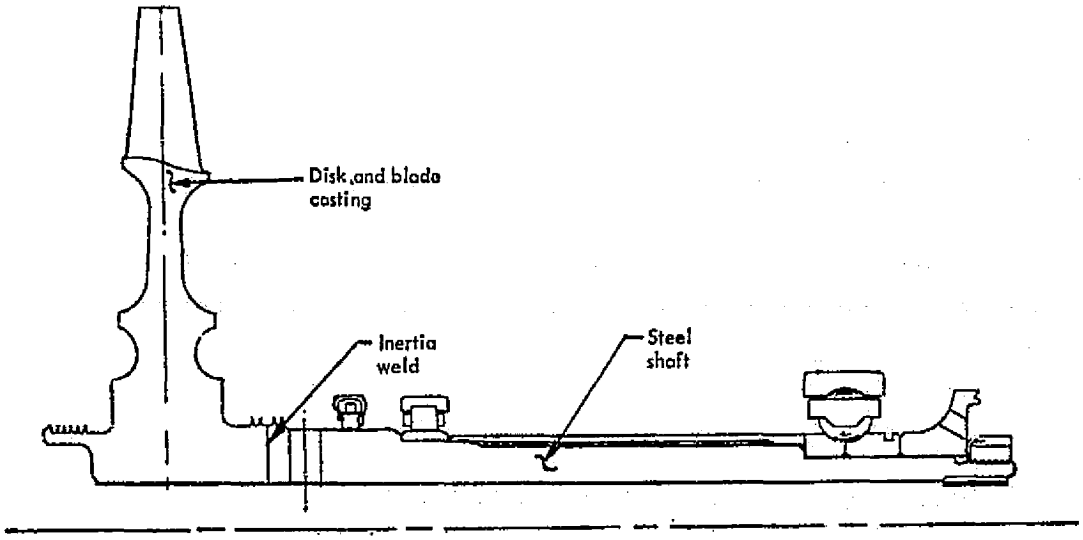

Figure 51. Base line power turbine rotor.

Turbine performance objectives for the base line engine were selected to match a performance cycle producing 224 shaft kW (300 hp) and 274 mg/W·h (0.45 lb/hp-hr) sfc. Power turbine design point performance conditions are listed in Table XXII. A full performance map for the base line power turbine is shown in Figure 52.

TABLE XXII. BASE LINE POWER TURBINE DESIGN POINT CONDITIONS

Parameters	Values	
Blade Inlet Total Temperature	814°C	(1498°F)
Vane Inlet Total Pressure	184.1 kN/m^2 abs	(26.71 psia)
Blade Inlet Gas Flow	1.488 kg/s	(3.280 lb/sec)
Blade Inlet Corrected Gas Flow	1.623 kg/s	(3.578 lb/sec)
Blade Inlet Fuel/Air Ratio		0.0113
Rotational Speed		30,705 rpm
		(90.0%)
Corrected Rotational Speed		15,980 rpm
Direction of Rotation as Viewed from the Rear of the Turbine		Clockwise
Power	212 kW	(285 hp)
Work	143 kJ/kg	(61.5 Btu/lb)
Corrected Work	38.8 kJ/kg	(16.7 Btu/lb)
Expansion Ratio		1.721
		(total-axial)
Efficiency Goal		89.7
		(total-axial)

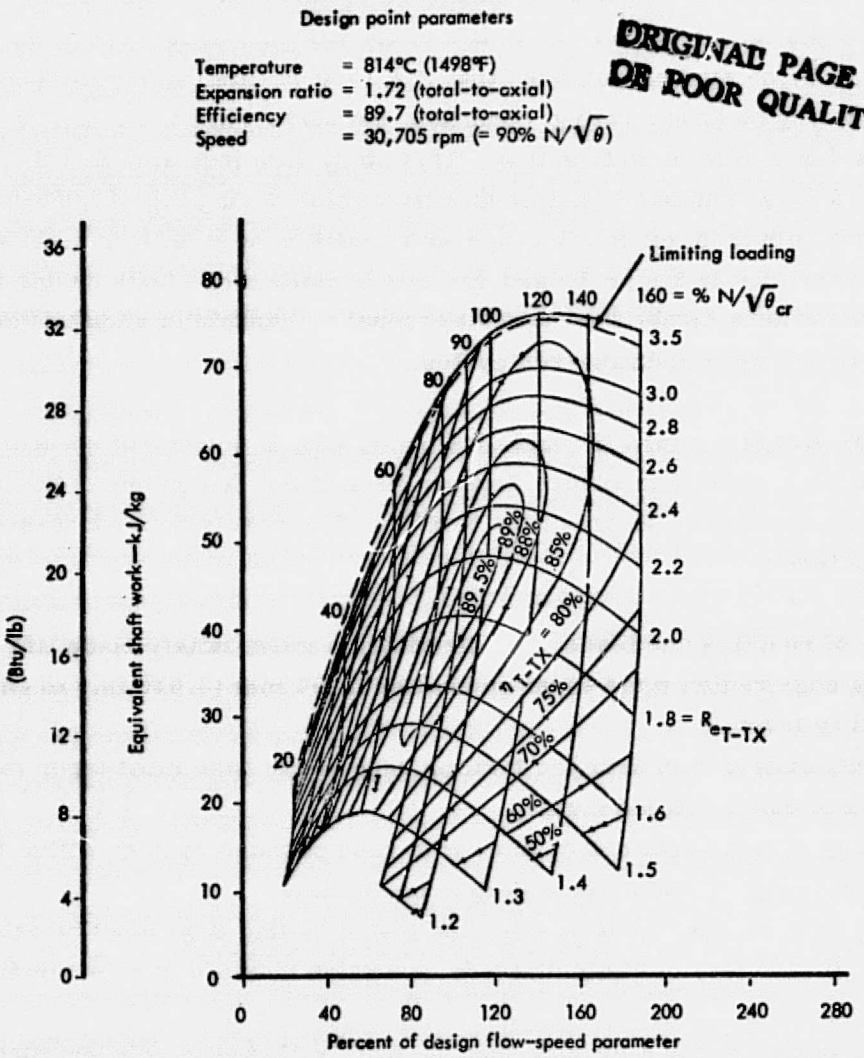

Figure 52. Base line power turbine performance map.

The approach in aerodynamic design considered the application of several technological advances to improve performance over previous development versions of the engine. The following are some of the more significant considerations which affected the power rotor:

- Controlled vortex velocity diagrams, which handle the continuity, momentum, and energy equations in a radial equilibrium flow solution, were used.
- Detailed flow analyses were used with iteration on airfoil contours to provide pressure and suction surface velocity distributions which minimize suction diffusion and loss.
- The power turbine requires peak efficiency at about 90% power turbine rpm when the gasifier is at 100% so as to have a wide range of output shaft rpm over which the engine sfc is close to optimum.

Vehicle mission simulation analyses were conducted to establish the sensitivity of turbine blade stress rupture life and turbine wheel cyclic life to the various vehicle operating modes and their distribution. These studies indicated that if a 1750-hr life can be provided in the power turbine blade at the engine power rating condition, the blade will have a 15,000-hr life capability at the normal mission condition distribution. This study also indicated that the turbine wheels will be exposed to a large number of major thermal cycles during this 15,000-hr mission life. These cycles result both from engine fire-ups which initiate at stabilized ambient conditions and from vehicle operation in the prolonged dynamic braking mode (with engine fuel shut off). Turbine cyclic life criteria established that disks must be capable of withstanding 7500 start-run-stop cycles and 37,500 run-brake-run cycles.

In addition to blade stress-rupture life and disk cyclic life, a number of specific mechanical parametric limits were defined to ensure that the mechanical design objectives would be achieved in accord with the aerodynamic design of the turbine. The constraints addressed the following power turbine problems:

- Rotor degree of reaction and blade area distribution must satisfy blade life objectives.
- Blade trailing edge radius must equal or exceed 0.254 mm (0.010 in.) to ensure adequate cast part quality level.
- Blade thickness distribution near the trailing edge at the base must taper radially to minimize fatigue concentration factor.
- Blade frequency should avoid coincidence with vane passage number within the engine operating speed range to avoid blade fatigue excitation.
- Axial spacing between vane trailing edge and blade leading edge must be equal to or greater than 6.35 mm (0.250 in.) to diminish blade excitation because of vane number in power turbines.
- Turbine blade geometry must provide that the passage between adjacent blades can be extracted along a straight line without rotation to facilitate high-volume/low-cost foundry practice.

The power turbine blade design was completed and all aerodynamic and mechanical considerations were satisfied.

The power turbine duty cycle requirements for the base line engine were given considerable attention in rotor designs. Temperature and stress distributions were established for the following conditions:

- Fire-up from stabilized ambient conditions
- Stabilized conditions at design point
- Prolonged dynamic braking from design point

Based on computed stress comparisons with available low cycle fatigue data available for Mar-M246 material, the power turbine disk design has a satisfactory steady-state and cyclic life.

BASE LINE TURBINE INLET PLENUM

The turbine inlet plenum is a transition piece which collects the combustor outlet gas flow and turns and directs it to the gasifier nozzle annulus. In the base line engine, the plenum is a metal structure mounted on the rear of the gasifier bearing support and piloted by a mating seal flange on the containment ring support (Figure 53). The combustor can is piloted in the ID of the plenum entrance opening, and the plenum exit annulus is spaced away from the gasifier nozzle annulus to allow for the introduction of boundary (muff) cooling flow. The net free body loads on the plenum induced by static pressure distribution are shown in Figure 54.

The shape of the plenum is designed to provide a gradually diminishing flow area from top to bottom as the gas flow is distributed to the nozzle annulus and is known as a "constant velocity" design. Because of requirements for strength and oxidation resistance, Hastelloy X has been selected as the plenum material.

The performance objective of the plenum is to distribute the combustor outlet gas flow uniformly to the gasifier nozzle annulus with a minimal total pressure loss ($\Delta P/P$). Based on testing in the burner rig, the performance objective has been satisfactorily met. The plenum durability

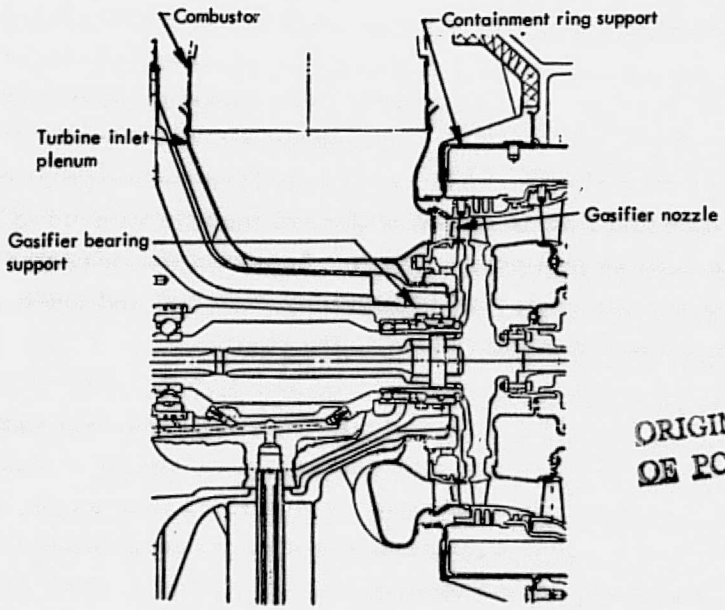

Figure 53. Base line turbine inlet plenum arrangement.

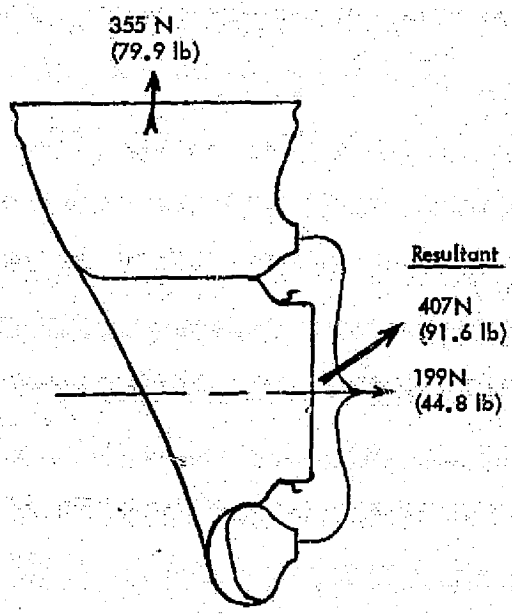

Figure 54. Aerodynamic loads on turbine inlet plenum at design power.

goal is an equivalent of 15,000 hours of engine operation. Although not substantiated by long-term durability testing, the life of the plenum appears to be acceptable based on metal temperature measurements and short-term testing. Figure 55 is a comparison of the measured peak metal temperature with turbine inlet temperature and shows the long-term material oxidation limit.

BASE LINE COMBUSTOR

In the base line engine, the combustor is a single can, mounted vertically in the top of the forward half of the engine block. It is fed by regenerated air in the forward block cavity and discharges into the turbine inlet plenum. The combustor forms a single chamber in which combustion is discontinuous—fuel flow is cut off with zero throttle demand to maximize engine dynamic braking and minimize fuel usage. Figure 56 shows the present design. The dome and walls of the combustor are composed of Lamilloy material and are attached to the burner cover through studs in a small casting welded to the dome.

Combustor performance is gaged by several characteristics including lighting, temperature pattern, emissions, and pressure drop. The current combustor is within acceptable limits, based on these characteristics. The combustor is projected to meet the durability goal of an equivalent of 15,000 hours of engine operation, based on an evaluation of metal temperature measurements from short-term engine testing.

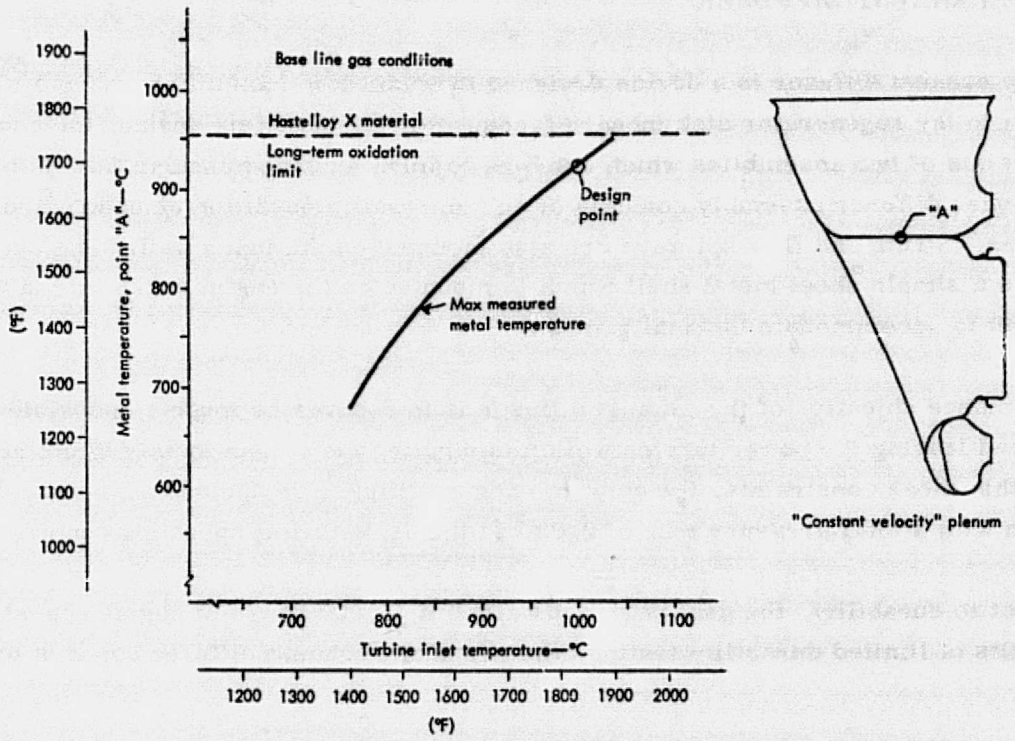

Figure 55. Effect of turbine inlet temperature on plenum metal temperature—base line engine.

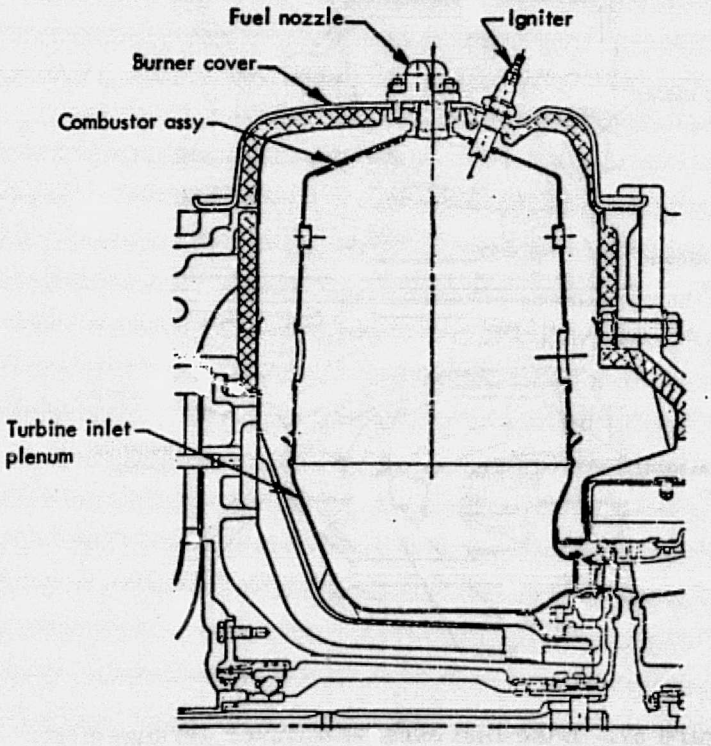

Figure 56. Base line combustor arrangement.

BASE LINE EXHAUST DIFFUSER

The turbine exhaust diffuser is a device designed to obtain low-loss diffusion from the power turbine exit to the regenerator disk inboard faces. For the base line engine, the configuration chosen consists of two assemblies which combine to form a curved annular flow path (Figure 57). The inner diffuser assembly consists of an inner wall, insulation blankets, and an insulation retainer. Struts and flow splitters are also mounted on the inner wall. The outer diffuser assembly is a simple sheet metal shell which is mounted on the engine bulkhead via a keying arrangement to accommodate thermal growth.

The performance objective of the exhaust diffuser is to recover as much as possible of the dynamic head leaving the power turbine while distributing the gas uniformly to the regenerator disks. Within these constraints, the current exhaust diffuser design has achieved adequate distribution with a total pressure loss of 2.62% at the design point operating conditions.

With respect to durability, the goal is an equivalent of 15,000 hours of engine operation. Based on the results of limited durability testing, the life of the exhaust diffuser appears to be acceptable.

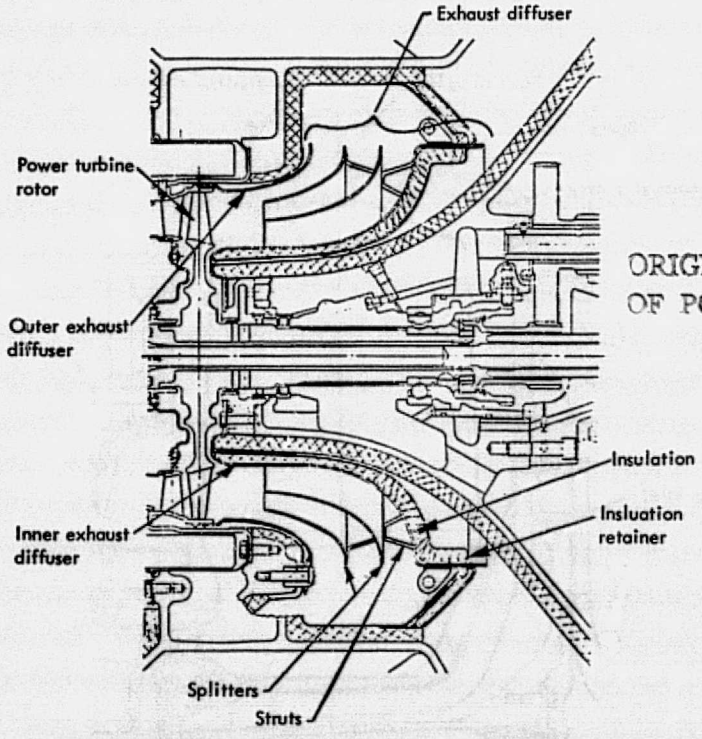

Figure 57. Base line exhaust diffuser arrangement.

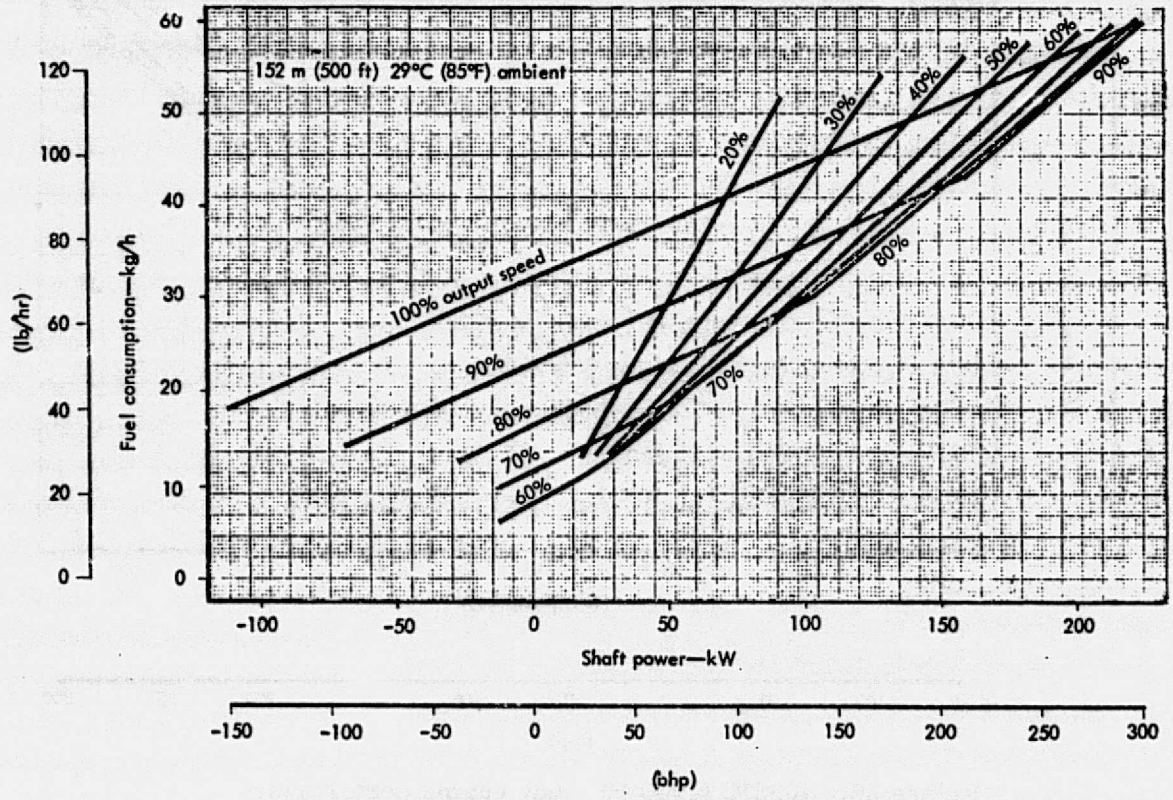

Figure 58. Base line engine performance.

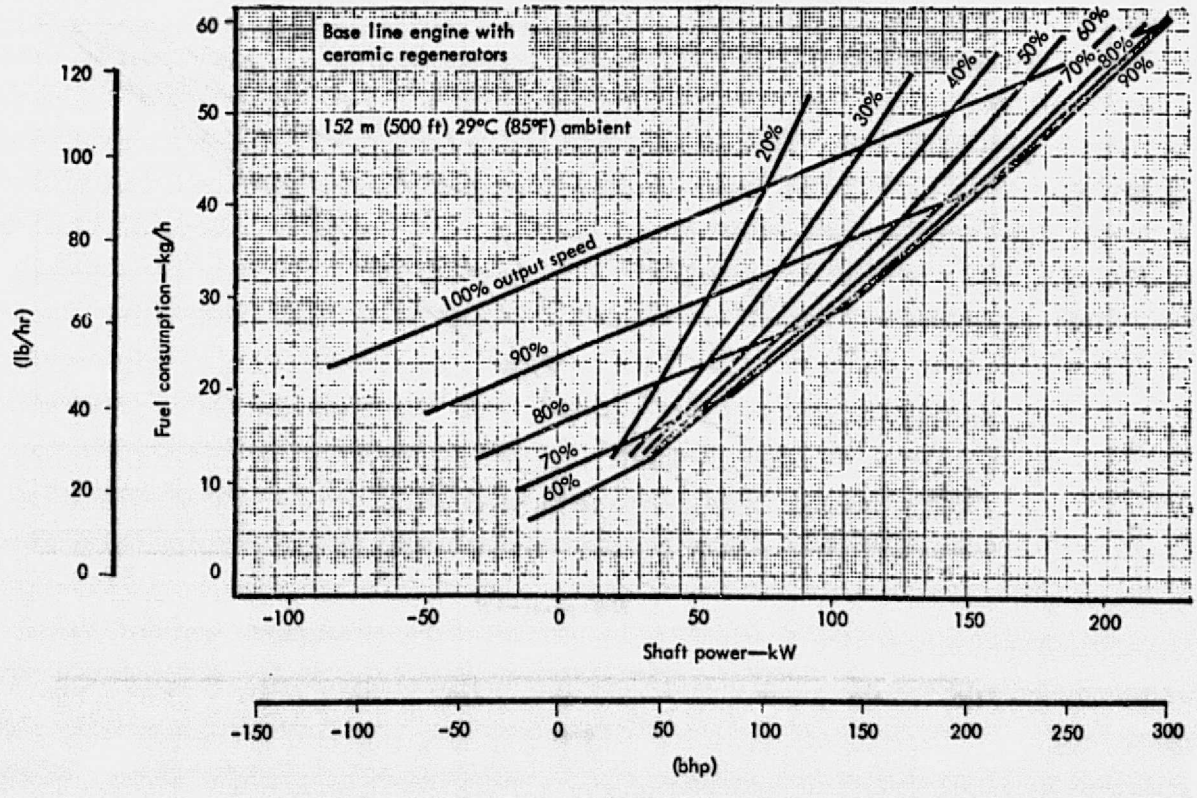

Figure 59. 1002°C (1835°F) study engine performance.

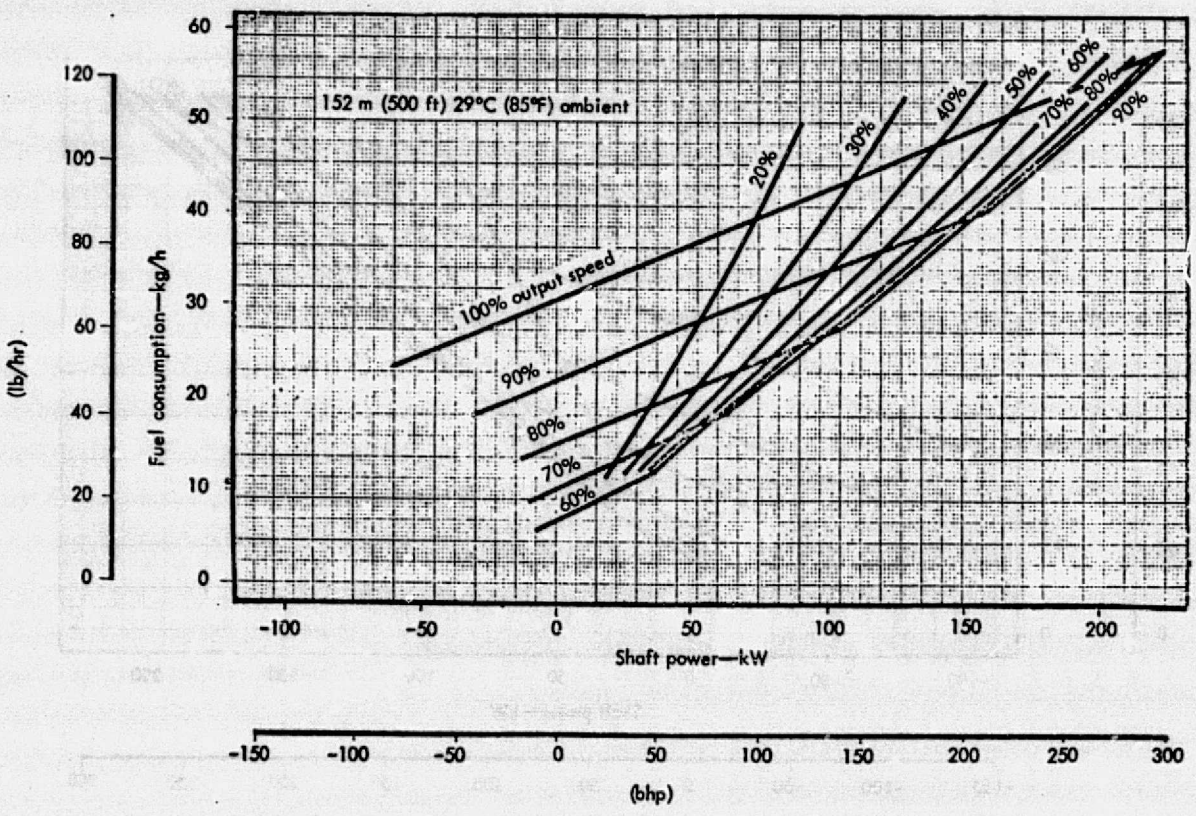

Figure 60. 1038°C (1900°F) study engine performance.

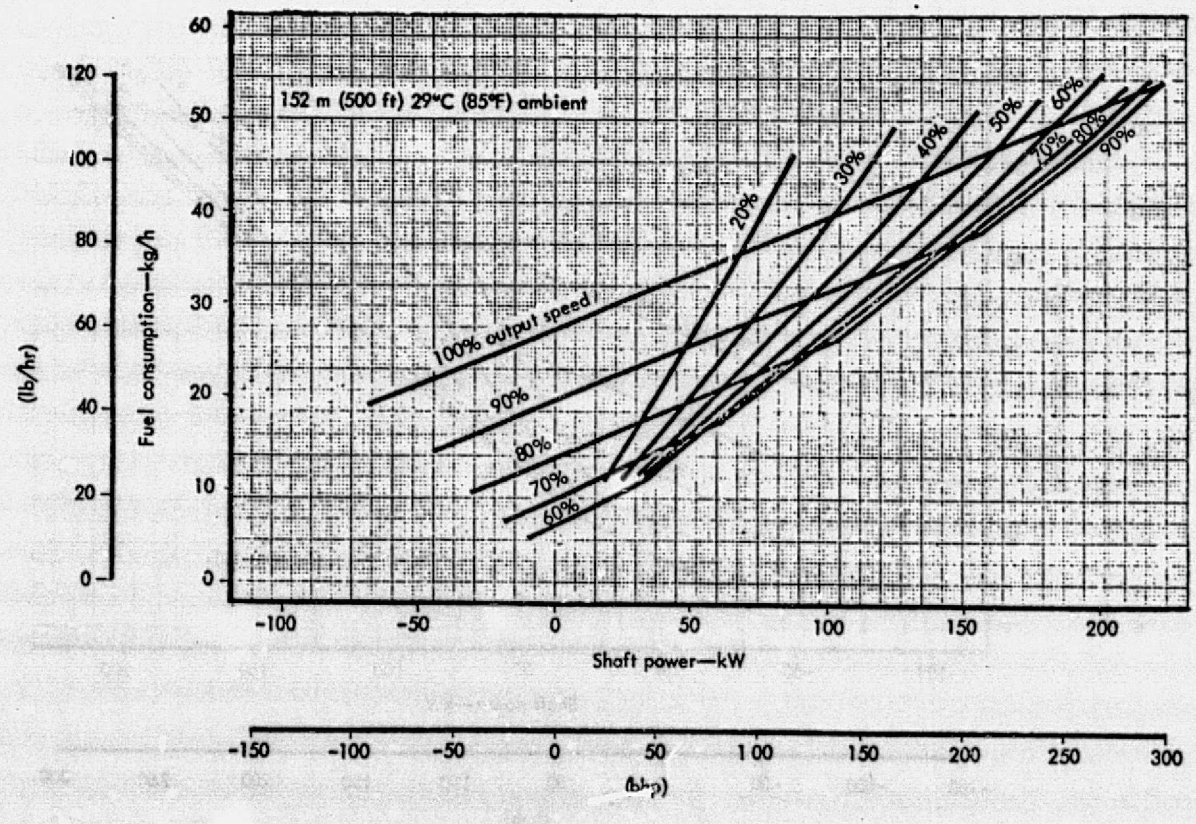

Figure 61. 1132°C (2070°F) study engine performance.

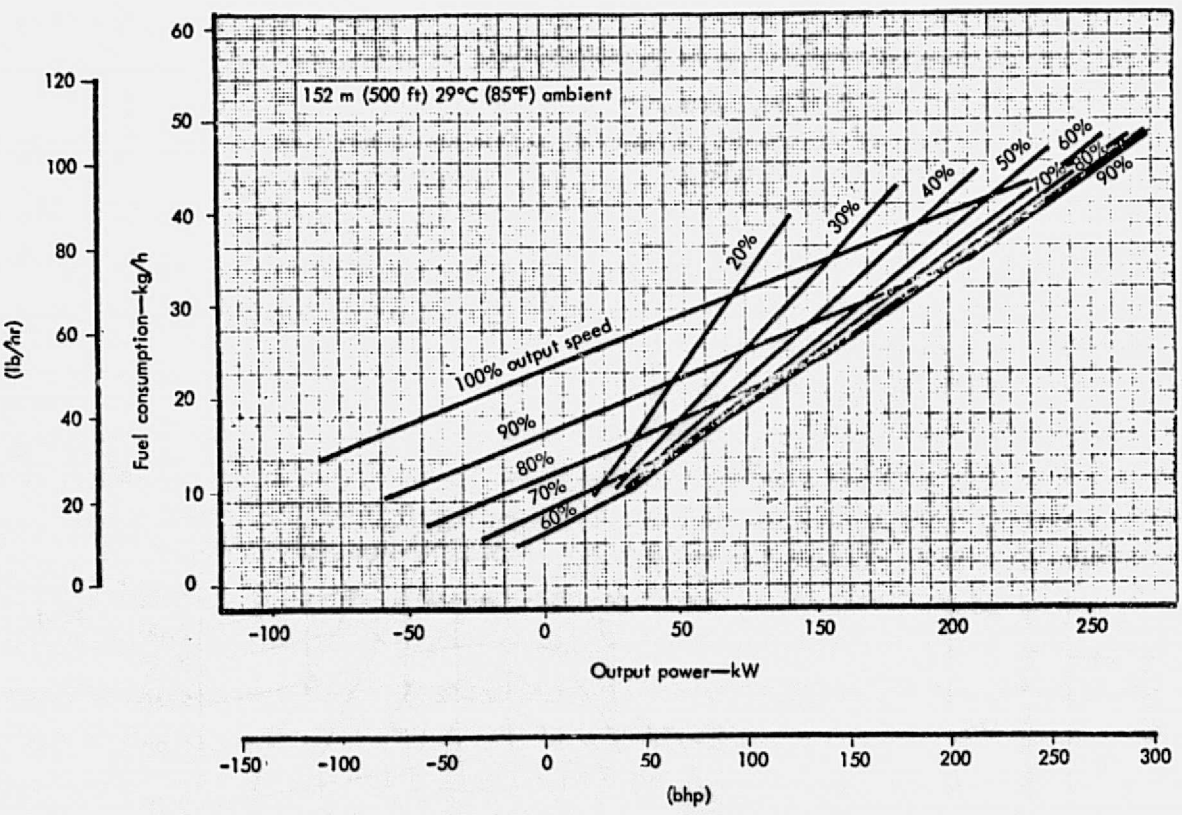

Figure 62. 1204°C (2200°F) study engine performance.

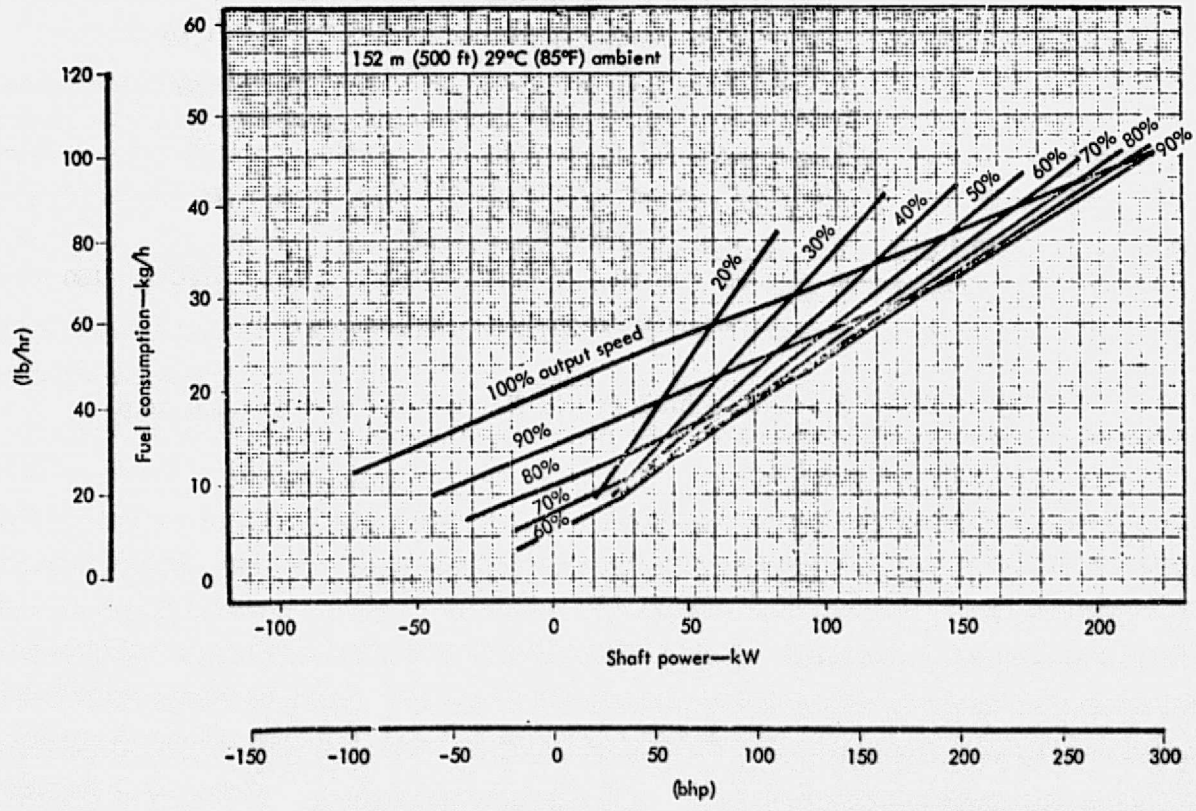

Figure 63. 1371°C (2500°F) study engine performance.

Design point parameters

Temperature = 1204°C (2200°F)
Expansion ratio = 1.929 (total-to-total)
Efficiency = 86.1% (total-to-total)
Speed = 43,000 rpm (= 100% $N/\sqrt{\theta}$)

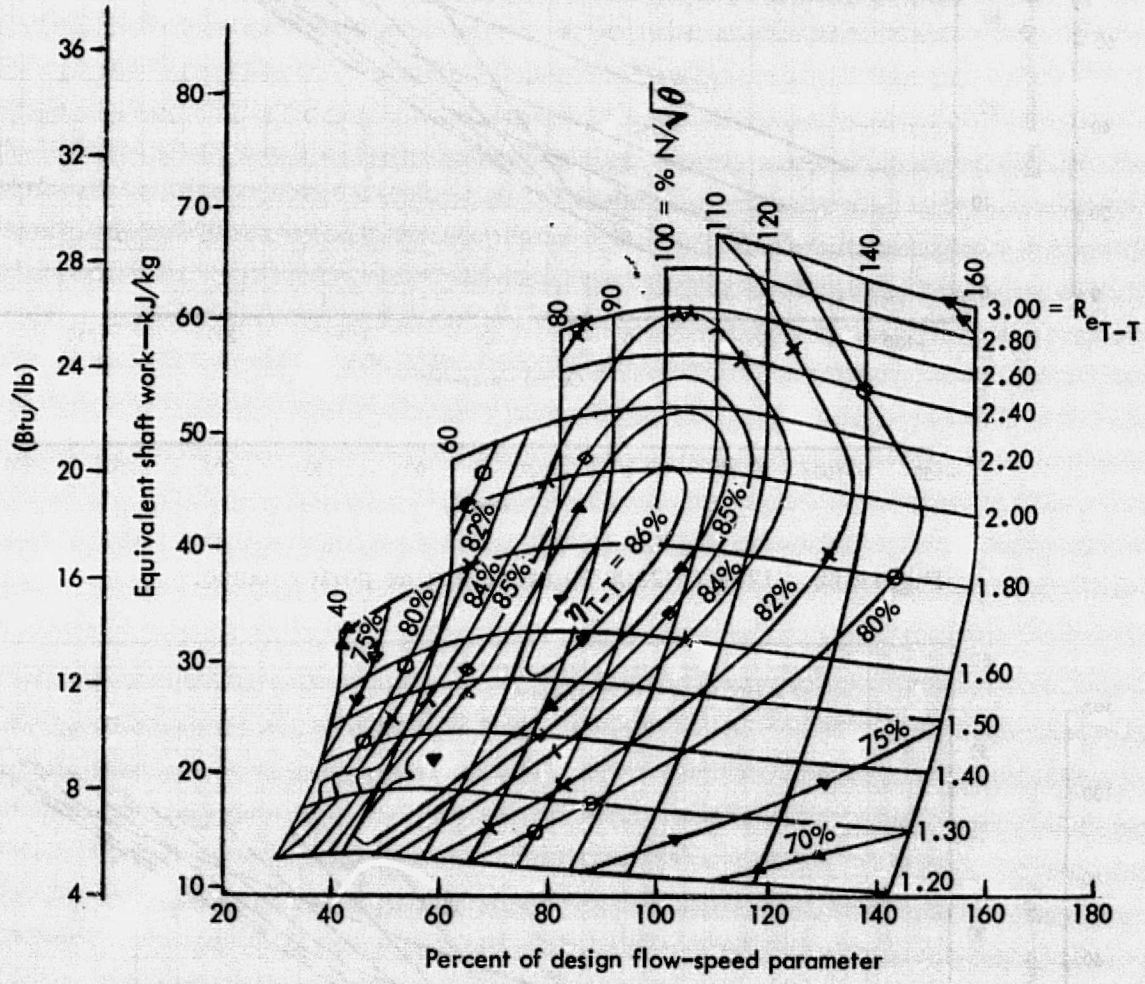

Figure 64. Advanced technology gasifier turbine performance map.

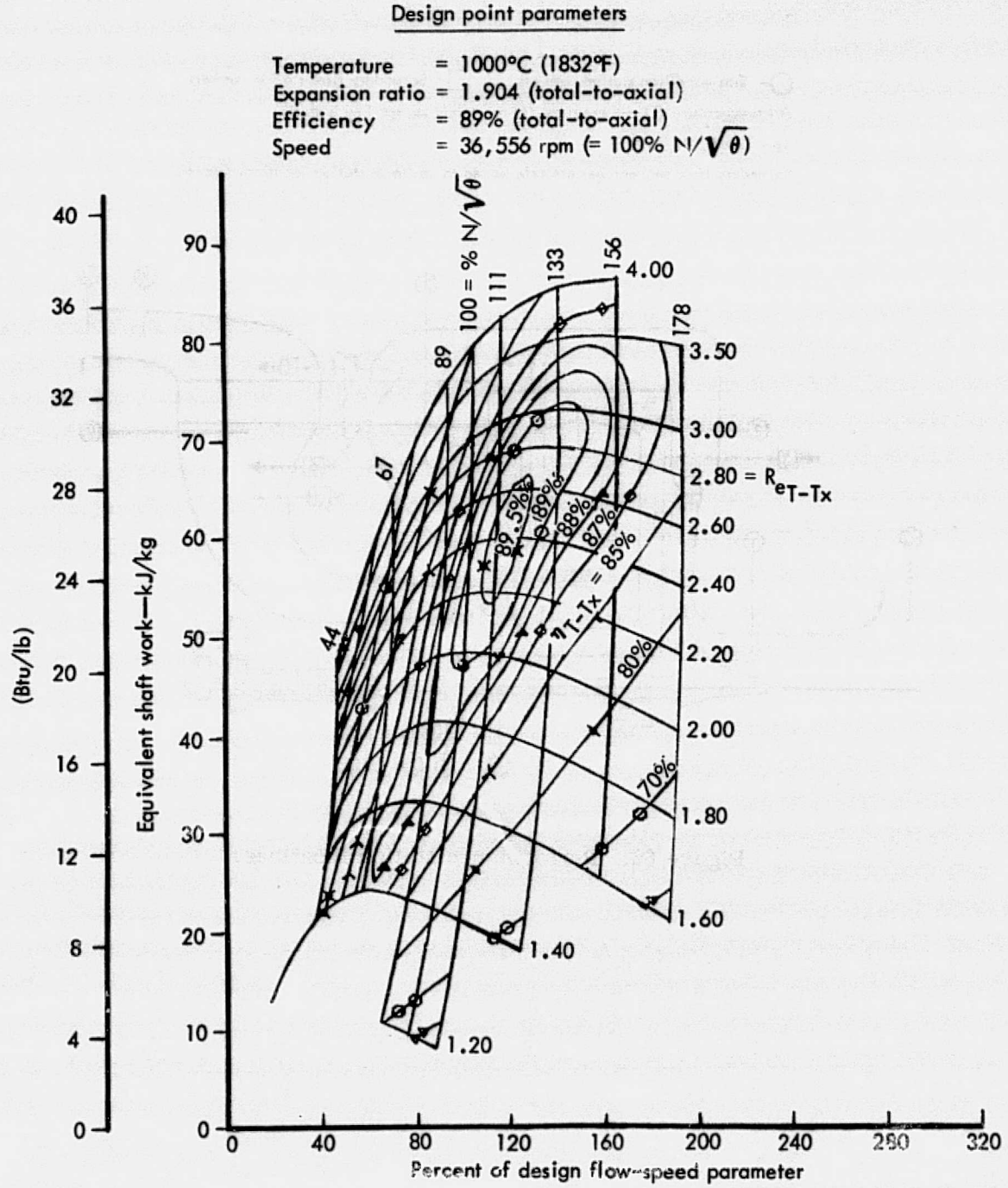

Figure 65. Advanced technology power turbine performance map.

○ - Gas condition station numbers □ - Secondary flow station numbers

All temperature (T) and pressures (P) are totals except T_{12} is static

To = TAMB, Po = PAMB

Secondary flow percentages are referenced to upstream station locations (approx)

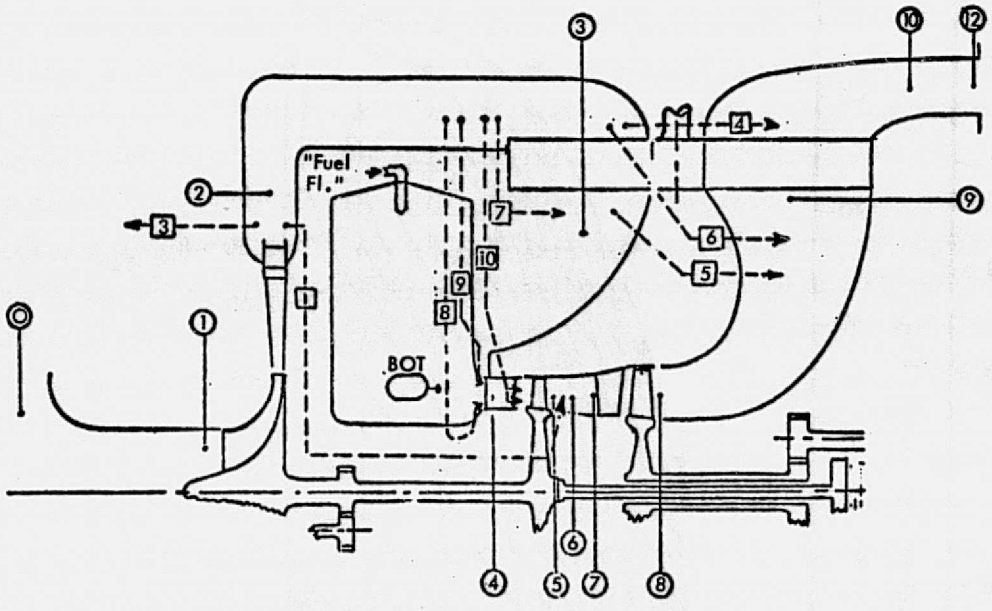

Figure 66. Performance station locations.

TABLE XXIII. BASE LINE ENGINE PERFORMANCE

100% Power

POWER 300 HP

SFC 0.450 LB/HP/HR

FUEL FLOW 135 LB/HR

STA NO.	°R TEMPERATURE	PSIA PRESSURE	LB/SEC CORR. FLOW	LB/SEC MASS FLOW	PRESSURE RATIOS	EFFICIENCY
1	0.544670E 03	0.142160E 02	0.365488E 01	0.345015E 01	0.399971E 01	0.823972E 00
2	0.863102E 03	0.568599E 02	0.103051E 01	0.309083E 01	0.177658E-02	0.0
3	0.162628E 04	0.567589E 02	0.139002E 01	0.303188E 01	0.220001E-01	0.976000E 00
4	0.229500E 04	0.555102E 02	0.183585E 01	0.322118E 01	0.206496E 01	0.869996E 00
5	0.197620E 04	0.268819E 02	0.343729E 01	0.322118E 01	0.100000E 01	0.0
6	0.195765E 04	0.268819E 02	0.348378E 01	0.328018E 01	0.690973E-02	0.0
7	0.195765E 04	0.266962E 02	0.357995E 01	0.328030E 01	0.172144E 01	0.897054E 00
8	0.173792E 04	0.155080E 02	0.569008E 01	0.328030E 01	0.275920E-01	0.0
9	0.172386E 04	0.150801E 02	0.603262E 01	0.339552E 01	0.306912E-01	0.888542E 00
10	0.104937E 04	0.146173E 02	0.492656E 01	0.344509E 01	0.0	0.0
11	0.0	0.0	0.0	0.344509E 01	0.0	0.0
12	0.104575E 04	0.144322E 02	0.0	0.344509E 01	0.128288E-01	0.0

50% Power (APPROX)

POWER 138 HP

SFC 0.500 LB/HP/HR

FUEL FLOW 69 LB/HR

STA NO.	TEMPERATURE	PRESSURE	CORR. FLOW	MASS FLOW	PRESSURE RATIOS	EFFICIENCY
1	0.544670E 03	0.142160E 02	0.232822E 01	0.219781E 01	0.259688E 01	0.825032E 00
2	0.750767E 03	0.369173E 02	0.942981E 00	0.196891E 01	0.254279E-02	0.0
3	0.176823E 04	0.368234E 02	0.142316E 01	0.193136E 01	0.230618E-01	0.976000E 00
4	0.228449E 04	0.359742E 02	0.179530E 01	0.204729E 01	0.177945E 01	0.862243E 00
5	0.202967E 04	0.202164E 02	0.294397E 01	0.204729E 01	0.100000E 01	0.0
6	0.200839E 04	0.202164E 02	0.298226E 01	0.208487E 01	0.502986E-02	0.0
7	0.200839E 04	0.201147E 02	0.305938E 01	0.208531E 01	0.134206E 01	0.987509E 00
8	0.188457E 04	0.149879E 02	0.389747E 01	0.208531E 01	0.127657E-01	0.0
9	0.186697E 04	0.147966E 02	0.406776E 01	0.215871E 01	0.200142E-01	0.913509E 00
10	0.964545E 03	0.145004E 02	0.302710E 01	0.219029E 01	0.0	0.0
11	0.0	0.0	0.0	0.219029E 01	0.0	0.0
12	0.963220E 03	0.144317E 02	0.0	0.219029E 01	0.476170E-02	0.0

Approx. Idle

POWER 3.3 HP

SFC 4.120 LB/HP/HR

FUEL FLOW 13.6 LB/HR

STA NO.	TEMPERATURE	PRESSURE	CORR. FLOW	MASS FLOW	PRESSURE RATIOS	EFFICIENCY
1	0.544670E 03	0.142160E 02	0.125231E 01	0.118216E 01	0.140962E 01	0.752050E 00
2	0.619234E 03	0.200391E 02	0.848625E 00	0.105904E 01	0.310445E-02	0.0
3	0.132227E 04	0.199769E 02	0.122019E 01	0.103884E 01	0.169531E-01	0.976000E 00
4	0.151629E 04	0.196383E 02	0.141982E 01	0.109489E 01	0.130750E 01	0.857538E 00
5	0.142913E 04	0.150197E 02	0.177824E 01	0.109489E 01	0.100000E 01	0.0
6	0.141519E 04	0.150197E 02	0.180221E 01	0.111510E 01	0.181538E-02	0.0
7	0.141519E 04	0.149924E 02	0.182746E 01	0.111519E 01	0.102753E 01	0.935326E 00
8	0.140585E 04	0.145907E 02	0.184921E 01	0.111519E 01	0.284588E-02	0.0
9	0.139323E 04	0.145492E 02	0.191153E 01	0.115466E 01	0.699639E-02	0.910341E 00
10	0.756428E 03	0.144474E 02	0.143925E 01	0.117165E 01	0.0	0.0
11	0.0	0.0	0.0	0.117165E 01	0.0	0.0
12	0.756186E 03	0.144320E 02	0.0	0.117165E 01	0.106716E-02	0.0

TABLE XXIV. 1002°C (1835°F) STUDY ENGINE PERFORMANCE

BASELINE ENGINE WITH CERAMIC REGENERATORS

100% Power

POWER 300 HP

SFC 0.450 LB/HP-HR

FUEL FLOW 135 LB/HR

STA NO.	°R TEMPERATURE	PSIA PRESSURE	LB/SEC CORR. FLOW	LB/SEC MASS FLOW	PRESSURE RATIOS	EFFICIENCY
1	0.544670E 03	0.142160E 02	0.365283E 01	0.344822E 01	0.400326E 01	0.824291E 00
2	0.863223E 03	0.568134E 02	0.102900E 01	0.308910E 01	0.264692E-02	0.0
3	0.164492E 04	0.567598E 02	0.139716E 01	0.303018E 01	0.222265E-01	0.976000E 00
4	0.229500E 04	0.554982E 02	0.193462E 01	0.321849E 01	0.205782E 01	0.870022E 00
5	0.197747E 04	0.269695E 02	0.342437E 01	0.321849E 01	0.100000E 01	0.0
6	0.195988E 04	0.269695E 02	0.347068E 01	0.327745E 01	0.685728E-02	0.0
7	0.195388E 04	0.267945E 02	0.356616E 01	0.327768E 01	0.170465E 01	0.896577E 00
8	0.174281E 04	0.157126E 02	0.561939E 01	0.327768E 01	0.268921E-01	0.0
9	0.172894E 04	0.152901E 02	0.595383E 01	0.339283E 01	0.441651E-01	0.904675E 00
10	0.103679E 04	0.146143E 02	0.489302E 01	0.344237E 01	0.0	0.0
11	0.0	0.0	0.0	0.344237E 01	0.0	0.0
12	0.103324E 04	0.144321E 02	0.0	0.344237E 01	0.126572E-01	0.0

50% Power (APPROX)

POWER 140 HP

SFC 0.471 LB/HP-HR

FUEL FLOW 66 LB/HR

STA NO.	°R TEMPERATURE	PSIA PRESSURE	LB/SEC CORR. FLOW	LB/SEC MASS FLOW	PRESSURE RATIOS	EFFICIENCY
1	0.544670E 03	0.142160E 02	0.232187E 01	0.719181E 01	0.260077E 01	0.825412E 00
2	0.751036E 03	0.368725E 02	0.939169E 00	0.196354E 01	0.356168E-02	0.0
3	0.181933E 04	0.368408E 02	0.143896E 01	0.192609E 01	0.235765E-01	0.976000E 00
4	0.229500E 04	0.359722E 02	0.179349E 01	0.204048E 01	0.177448E 01	0.862181E 00
5	0.204012E 04	0.202720E 02	0.293366E 01	0.204048E 01	0.100000E 01	0.0
6	0.201864E 04	0.202720E 02	0.297177E 01	0.207796E 01	0.499421E-02	0.0
7	0.201864E 04	0.201758E 02	0.304854E 01	0.207844E 01	0.133763E 01	0.887101E 00
8	0.180553E 04	0.150795E 02	0.387227E 01	0.207844E 01	0.125964E-01	0.0
9	0.179258E 04	0.148896E 02	0.404160E 01	0.215163E 01	0.263730E-01	0.949414E 00
10	0.926063E 03	0.144968E 02	0.295712E 01	0.218312E 01	0.0	0.0
11	0.0	0.0	0.0	0.218312E 01	0.0	0.0
12	0.924849E 03	0.144313E 02	0.0	0.218312E 01	0.454235E-02	0.0

Approx. Idle

POWER 3.3 HP

SFC 3.641 LB/HP-HR

FUEL FLOW 12.0

STA NO.	°R TEMPERATURE	PSIA PRESSURE	LB/SEC CORR. FLOW	LB/SEC MASS FLOW	PRESSURE RATIOS	EFFICIENCY
1	0.544670E 03	0.142160E 02	0.124701E 01	0.117716E 01	0.141275E 01	0.755746E 00
2	0.619375E 03	0.200837E 02	0.843254E 00	0.105456E 01	0.453883E-02	0.0
3	0.136938E 04	0.199925E 02	0.123551E 01	0.103445E 01	0.173810E-01	0.976000E 00
4	0.152753E 04	0.196450E 02	0.141792E 01	0.108967E 01	0.130595E 01	0.857317E 00
5	0.144016E 04	0.150428E 02	0.177387E 01	0.108967E 01	0.100000E 01	0.0
6	0.142602E 04	0.150428E 02	0.179774E 01	0.110980E 01	0.180686E-02	0.0
7	0.142602E 04	0.150156E 02	0.183306E 01	0.110991E 01	0.102660E 01	0.935212E 00
8	0.141693E 04	0.146265E 02	0.194317E 01	0.110991E 01	0.292508E-02	0.0
9	0.140484E 04	0.145852E 02	0.190571E 01	0.114922E 01	0.950789E-02	0.957074E 00
10	0.722683E 03	0.144465E 02	0.140024E 01	0.116613E 01	0.0	0.0
11	0.0	0.0	0.0	0.116613E 01	0.0	0.0
12	0.722468E 03	0.144319E 02	0.0	0.116613E 01	0.100994E-02	0.0

TABLE XXV. 1038°C (1900°F) STUDY ENGINE PERFORMANCE

100% Power

POWER 300 HP

SFC 0.425 LB/HP-HR

FUEL FLOW 127 LB/HR

STA NO.	°R TEMPERATURE	PSIA PRESSURE	LB/SEC CORR. FLOW	LB/SEC MASS FLOW	PRESSURE RATIOS	EFFICIENCY
1	0.544670E 03	0.142160E 02	0.363284E 01	0.342934E 01	0.403223E 01	0.826643E 00
2	0.864297E 03	0.573222E 02	0.102649E 01	0.310164E 01	0.267631E-02	0.0
3	0.168690E 04	0.571688E 02	0.141075E 01	0.304312E 01	0.226610E-01	0.976000E 00
4	0.236000E 04	0.559733E 02	0.183705E 01	0.319801E 01	0.205791E 01	0.869855E 00
5	0.203515E 04	0.271505E 02	0.342884E 01	0.319801E 01	0.100000E 01	0.0
6	0.201430E 04	0.271505E 02	0.347817E 01	0.326077E 01	0.688857E-02	0.0
7	0.201430E 04	0.269634E 02	0.357617E 01	0.326103E 01	0.171391E 01	0.897362E 00
8	0.179095E 04	0.157321E 02	0.566050E 01	0.326103E 01	0.273015E-01	0.0
9	0.177638E 04	0.153026E 02	0.599904E 01	0.337541E 01	0.450247E-01	0.903723E 00
10	0.104215E 04	0.146136E 02	0.488163E 01	0.342462E 01	0.0	0.0
11	0.0	0.0	0.0	0.342462E 01	0.0	0.0
12	0.103861E 04	0.144319E 02	0.0	0.342462E 01	0.125914E-01	0.0

50% Power (APPROX)

POWER 138 HP

SFC 0.446 LB/HP-HR

FUEL FLOW 61 LB/HR

STA NO.	TEMPERATURE	PRESSURE	CORR. FLOW	MASS FLOW	PRESSURE RATIOS	EFFICIENCY
1	0.544670E 03	0.142160E 02	0.230324E 01	0.217422E 01	0.261067E 01	0.826746E 00
2	0.751758E 03	0.371133E 02	0.937448E 00	0.196646E 01	0.360656E-02	0.0
3	0.136697E 04	0.369795E 02	0.145467E 01	0.192935E 01	0.240942E-01	0.976000E 00
4	0.236000E 04	0.360585E 02	0.179729E 01	0.202204E 01	0.177470E 01	0.860929E 00
5	0.209947E 04	0.203350E 02	0.294000E 01	0.202204E 01	0.100000E 01	0.0
6	0.207549E 04	0.203350E 02	0.298069E 01	0.206183E 01	0.502449E-02	0.0
7	0.207549E 04	0.202328E 02	0.305947E 01	0.206231E 01	0.134099E 01	0.888963E 00
8	0.194828E 04	0.150879E 02	0.389310E 01	0.206231E 01	0.127251E-01	0.0
9	0.193054E 04	0.148959E 02	0.406342E 01	0.213482E 01	0.268549E-01	0.947976E 00
10	0.927554E 03	0.144959E 02	0.293655E 01	0.216602E 01	0.0	0.0
11	0.0	0.0	0.0	0.216602E 01	0.0	0.0
12	0.926362E 03	0.144311E 02	0.0	0.216602E 01	0.447750E-02	0.0

Approx. Idle

POWER 3.1 HP

SFC 3.437 LB/HP-HR

FUEL FLOW 10.7 LB/HR

STA NO.	TEMPERATURE	PRESSURE	CORR. FLOW	MASS FLOW	PRESSURE RATIOS	EFFICIENCY
1	0.544670E 03	0.142160E 02	0.124648E 01	0.117665E 01	0.141306E 01	0.756105E 00
2	0.619386E 03	0.200880E 02	0.850501E 00	0.106422E 01	0.458497E-02	0.0
3	0.137060E 04	0.199959E 02	0.124744E 01	0.104414E 01	0.177183E-01	0.976000E 00
4	0.153140E 04	0.196416E 02	0.141756E 01	0.108781E 01	0.130560E 01	0.857225E 00
5	0.144393E 04	0.150442E 02	0.177290E 01	0.108781E 01	0.100000E 01	0.0
6	0.142873E 04	0.150442E 02	0.179854E 01	0.110934E 01	0.180811E-02	0.0
7	0.142873E 04	0.150169E 02	0.182389E 01	0.110946E 01	0.102676E 01	0.934907E 00
8	0.141957E 04	0.146256E 02	0.184425E 01	0.110946E 01	0.283080E-02	0.0
9	0.140744E 04	0.145842E 02	0.190674E 01	0.114870E 01	0.945634E-02	0.955494E 00
10	0.717498E 03	0.144463E 02	0.139458E 01	0.116559E 01	0.0	0.0
11	0.0	0.0	0.0	0.116559E 01	0.0	0.0
12	0.717286E 03	0.144318E 02	0.0	0.116559E 01	0.100231E-02	0.0

TABLE XXVI. 1132°C (2070°F) STUDY ENGINE PERFORMANCE

100% Power

POWER 300 HP

SFC 0.404 LB/HP-HR

FUEL FLOW 121 LB/HP

STA NO.	°R TEMPERATURE	PSIA PRESSURE	LB/SEC CORR. FLOW	LB/SEC MASS FLOW	PRESSURE RATIOS	EFFICIENCY
1	0.544670E+03	0.142160E+02	0.309963E+01	0.292600E+01	0.400000E+01	0.822000E+00
2	0.863873E+03	0.568640E+02	0.868509E+00	0.260395E+01	0.241643E-02	0.0
3	0.182960E+04	0.567266E+02	0.123884E+01	0.254612E+01	0.220008E-01	0.976000E+00
4	0.253000E+04	0.554786E+02	0.160661E+01	0.267883E+01	0.198278E-01	0.864000E+00
5	0.220452E+04	0.279802E+02	0.290067E+01	0.267883E+01	0.100000E+01	0.0
6	0.217007E+04	0.279802E+02	0.296059E+01	0.275579E+01	0.692260E-02	0.0
7	0.217007E+04	0.277865E+02	0.304844E+01	0.275579E+01	0.177742E+01	0.889000E+00
8	0.191991E+04	0.156330E+02	0.498413E+01	0.275579E+01	0.260000E-01	0.0
9	0.190134E+04	0.152266E+02	0.530101E+01	0.286865E+01	0.399984E-01	0.932976E+00
10	0.104995E+04	0.146175E+02	0.417277E+01	0.291722E+01	0.0	0.0
11	0.0	0.0	0.0	0.291722E+01	0.0	0.0
12	0.104632E+04	0.144325E+02	0.0	0.291722E+01	0.128202E-01	0.0

50% Power (APPROX)

POWER 136

SFC 0.433 LB/HP-HR

FUEL FLOW 59 LB/HP

STA NO.	TEMPERATURE	PRESSURE	CORR. FLOW	MASS FLOW	PRESSURE RATIOS	EFFICIENCY
1	0.544670E+03	0.142160E+02	0.197307E+01	0.186255E+01	0.259801E+01	0.823143E+00
2	0.751344E+03	0.369334E+02	0.793817E+00	0.165755E+01	0.333822E-02	0.0
3	0.200094E+04	0.368101E+02	0.127089E+01	0.162073E+01	0.231539E-01	0.976000E+00
4	0.253000E+04	0.359578E+02	0.157250E+01	0.170037E+01	0.172153E+01	0.856052E+00
5	0.226930E+04	0.208872E+02	0.250239E+01	0.170037E+01	0.100000E+01	0.0
6	0.223029E+04	0.208872E+02	0.255225E+01	0.174935E+01	0.512105E-02	0.0
7	0.223029E+04	0.207802E+02	0.262513E+01	0.175076E+01	0.137922E+01	0.881104E+00
8	0.208423E+04	0.150667E+02	0.342317E+01	0.175076E+01	0.121300E-01	0.0
9	0.206157E+04	0.148839E+02	0.358779E+01	0.182260E+01	0.259311E-01	0.956152E+00
10	0.954100E+03	0.144980E+02	0.254820E+01	0.185352E+01	0.0	0.0
11	0.0	0.0	0.0	0.185352E+01	0.0	0.0
12	0.952870E+03	0.144299E+02	0.0	0.185352E+01	0.471878E-02	0.0

Approx. Idle

POWER 2.9 HP

SFC 3.335 LB/HP-HR

FUEL FLOW 9.7 LB/HP

STA NO.	TEMPERATURE	PRESSURE	CORR. FLOW	MASS FLOW	PRESSURE RATIOS	EFFICIENCY
1	0.544670E+03	0.142160E+02	0.106002E+01	0.100064E+01	0.141108E+01	0.751954E+00
2	0.619478E+03	0.200599E+02	0.712979E+00	0.890510E+00	0.410151E-02	0.0
3	0.151409E+04	0.199776E+02	0.109437E+01	0.870731E+00	0.171686E-01	0.976000E+00
4	0.169978E+04	0.196346E+02	0.124952E+01	0.907762E+00	0.128809E+01	0.850550E+00
5	0.160574E+04	0.152432E+02	0.154177E+01	0.907762E+00	0.100000E+01	0.0
6	0.158348E+04	0.152432E+02	0.157347E+01	0.934079E+00	0.192943E-02	0.0
7	0.158348E+04	0.152139E+02	0.159956E+01	0.934221E+00	0.104066E+01	0.919102E+00
8	0.156869E+04	0.146154E+02	0.163318E+01	0.934221E+00	0.273567E-02	0.0
9	0.155218E+04	0.145793E+02	0.169636E+01	0.972818E+00	0.899488E-02	0.961495E+00
10	0.741824E+03	0.144482E+02	0.120356E+01	0.989428E+00	0.0	0.0
11	0.0	0.0	0.0	0.989428E+00	0.0	0.0
12	0.741592E+03	0.144332E+02	0.0	0.989428E+00	0.104237E-02	0.0

TABLE XXVII. 1204°C (2200°F) STUDY ENGINE PERFORMANCE

100% Power

POWER 300 HP

SFC 0.357 LB/HP-HR

FUEL FLOW 107 LB/HR

STA NO.	°R TEMPERATURE	PSIA PRESSURE	LB/SEC CORR. FLOW	LB/SEC MASS FLOW	PRESSURE RATIOS	EFFICIENCY
1	0.544670E+03	0.142521E+02	0.268071E+01	0.253697E+01	0.400305E+01	0.829305E+00
2	0.861212E+03	0.570091E+02	0.750111E+00	0.225819E+01	0.199281E-02	0.0
3	0.194022E+04	0.558961E+02	0.110575E+01	0.221305E+01	0.220010E-01	0.978000E+00
4	0.265000E+04	0.556443E+02	0.142930E+01	0.232926E+01	0.190278E+01	0.870999E+00
5	0.253675E+04	0.292437E+02	0.248461E+01	0.232926E+01	0.100000E+01	0.0
6	0.229359E+04	0.292437E+02	0.254294E+01	0.240639E+01	0.0	0.0
7	0.229359E+04	0.292437E+02	0.260277E+01	0.240625E+01	0.189515E+01	0.891997E+00
8	0.220345E+04	0.154508E+02	0.450390E+01	0.240625E+01	0.245935E-01	0.0
9	0.198597E+04	0.150513E+02	0.476800E+01	0.249557E+01	0.281224E-01	0.962418E+00
10	0.133555E+04	0.145280E+02	0.359369E+01	0.253392E+01	0.0	0.0
11	0.0	0.0	0.0	0.253392E+01	0.0	0.0
12	0.103276E+04	0.144329E+02	0.0	0.253392E+01	0.135164E-01	0.0

50% Power (APPROX)

POWER 137 HP

SFC 0.393 LB/HP-HR

FUEL FLOW 54 LB/HR

STA NO.	TEMPERATURE	PRESSURE	CORR. FLOW	MASS FLOW	PRESSURE RATIOS	EFFICIENCY
1	0.544670E+03	0.142521E+02	0.170725E+01	0.161618E+01	0.259639E+01	0.830039E+00
2	0.749531E+03	0.370111E+02	0.686673E+00	0.143858E+01	0.290698E-02	0.0
3	0.211315E+04	0.369035E+02	0.113320E+01	0.140982E+01	0.231058E-01	0.978000E+00
4	0.265000E+04	0.360505E+02	0.140077E+01	0.147982E+01	0.147808E+01	0.866041E+00
5	0.239693E+04	0.214834E+02	0.217613E+01	0.147982E+01	0.100000E+01	0.0
6	0.234854E+04	0.214834E+02	0.222554E+01	0.152805E+01	0.0	0.0
7	0.234854E+04	0.214834E+02	0.227747E+01	0.152882E+01	0.143577E+01	0.883105E+00
8	0.217705E+04	0.149525E+02	0.307938E+01	0.152882E+01	0.113839E-01	0.0
9	0.215555E+04	0.147823E+02	0.321379E+01	0.158572E+01	0.187543E-01	0.972272E+00
10	0.750371E+03	0.145151E+02	0.220785E+01	0.161015E+01	0.0	0.0
11	0.0	0.0	0.0	0.161015E+01	0.0	0.0
12	0.748771E+03	0.144329E+02	0.0	0.161015E+01	0.499821E-02	0.0

Approx. Idle

POWER 8.0 HP

SFC 1.218 LB/HP-HR

FUEL FLOW 10.3 LB/HR

STA NO.	TEMPERATURE	PRESSURE	CORR. FLOW	MASS FLOW	PRESSURE RATIOS	EFFICIENCY
1	0.544670E+03	0.142521E+02	0.913220E+00	0.864254E+00	0.141391E+01	0.761690E+00
2	0.619974E+03	0.201511E+02	0.612883E+00	0.769284E+00	0.359529E-02	0.0
3	0.166802E+04	0.200787E+02	0.980593E+00	0.753905E+00	0.173025E-01	0.978000E+00
4	0.183353E+04	0.197313E+02	0.112052E+01	0.786390E+00	0.126060E+01	0.863833E+00
5	0.174420E+04	0.156523E+02	0.135396E+01	0.786390E+00	0.100000E+01	0.0
6	0.171017E+04	0.156523E+02	0.138548E+01	0.812663E+00	0.0	0.0
7	0.171017E+04	0.156523E+02	0.140701E+01	0.812256E+00	0.107311E+01	0.899603E+00
8	0.168294E+04	0.145859E+02	0.147414E+01	0.812256E+00	0.259411E-02	0.0
9	0.166655E+04	0.145491E+02	0.152588E+01	0.842683E+00	0.567536E-02	0.974422E+00
10	0.746589E+03	0.144510E+02	0.104408E+01	0.855747E+00	0.0	0.0
11	0.0	0.0	0.0	0.855747E+00	0.0	0.0
12	0.746541E+03	0.144350E+02	0.0	0.855747E+00	0.110722E-02	0.0

TABLE XXVIII. 1371°C (2500°F) STUDY ENGINE PERFORMANCE

100% Power

POWER 300 HP

SFC 0.344 LB/HP-HR

FUEL FLOW 103 LB/HR

STA NO.	°R TEMPERATURE	PSIA PRESSURE	LB/SEC CORR. FLOW	LB/SEC MASS FLOW	PRESSURE RATIOS	EFFICIENCY
1	0.544670E+03	0.142521E+02	0.224011E+01	0.212000E+01	0.400000E+01	0.822000E+00
2	0.863873E+03	0.570083E+02	0.617611E+00	0.185641E+01	0.179952E-02	0.0
3	0.215897E+04	0.569057E+02	0.954602E+00	0.181180E+01	0.219269E-01	0.978000E+00
4	0.296000E+04	0.556579E+02	0.123919E+01	0.191140E+01	0.183286E+01	0.866000E+00
5	0.262685E+04	0.303667E+02	0.208170E+01	0.191140E+01	0.100000E+01	0.0
6	0.256423E+04	0.303667E+02	0.214022E+01	0.198899E+01	0.0	0.0
7	0.256423E+04	0.303667E+02	0.219529E+01	0.198899E+01	0.198280E+01	0.838000E+00
8	0.222686E+04	0.153150E+02	0.395464E+01	0.198899E+01	0.181000E-01	0.0
9	0.220240E+04	0.150378E+02	0.418351E+01	0.207742E+01	0.278147E-01	0.970479E+00
10	0.108263E+04	0.146195E+02	0.307217E+01	0.211540E+01	0.0	0.0
11	0.0	0.0	0.0	0.211540E+01	0.0	0.0
12	0.107888E+04	0.144325E+02	0.0	0.211540E+01	0.129595E-01	0.0

50% Power (APPROX)

POWER 121 HP

SFC 0.398 LB/HP-HR

FUEL FLOW 48 LB/HR

STA NO.	TEMPERATURE	PRESSURE	CORR. FLOW	MASS FLOW	PRESSURE RATIOS	EFFICIENCY
1	0.544670E+03	0.142521E+02	0.145493E+01	0.137692E+01	0.256440E+01	0.818605E+00
2	0.749267E+03	0.365480E+02	0.582713E+00	0.120572E+01	0.252384E-02	0.0
3	0.219187E+04	0.364556E+02	0.975144E+00	0.117674E+01	0.228829E-01	0.978000E+00
4	0.276609E+04	0.356216E+02	0.120856E+01	0.123634E+01	0.162216E+01	0.863241E+00
5	0.251183E+04	0.219594E+02	0.182079E+01	0.123634E+01	0.100000E+01	0.0
6	0.244880E+04	0.219594E+02	0.187108E+01	0.128674E+01	0.0	0.0
7	0.244880E+04	0.219594E+02	0.191778E+01	0.128768E+01	0.147701E+01	0.876009E+00
8	0.225985E+04	0.148674E+02	0.265660E+01	0.128768E+01	0.910968E-02	0.0
9	0.223285E+04	0.147469E+02	0.278127E+01	0.134511E+01	0.168981E-01	0.975271E+00
10	0.974490E+03	0.144977E+02	0.190322E+01	0.136978E+01	0.0	0.0
11	0.0	0.0	0.0	0.136978E+01	0.0	0.0
12	0.973185E+03	0.144269E+02	0.0	0.136978E+01	0.490665E-02	0.0

Approx. Idle

POWER 6.4 HP

SFC 1.404 LB/HP-HR

FUEL FLOW 9.0 LB/HR

STA NO.	TEMPERATURE	PRESSURE	CORR. FLOW	MASS FLOW	PRESSURE RATIOS	EFFICIENCY
1	0.544670E+03	0.142521E+02	0.758524E+00	0.717952E+00	0.141814E+01	0.760112E+00
2	0.619802E+03	0.202114E+02	0.499641E+00	0.628600E+00	0.315577E-02	0.0
3	0.185999E+04	0.201476E+02	0.847396E+00	0.613492E+00	0.172805E-01	0.978000E+00
4	0.210145E+04	0.197995E+02	0.976669E+00	0.640677E+00	0.124292E+01	0.857803E+00
5	0.200318E+04	0.159298E+02	0.116299E+01	0.640677E+00	0.100000E+01	0.0
6	0.195753E+04	0.159298E+02	0.119532E+01	0.666950E+00	0.0	0.0
7	0.195753E+04	0.159298E+02	0.121802E+01	0.666961E+00	0.109348E+01	0.886500E+00
8	0.191958E+04	0.145680E+02	0.129435E+01	0.666961E+00	0.191319E-02	0.0
9	0.189587E+04	0.145401E+02	0.134668E+01	0.696904E+00	0.632519E-02	0.974794E+00
10	0.793808E+03	0.144481E+02	0.893115E+00	0.709766E+00	0.0	0.0
11	0.0	0.0	0.0	0.709766E+00	0.0	0.0
12	0.793552E+03	0.144327E+02	0.0	0.709766E+00	0.106812E-02	0.0

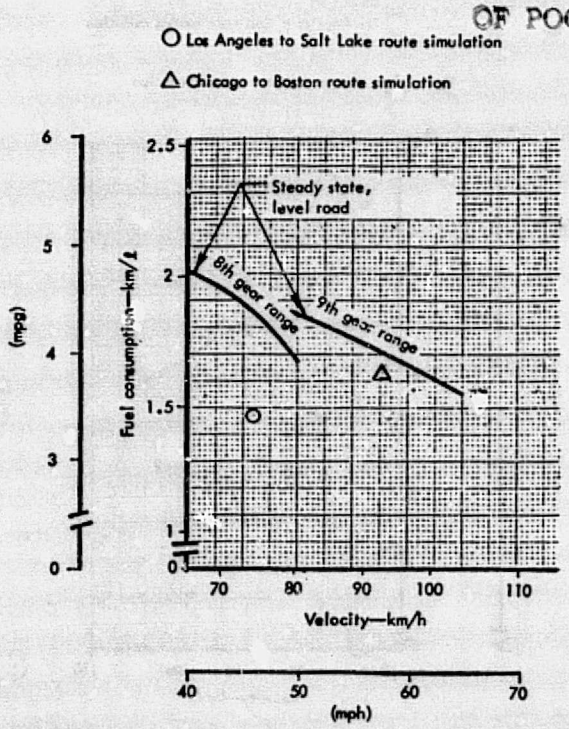

Figure 67. Line haul truck fuel consumption with base line engine.

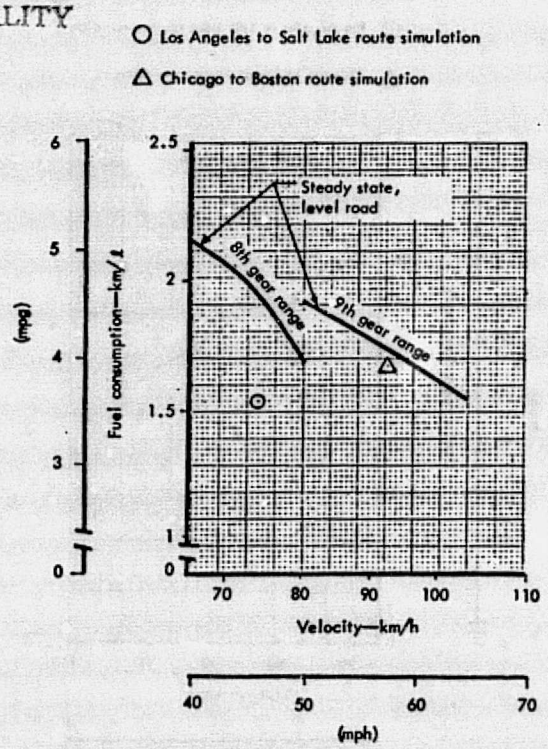

Figure 68. Line haul truck fuel consumption with 1002°C (1835°F) study engine.

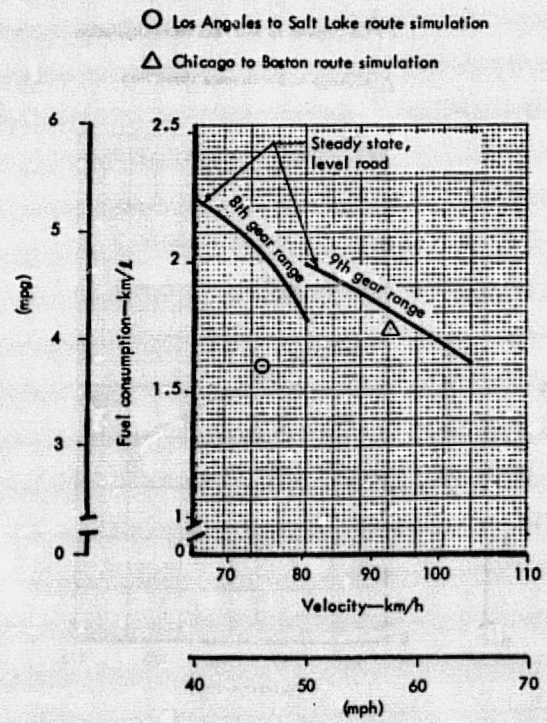

Figure 69. Line haul truck fuel consumption with 1038°C (1900°F) study engine.

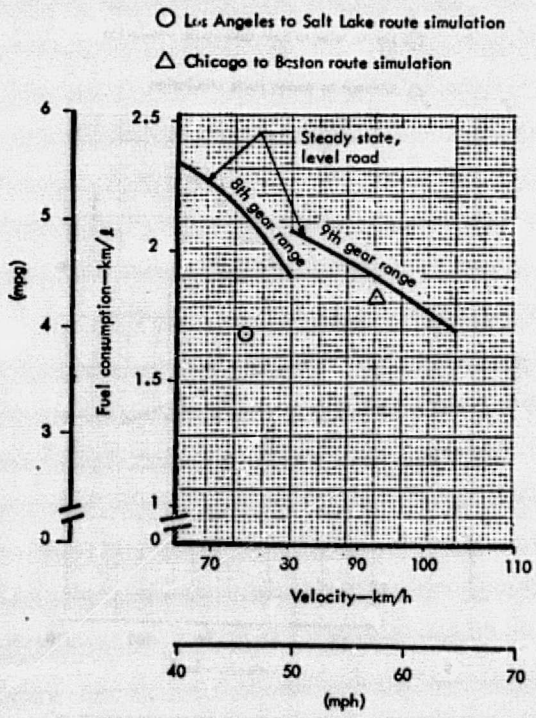

Figure 70. Line haul truck fuel consumption with 1132°C (2070°F) study engine.

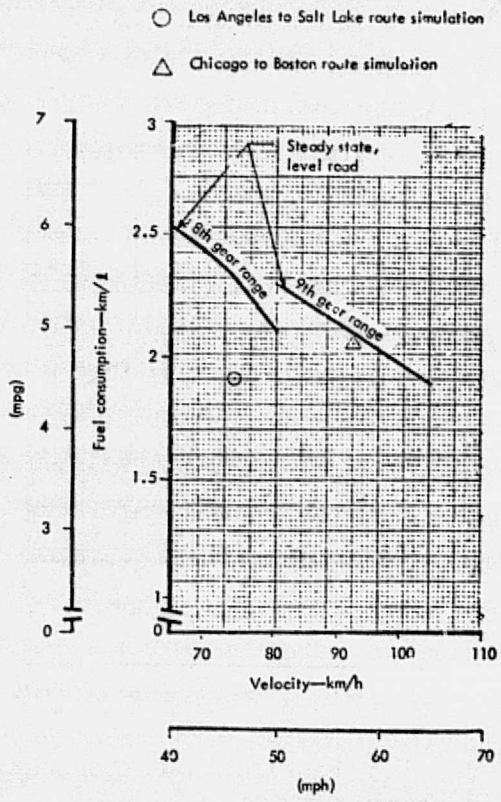

Figure 71. Line haul truck fuel consumption with 1204°C (2200°F) study engine.

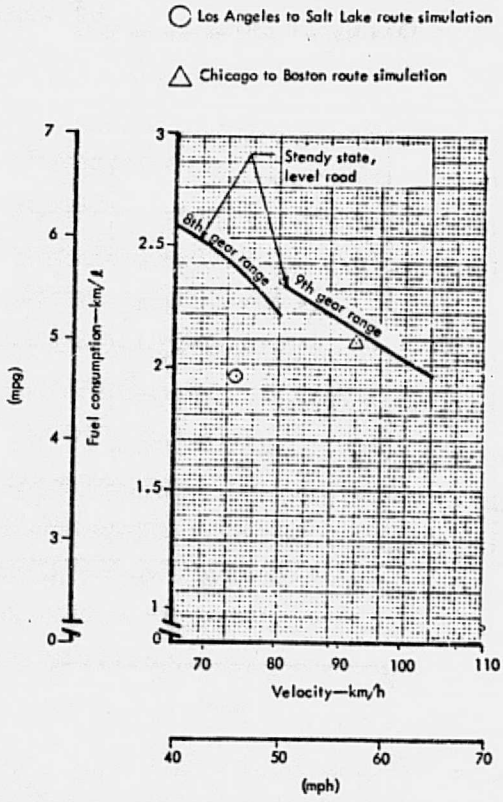

Figure 72. Line haul truck fuel consumption with 1371°C (2500°F) study engine.

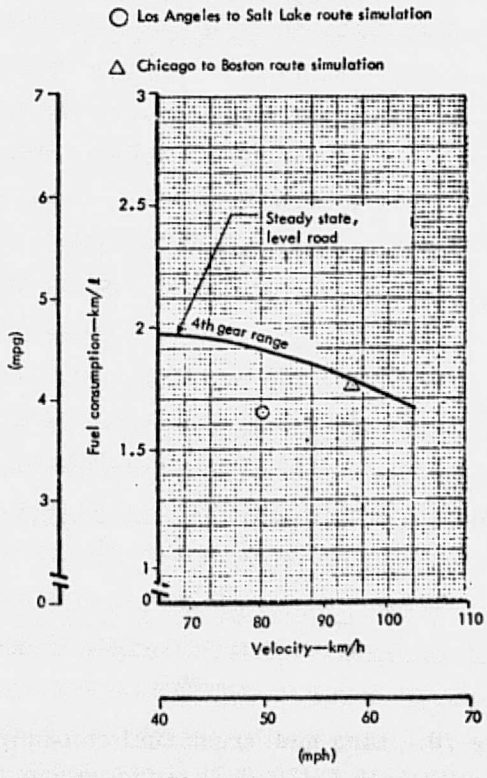

Figure 73. Intercity bus fuel consumption with base line engine.

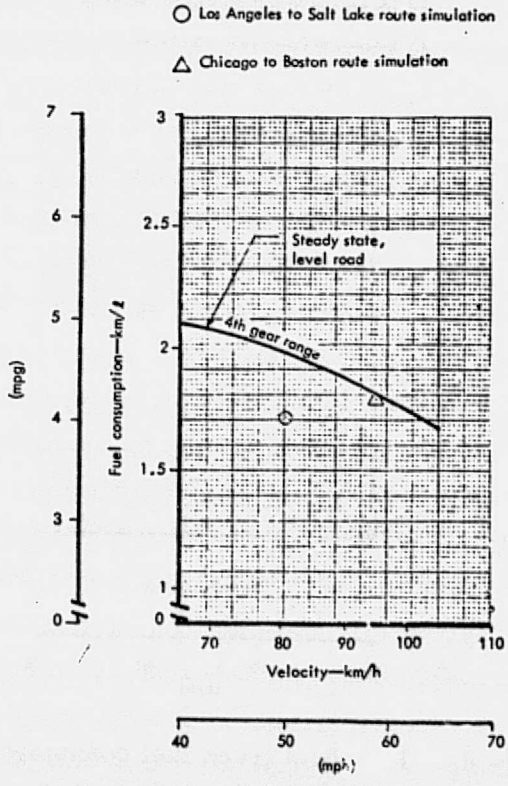

Figure 74. Intercity bus fuel consumption with 1002°C (1835°F) study engine.

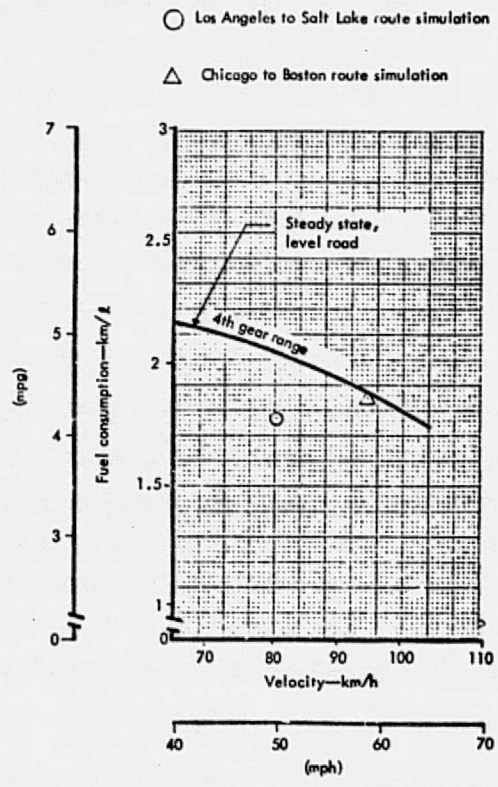

Figure 75. Intercity bus fuel consumption with 1038°C (1900°F) study engine.

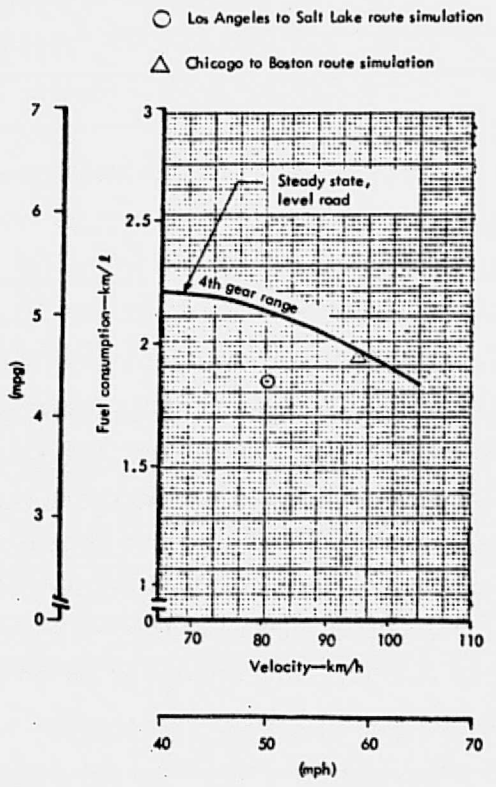

Figure 76. Intercity bus fuel consumption with 1132°C (2070°F) study engine.

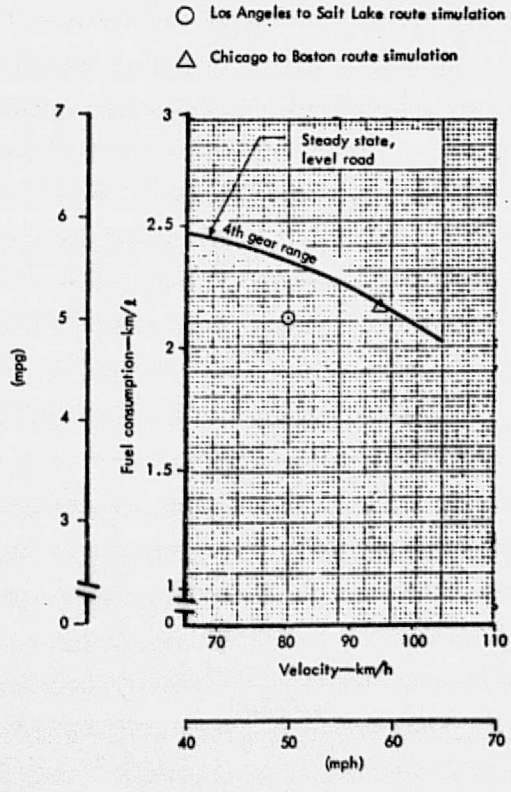

Figure 77. Intercity bus fuel consumption with 1204°C (2200°F) study engine.

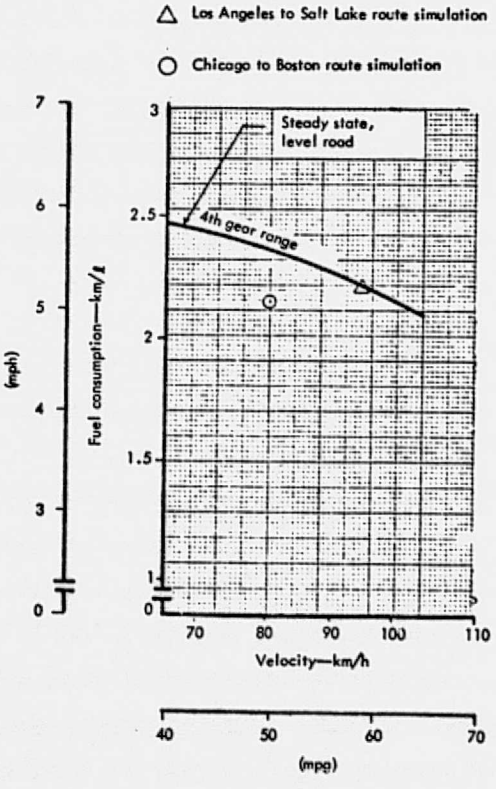

Figure 78. Intercity bus fuel consumption with 1371°C (2500°F) study engine.